

Some pages of this thesis may have been removed for copyright restrictions.

If you have discovered material in AURA which is unlawful e.g. breaches copyright, (either yours or that of a third party) or any other law, including but not limited to those relating to patent, trademark, confidentiality, data protection, obscenity, defamation, libel, then please read our [Takedown Policy](#) and [contact the service](#) immediately

Improving the solubility and dissolution of poorly soluble drugs by salt formation and the consequent effect on mechanical properties

Sarah David

Doctor of Philosophy

Aston University

April 2005

This copy of the thesis has been supplied on condition that anyone who consults it is understood to recognise that its copyright rests with its author and that no quotation from the thesis and no information derived from it may be published without proper acknowledgement.

Thesis Summary

Aston University

Improving the solubility and dissolution of poorly soluble drugs by salt formation and the consequent effects on mechanical properties

Sarah David

Doctor of Philosophy

April 2005

The bioavailability of BCS II compounds may be improved by an enhanced solubility and dissolution rate. Four carboxylic acid drugs were selected, which were flurbiprofen, etodolac, ibuprofen and gemfibrozil. The drugs were chosen because they are weak acids with poor aqueous solubility and should readily form salts. The counterions used for salt formation were: butylamine, pentylamine, hexylamine, octylamine, benzylamine, cyclohexylamine, tert-butylamine, 2-amino-2-methylpropan-2-ol, 2-amino-2-methylpropan-1,3-ol and tromethamine.

Salt formation was confirmed by NMR, DSC, TGA, DVS and FTIR. The saturated solubility in water was obtained for each of the salts together with dissolution data under different pH conditions. Dissolution was performed at one and two pH units above the parent drug pK_a . Solubility was partially controlled by the saturated solution pH with the butylamine counterion increasing the solution pH and solubility and dissolution to the greatest extent. As the chain length increased, solubility was reduced due to the increasing lipophilic nature of the counterion. The benzylamine and cyclohexylamine counterions produced crystalline, stable salts but did not improve solubility and dissolution significantly compared to the parent compound. The substitution of hydroxyl groups to tert-butylamine counterions produced an increase in solubility and dissolution. AMP2 resulted in the most enhanced solubility and dissolution compared to the parent drug but using the tris salt did not further improve solubility due to a very stable crystal lattice structure.

The parent drugs were very difficult to compress due to orientation effects and lamination. Compacts were prepared of each parent drug and salt and their modulus of elasticity values were measured using a three-point bend (Young's modulus, E_0) were extrapolated to zero porosity and compared. Compressibility and E_0 were improved with the butylamine, tert-butylamine, cyclohexylamine and AMP2 counterions. The most significant improvement in compression and E_0 was with the AMP2 salts. Mechanical properties were related to the hydrogen bonding within the crystal lattice structure for the gemfibrozil salt series. As the number of hydrogen bonds increased within the crystal structure the compressibility improved, increasing the E_0 value.

Key words: enhancement, compression properties, Young's modulus, counterion, modification of physicochemical properties

Acknowledgements

I would like to thank my supervisors, Dr Barbara Conway, Professor Bill Irwin and Professor Peter Timmins because without their support and encouragement this thesis would not have been possible. They have been an inspiration and source of important knowledge and experience which is invaluable to a PhD student.

Thanks to Professor Kenneth Harris and Dr Eugene Cheung of Cardiff University for the powder X-ray single crystal unit cell information for gemfibrozil and some of its amine salts. I would like to thank Eugene for his help, explanations and enthusiasm to complete this part of the thesis. Dr Carl Schwalbe performed the single crystal X-ray diffraction and I would like to extend my appreciation to him for his time and assistance.

Thank you to all the technical staff at Aston including Chris Bache, Jiteen Kansaris who have helped me through equipment failure. I would also like to express my gratitude to all my friends and family who have always supported me, even through the difficult times when my motivation was nearly lost.

List of Contents

Chapter 1 Introduction	25
1.1 The drug discovery process	25
1.2 The oral absorption route	26
1.2.1 The gastro-intestinal tract (GIT)	26
1.2.1.1 The stomach	27
1.2.1.2 The small intestine	28
1.2.1.3 The colon	31
1.2.1.4 Gastric emptying and small intestinal transit	31
1.2.1.5 Variation in pH of the gastrointestinal tract	33
1.3 Poorly soluble drugs	34
1.4 The Biopharmaceutics Classification System (BCS)	35
1.4.1 Class I drugs	35
1.4.2 Class II drugs	36
1.4.3 Class III drugs	36
1.4.4 Class IV drugs	36
1.5 Improving the solubility of drugs	36
1.6 The importance of salts	38
1.7 The salt selection process	42
1.8 Salt selection strategies	43
1.9 Tableting drugs	44
1.10 Improving the mechanical properties of drugs	45
1.11 Selecting model drugs	46
1.11.1 Properties of carboxylic acids	46
1.11.3 Carboxylic acids as drugs	48
1.11.4 Flurbiprofen	49
1.11.5 Ibuprofen	50
1.11.6 Etodolac	51
1.11.7 Gemfibrozil	52
1.12 Selecting counterions	53

1.12.1 Homologous alkyl series	53
1.12.2 Cyclic compounds	54
1.12.3 Hydrophilic series (hydroxyl substituted tert-butylamine)	55
1.13 Toxicology considerations	55
1.14 Experimental aims and objectives	56
 Chapter 2 HPLC methods and pH measurement	 58
2.1 HPLC	58
2.1.1 General Method for HPLC analysis	58
2.1.1.1 Materials	58
2.1.1.2 Equipment	58
2.1.1.3 Method	58
2.1.2 Gemfibrozil assay by HPLC	59
2.1.2.1 Materials	59
2.1.2.2 Methods	59
2.1.2.3 Example Data	59
2.1.3 Flurbiprofen assay by HPLC	60
2.1.3.1 Materials	60
2.1.3.2 Method	60
2.1.3.3 Example data	61
2.1.4 Ibuprofen assay by HPLC	61
2.1.4.1 Materials	61
2.1.4.2 Method	61
2.1.4.3 Example data	62
2.1.5 Etodolac assay by HPLC	62
2.1.5.1 Materials	62
2.1.5.2 Method	62
2.1.5.3 Example data	63
2.1.6 Naproxen assay by HPLC	63
2.1.6.1 Materials	63
2.1.6.2 Method	63
2.1.6.3 Example data	64
2.1.7 Piroxicam assay by HPLC	64
2.1.7.1 Materials	64
2.1.7.2 Method	64

2.1.7.3 Example data	65
2.2 pH measurements	65
 Chapter 3 Preparation and characterisation of salts of model acidic drugs	66
3.1 Introduction	66
3.2 Salt Preparation	67
3.2.1 Introduction	67
3.2.2 Homologous alkylamine series	67
3.2.2.1 Materials	67
3.2.2.2 Methods	68
3.2.3 Hydrophilic series	68
3.2.3.1 Materials	68
3.2.3.2 Methods	68
3.2.4 Cyclic compounds	69
3.2.4.1 Materials	69
3.2.4.2 Methods	69
3.3 Structural analysis	69
3.3.1 Introduction	69
3.3.2 Yield and salt purity	70
3.3.2.1 Materials	70
3.3.2.2 Equipment	70
3.3.2.3 Methods	70
3.3.2.4 Results	70
3.3.3 Confirmation of salt formation	71
3.3.3.1 FTIR	72
3.3.3.1.1 Materials	72
3.3.3.1.2 Equipment	72
3.3.3.1.3 Method	72
3.3.3.1.4 Results and discussion	73
3.3.3.2 NMR	73
3.3.3.2.1 Materials	74
3.3.3.2.2 Equipment	74
3.3.3.2.3 Method	74
3.3.3.2.4 Results and discussion	74

3.4 Physicochemical characteristics	75
3.4.1 Introduction	75
3.4.2 Differential scanning calorimetry (DSC) and Thermogravimetric analysis (TGA)	75
3.4.2.1 Materials	76
3.4.2.2 Equipment	76
3.4.2.3 Method	76
3.4.2.4 Results and discussion	76
3.4.3 Calculation of Log P and Log D values	83
3.4.3.1 Introduction	83
3.4.3.2 Method	83
3.4.3.3 Results and discussion	84
3.4.4 Determination of pKa for the salt forms	85
3.4.4.1 Method	85
3.4.4.2 Results	86
3.4.5 Surface area	87
3.4.5.1 Introduction	87
3.4.5.2 Materials and experimental	89
3.4.5.3 Method	89
3.4.5.4 Results and discussion	89
3.4.6 Dynamic vapour sorption (DVS)	90
3.4.6.1 Introduction	90
3.4.6.2 Materials and Experimental	91
3.4.6.3 Results and discussion	92
3.5 Physicochemical studies	95
3.5.1 Introduction	95
3.5.1.1 The theory of salt dissolution	98
3.5.1.2 The theory of salt solubility	100
3.5.2 pH solubility profile of model drugs	101
3.5.2.1 Introduction	101
3.5.2.1 Materials	103
3.5.2.2 Equipment	103
3.5.2.3 Methods	103
3.5.2.4 Results and discussion	103
3.5.3 Saturated solubility of model drug and salt in water	109
3.5.3.1. Materials and Experimental	109
3.5.3.2 Methods	109

3.5.3.3 Results and discussion	109
3.4.3.4 Relating solubility to physicochemical characteristics	114
3.4.3.4.1 pH-solubility relationships	114
3.4.3.4.2 Relationships between salt melting points and solubility	116
3.5.4 Contact-angle measurements	117
3.5.4.1 Introduction	117
3.5.4.2 Materials	118
3.5.4.3 Equipment	118
3.5.5.4 Method	119
3.5.4.5 Results and discussion	119
3.5.5 Estimation of solubility using the SPARC on-line calculator	120
3.5.5.1 Method	121
3.5.5.2 Results	121
3.5.6 Salt solubility in buffer	123
3.4.6.1 Introduction	123
3.4.6.2 Materials and Experimental	123
3.4.6.3 Methods	123
3.4.6.4 Results and discussion	124
3.5.7 Dissolution	127
3.5.7.1 Introduction	127
3.4.7.2 Statistical Analysis	128
3.5.7.3 Powder dissolution	130
3.5.7.4 Dissolution at pH 7.2	130
3.5.7.4.1 Materials	130
3.5.7.4.2 Equipment	130
3.5.7.4.3 Method	131
3.5.7.4.4 Results and discussion	131
3.5.7.4.4.1 Flurbiprofen	132
3.5.7.4.4.2 Gemfibrozil	135
3.5.7.5 Dissolution at pH 5	137
3.5.7.5.1 Materials	137
3.5.7.6.2 Equipment	137
3.5.7.6.3 Method	137
3.5.7.6.4 Results and discussion	137
3.5.8 Intrinsic Dissolution of salt forms	144

3.5.8.1 Materials	148
3.5.8.2 Equipment	148
3.5.8.3 Method	148
3.5.8.4 Results and discussion	148
3.5.8.5 Conclusions	153
Chapter 4 The Common Ion Effect	155
4.1 Introduction	155
4.1.1 Salting in and salting out	155
4.1.2 Common-ion effect	156
4.2 Experimental	160
4.2.1 Materials	160
4.2.2 Equipment	160
4.2.3 Method	160
4.2.3.1 Solubility screen in 2 M sodium hydroxide	160
4.2.3.2 Solubility of NSAID in sodium hydroxide	160
4.2.3.3 The effect of added NaCl on a saturated solution of NSAID in sodium hydroxide	161
4.2.4 Results and Discussion	162
4.2.4.1 Solubility screen in 2 M sodium hydroxide	162
4.2.4.2 NSAID solubility in increasing concentrations of sodium hydroxide	163
4.2.4.3 The effect of added NaCl on a saturated solution of NSAID in sodium hydroxide	167
4.2.5 Further work: examination of crystal structure	172
Chapter 5 Surface active characteristics of drug-salt systems	174
5.1 Introduction	174
5.1.1 Amphipathic compounds	174
5.1.2 Factors affecting the CMC	177
5.1.2.1 The effect of chain length	177
5.1.2.2 The effect of added electrolytes	178
5.1.2.3 The effect of hydrophilicity on micelle formation	178
5.1.2.4 The effect of pH	179
5.1.2.5 Studying the micellisation process	179
5.1.3 Surface activity of drugs	179
5.1.3.1 Closed Association	181
5.1.3.2 Open Association	182

5.1.3.3 Previous studies on surface-active drug systems	183
5.1.3.4 The effect of the counterion on micelle formation	186
5.1.4 Surface activity effects of amphiphilic drug-membrane interactions	186
5.2 Experimental	187
5.2.1 Materials	187
5.2.2 Equipment	187
5.2.3 Surface Tension determination	188
5.2.3.1 Method	188
5.2.3.2 Results and Discussion	189
5.2.3.3 Conclusions	198
5.2.4 Photon Correlation Spectroscopy (PCS)	199
5.2.4.1 Method	199
<u>Experiment 1: Etodolac and ibuprofen AMP2</u>	199
<u>Experiment 2: Amine salt solutions</u>	199
5.2.4.2 Results and Discussion	200
<u>Experiment 1: Etodolac and ibuprofen AMP2</u>	200
<u>Experiment 2: Amine salt solutions</u>	201
5.2.4.3 Conclusions	204
Chapter 6 X-ray Crystallography	206
6.1 Introduction	206
6.1.1 Using Single Crystals	206
6.1.2 Crystal growth	210
6.1.3 Powder diffraction	211
6.1.4 <i>Ab initio</i> crystal structure prediction	212
6.1.5 Relating crystal structure to physicochemical characteristics and mechanical properties; the future: growing crystals with specific properties.	213
6.2 Single crystal X-ray crystallography: experimental work	214
6.2.1 Crystal growth	214
6.2.2 Structure determination and refinement	215
6.2.2.1 Method of structure determination and refinement.	215

behaviour	245
7.2.5.1. Crystal Habit	245
7.2.5.2 Crystal form	245
7.2.6 Molecular structure and the prediction of mechanical properties	247
7.3 Experimental	248
7.3.1 Introduction	248
7.3.2 Experimental Aims	250
7.3.3 Experiment 1	250
7.3.3.1 Equipment	250
7.3.3.1.1 QTS-25 Texture Analyser from CNS Farnell (UK)	250
7.3.3.1.2 Specac Die and Press	252
7.3.3.2 Methods	252
7.3.3.3 Results	253
7.3.3.4 Experimental Limitations	258
7.3.4 Experiment 2	259
7.3.4.1 Equipment	259
7.3.4.1.1 Variable depth die (120 x 7 mm)	259
7.3.4.1.2 Bespoke die (20 x 7 x 1 mm)	260
7.3.4.1.3 Hounsfield Universal Tester S Series H10KS-0393	261
7.3.4.1.4 Stretching apparatus	261
7.3.4.1.5 Bespoke miniature three-point bend apparatus	263
7.3.4 Three-point bend determination of Young's modulus	264
7.3.4.1 Method	264
7.3.4.2 Results	265
7.3.4.3 Discussion of the mechanical properties of the salts; the effect of the counterion	270
7.3.4.3.1 Etodolac and Salts	270
7.3.4.3.2 Gemfibrozil and salts	274
7.3.4.3.3 Flurbiprofen and salts	276
7.3.4.3.4 Ibuprofen and salts	279
7.3.4.4 DSC	281
7.3.4.5 X-ray	283
7.3.4.6 Conclusions	285
Chapter 8 Concluding remarks and further work	286
Appendix	289
References	306

6.2.2.2 Redetermination from data collected with synchrotron radiation.	215
6.2.3 Results and Conclusions	216
6.2.3.1 Description of the structure.	216
6.2.3.2 Relationship of crystal structure to solubility	218
6.3 Structure determination using powder diffraction data: experimental work	219
6.3.1 Introduction	219
6.3.2 Experimental	219
6.3.3 Results	220
6.3.3.1 Gemfibrozil	220
6.3.3.2 Gemfibrozil butylamine	221
6.3.3.3 Gemfibrozil pentylamine	223
6.3.3.4 Gemfibrozil hexylamine	225
6.3.3.5 Gemfibrozil AMP2	226
6.3.3.6 Gemfibrozil Tris	227
6.3.4 Discussion	229
Chapter 7 Mechanical Properties of Salts	230
7.1 Introduction	230
7.1.1 Summary	230
7.1.2 The Process of Compression	230
7.1.2.1 Particle Rearrangement	231
7.1.2.2 Deformation	231
7.1.2.3 Fragmentation	232
7.1.2.4 Bonding	232
7.1.2.5 Decompression and Ejection	233
7.1.2.6 The Heckel Plot	233
7.1.2.7 Tablet Indices	235
7.2.2.8 Leuenberger theory of powder compression	238
7.2.3 The effect of compression on tablet characteristics	239
7.2.3.1 Density and Porosity	239
7.2.3.2 Fracture	240
7.2.3.3 Disintegration and dissolution	241
7.2.4 Mechanical Properties	241
7.2.4.1 Young's Modulus	241
7.2.5 The effect of crystallographic forms on tableting	

List of Figures

Figure		Page
Figure 1.1	Components of the digestive system	27
Figure 1.2	Anatomy of the stomach	28
Figure 1.3	Gross structure of the small intestine	30
Figure 1.4	pH in the small intestine in healthy humans in the fed and fasted state	33
Figure 1.5	Distribution of the most commonly occurring salt forms for acids	39
Figure 1.6	Distribution of the most commonly occurring salts for bases	39
Figure 1.7	Structure of a carboxylic acid	47
Figure 1.8	Chemical structure of flurbiprofen	50
Figure 1.9	The chemical structure of ibuprofen	51
Figure 1.10	Chemical structure of etodolac	51
Figure 1.11	Chemical structure of gemfibrozil	52
Figure 1.12	The chemical structure of the homologous series of linear chain amines	54
Figure 1.13	The chemical structures of benzylamine and cyclohexylamine	54
Figure 1.14	The chemical structures of hydroxyl substituted tert, AMP1, AMP2 and tris	55
Figure 2.1	Typical HPLC chromatogram of a gemfibrozil peak of concentration 0.5 mg/ml at 276 nm.	60
Figure 2.2	Typical HPLC chromatogram of flurbiprofen 1 mg/ml at 250 nm	61
Figure 2.3	Typical chromatogram of the ibuprofen peak of 1 mg/ml at 225 nm	62
Figure 2.4	Typical HPLC chromatogram of the etodolac peak of 2 mg/ml at 275 nm	63
Figure 2.5	Typical HPLC chromatogram of the naproxen peak of 1 mg/ml at 225 nm	64

Figure 2.6	Typical HPLC chromatogram for piroxicam 1 mg/ml and 254 nm	65
Figure 3.1	DSC scans for the homologous salts of the gemfibrozil series	79
Figure 3.2	DSC scans of ibuprofen and its benzylamine, cyclohexylamine, tris, AMP2, AMP1 and tert-butylamine salts.	80
Figure 3.3	TGA of ibuprofen benzylamine	80
Figure 3.4	DSC scans for the cyclohexylamine and benzylamine salt of gemfibrozil	81
Figure 3.5	DSC (green) and TGA (blue) trace of etodolac AMP2	82
Figure 3.8	DVS data for etodolac butylamine	93
Figure 3.7	DVS data for ibuprofen benzylamine	94
Figure 3.8	DVS data for etodolac butylamine	94
Figure 3.9	Diffusion layer model of drug diffusion	97
Figure 3.10	The solubility/pH profile for flurbiprofen	107
Figure 3.11	The solubility/pH profile for gemfibrozil	107
Figure 3.12	The solubility/pH profile for etodolac	108
Figure 3.13	The solubility/pH profile for ibuprofen	108
Figure 3.14	The saturated aqueous solubility of etodolac, flurbiprofen, gemfibrozil and ibuprofen and their amine salts.	112
Figure 3.15	Saturated aqueous solubilities of etodolac, flurbiprofen, gemfibrozil and ibuprofen and their hydrophilic amine salts.	114
Figure 3.16	Relationship between melting point and solubility for a range of amine salts for the drugs etodolac, flurbiprofen, gemfibrozil and ibuprofen.	117
Figure 3.17	Contact angle (CA) measurements for gemfibrozil butylamine (n=2) in seconds (s).	119
Figure 3.17	Contact angle (CA) measurements for gemfibrozil (n=2) in seconds (s).	120

Figure 3.18	Aqueous solubilities of the butylamine, hexylamine, AMP1 and AMP2 salts of etodolac and ibuprofen in pH 6 buffer	125
Figure 3.19	Aqueous solubilities of the butylamine, hexylamine and AMP1 salts of flurbiprofen and gemfibrozil at pH 6	126
Figure 3.20	The powder dissolution of flurbiprofen and its benzylamine, cyclohexylamine, hexylamine and tert-butylamine salts at pH 7.2	134
Figure 3.21	The powder dissolution of flurbiprofen and its AMP1, AMP2 and tris salts at pH 7.2.	134
Figure 3.22	The powder dissolution of gemfibrozil and its butylamine, benzylamine, hexylamine and cyclohexylamine salts at pH 7.2.	136
Figure 3.23	The powder dissolution of gemfibrozil and its tris, AMP1 and AMP2 salts.	136
Figure 3.24	Powder dissolution of etodolac and its butylamine, hexylamine and AMP1 salts at pH 5.2.	140
Figure 3.25	Powder dissolution of flurbiprofen and its butylamine, hexylamine and AMP1 salts at pH 5.2.	141
Figure 3.26	Powder dissolution of gemfibrozil and its tris, AMP2 and AMP1 salts at pH 5.6.	143
Figure 3.27	Powder dissolution of ibuprofen and its butylamine, hexylamine and AMP1 salts at pH 5.4.	144
Figure 3.28	Diagram of PTFE disk holders used in IDR experiments, not to scale.	146
Figure 3.29	Intrinsic disk dissolution of flurbiprofen and its benzylamine, cyclohexylamine and tert-butylamine salts at pH 6.8.	152
Figure 3.30	Intrinsic disk dissolution of gemfibrozil and its butylamine, benzylamine and tert-butylamine salts at pH 7.2.	153
Figure 4.1	Graph to show the solubility of flurbiprofen in sodium hydroxide solution, from 0.1-2M.	163

Figure 4.2	Graph to show the solubility of piroxicam in sodium hydroxide solution, from 0.1-2M.	164
Figure 4.3	Graph to show the solubility of naproxen in sodium hydroxide solution, from 0.1-2M.	165
Figure 4.4	Graph to show the solubility of naproxen in sodium hydroxide solution, from 1-1.5M.	166
Figure 4.5	Graph to show the effect of added sodium chloride on the solubility of flurbiprofen in 0.1M sodium hydroxide solution.	167
Figure 4.6	Graph to show the effect of added sodium chloride on the solubility of naproxen in 1M sodium hydroxide solution.	168
Figure 4.7	Graph to show the effect of added sodium chloride on the solubility of piroxicam in 0.1M sodium hydroxide solution.	168
Figure 4.8	Plots of solubility mg/ml against log concentration (mmol/ml) sodium chloride added for flurbiprofen (0.1 M sodium hydroxide), piroxicam (0.1 M sodium hydroxide) and naproxen (1 M sodium hydroxide) in sodium hydroxide solutions.	171
Figure 5.1	Surface tension versus log concentration plots for a model compound illustrating typical surfactant behaviour (schematic).	176
Figure 5.2	Schematic diagram of the conformation of a typical micelle	176
Figure 5.3	Structure of typical diphenylmethane derivatives. Diphenhydramine $R_1 = OCH_2CH_2N^+H(CH_3)_2$ $R_2 = H$	181
Figure 5.4	Schematic representation of a typical micelle of ionic surfactant molecules	182
Figure 5.5	Structures of drugs that exhibit continuous association patterns in aqueous solution: L-R clockwise propantheline, methantheline, pavatrine and chlordiazepoxide.	183

Figure 5.6	Structure of clomipramine and imipramine	184
Figure 5.7	Structures of trimeprazine tartrate (A) and promethazine hydrochloride (B).	185
Figure 5.8	Surface tension measurements against concentration of aqueous solutions of etodolac AMP2 and ibuprofen AMP2.	190
Figure 5.9	Surface tension v log concentration (mg/ml) for aqueous solutions of ibuprofen AMP2 used to calculate the CMC.	190
Figure 5.10	Surface tension v log concentration (mg/ml) for aqueous solutions of etodolac AMP2 used to calculate the CMC.	191
Figure 5.11	Surface tension of aqueous solutions of ibuprofen, etodolac and gemfibrozil.	193
Figure 5.12	Surface tension measurements as of a function of concentration for the aqueous solutions of the butylamine salts of etodolac, flurbiprofen, gemfibrozil and ibuprofen.	195
Figure 5.13	Surface tension measurements as a function of concentration for the aqueous solutions of the hexylamine salts of etodolac, flurbiprofen, gemfibrozil and ibuprofen.	196
Figure 5.14	Surface tension measurements as a function of concentration for an aqueous solution of the AMP1 salts of etodolac and ibuprofen.	197
Figure 5.15	Surface tension measurements for the aqueous solution of gemfibrozil AMP1, AMP2 and flurbiprofen AMP1, AMP2.	198
Figure 5.16	Plot of micelle effective diameter (nm) against concentration (mg/ml) for etodolac and ibuprofen AMP2 using photon correlation spectroscopy.	200
Figure 5.17	Particle size versus concentration for the salts showing evidence of micellisation as determined by	203

	PCS.	
Figure 6.1	Photographic imaging of crystals using X-rays and the ionisation spectrometer used by W. H. Bragg to conduct the first investigations of the X-ray spectra.	207
Figure 6.2	Crystal structure of flurbiprofen cyclohexylamine	217
Figure 6.3	Crystal structure of flurbiprofen cyclohexylamine	217
Figure 6.4	The crystal structure and unit cell of gemfibrozil	221
Figure 6.5	The unit cell of gemfibrozil butylamine	222
Figure 6.6	The unit cell of gemfibrozil pentylamine	224
Figure 6.7	Unit cell of gemfibrozil pentylamine re-oriented	224
Figure 6.8	The unit cell of gemfibrozil hexylamine	225
Figure 6.9	The unit cell of gemfibrozil AMP2	227
Figure 6.10	The unit cell for gemfibrozil tris	228
Figure 7.1	The QTS-25 Texture Analyser	251
Figure 7.2	Tensile strength of etodolac and its amine salt compacts with 10% Avicel PH 105.	255
Figure 7.3	Tensile strength of ibuprofen and its amine salts with 10% Avicel PH 105.	256
Figure 7.4	Tensile strength of gemfibrozil and its amine salts with 10% Avicel PH 105.	256
Figure 7.5	Tensile strength of flurbiprofen and its amine salts with 10% Avicel PH 105.	258
Figure 7.6	Roberts 20 x 7 mm four piece stainless steel die held together with screws	259
Figure 7.7	New punch and die set. One piece hardened steel die of 20 x 7 mm made to fit existing punches with 1 mm gap and longer punch for ejection.	260
Figure 7.8	The Hounsfield S Series Universal Testing Machine	261
Figure 7.9	Avicel PH105 wafer held between upper and lower clamps for elongation	262
Figure 7.10	Bespoke miniature three point bend jig	264
Figure 7.11	Typical force against displacement data for an Avicel wafer using QMAT Testzone for Hounsfield S series.	265

Figure 7.12	Typical force against displacement data curve of an ibuprofen wafer of porosity -0.08, using QMAT Testzone for Hounsfield S series.	266
Figure 7.13	Young's Modulus versus porosity for Avicel PH105®, etodolac, flurbiprofen, ibuprofen and gemfibrozil.	267
Figure 7.14	Young's modulus versus porosity for etodolac butylamine, etodolac hexylamine and etodolac octylamine.	271
Figure 7.15	Young's modulus versus porosity for etodolac cyclohexylamine and etodolac benzylamine.	272
Figure 7.16	Young's modulus versus porosity for etodolac tert-butylamine, etodolac AMP1, etodolac AMP2.	273
Figure 7.17	Young's modulus versus porosity for gemfibrozil butylamine and gemfibrozil hexylamine.	274
Figure 7.18	Young's modulus versus porosity for gemfibrozil tert-butylamine, gemfibrozil AMP2 and gemfibrozil tris.	275
Figure 7.19	Young's modulus versus porosity for flurbiprofen butylamine and flurbiprofen hexylamine.	277
Figure 7.20	Young's modulus versus porosity for flurbiprofen cyclohexylamine and flurbiprofen benzylamine.	278
Figure 7.21	Young's modulus versus porosity for flurbiprofen tert-butylamine, flurbiprofen AMP2 and flurbiprofen tris.	278
Figure 7.22	Young's modulus versus porosity for ibuprofen tert-butylamine and ibuprofen AMP2.	280
Figure 7.23	Young's modulus versus porosity for ibuprofen AMP1 demonstrating eliminated points (pink).	281
Figure 7.24	The DSC traces of Ibuprofen and its compacts	282
Figure 7.25	The DSC traces of etodolac and its compacts	283
Figure 7.26	The X-ray image of an ibuprofen compact of positive porosity showing random orientation	284
Figure 7.27	The X-ray image of an ibuprofen compact of negative porosity showing preferred orientation	284

List of Tables

Table		Page
Table 1.1	Solubility terms and solubility ranges as used by Martindale (1999)	50
Table 3.1	Weights and volumes of reagents used in salts preparation.	68
Table 3.2	Purity of four selected amine salts of flurbiprofen	71
Table 3.3	Purity of four selected amine salts of gemfibrozil	71
Table 3.4	Melting points and enthalpies of fusion for the amine salts of etodolac and flurbiprofen determined using DSC.	78
Table 3.5	Melting points and enthalpies of fusion for the amine salts of gemfibrozil and ibuprofen determined using DSC.	78
Table 3.6	Estimated ClogP values from the computer program ClogP V4.0.	84
Table 3.7	Calculated pKa values using the SPARC online calculator for the model drugs and their counterions.	86
Table 3.8	Calculated pKa values using the SPARC online calculator for the amine salts of etodolac and flurbiprofen.	86
Table 3.9	Calculated pKa values using the SPARC online calculator for the amine salts of ibuprofen and gemfibrozil.	86
Table 3.10	Surface area and saturated water solubility measurements of ibuprofen, ibuprofen butylamine, ibuprofen octylamine and ibuprofen AMP2.	90
Table 3.11	DVS analysis of a selection of model drugs and salts from 0-100% humidity over time.	92
Table 3.12	SPARC calculation of pKa for the model drugs	104
Table 3.13	Table to indicate the calculated pK _a values for the weak acids used and their regression fit to theory.	104
Table 3.14	The pH/solubility relationship for flurbiprofen and	106

	gemfibrozil in phosphate buffer solutions.	
Table 3.15	The pH/solubility relationship for etodolac and ibuprofen in phosphate buffer solution.	106
Table 3.16	Aqueous solubilities of the drugs and their amine salts as molar concentrations. Results are calculated from mean values	110
Table 3.17	The saturated aqueous solubilities, corresponding pH values and the solubility increase factor of the amine salts of etodolac and gemfibrozil.	111
Table 3.18	The saturated aqueous solubilities, corresponding pH values and the solubility increase factor of the amine salts of flurbiprofen and ibuprofen.	111
Table 3.19	The saturated aqueous solubility and measured pH values against the solubility data from the pH-solubility profiles of each drug, etodolac, flurbiprofen, gemfibrozil and ibuprofen.	115
Table 3.20	SPARC versus measured aqueous solubilities (mg/ml) of etodolac and flurbiprofen salts	122
Table 3.21	SPARC versus measured aqueous solubilities (mg/ml) of ibuprofen and gemfibrozil salts	122
Table 3.22	Solubility of the butylamine, hexylamine and AMP1 salts of etodolac and flurbiprofen, including etodolac AMP2 in pH 6 buffer	124
Table 3.23	Solubility of the butylamine, hexylamine and AMP1 salts of gemfibrozil and ibuprofen, including ibuprofen AMP2 in pH 6 buffer	124
Table 3.24	F ₂ fit factors for classification of dissolution curves into categories	129
Table 3.25	f ₂ fit factor results for the powder dissolution of flurbiprofen and a selection of its amine salts at pH 7.2	132
Table 3.26	f ₂ fit factor results for the powder dissolution of gemfibrozil and a selection of its amine salts at pH	132

	7.2	
Table 3.27	f_2 fit factor results for the powder dissolution of gemfibrozil and a selection of its amine salts at pH 7.2	135
Table 3.28	f_2 fit factor results for the powder dissolution of etodolac and its butylamine, hexylamine and AMP1 amine salts at pH 5.2	138
Table 3.29	f_2 fit factor results for the powder dissolution of flurbiprofen and its butylamine, hexylamine and AMP1 amine salts at pH 5.2	138
Table 3.30	f_2 fit factor results for the powder dissolution of gemfibrozil and a selection of its amine salts at pH 5.6	138
Table 3.31	f_2 fit factor results for the powder dissolution of ibuprofen and its butylamine, hexylamine and AMP1 amine salts at pH 5.5	138
Table 3.32	IDR results for flurbiprofen and its cyclohexylamine, tert-butylamine and benzylamine salts	150
Table 3.33	IDR results for gemfibrozil and its butylamine, tert-butylamine and benzylamine salts	150
Table 3.34	The f_2 fit values for the intrinsic disk dissolution of flurbiprofen and its benzylamine, cyclohexylamine and tert-butylamine salts at pH 6.8	151
Table 3.35	The f_2 fit values for the intrinsic disk dissolution of gemfibrozil and its benzylamine, cyclohexylamine and tert-butylamine salts at pH 7.2.	152
Table 4.1	Table detailing sample volume and additional sodium chloride to investigate the common ion effect on saturated NSAID solutions.	162
Table 4.2	The behaviour of selected NSAIDs in 2M sodium hydroxide solution.	162
Table 5.1	Classification of surfactants	174
Table 5.2	CMC values of singly dispersed anionic ^a and non-	178

	ionic surfactants (Shinoda et al., 1996). ^a Attwood and Florence (1983).	
Table 5.3	Micellar properties of some non-peptide surface active drugs in water	181
Table 5.4	Summary of the solution properties of etodolac, flurbiprofen, gemfibrozil, ibuprofen and their butylamine, hexylamine, AMP1 and AMP2 salts	192
Table 5.5	Effective particle size (nm) measured by PCS and aqueous solubility data (mg/ml) for the AMP1, butylamine and hexylamine salts of etodolac, flurbiprofen, gemfibrozil and ibuprofen.	202
Table 7.1	Young's modulus of drug substances as determined by three point beam testing (Roberts, 1991)	249
Table 7.2	The true density of etodolac and flurbiprofen amine salts	254
Table 7.3	The true density of gemfibrozil and ibuprofen amine salts	254
Table 7.4	Young's modulus of all the materials as determined by three-point bend testing for etodolac and gemfibrozil salt compacts	269
Table 7.5	Young's modulus of all the materials as determined by three-point bend testing for flurbiprofen and ibuprofen salt compacts	270

List of Abbreviations

BCS	Biopharmaceutics Classification System
BP	British Pharmacopoeia
cm	Centimetre
DMSO	Dimethyl Sulfoxide
e-	Etodolac-counterion
f-	Flurbiprofen-counterion
FDA	Federal Drug Administration
FTIR	Fourier Transform Infrared Spectroscopy
g-	Gemfibrozil-counterion
g	Gram
gut/GIT	Gastrointestinal
h or hr	Hour
HCl	Hydrochloric acid
Hplc or HPLC	High Performance Liquid Chromatography
i-	Ibuprofen
IDR	Intrinsic Dissolution Rate
J	Joules
kg	Kilograms
M	Molar
mg	Milligram
min	Minutes
ml	Millimetres
mM	Millimolar
mmol	Millimolar
NaOH	Sodium Hydroxide
NMR	Nuclear Magnetic Resonance
NSAID	Non-Steroidal Anti-inflammatory Drug
PCS	Photon Correlation Spectroscopy
R or r^2	Correlation coefficient
RH	Relative Humidity
RPM	Revolutions <i>per</i> minute
s	Seconds
SD	Standard Deviation
USP	United States Pharmacopoeia
UV	Ultraviolet
μ g	Micrograms
C	Degrees Celsius
%	Percentage

Chapter 1 Introduction

1.1 The drug discovery process

In a commercial environment, the drug discovery process strives to chemically synthesise a potent, active compound. The pre-requisites are high potency, or a compound that binds selectively and reversibly to the appropriate receptor. The active compound should have low toxicity, low or no teratogenicity and a good side effect profile. Once the compound is selected it is passed to the formulation scientist to create an appropriate dosage form. The active chemical entity must have acceptable aqueous solubility in order for it to be absorbed from the gastrointestinal tract and have a good bioavailability (the rate and extent of absorption). Many drug discovery processes result in an active pharmaceutical that is poorly soluble in water which leads to many problems when formulating a dosage form.

Over the last 15 years there has been a change towards the use of combinatorial-chemistry techniques that have the ability to produce thousands of molecules per year. Initial screening techniques generally involve an automated high throughput screen using the compound dissolved in dimethyl sulfoxide (DMSO). The screening allows for activity in enzyme- or receptor-based assay systems to be assessed quickly. The screening is then refined to give a manageable number of 'hits' and then further structural refinement is usually required to make the molecules more potent. The 'candidate' drugs can be relatively impure free bases, free acids or neutral molecules, and are often amorphous. Because they are often dissolved in DMSO prior to screening it is not necessary to ensure the crystallinity, also solubility is better in DMSO than in aqueous solvents.

Drugs are often designed to have a high binding affinity to endogenous receptors, so their action is selective and potent. In this way drugs are designed to exert their pharmacological effect with a small dose producing little or no side effects so they are acceptable to the patient and improve compliance. When a selection of candidate drugs are screened for affinity for the appropriate receptor, the most potent molecule may be lipophilic because of the drug discovery process. If a drug is highly lipophilic it probably will have limited solubility in water. This will lead to unsatisfactory

dissolution of the drug in the gastrointestinal tract and therefore a small amount of the dose will be absorbed into the systemic circulation.

Drugs with poor solubility are becoming an increasing problem in the pharmaceutical industry and strategies to overcome poor solubility are being employed by formulation scientists and medicinal chemists to maintain good bioavailability of new drugs. Because drug substances are designed to bind to a receptor, enzyme or protein *etc.*, they normally possess several functional groups capable of hydrogen bonding. Some of these functional groups may give the potential for salt formation and thus increased hydrophilicity. Salt formation gives the formulation scientist the opportunity to modify the physicochemical characteristics *e.g.* melting point, hygroscopicity, chemical stability, dissolution rate, solution pH, crystal form *etc.* and mechanical properties *e.g.* hardness, elasticity *etc.* of the potential drug substance and to develop dosage forms with acceptable bioavailability, stability, manufacturability and patient compliance.

1.2 The oral absorption route

1.2.1 The gastro-intestinal tract (GIT)

The gastro-intestinal tract (GIT) is a highly specialised region of the body that is involved in secretion, digestion and absorption. All nutrients required by the body apart from oxygen must be ingested orally, processed by the GIT and made available for absorption into the bloodstream before their benefits can be realised. The GIT is responsible for ejecting noxious or irritating materials to prevent toxicity and it removes these by vomiting or diarrhoea. Therefore the GIT represents a significant barrier to the environment and to foreign substances, like some drugs.



Illustration removed for copyright restrictions

Figure 1.1 Components of the digestive system adapted from Human Physiology (2004)

The GIT is represented pictorially in figure 1.1 and it shows the main functional regions within the GIT. The liver, gallbladder and pancreas secrete materials vital to the digestive and some absorptive process. The small intestine, comprising of the duodenum (0.3 m), jejunum (2.4 m), ileum (3.6 m) represents over 60% of the length of the GIT, which is consistent with its primary digestive and absorptive functions. The large intestine or colon is commonly 0.9 to 1.5 m in length.

1.2.1.1 The stomach

The stomach is the first major barrier to most ingested materials; its primary function is breaking down components with the aid of enzymes and a high acid environment to chyme and the storage and mixing of the stomach contents. The stomach is then emptied in a controlled manner to the small intestine for further digestion and absorption. The stomach consists of three main parts: the fundus and body, which is a storage region and the walls can distend outwards to accommodate a large meal and the antrum, as illustrated in figure 1.2, is the major site for mixing motions and acts as a pump to assist gastric emptying.



Illustration removed for copyright restrictions

Figure 1.2 The anatomy of the stomach adapted from Human Physiology (2004)

The mucosal surface of the stomach is lined by an epithelial layer of columnar cells. Along the surface are many gastric pits, at the bottom of which secretory cells produce about 2 L of fluid a day. The epithelial cells rapidly proliferate and renew the layer every 1 to 3 days. Covering the surface is a layer of mucus which is constantly being renewed. The mucus acts as a protective lubricating coat for the cell lining. The parietal cells produce acid (HCl) and maintain the pH of the stomach between 1 and 3.5, in the fasted state. Pepsins are present in the stomach which are only active below pH 5, these are secreted by the peptic cells and break down proteins.

Very little drug absorption occurs in the stomach owing to its small surface area compared to the small intestine.

1.2.1.2 The small intestine

The small intestine is the longest and most convoluted part of the GIT. The wall of the small intestine has a unique structure, making it ideally suited for digestion and absorption because it greatly increases its effective luminal surface area. The small intestine has a rich network of blood vessels; it is supplied with blood from the mesenteric artery via branched arterioles and the blood leaving the small intestine flows into the hepatic portal vein, which carries it to the liver and then to the systemic

circulation. Drugs that are metabolised by the liver before reaching the systemic circulation are degraded and are subject to first pass metabolism. The walls of the small intestine are also well supplied by the lymphatic system. Peyer's patches on the surface of the ileum are areas of lymphoid tissue that play a key role in the immune response as they transport macromolecules and are involved in antigen uptake. The lymphatic system is involved in the transport of fats from the gastrointestinal tract.

The increased surface area of the small intestine is because of the submucosal folds of Kerckring and the villi and microvilli that have evolved at the epithelial surface. Lining the epithelium are the villi which are finger-like projections into the lumen of approximately 0.5 to 1.5 mm in length and 0.1 mm in diameter. They are well supplied with blood and lymph vessels (figure 1.3). Projecting from the villi surface are the microvilli, there are approximately 600-1000 of these brush-like structures that cover each villus and they are approximately 1 μm in length and depth. The microvilli region is also referred to as the 'brush border' and it is in this region that absorption is initiated.



Illustration removed for copyright restrictions

Figure 1.3 Gross structure of the small intestine showing the circular folds that increase the total surface area for absorption, the microscopic luminal projections known as the villi and a pictorial representation of a villus epithelial cell depicting microvilli on its luminal border.

Adapted from Human Physiology (2004)

The luminal pH of the small intestine increases to between 6 and 7.5 because of secretions of bicarbonate by the Brunner's glands in the duodenum which neutralise the acids from the stomach. Other secretions include mucus and enzymes by intestinal cells, hydrolases and proteases continue the digestive process. The pancreas lies below the stomach and secretes digestive enzymes and an aqueous alkaline fluid into the duodenum *via* a duct. Pancreatic proteolytic enzymes including trypsin, chymotrypsin and carboxypeptidases are all secreted in their inactive form and digest protein when activated by enterokinase. Pancreatic amylase and lipase are secreted in their active form and digest carbohydrate and fats. Bicarbonate is also secreted to neutralise the stomach contents that have been emptied into the small intestine. The secretion of bicarbonate is controlled by the pH of the chyme delivered by the stomach so that enzymatic activity is facilitated because pancreatic enzymes function best in a neutral or slightly alkaline environment. Bile is continuously secreted by hepatocytes in the liver and is diverted to the gallbladder between meals. The bile is stored and concentrated in the gallbladder by the removal

of sodium ions, chloride and water, and delivered in the duodenum. Bile is an alkaline fluid containing bile salts, cholesterol, lecithin and bilirubin. The bile acids are reabsorbed back into the blood by an active transport mechanism referred to as the enterohepatic circulation. Bile pigments including bilirubin, are excreted in the faeces. The main function of the bile is to aid fat digestion and absorption by emulsifying the fats present in the lumen and to facilitate fat absorption by participation in the formation of micelles.

1.2.1.3 The colon

The colon is the final part of the gastro-intestinal tract; its length is approximately 1.5 m. The main functions of the colon are the absorption of sodium ions, chloride ions and water from the lumen in exchange for bicarbonate and potassium ions. Thus the colon has a significant homeostatic role in the body. The pH of the upper part of the colon is around 6 to 6.5 and this increases to around 7 to 7.5 towards the distal parts of the colon. The gases hydrogen, methane and carbon dioxide are produced by the masses of bacteria present in the colon which break down undigested carbohydrates to short-chain fatty acids which lower the pH.

1.2.1.4 Gastric emptying and small intestinal transit

The transit time of pharmaceuticals in the gastrointestinal tract is a very important consideration when designing a formulation. If a controlled release delivery system is being developed it is important to consider factors that will affect absorption of the drug. If it is to be absorbed in the small intestine, the major site for drug absorption, then the time a drug is present in this part of the gastrointestinal tract is highly significant.

In general, most dosage forms when taken in the upright position transit through the oesophagus in less than 15 seconds. If the dose is taken in the supine position they are liable to lodge in the oesophagus and reduce their effectiveness. Gastric emptying of pharmaceuticals is highly variable and is dependent on the dosage form and whether the stomach is in a fed or fasted state. Normal gastric residence times are between 5 minutes and 2 hours, although much longer times have been recorded (over 12 hours). In the fasted state there are four phases of contraction; Phase I and II are relatively inactive stages that last 40-60 minutes. Phase III clears the stomach

contents by powerful peristaltic contractions and Phase IV is a short transitional period before Phase I begins again. The cycle repeats itself every 2 hours until a meal is ingested. When a meal is ingested the stomach walls relax to accept the food and peristalsis begins to break down food particles and move them to the pyloric sphincter. Thus, in the fed state, disintegrated tablets will empty into the small intestine with food yet sustained release single unit tablets can be retained in the stomach for long periods of time. Gastric emptying in the fasted state is related to the position in the stomach cycle at which the formulation is ingested.

Many factors influence gastric emptying including postural position, the presence of disease states, the presence of food and the type of food. Fatty foods can delay gastric emptying and delay the absorption of drugs. Drugs can affect the gastric emptying rate; metoclopramide has been shown to increase the absorption of paracetamol because it increased gastric emptying. Propantheline delays gastric emptying and therefore delays the absorption of paracetamol (Nimmo *et al.*, 1973).

Small intestinal transit has been found to be relatively constant, at around 3 hours. In contrast to the stomach the small intestine does not differentiate between the fed and fasted state. The propulsive motion of the small intestine determines the transit rate and hence the residence time of the drug or dosage form. As the small intestine is the major site for absorption, the transit time is most important when considering oral drug bioavailability. Small intestine residence time is particularly important for controlled release systems as their absorption continues along the length of the gastrointestinal tract. Enteric coated (EC) systems, for example ibuprofen and diclofenac EC tablets only release their drug when they reach an area in the small intestine of a particular pH. In this case disintegration of the formulation has to occur before dissolution and absorption can take place. This can extend the onset of physiological action. Drugs that dissolve slowly in intestinal fluid and drugs that are absorbed by intestinal carrier-mediated transport systems can be severely affected by small intestine residence time. The most reliable and rapid method of administering a drug is on an empty stomach with a glass of water.

1.2.1.5 Variation in pH of the gastrointestinal tract

Variation in gastrointestinal pH can be a significant barrier to drug absorption, particularly with drugs that have pH dependent solubility e.g. organic carboxylic acids. Gastric fluid is highly acidic, normally between pH 1 and 3.5 in healthy people in the fasted state. Following the ingestion of a meal, the gastric juice is buffered by the contents and the pH rises, depending on the contents of the meal to pH 3 to 7. The pH of the stomach returns to fasted state values within 2 to 3 hours. Thus only a dosage form ingested after a meal will encounter such elevated pH conditions, although the presence of food can affect drug dissolution and absorption.

Intestinal pH values are higher than gastric pH because of the alkaline secretions into the lumen of the small intestine. The pH along the small intestine can vary and a gradual rise in pH is observed along the length of the intestine from the duodenum to the ileum. Figure 1.4 summarises the literature recorded values for intestinal pH. The pH of the colon lowers to around 6.5 due to bacterial enzymes in the colon breaking down undigested carbohydrates to short-chain fatty acids.

Figure 1.4 pH in the small intestine in healthy humans in the fasted and fasted state (Gray and Dressman, 1996)

Location	Fasted State pH	Fed state pH
Mid-distal duodenum	4.9	5.2
	6.1	5.4
	6.2	5.1
Jejunum	4.4 - 6.5	5.2 – 6.0
	6.6	6.2
Ileum	6.5	6.8 – 7.8
	6.8 – 8.0	6.8 – 8.

The gastrointestinal pH may influence the absorption of drugs in a variety of ways. Chemical degradation due to pH-dependent hydrolysis can occur in the gastrointestinal tract; this can influence the chemical stability of the drug in the lumen. The result of this instability is incomplete bioavailability, as only a small proportion of drug reaches the systemic circulation. Gastric pH degrades penicillin G (benzylpenicillin) so that absorption from the gastrointestinal tract is low and therefore

the bioavailability is extremely poor. Penicillin V (phenoxymethylpenicillin) is not susceptible to gastric acid but has unpredictable absorption and variable plasma levels. It is therefore advised to take penicillin V on an empty stomach with a glass of water to optimise bioavailability (BNF No. 49, 2005).

If the drug is a weak electrolyte then the pH of the lumen will affect its solubility and dissolution in the gastrointestinal tract. Weak acids (pK_a 4-5) may become freely soluble in the latter part of the small intestine, so dissolution and absorption must occur within the small intestine transit time (3 hours or less).

1.3 Poorly soluble drugs

If a drug is poorly soluble in the pH of the stomach or small intestine then the dose may not be fully absorbed and therefore the pharmacological response may be unpredictable and blood plasma levels may vary. Poor water solubility is becoming an increasing problem and presents difficulties when designing a suitable formulation for oral drug delivery. This is a particular problem for certain classes of drugs such as the HIV protease inhibitors, the glycoprotein IIb/IIIa inhibitors, many anti-infectives and anticancer drugs (Aulton, 2002). Medicinal chemists are aware that the drug discovery process commonly produces poorly soluble drugs that cause difficulties formulating an appropriate dosage form that gives an appropriate pharmacological response and a good side effect profile. Strategies employed by medicinal chemists include: introducing ionisable groups, reducing melting points, using prodrugs and changing polymorphs to improve solubility. Pharmaceutical scientists improve dissolution of poorly soluble drugs by formulation approaches. Formulating reduced particle sizes, using solid dispersions or self-emulsifying drug delivery systems, stabilising amorphous forms of the drug substance, formulating with cyclodextrins or encapsulation are some techniques used. Poor solubility can be exploited when designing sustained release formulations. Retarding the aqueous solubility may result in a slow dissolution and continuous absorption of the drug into the systemic circulation.

1.4 The Biopharmaceutics Classification System (BCS)

Amidon *et al.* (1995) developed a biopharmaceutical classification scheme which classifies drugs in four classes according to their solubility across the gastrointestinal mucosa. The system was originally designed to identify which immediate release solid oral products did not require bioequivalence tests. It is a useful system to classify drugs and identify and predict which bioavailability issues may arise during the various stages of the development process.

The four classes are:

- Class I : high solubility/high permeability
- Class II : low solubility/high permeability
- Class III : high solubility/low permeability
- Class IV : low solubility/low permeability

A drug is considered to be highly soluble where the highest dose is soluble in 250 ml or less of aqueous media over the pH range 1-8. The volume is approximately the same as the minimum volume anticipated in the stomach when the dose is taken in the fasted state with a glass of water. If the intended dose is soluble in a volume greater than 250 ml over a pH range of 1 to 8 then the drug is considered to have a low solubility. The classification therefore takes into consideration the dose of the drug as well as its solubility. A highly permeable drug is considered when the extent of absorption in humans is expected to be greater than 90% of the administered dose.

1.4.1 Class I drugs

Class I drugs will dissolve rapidly when administered as immediate-release dosage forms, and are also rapidly transported across the gastrointestinal epithelia to the systemic circulation. Therefore, unless they form insoluble complexes or undergo presystemic clearance, it is expected that such drugs will be rapidly absorbed and show good bioavailability. Examples of class I drugs are the β -blockers metoprolol and propranolol (Aulton, 2002).

1.4.2 Class II drugs

The rate-limiting step to absorption is the dissolution rate of the dose in gastric fluids for class II compounds. For this class of drugs, therefore, it should be possible to generate a strong correlation between in vitro dissolution and in vivo absorption. Examples of class II drugs are the non-steroidal anti-inflammatory drug ketoprofen and the antiepileptic carbamazepine. The solubility of this class can often be improved by formulation approaches to enhance the dissolution rate and oral bioavailability.

1.4.3 Class III drugs

Class III drugs dissolve rapidly but are poorly permeable through the gastric lining. Examples are the H₂-antagonist ranitidine and the β -blocker atenolol. It is important that these drugs are released rapidly from a formulation in order to maximise the amount of time these drugs are present in the gastrointestinal tract because these drugs are slow to permeate the gastric epithelium.

1.4.4 Class IV drugs

Drugs with poor solubility and poor permeability are liable to have poor oral bioavailability, or the absorption may be so slow the oral route is not possible. Class IV drugs include the diuretics hydrochlorothiazide and furosemide. Approaches to overcome this problem include forming prodrugs of class IV compounds or finding alternative routes of delivery which can significantly improve their absorption into the systemic circulation.

1.5 Improving the solubility of drugs

Improving the solubility of poorly soluble drugs will improve dissolution and therefore the drug will act quicker. If fast onset of action is required then a number of parameters can be modified to improve the bioavailability of the drug. Factors that affect the dissolution of a drug are the particle size, the wettability, the solubility and the form of the drug (whether a salt form or a free form, crystalline or amorphous).

A decrease in particle size will cause an increase in the total surface area of drug in contact with the gastrointestinal fluids. According to the Noyes-Whitney equation this will cause an increase in dissolution rate (equation 1.1).

$$\frac{dC}{dt} = \frac{DA(C_s - C)}{h} \quad \text{equation 1.1}$$

where dC/dt is the rate of dissolution, D is the diffusion coefficient of the drug in solution, A is the effective surface area, h is the thickness of the diffusion layer, C_s is the saturated solubility of the drug in the diffusion layer and C is the concentration of drug in the gastrointestinal fluids.

Provided each particle is wetted by the gastrointestinal fluids, the effective surface area exhibited by the drug will be proportional to the particle size. Hence the smaller the particle size, the larger the effective surface area of drug and therefore the dissolution rate is higher. Particle size reduction will only improve bioavailability if the drug has dissolution rate limited absorption.

Particle size reduction has been shown to improve the rate and extent of oral absorption in drugs such as digoxin, nitrofurantoin, danazol, tolbutamide, aspirin, naproxen and ibuprofen (Aulton, 2002). The oral bioavailability of griseofulvin was approximately doubled by the reduction in particle size from about 10 μm to 2.7 μm (Aulton, 2002). Particle size reduction techniques include; micronisation or fluid energy milling, ball milling, spray-drying and using supercritical fluids. For some drugs, particularly those that are hydrophobic in nature, micronisation and other particle size-reduction techniques can result in aggregation of the material which will not improve the effective surface area exposed to the luminal fluids and so bioavailability is not improved. Aspirin and phenobarbitone are prone to aggregation during particle size reduction; one approach that may overcome this problem is milling the material with a hydrophilic carrier or wetting agent.

The effective surface area of drugs can also be increased by co-formulating a polymer with a poorly soluble drug as a fine particle size. This is termed a solid dispersion and the drug can be formulated as an amorphous solid to improve the overall solubility. The dispersed particles and the fine particle size significantly improve the effective surface area and dissolution can therefore be improved; this has been described by Leuner and Dressman (2000). Recently Urbanetz and Lippold

(2005) have improved the dissolution of nimodipine by the use of solid dispersions or solid solutions.

1.6 The importance of salts

When the first 'drugs' or alkaloids were isolated from plant materials they were purified as well-crystallising salts. In contrast to the free bases, the salts were found to be water soluble and also more stable. Such properties rendered the salts ideal for use as therapeutic agents, these included: morphine hydrochloride, atropine sulphate, codeine phosphate, quinine sulphate, pilocarpine nitrate *etc.* Endogenous biological agents commonly contain nitrogen *e.g.* neurotransmitters and can easily form salts. Salt formation is a natural solution to make an organic molecule more water soluble.

Modification of the solid state and solution properties are possible by salt formation. The main purpose of formulating a salt is that solubility can be improved due to the selection of an appropriate counterion. Typical pharmaceutical salt counter-ions are shown in figures 1.5 and 1.6. Typically inorganic counterions are used to form salts with acidic drugs, for example sodium, potassium and calcium *etc* which make up 90% of all the counterions used. Diethanolamine is the only organic counterion in the group. Around 50% of basic drugs form salts with inorganic counterions and the remaining 50% with organic counterions. The most common counterions are the hydrochloride ion with 43% and the sodium ion with 62% usage (Stahl and Wermuth, 2002). Organic counterions are increasingly being used as salt formers as there is a wide variety of molecules available. Usage of organic counterions has risen to up to 50% with basic drugs and organic counterions are probably under-used with acidic drugs. The possibility of using more organic counterions, particularly with acidic drugs means that drug properties could be further modified and improved in future.

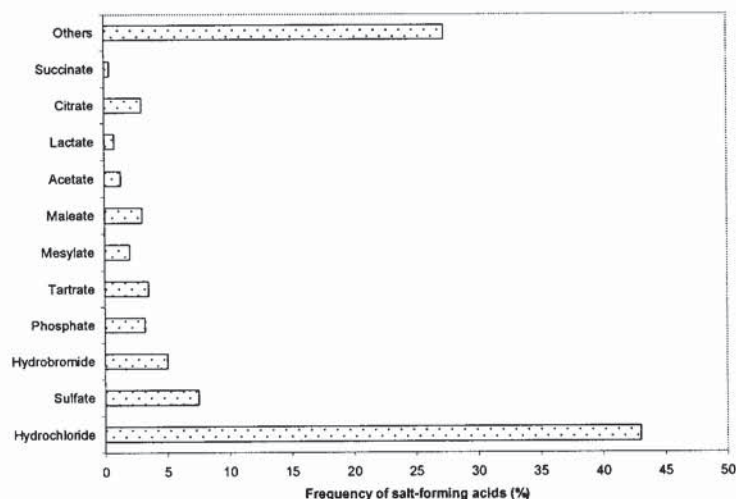


Figure 1.5 Distribution of the most commonly occurring salt forms for acids (anions) (Stahl and Wermuth, 2002)

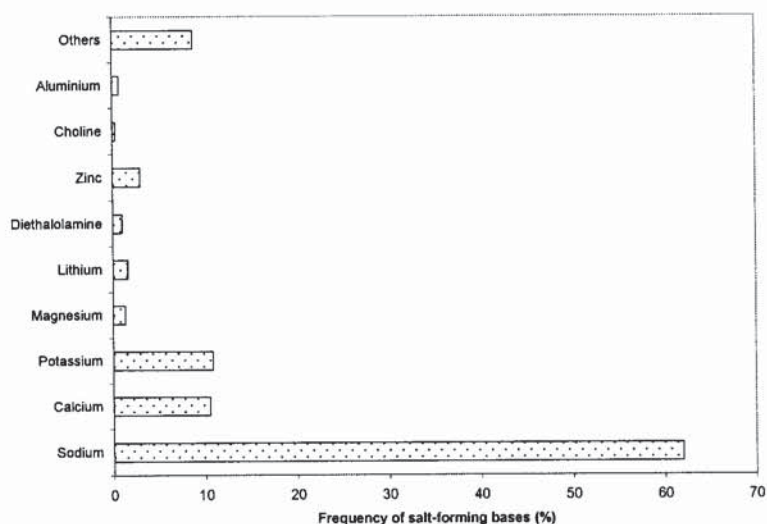


Figure 1.6 Distribution of the most commonly occurring salts for bases (cations) (Stahl and Wermuth, 2002)

Salts are usually formed with weak acids and bases because using strong acids and bases can lead to instability. Salts may be less soluble than those formed with strong acids and bases but they are less hygroscopic and form less acidic or basic solutions in water. A very alkaline solution will attack glass packaging and hydrochloride salts react with propellants used in aerosol cans and will corrode the canister.

The intrinsic pH of a drug can be altered by the formation of a salt; the pH of a weak base can be significantly reduced by the addition of a counterion or conversely the pH of a weak acid can be increased. As a consequence of the change in pH the solubility rises exponentially (see section 1.11.1). This effect has important implications in the gastrointestinal tract; a weak acid with a low intrinsic solubility will have minimal dissolution in the stomach but will become more soluble in the small intestine. Unfortunately as dissolution increases so absorption falls because the drug is less likely to be absorbed in the ionised form. The pH partition theory states that lipid soluble drugs will diffuse across the epithelia by passive diffusion and therefore the unionised form will be absorbed. In theory, a weak acid will be absorbed from the stomach; however, in practice the massive increase in surface area provided by the small intestine means that absorption occurs in this region. The longer residence time in the small intestine and a lower microclimate pH at the surface of the mucosa that is lower than that of luminal pH also aids the absorption of weak acids. Diffusion of drugs across the unstirred layer of the surface mucosa is dependent on molecular size. Formulating a salt provides some control of the pH of the diffusion layer which is the saturated solution immediately adjacent to the dissolving surface also known as the pH microenvironment.

The sodium and potassium salts of a weak acid dissolve much more rapidly than the parent acids. This is why diclofenac, for example, is formulated as the sodium salt as it has higher solubility than the free acid, and an immediate release preparation contains the potassium salt (Voltarol Rapid®) which is even more soluble. These salts would be expected to have limited dissolution in the stomach but the dissolution rate is governed by the pH of the diffusion layer and not the pH of the bulk solution. The buffering capacity of the salt improves the solubility in these conditions. It is thought that when the dissolved drug diffuses out of the diffusion layer into the bulk solution, precipitation is likely to occur in the lower gastric pH environment. Thus the free acid form of the drug is present in the form of very fine, non-ionised wetted particles which exhibit a very large effective surface area in contact with the gastric fluids. This large surface area facilitates re-dissolution of the drug if more gastric fluid becomes available or the stomach contents are emptied into the small intestine. In the intestine the salt does not depress the pH and in the diffusion layer, pH is raised promoting

dissolution. By controlling the diffusion layer pH, the dissolution rate can be increased substantially, independently of its position in the gastrointestinal tract. The NSAID naproxen was first marketed as the free acid for the treatment of chronic inflammatory conditions. However the sodium salt has replaced its use as it has a greater dissolution rate, is absorbed faster and is more effective for mild to moderate pain (Sevelius *et al.*, 1980).

Occasionally salts are prepared to decrease the solubility, particularly for suspension formulations where low solubility is necessary to prevent 'Ostwald ripening', or to prepare an extended release product. Salt formation may also confer a higher melting point than the free acid or base and may thus improve stability. Different salts of a drug rarely change the pharmacological action or response significantly (Stahl and Wermuth, 2002). The new salt form will have very different physico-chemical characteristics, any change in melting point may affect stability and the process may produce polymorphic forms which can be difficult to isolate. Changes in solubility and dissolution will affect the bioavailability of the drug which will consequently alter the pharmacokinetic profile. Toxicity of any counterions will be scrutinised thoroughly by regulatory authorities and it is important to consider only inert or non-toxic counterions. Each potential salt form will behave differently to each other and the parent drug and careful selection is therefore required when selecting an appropriate counterion for use in formulations.

One of the negative aspects of salt formation is that by using a large counterion with a high molecular weight with a drug with a low activity, may mean that a large dose is required. Thus 20-50% of the overall weight of drug substance can be due to an inactive counterion. This may lead to problems when tableting; if the dose is high, excipients are necessary to improve flow and compressibility. The final powder mix or granule mix may require 40-70% of excipients for successful encapsulation or tableting, which would result in large tablets or a dose of multiple tablets. This would reduce compliance and increase costs.

Other problems that occur commonly with salt forms are the tendency for hydrate formation or the production of polymorphs. Hydrates may form over time, while in storage if the formulation contains a water-bound excipient such as lactose

monohydrate. The stability of the active compound may be impaired. In some cases, salts prepared from strong acids or bases are freely soluble in water but are very hygroscopic solids. This leads to instability in the formulation if the drug is in a tablet or capsule, because the drug will slowly dissolve any absorbed moisture.

1.7 The salt selection process

Important physicochemical information is gathered on a new chemical entity once discovery chemistry has identified an active compound. The dissociation constant (pK_a) of each ionisable group in the molecule is one of the first pieces of information gathered; it is usually performed by potentiometric titration on an automated instrument. Log P, the octanol-water coefficient of the molecule is another important parameter measured using an octanol-loaded HPLC column.

Once the pK_a of each ionisable group is known a number of counter-ions can be selected. For a stable salt to form there must be a minimum difference of 3 pK_a units between the salt former and counterion (Stahl and Wermuth, 2002). This is particularly important when the salt former is a weak acid or base where disproportionation back to the component parts often occurs in solution, and precipitation of the free acid or base occurs.

Once a number of potential counterions have been identified then further physicochemical tests are required to assess crystallinity or amorphous content and to look at possible polymorphism. Melting points are determined by differential scanning calorimetry (DSC) and thermal gravimetric analysis (TGA) can give information on the existence of solvates and hydrates. Crystallinity is determined by a powder X-ray study and hygroscopicity can be evaluated by dynamic vapour sorption (DVS). These tests can help with the identification of future problems that may hinder the development of a dosage form. The target aqueous solubility should be over 1 mg/ml with a saturated solution pH of around that found in the gastrointestinal tract for dissolution and absorption to be maximised. If these parameters are unfavourable then salt formation can be used to maximise the bioavailability.

Occasionally the properties of the free acid/base are much better than any of the salts. This occurs frequently where the candidate base has a low pK_a value, or a high pK_a value if an acid and the resulting salts are less stable than required. Salts can also exhibit hygroscopicity particularly if they are very soluble or exhibit complex polymorphism/pseudopolymorphism (hydration or solvation). These complex interactions can lead to the free acid or base being considered for the formulation.

When the initial investigative experiments are concluded then it is possible to assess the new chemical entity in terms of its crystallinity, stability, solubility in water *etc.* These parameters will determine whether a salt form is required to modify the drug's properties to overcome any potential formulation or bioavailability problems.

1.8 Salt selection strategies

The choice of counter-ion depends on several factors. The salt should be crystalline as ease of crystallinity allows for purification and removal of unwanted impurities. Lack of crystallinity can lead to unpredictable amorphous/crystalline content and may cause problems in the formulation. The prospect of uncontrolled crystallisation either in a formulation or upon storage is not acceptable to the regulatory authorities.

Commonly basic drugs with low pK_a values require strong acid groups e.g. mineral acids or sulfonic acids to form a stable salt (hydrochloride, sulphate, citrate). Organic acids would not be expected to form a stable salt e.g. tartrate, mesylate. In this scenario it is likely that any salts formed may be hygroscopic or may show polymorphism and the free acid may precipitate out once in solution. Therefore the free acid may be the preferred form to be used in the formulation. Each salt is selected because of historical use and previous experience with toxicity of the counterions. There is a small range of potential counterions and there are no new and emerging counterions because of safety concerns. Screening of a selection of salts allows for the development of the salt with the most desirable properties. Presently salt selection is an empirical process and is applied in the same way to each potential salt former. A more useful scenario would be to be able to examine the drug as a crystal structure together with its physicochemical information and predict a potential counterion which would confer desirable properties.

1.9 Tableting drugs

The compression properties of most drug powders are extremely poor and require the addition of compression aids. When the dose is less than 50 mg, tablets can usually be prepared by direct compression which is an easy, cost effective method of tablet formation. At higher doses the preferred method would be wet massing which introduces potential interactions of water and temperature with the active pharmaceutical ingredient or excipients.

Tabletted material should be plastic, *i.e* capable of permanent deformation, it should also exhibit a degree of brittleness (fragmentation). Thus if the dose is high and it behaves plastically, the chosen excipients should fragment *e.g.* lactose, calcium phosphate. If the drug is brittle or elastic, the excipients should be plastic, *e.g.* microcrystalline cellulose, or plastic binders should be used in wet massing. If the dose is between 10 to 20% of the overall mass, it will influence the mechanical properties of the formulation therefore careful choice of excipients is required.

When materials are ductile they deform by changing shape (plastic flow). As there is no fracture, no new surfaces are generated during compression that could be available for additional bonding so an increased lubricant mixing time does not increase tensile strength. Plastic materials bond after viscoelastic deformation, and because this is time dependent, increasing the dwell time will increase bonding strength. If a material is fragmenting during compression then dwell time and lubricant mixing time will not affect tensile strength. Fragmenting powders compress to form brittle tablets that are hard but have a high propensity for fracture. Some materials are elastic *e.g.* paracetamol, and there is very little permanent change either by plastic flow or fragmentation caused by compression: the material rebounds (recovers elastically) when the compression load is released. If bonding is weak the compact will self-destruct and the top will detach (capping), or the whole cylinder cracks into horizontal layers (lamination). Elastic material can also maintain integrity but be very weak after compression; these properties can be improved by addition of a plastic excipient to induce plasticity. See section 7.1.2.

1.10 Improving the mechanical properties of drugs

Because most drug substances have flow properties that are non-ideal, it is necessary to formulate them with suitable excipients for tableting. If the dose is large then there is less capacity for excipients to improve the tableting properties. It may be possible to improve tableting properties with addition of a counterion (salt formation) or to alter the structure of the drug to improve the compression properties. This would benefit the formulation reducing the need for excipients hence producing smaller tablets with better patient compliance. Also better mechanical properties would benefit the tableting process as more economical dry tablet compression (direct tableting, compacting replacing wet granulation) will become the technology of choice.

It is well recognised that salt formation will affect the mechanical properties of the drug substance; the additional number of ionic bonds may increase the brittleness, for example. There have been few studies that examine the relationship between the chemical lattice structures and mechanical properties or the effect of the counterion on the mechanical properties of the drug. Sulfonic acid salts resulted in materials deforming predominantly by plastic deformation (yield pressure), whereas mineral acids salts underwent brittle fracture. Sun and Grant (1999) examined the salt forms of L-lysine; the tensile strength increased linearly with the compaction pressure. At high compaction pressures the tensile strength is determined by the interparticulate bonding strength and at low compaction pressures, yield strength predominates. They also found that compact tensile strength increases linearly with increasing melting temperature of the salts. Sun and Grant (2004) found that they could improve the mechanical properties of p-hydroxybenzoic acid with water of crystallisation; the mechanical properties were successfully related to the crystal structure.

1.11 Selecting model drugs

Four similar molecules were selected as possible salt formers in this project. They were chosen because they are freely available as the raw drug and did not require extraction from a commercial formulation. Affordability was also a consideration and the most cost-effective drugs were picked.

An estimated half of all the drug molecules used in medicinal therapy are administered as salts. 74% of these drugs have basic functions, and most research has been directed at this group of drugs (Aulton, 2002). Therefore the remaining 26% of salts contain an acidic drug e.g. many with carboxylic acid functional groups. Less is known about this group of compounds so it becomes an attractive area for research. Although there are many different acidic functions, the type of group determines the salt forming ability of the active compound e.g. sulphates are not ideal salt formers due to incomplete dissociation in solution but carboxylic acids can easily form salts. Therefore carboxylic acids were selected as salt formers in this project.

1.11.1 Properties of carboxylic acids

Seventy-five percent of all drugs are weak bases; 20% are weak acids and only 5% are non-ionic, amphoteric or alcohols. Carboxylic acids are weak acids, they make a large contribution to the 20% of weak acids as drugs; they commonly have a dissociation constant, pK_a of between 4 and 5 and they can be poorly soluble in water. The solubility of a weak acid is described by equations 1.2, 1.3 and 1.4:

$$S = [HA] + [A^-] \quad \text{equation 1.2}$$

$$S = S_o \left(1 + \frac{K_a}{[H^+]} \right) \quad \text{equation 1.3}$$

where S is the total solubility at any given pH, S_o is the intrinsic solubility of the free acid, $[HA]$ and $[A^-]$ represent concentrations of the undissociated and dissociated forms, respectively, in solution and K_a is the acid dissociation constant, defined as:

$$K_a = \frac{[H^+].[A^-]}{[HA]} \quad \text{equation 1.4}$$

Weak acids such as carboxylic acids usually have poor water solubility. This is because the acid dissociates in solution releasing hydrogen ions to make the solution

acidic. As the solution becomes increasingly acidic the dissolution and solubility is inhibited because there is pH dependent solubility, due to equation 1.2. If the pH of the solution is raised then dissolution can be improved (see also section 5).

Carboxylic acids are ideal salt formers; the functional group exists as a carbon double bonded to an oxygen and an oxygen atom attached to a hydrogen atom, figure 1.7.

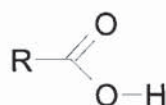


Figure 1.7 Structure of a carboxylic acid

Oxygen is a very electronegative atom as it has a high charge density and can accept hydrogen atoms from the environment to form hydrogen bonds. In a carboxylic acid functional group, there is much electronegativity caused by the two oxygen atoms being in close proximity to each other. The hydroxyl group is eclipsed with the carbonyl group to get an overlap of π orbital with orbital of the lone pair of electrons on oxygen. The bond angles are close to 120° . This causes the hydrogen to be easily lost i.e. the molecule becomes ionised when in solution and this results in a charged functional group. When the molecule becomes ionised it is said to dissociate in solution.

Carboxylic acids can form salts due to the attraction of a positive ion to the functional group. The positive ion can either be inorganic (Na^+ , K^+) or organic (organic molecules containing nitrogen can form salts). Nitrogen is an electron-donating atom and can easily share its lone pair to form a positive ion, which is consequently attracted to the negative charge of the carboxylic acid function. The degree of dissociation of the two ions affects the formation of the salt; there must be ample dissociation of each ion in solution for a stable salt to be formed.

1.11.3 Carboxylic acids as drugs

Examples of carboxylic acids as drugs are: NSAIDs, fibrates (gemfibrozil, bezafibrate), acetylcysteine, acetyltryptophan, acetyltryrosine, alprostadil, aminocaproic acid, β -lactam antibiotics, betamethasone, cetirazine, chlorambucil.

Nonsteroidal anti-inflammatory drugs (NSAIDs) are a group of organic acids that have analgesic, anti-inflammatory, and antipyretic properties. NSAIDs are inhibitors of the enzyme cyclo-oxygenase, which results in the direct inhibition of the biosynthesis of prostaglandins and thromboxanes from arachadonic acid. There are three forms of cyclo-oxygenase known, COX-1 which is the constitutive form of the enzyme, and COX-2, which is the form induced by the presence of injury and inflammation. Inhibition of COX-2 is therefore considered to be responsible for some of the analgesic, antipyretic and anti-inflammatory properties of NSAIDs. Inhibition of COX-1 is thought to produce some of their toxic effects, including damage to the intestinal tract and nephrotoxicity. Selective COX-2 inhibitors may be used in preference to non-selective NSAIDs for patients at high risk of developing serious gastro-intestinal side effects. Selective COX-2 inhibitors include: celecoxib, etodolac, meloxicam and rofecoxib. Propionic acid derivatives include ibuprofen, naproxen, fenbufen, flurbiprofen, ketoprofen and tiaprofenic acid. Other drugs with similar properties include: azapropazone, diclofenac, diflunisal, indomethacin, mefenamic acid, piroxicam, sundilac, tenoxicam, and ketorolac. COX-3 is also an inflammatory mediator and could represent a primary central mechanism by which paracetamol decreases pain and possibly fever (Chandrasekharan et al. 2002).

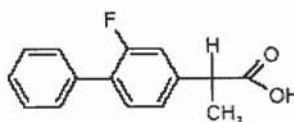
This group of active medicinal materials are Class II compounds, as described by the BCS, as having dissolution rate limited absorption. Absorption of these compounds is not usually a problem as the molecules are lipophilic, containing benzene rings or hydrocarbon chains with carboxylic functions attached. The rate limiting step to absorption for BCS class 2 compounds is the dissolution process. In the case of carboxylic acids, solubility is poor in the stomach as the pH is low (below 4) and the molecule is predominantly unionised. Dissolution occurs in the small intestine as the pH rises along the gastro-intestinal tract; under these conditions dissolution is promoted by the changing pH. Absorption occurs when the solid has dissolved in the fluids in the gastro-intestinal tract; the large surface area of the intestines promotes absorption. The limiting step is the time taken for complete dissolution which is

controlled by gastric emptying and gut transit time. It can take up to 30-45 minutes to achieve maximum blood levels and achieve a clinical effect e.g. ibuprofen is a carboxylic acid, it is also an analgesic, it is therefore not ideal to wait 30-45 minutes for pain relief. To accelerate the rate limiting step *i.e.* the time taken for dissolution, would improve the clinical effect because absorption would be quicker and analgesia would be more immediate.

The drugs selected for use are to be used as model drugs to represent Class II compounds and practically *insoluble* drugs. All of the drugs selected are administered as the free acid; although they are classified as practically *insoluble* in water, they are readily absorbed from the gastrointestinal tract. Peak plasma levels of these drugs reach a maximum between 1 to 2 hours of administration, therefore, the onset of analgesia or clinical effect will be delayed by their poor water solubility. These drugs are ideal candidates for salt formation as if solubility could be improved then analgesia will be quicker. This would be ideal for treating acute pain where instant pain relief would be preferred e.g. migraine treatment or dental pain. Ibuprofen lysine (Nurofen advance®) and diclofenac potassium (Voltarol Rapid®) have been prepared and are licensed for the treatment of acute pain.

1.11.4 Flurbiprofen

Flurbiprofen is a white or almost white crystalline powder. It is practically *insoluble* in water (see table 1.1 for definition), freely soluble in alcohol, in acetone, in chloroform and in ether; soluble in acetonitrile. Flurbiprofen sodium is a white to creamy-white, crystalline powder which is *sparingly* soluble in water (Martindale, 1999). The structure of flurbiprofen is shown below (figure 1.8), its chemical name is 2-(2-Fluorobiphenyl-4-yl)propanoic acid and its molecular weight is 244.3.



Flurbiprofen

Figure 1.8 The chemical structure of flurbiprofen

Flurbiprofen is readily absorbed from the gastrointestinal tract with peak plasma levels occurring about 1 to 2 hours after ingestion. It is 99% bound to plasma proteins and has a plasma half-life of about 3 to 6 hours. It is metabolised mainly by hydroxylation and conjugation in the liver and excreted in urine. Flurbiprofen is an NSAID and is used to treat acute and chronic inflammatory conditions including musculoskeletal and joint disorders. It is used for mild to moderate pain including sprains and strains as well as migraine and dysmenorrhoea.

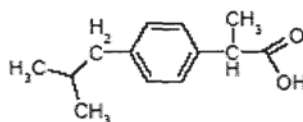
Flurbiprofen is given orally in divided doses of between 150 mg and 200 mg per day, increased to 300 mg in acute or severe conditions.

Table 1.1 Solubility terms and solubility ranges as used by Martindale (1999)

Solubility	
Very soluble	1 in less than 1
Freely soluble	1 in 1 to 1 in 10
Soluble	1 in 10 to 1 in 30
Sparingly soluble	1 in 30 to 1 in 100
Slightly soluble	1 in 100 to 1 in 1000
Very slightly soluble	1 in 1000 to 1 in 10 000
Practically insoluble	1 in more than 10 000

1.11.5 Ibuprofen

Ibuprofen is also known as 2-(4-iso-butylphenyl)propanoic acid, it is a carboxylic acid and has a molecular mass of 206.3. The structure of ibuprofen is detailed in figure 1.9. It is a white crystalline powder that is practically *insoluble* in water, very soluble in alcohol and in chloroform (Martindale, 1999).



Ibuprofen

Figure 1.9 The chemical structure of ibuprofen

Ibuprofen is absorbed from the gastro-intestinal tract and peak plasma levels occur 1 to 2 hours after administration. It is 90 to 99% bound to plasma proteins and has a plasma half life of about 2 hours. It is rapidly excreted from the urine mainly as metabolites and their conjugates. Ibuprofen is a racemic mixture containing the inactive (R)-enantiomer, some of which is converted to the active (S)-enantiomer by metabolic processes.

The dose by mouth for painful conditions in adults is 1.2 to 1.8 g daily in divided doses; the maximum daily dose is recommended to be 2.4 g. Ibuprofen is usually given as the free base but the lysine salt is licensed for the treatment of migraine.

1.11.6 Etodolac

Etodolac is a non-steroidal anti-inflammatory drug; it is classified as a selective COX-2 inhibitor and so is expected to have less gastrointestinal side-effects than conventional NSAID's. It is a white or almost white crystalline powder which is practically *insoluble* in water and freely soluble in alcohol (Martindale, 1999). Its chemical name is 1,8-Diethyl-1,3,4,9-tetrahydropyranol[3,4-b]indol-1-ylacetic acid and it has a molecular mass of 287.4. The structure of etodolac is detailed in figure 1.10.

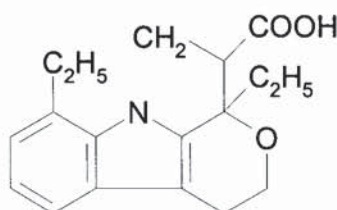


Figure 1.10 The chemical structure of etodolac

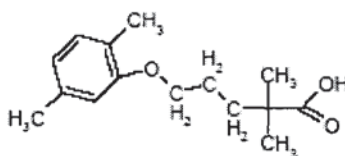
Etodolac is a chiral compound given as a racemic solution containing the active (S)-enantiomer and the inactive (R)-enantiomer. Peak plasma levels are usually obtained within 2 hours of administration by mouth; both enantiomers are tightly bound to plasma protein. The plasma half life of total etodolac has been reported to be about 7

hours; excretion is predominantly in the urine, it is hydroxylated in the liver and also excreted as glucuronide conjugates.

Etodolac is an anti-inflammatory used for the treatment of mild to moderate pain; it is used for rheumatoid arthritis and osteoarthritis and for the treatment of acute pain. The recommended dose is 600 mg per day and it is available as a modified release tablet with a once daily dosage regime (Lodine SR®).

1.11.7 Gemfibrozil

Gemfibrozil is a lipid regulating drug; it is a carboxylic acid known as 2,2-Dimethyl-5-(2,5-xylyloxy)valeric acid with a molecular mass of 250.3 (figure 1.11). It is a white waxy crystalline powder with a melting point of 58-61 °C (Martindale, 1999). It is practically *insoluble* in water, soluble in alcohol and chloroform.



Gemfibrozil

Figure 1.11 The chemical structure of gemfibrozil

Gemfibrozil is readily absorbed from the gastrointestinal tract, peak concentrations in plasma occur within 1 to 2 hours, the half life is about 1.5 hours. Plasma protein binding of gemfibrozil is about 98%; about 70% of a dose is excreted in the urine mainly as glucuronide conjugates of gemfibrozil and its metabolites. It is given via the oral route in 2 divided doses given 30 minutes before morning and evening meals. The dosage may vary between 0.9 and 1.5 g daily.

Gemfibrozil is a fibric acid derivative and is a lipid regulating drug. It is used in the treatment of hyperlipoproteinaemias. Gemfibrozil reduces serum triglycerides by reducing the concentration of very-low-density lipoproteins (VLDL). It reduces elevated plasma concentrations of cholesterol to a lesser extent, but the effect is variable. Gemfibrozil displaces other protein bound drugs including warfarin,

tolbutamide, phenytoin, frusemide. Fibrates may enhance the effects of oral anticoagulants and the dose may have to be reduced. There is an increased risk of myopathy if fibrates are given concurrently with statins, this is the major reason why the use of fibrates has reduced dramatically over the last 5 years. Also the introduction of statins; has eclipsed the use of fibrates as they have a better side effect profile and they reduce total serum triglyceride concentration (Martindale, 1999).

1.12 Selecting counterions

Conventional counterions including sodium, potassium and calcium have been widely used to form salts with NSAIDs to improve the solubility and dissolution (Anderson and Conradi, 1985; O'Connor and Corrigan, 2001a). Although amine counterions account for less than 5% of salt forms, the potential number of counterions in this group is huge. The chemical construction of amines can be altered at will and specific counterions can be synthesised easily to represent particular molecules.

Three groups of counterion were identified for investigation:

- The effect of chain length on salt formation including solubility and physico-chemical characteristics
- The effect of an unsaturated ring versus a saturated ring on solubility
- The effect of increasing hydrophilicity on solubility

1.12.1 Homologous alkyl series

The effect of chain length on salt formation and solubility was investigated using an amine chain. Butylamine (C4), pentylamine (C5), hexylamine (C6), octylamine (C8) and decylamine (C10) are commercially available (figure 1.12) and were used to make a homologous series. Butylamine, pentylamine *etc.* are available as liquids, they are insoluble in water but freely soluble in alcohols and acetonitrile. Below C3 the amines were available as gases and were therefore unsuitable for use. The pK_a of the amines are approximately 10.3 (SPARC online calculator, <http://ibmlc2.chem.uga.edu/sparc/index.cfm>) and salt formation will therefore not be a foreseeable problem with the drugs selected.

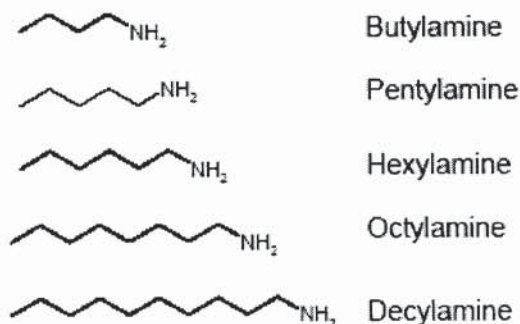


Figure 1.12 The chemical structure of the homologous series of linear chain amines

1.12.2 Cyclic compounds

Benzylamine has an unsaturated benzene ring attached to an amine group, it has a pK_a of 9.4 (figure 1.10). Cyclohexylamine (figure 1.13) has an amine group directly attached to a saturated ring (C6), it is therefore a stronger base than benzylamine and has a pK_a of 10.5. They are liquids at room temperature and freely soluble in alcohols but insoluble in water.

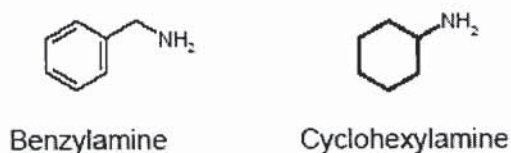


Figure 1.13 The chemical structures of benzylamine and cyclohexylamine

1.12.3 Hydrophilic series (hydroxyl substituted tert-butylamine)

A hydrophilic series was devised from tert-butylamine as the initial molecule. Tert-butylamine was considered suitable as each methyl group could easily be substituted with hydroxyl functional groups. Tert, AMP1, AMP2 and tris were all commercially available; the chemical structure of each counterion is detailed in figure 1.14. Tert-butylamine is a liquid at room temperature, it is freely soluble in alcohols and

acetonitrile and it has a pK_a of 10.5. 2-amino-2-methylpropan-1-ol is also a liquid at room temperature; it is freely soluble in alcohol and acetonitrile and has a pK_a of 9.2.

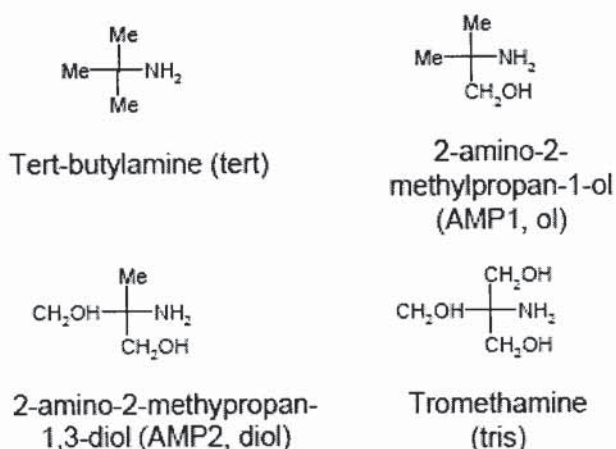


Figure 1.14 The chemical structures of hydroxyl substituted tert, AMP1, AMP2 and tris

2-amino-2-methylpropan-1,3-diol has a pK_a of 7.9, it is a solid at room temperature. Tris has a pK_a of 6.4, it is a solid at room temperature and is soluble in methanol (Data sheet, Sigma-Aldrich).

1.13 Toxicology considerations

The safety considerations of potential counterions are closely related to their abundance in the body under normal physiological conditions. As long as their intake is marginal compared to their intake by food and beverages then there is no safety concern (Stahl and Wermuth, 2002). Sodium, potassium, calcium and magnesium are all regularly consumed and have no safety concerns. Denser metals e.g. lithium are less suitable as they exert a physiological response, lithium is used in the treatment of manic depressive disorders. The essential amino acids have no safety concern as do other bases that are rapidly metabolised and eliminated before they can exert toxic effects.

Tromethamine (tris) has been used as a counterion to form salts with carboprost, ketorolac, lodoxamide, desglugastrin, fosfomycin (Stahl and Wermuth, 2002). In July 1981 the tris salt of prostaglandin $F_{2\alpha}$ was approved by the FDA for abortion of

feedlot cattle. The tris salt of ketorolac has been approved by the FDA in 1991 for oral administration (Approved Drug Products, 1992). Perindopril tert-butylamine has been approved by the FDA and MCA for the treatment of hypertension; it is usually administered as a 2 or 4 mg dose once daily. The daily dose of the drug is small therefore the amount of amine entering the systemic blood circulation will also be small, minimising any toxicity.

1.14 Experimental aims and objectives

The main aim was to form amine salts for a series of carboxylic acid drugs and to explore the relationships between their physicochemical and mechanical properties.

The experimental objectives were:

- To form amine salts with a selection of carboxylic acid drugs.
- Investigate the physicochemical characteristics of the salts using a range of analytical techniques
- Improve the solubility and dissolution of the carboxylic acid drugs.
- Form rules using the physicochemical characteristics of the salts to identify the counterions that most enhance solubility and dissolution.
- Investigate how different counterions affect the solubility by looking at the crystal structure
- Characterise the mechanical properties of drug and salt powder by compressing the powders and testing the compact
- Identify a suitable mechanical test and instrument to investigate the mechanical properties of drug and salt compacts
- Investigate the effect of the counterion on mechanical properties
- Form rules to identify which counterions consistently improve compression properties
- Relate solubility and mechanical properties to salt selection

The first four objectives are addressed in Chapters 2 – 5. The fifth objective is dealt with in Chapter 6, and the next four objectives in Chapter 7. The integration of concepts and results envisaged in the final objective is presented in Chapter 8.

Chapter 2 HPLC methods and pH measurement

2.1 HPLC

There was no internal standard used in the following experiments as the analysis of samples was straightforward because no mixtures were used. In each case the drug was dissolved in a solvent that did not absorb UV radiation and the counterions did not interfere with the analysis of the drug at the selected wavelength of analysis. It was considered appropriate to produce a calibration curve of the concentration range of interest before the experiment. The injection volume was accurately delivered reproducibly by the Aligent auto sampler therefore an internal standard was not required.

2.1.1 General Method for HPLC analysis

2.1.1.1 Materials

Purity was assigned as 100% for the parent compound as the same batch of drug was used for sample, salt and standard preparations throughout. Acetonitrile and orthophosphoric acid were supplied from Aldrich (Poole, UK). Double-distilled water was produced in-house using a Fison's FiStream still. All materials were of analytical, pharmaceutical or HPLC grade as appropriate.

2.1.1.2 Equipment

The HPLC system comprised a Hewlett Packard Aligent 1100 system with G1312A Binary Pump, G1313A ALS Auto-injector, G1316A COLCOM column section and a G1314A VWD variable wavelength detector. The HPLC was controlled by Chemstation software which ran on Windows 2000.

2.1.1.3 Method

All calibration and sample dilutions were made with solvent mixture (65:35 acetonitrile:water); each drug was freely soluble in this mix. Linear regression analysis was performed on a plot of standard concentration against peak area and

the resultant equation of the line was used to calculate the sample concentration from the response.

2.1.2 Gemfibrozil assay by HPLC

2.1.2.1. Materials

Gemfibrozil was supplied by DiPharma (Italy) and was of USP-BP grade.

2.1.2.2 Methods

Working standards of 0.01 to 0.75 mg/ml were prepared by serial dilution from a stock solution of 1 mg/ml; the specific concentration range was dependent on the experiment.

The chromatographic conditions were:

Injection volume	:	20 or 1 μ l
Mobile phase	:	Acetonitrile:water 65:35 (phosphoric acid 0.005% v/v)
Wavelength	:	276 nm
Flow rate	:	1 ml/min
Run time	:	7 minutes
Column	:	Thermo ODS-2 Hypersil 150 mm x 4.6 mm 5 μ m

2.1.2 Example Data

A typical chromatogram of gemfibrozil is presented in figure 2.1:

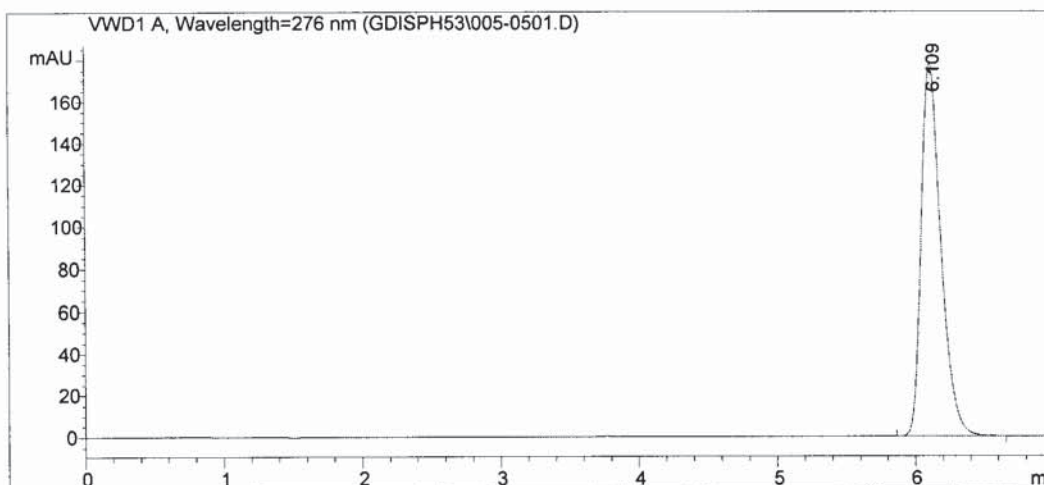


Figure 2.1 Typical HPLC chromatogram gemfibrozil (concentration 0.5 mg/ml at 276 nm).

Typical calibration data and UV scans for gemfibrozil are in appendix A.

2.1.3 Flurbiprofen assay by HPLC

2.1.3.1 Materials

Flurbiprofen was supplied by Erregierre (Italy) and was of USP grade.

2.1.3.2 Method

Working standards were prepared by serial dilution of a stock solution to produce standards in the range of 0.001, 0.01 0.1, 0.5, 1, 2, 3 mg/ml in 65:35 acetonitrile:water, the exact concentration range was dependent on the experiment.

The chromatographic conditions were:

Injection volume	:	20 µl, 1 µl
Mobile phase	:	Acetonitrile:water 65:35 (phosphoric acid 0.005%)
Wavelength	:	250 nm
Flow rate	:	1 ml/min
Runtime	:	6 minutes
Column	:	Thermo ODS-2 Hypersil 150 mm x 4.6 mm 5 µm

2.1.3.3 Example data

A typical chromatogram of flurbiprofen is presented in figure 2.2:

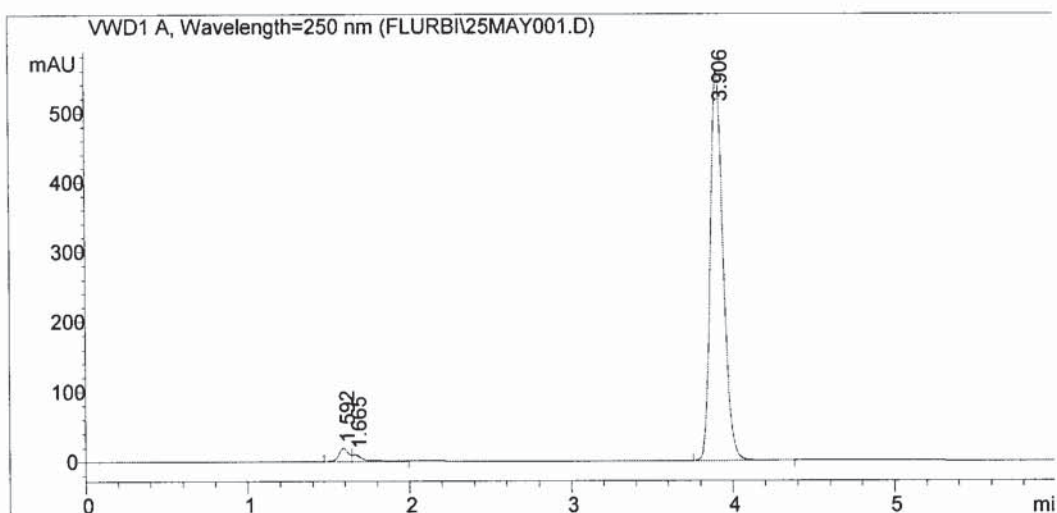


Figure 2.2 Typical HPLC chromatogram of flurbiprofen (concentration 1 mg/ml at 250 nm).

Typical UV scans and example calibration data for flurbiprofen are in appendix A.

2.1.4 Ibuprofen HPLC assay

2.1.4.1 Materials

Ibuprofen was supplied by GSK (Weybridge, UK).

2.1.4.2 Method

Working standards were prepared by serial dilution of a stock solution to produce standards in the range of 0.001-3 mg/ml, the exact concentration range dependent on the experiment.

Chromatographic conditions:

Injection volume	:	1 μ l
Mobile phase	:	Acetonitrile:water 65:35 (phosphoric acid 0.005%)
Wavelength	:	225 nm
Flow rate	:	1 ml/min
Runtime	:	7 minutes

Column : Thermo ODS-2 Hypersil 150 mm x 4.6 mm 5 μ m

2.1.4.3 Example data

A typical chromatogram for ibuprofen is presented in figure 2.3.

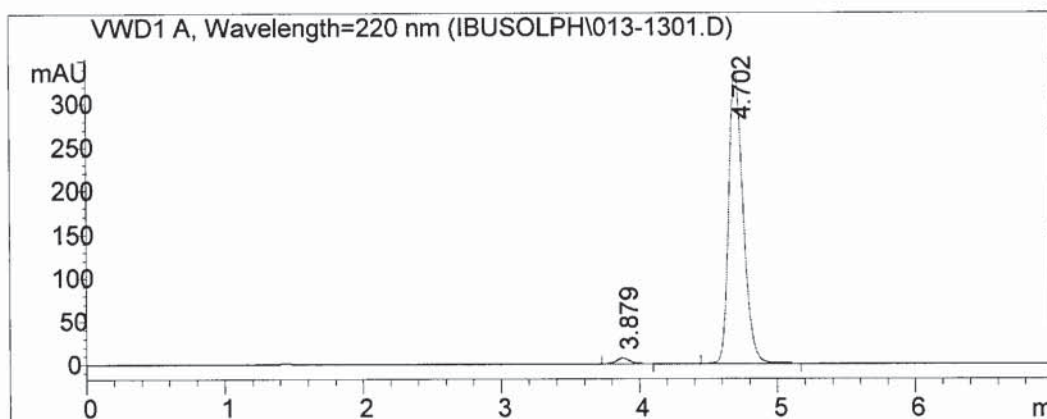


Figure 2.3 Typical chromatogram of ibuprofen (concentration 1 m/ml at 225 nm).

Typical calibration data and UV scans for ibuprofen are in appendix A.

2.1.5 Etodolac assay by HPLC

2.1.5.1 Materials

Etodolac was supplied by Ulkar Kimya (Istanbul) and was considered 100% pure for all experiments.

2.1.5.2 Method/chromatographic conditions

Working standards were prepared by serial dilution of a stock solution to produce standards in the range of 0.01 to 10 mg/ml, the exact concentration range dependent on the experiment.

Chromatographic conditions:

Injection volume	:	1 μ l
Mobile phase	:	Acetonitrile:water 65:35 (phosphoric acid 0.005%)
Wavelength	:	254 nm
Flow rate	:	1 ml/min

Runtime : 6 minutes
Column : Thermo ODS-2 Hypersil 150 mm x 4.6 mm 5 μ m

2.1.5.3 Example data

A typical chromatogram for etodolac is presented in figure 2.4.

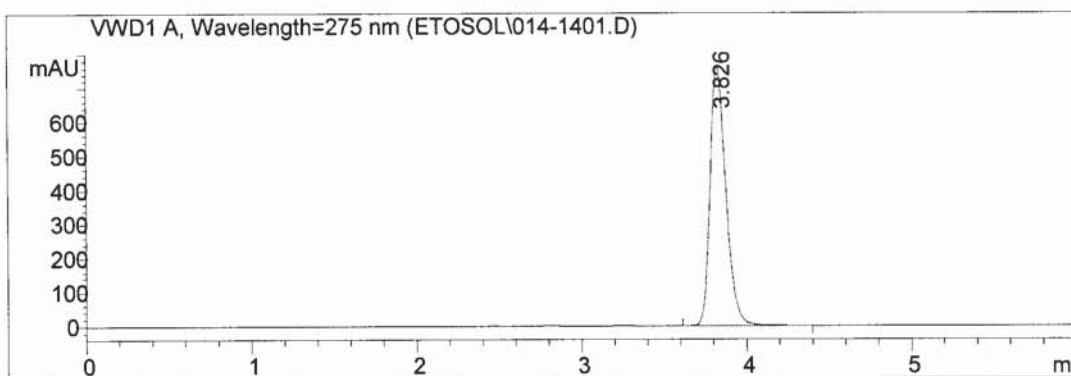


Figure 2.4 Typical HPLC chromatogram of etodolac (concentration 2 mg/ml at 275 nm).

Typical calibration data and UV scans for etodolac are in appendix A.

2.1.6 Naproxen HPLC assay

2.1.6.1 Materials

Naproxen was supplied by Sigma-Aldrich (Poole, UK).

2.1.6.2 Method/chromatographic conditions

Working standards were prepared by serial dilution of a stock solution to produce standards in the range of 0.01 to 1 mg/ml in 65:35 acetonitrile:water, the exact concentration range dependent on the experiment.

Chromatographic conditions:

Injection volume : 1 μ l
Mobile phase : Acetonitrile:water 65:35 (phosphoric acid 0.005%)
Wavelength : 225 nm
Flow rate : 1 ml/min
Runtime : 5 minutes

Column : Thermo ODS-2 Hypersil 150 mm x 4.6 mm 5 μ m

2.1.6.3 Example data

A typical chromatogram for naproxen is presented in figure 2.5.

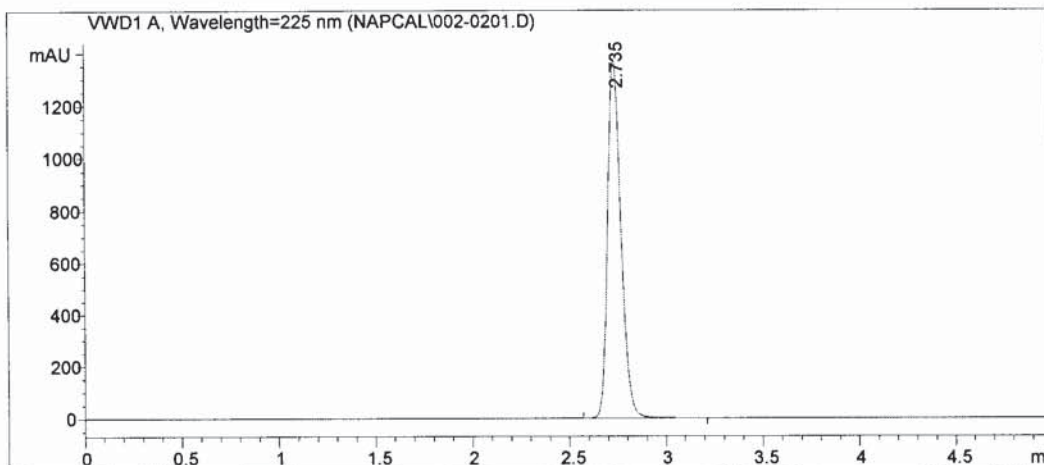


Figure 2.5. Typical HPLC chromatogram of naproxen (concentration 1 mg/ml at 225 nm).

Typical calibration data and UV scans for naproxen are in appendix A.

2.1.7 Piroxicam assay by HPLC

2.1.7.1 Materials

Piroxicam was supplied by Sigma-Aldrich (Poole, UK) and was considered 100% pure.

2.1.7.4 Method/chromatographic conditions

Working standards were prepared by serial dilution of a stock solution to produce standards in the range of 0.01 to 1 mg/ml in 65:35 acetonitrile:water, the exact concentration range dependent on the experiment.

Chromatographic conditions:

Injection volume : 1 μ l

Mobile phase : Acetonitrile:water 65:35 (phosphoric acid 0.005%) plus 2-3 drops of triethylamine per 500ml

Wavelength : 254 nm
Flow rate : 1 ml/min
Runtime : 6 minutes
Column : Thermo ODS-2 Hypersil 150 mm x 4.6 mm 5 μ m

2.1.7.3 Example data

A typical chromatogram for piroxicam is presented in figure 2.6.

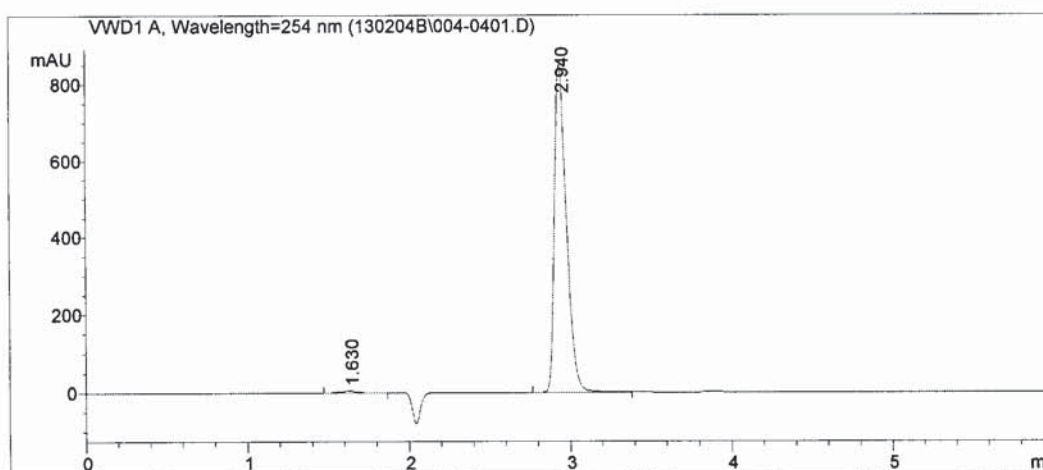


Figure 2.6 Typical HPLC chromatogram for piroxicam (concentration 1 mg/ml and 254 nm).

Typical calibration data and UV scans for piroxicam are in appendix A.

2.3 pH measurements

pH measurements were determined with a Mettler Toledo MP 230 pH meter to 3 decimal places. The instrument was calibrated before use with standard pH buffer solutions (Fisher, Loughborough, UK), *i.e.* pH 7 and either pH 4 or 10 depending on the region of interest.

Chapter 3 Preparation and characterisation of salts of model acidic drugs

3.1 Introduction

The drugs selected were:

- etodolac, an NSAID with selective COX-2 inhibition; it is available as Lodine SR®.
- flurbiprofen, NSAID prescribed generically for arthritis and dysmenorrhoea (Froben®)
- gemfibrozil, a fibrate used to lower serum triglycerides (Lopoid®)
- ibuprofen, a NSAID available generically and launched as an over-the-counter product in 1983 as Nurofen®.

Four carboxylic acids were selected because they were:

- commonly used molecules,
- they had limited solubility in water (solubility below 1 mg/ml),
- BCS class II compounds,
- readily available,
- potential salt formers

The molecular structures of the drug molecules are shown in Appendix A.

Inorganic ions have traditionally been used to form salts with acidic drugs, commonly sodium, potassium or calcium ions. Examples include: diclofenac sodium (Voltarol®), diclofenac potassium (Voltarol Rapid®). Recently alternative counterions have been explored due to limitations using the inorganic ions. For example amino acids have been used successfully, e.g. Nurofen Advance® contains ibuprofen lysine licensed for the treatment of migraines, a condition that requires rapid analgesia. Amine counterions are an emerging group of counterions suitable for salt formation; this is a large group so the variety of molecules available containing large, small and differently shaped hydrocarbon groups is enormous.

Although there are concerns over the safety of secondary amine molecules, if the salt forming group is small compared to the drug then these problems can be minimised.

A linear homologous amine series was selected to form salts with the carboxylic acids, in which the chain length increased. This included butylamine (4C hydrocarbon chain) and extended to octylamine (8C hydrocarbon chain). This series was chosen to observe and understand the effect of chain length on salt formation and solubility of the salt form. A saturated cyclic counterion was chosen, cyclohexylamine together with an unsaturated cyclic molecule, benzylamine to examine the effect of saturation of the ring structure on solubility. A hydrophilic series was also used based on the tert-butylamine molecule. Sequential substitution of each methyl group with hydroxyl groups produced a series of increasing hydrophilicity as the number of hydroxyl groups increased. They were used to investigate the effect of increasing hydrophilicity on salt formation and solubility. The structures of the amine counterions used in these studies are illustrated in Appendix A.2.

3.2 Salt Preparation

3.2.1 Introduction

Salts were formed with gemfibrozil (DiPharma, Italy), flurbiprofen (Erregierre, Italy), ibuprofen (GSK, Weybridge, UK) and etodolac (Ulkar Kimya, Istanbul). These substances are all carboxylic acids and readily formed salts with the amine counterions used.

3.2.2 Homologous alkylamine series

3.2.2.1 Materials

The counterions: propylamine, butylamine, hexylamine, octylamine and decylamine were supplied by Sigma-Aldrich (Poole, UK). Pentylamine was supplied by Fluka chemicals (Poole, UK), acetonitrile was supplied by Fisher (Loughborough, UK). All materials were of pharmaceutical, analytical or HPLC grade as appropriate.

3.2.2.2 Methods

The method of salt preparation was adapted from Anderson and Conradi (1985). 0.01 moles (a table of weights used is detailed in table 3.1) of drug and counterion were accurately measured on a Sartorius bench top balance; each material was dissolved in 40 ml of acetonitrile. The solutions were added together and produced a precipitate which was recovered by filtration under vacuum. If a precipitate did not form immediately the solution was stored at -4°C for 12 hours (or until a precipitate formed) and then filtered under vacuum. Products were dried overnight at 40°C under vacuum using a Gallenkamp vacuum oven. The powders were stored in sealed containers at room temperature until used.

Table 3.1 Weights and volumes of reagents used in salts preparation.

Material	Molecular weight	Density g/cc	Quantity used	Material	Molecular weight	Density g/cc	Quantity used
Etodolac	287.4	-	2.874 g	Benzylamine	107.16	0.981	1.09 ml
Flurbiprofen	244.3	-	2.443 g	Cyclohexylamine	99.18	0.87	1.14 ml
Gemfibrozil	250.3	-	2.503 g	Tert-butylamine	73.14	0.696	1.05 ml
Ibuprofen	206.3	-	2.063 g	AMP1	89.14	0.931	0.96 ml
Butylamine	73.14	0.722	1.01 ml	AMP2	105.14	-	1.051 g
Pentylamine	87.17	0.753	1.16 ml	Tris	121	-	1.210 g
Hexylamine	101.19	0.766	1.32 ml	Octylamine	129.25	0.782	1.65 ml

3.2.3 Hydrophilic series

3.2.3.1 Materials

The counterions: tert-butylamine (tert), 2-methyl-2-aminopropan-1-ol (AMP1), 2-methyl-2-aminopropan-1,3-diol (AMP2) and tris(hydroxymethyl)aminomethane base or tromethamine (tris) were supplied by Sigma-Aldrich (Poole, UK). Acetonitrile and methanol were supplied by Fisher (Loughborough, UK). All materials were of pharmaceutical, analytical or HPLC grade as appropriate.

3.2.3.2 Methods

The method of salt preparation for the tert-butylamine and AMP1 counterions was identical to that described in section 3.2.2.2. To prepare the salts of AMP2 and tris,

each counterion (0.01 moles) was dissolved in a warmed solution of methanol (40 ml). This was then added to solution of the drug in acetonitrile (40 ml). The precipitate was collected and dried as detailed in section 3.2.2.2.

3.2.4 Cyclic compounds

3.1.4.1 Materials

The counterions: benzylamine and cyclohexylamine were supplied by Sigma-Aldrich (Poole, UK). Acetonitrile was supplied by Fisher (Loughborough, UK). All materials were of pharmaceutical, analytical or HPLC grade as appropriate.

3.2.4.2 Methods

The method of salt preparation was as in section 3.2.2.2.

3.3 Structural analysis

3.3.1 Introduction

The aim of this section was to examine the solid state properties of the model drugs and the salts formed with the amine counterions. It is important to characterise the salts using as many analytical techniques as possible to gain an understanding of the properties of the salt forms with a view to relating them to solubility.

Once the salt had been formed, it was important to determine that a salt species had actually been made. This was confirmed by FTIR, NMR and purity experiments. It was also essential to confirm that a true salt had been made and it had the correct ratio of atoms within the molecule; this was done by NMR. A true salt was expected to: have one melting point, for one mole of acid to form a salt with one mole of base, to be crystalline and to have an approximately neutral solution pH.

3.3.2 Yield and salt purity

3.3.2.1 Materials

The amine salts were produced as detailed in section 2.2. Acetonitrile (Fisher, Loughborough) was of HPLC grade, double distilled water was generated in-house using a Fisons Fi-streem still.

3.3.2.2. Equipment

A multipoint magnetic stirrer (Variomag) set at 500 rpm was used for sample preparation. HPLC equipment was used as detailed in section 2.1.1.2.

3.3.2.3 Methods

Eight salts were selected to determine their relative purity: F hex, F benz, F cyclo, F tert and G hex, G benz, G cyclo, G tert. This was done by measuring the amount of parent drug in the salt and this was compared with the theoretical ratio. Each salt (100 mg) was accurately weighed and placed in a 100 ml class B volumetric flask and made up to volume with acetonitrile:water 65:35 solvent to give a solution of 1 mg/ml. 1 ml was placed in a 10 ml class B volumetric flask and filled to volume with solvent mix. The solution was then analysed by HPLC with appropriate calibration standards.

3.3.2.4 Results

The model drug content was determined for all eight salts (table 3.2 and 3.3). The yields were between 90-100 % for all the salts tested. The salts were not further purified by crystallisation because this would have extended the manufacturing time beyond a reasonable level. It was important to keep the manufacturing time as short as possible as a lot of material was required for the solubility, dissolution and compression work.

This method of salt formation was satisfactory in producing a reasonable yield, with little wastage and an acceptable level of purity. The method of salt formation was deemed to be appropriate because of the following reasons:

- Simple procedure
- Ease of precipitation and recovery
- Short manufacturing time
- Large batches possible (up to 5 g)
- Purity of over 90%

Table 3.2 Purity of four selected amine salts of flurbiprofen

	% flurbiprofen content (experimental)	% flurbiprofen content (theoretical)	Purity of flurbiprofen salts (% of theoretical)
F.hex	69.8	70.7	96
F.benz	68.8	69.5	99
F.cyclo	68.2	71.2	90
F.tert	69.3	77	99

Table 3.3 Purity of four selected amine salts of gemfibrozil

	% gemfibrozil content (experimental)	% gemfibrozil content (theoretical)	Purity of gemfibrozil salts(% of theoretical)
G.hex	66.8	71.7	93
G.benz	66.3	71.2	93
G.cyclo	64.7	70.1	92
G.tert	72.2	77.4	93

3.3.3 Confirmation of salt formation

The salts are formed by combining an amine ($R-NH_3^+$) ion with an organic carboxylic acid (model drug- COO^-). As these ions have a valency of one they are expected to combine to give a neutral molecule at a 1:1 ratio. The loss of the COO^- group is expected to be confirmed by Fourier Transform Infra-red spectroscopy (FTIR), whereas the 1:1 ratio was investigated by nuclear magnetic resonance spectroscopy (NMR). The total proton count will confirm salt formation.

3.3.3.1 FTIR

IR spectroscopy uses electromagnetic radiation ranging between 500 cm^{-1} and 4000 cm^{-1} which is passed through a sample and is absorbed by the bonds of the molecules in the sample, causing them to stretch or bend. The wavelength of the radiation absorbed is characteristic of the bond absorbing it. The advantage of FTIR over conventional IR spectroscopy is that several scans can be taken very quickly and averaged to improve the signal:noise ratio for the spectrum. IR provides a qualitative fingerprint check for the identity of drugs and polymorphs as fingerprint regions are unique to the compound being examined. It can be used to identify the presence or absence of carbonyl groups, which can be difficult to check by any other methods. IR is rarely used for quantitative analysis because of relative difficulty in sample preparation and the complexity of the spectra. The technique suffers because sample preparation requires a level of skill and not all materials compress well to form disks; this means that it may not be possible to analyse certain materials. Some of the salts were so poorly compressible that FTIR was not possible. IR can only usually detect gross impurities within a sample.

3.3.3.1.1 Materials

Potassium bromide (KBr) of FTIR grade was supplied by Sigma-Aldrich (Poole, UK) and kept free of moisture in a desiccator. The salts used were made as detailed in section 3.2.

3.3.3.1.2 Equipment

Disks for analysis were prepared with a Specac KBr press using a 13 mm die. A Unicam Mattson 3000 FTIR was used to analyse the samples and Galaxy software was used to interpret the results.

3.3.3.1.3 Method

Approximately 1 mg of sample was ground to a fine powder in a marble mortar together with approximately 10 mg KBr to form a fine powder. A small amount of sample was placed in the die and subjected to 8 tonnes pressure for 6 minutes to form a thin opaque disk.

3.3.3.1.4 Results and discussion

The signal at 1684 cm^{-1} in the spectrum for the model drugs was attributed to a C=O stretching of the carboxylic acid group (Silverstein and Webster, 1998; Palomo et al., 1999; O'Connor and Corrigan, 2001). Salt formation was confirmed by: the absence of the 1684 cm^{-1} carboxylic acid peak; the presence of bands characteristic of carboxylic acid salts, at $1650\text{--}1550\text{ cm}^{-1}$ and $1440\text{--}1335\text{ cm}^{-1}$ (Socrates, 1994); and absorption at $3350\text{--}3150\text{ cm}^{-1}$, attributable to NH_3^+ stretching of solid amine salts (Socrates, 1994). This method has been used previously by O'Connor and Corrigan (2001) and allowed confirmation of salt formation. Examples of spectra are in appendix C.

3.3.3.2 NMR

The principle of NMR is that radiation is used to excite the nuclei of the atoms, usually protons (hydrogen atoms) or carbon-13 atoms, so that in an extreme magnetic field their spins switch from being aligned with, to being aligned against, an applied magnetic field (Watson, 1999). The range of frequencies required for excitation and the complex splitting patterns produced are very characteristic of the chemical structure of the molecule. It is a very powerful technique that is used to derive the exact structure of a material once the chemical formula is known. It can detect impurities at a low % w/w level, including enantiomeric impurities.

The sample is placed in a narrow glass NMR tube and is spun in a fixed magnetic field by way of an air turbine, thus ensuring uniformity of the magnetic field across the sample in a horizontal direction. The sample is analysed in deuterated solvent to ensure there is no interference from protons in the solvent. The reference point is taken as 7.25 ppm relative to tetramethylsilane (TMS) as this is the frequency at which the residual proton in chloroform absorbs. As well as determining the frequency at which protons in the molecule absorb, the instrument determines the area of each signal, which is proportional to the number of protons absorbing radiation, e.g. three protons give an area three times as large as a signal due to one proton in the same molecule. Thus this technique can be used to identify salt formation.

Proton (^1H) NMR (200-600 MHz) is the most commonly used form of NMR because of the large amount of structural information it yields. The exact absorption or resonance frequency of a proton depends on its environment; proton shifts depend

on the strength of the magnetic field required to excite a proton. The proton shift is determined by the degree of shielding provided by the groups to which it is attached. If the hydrogen atom in question is attached to an aromatic ring, the chemical shift, σ , will increase due to the electron withdrawing nature of the conjugated ring. The more a proton is shielded by its environment, the lower the σ value, e.g. alkyl protons such as CH_3 and CH_2 groups not attached to electronegative groups resonate between δ 0.2-2 ppm. Protons on CH_3 , CH_2 and CH groups attached to electronegative atoms or groups such as O, N, F, $\text{C}=\text{O}$ resonate between δ 2-5. Protons attached to aromatic rings resonate between δ 6-9.

3.3.3.2.1 Materials

Deuterated chloroform was supplied by Sigma-Aldrich (Poole, UK). The salts used were made as detailed in section 3.2.

3.3.3.2.2 Equipment

The samples were analysed on a Bruker AC 250 NMR (250 MHz) and a MAC Quadra 800 PC using WIN-NMR V3.0 software was used to interpret the results.

3.3.3.2.3 Method

Samples of approximately 10 mg were dissolved in 10 ml of deuterated chloroform and placed in a sample capillary vial, to a height of 10-15 cm. The vial was placed in the NMR machine and the sample was tested for the presence of hydrogen atoms (^1H -NMR).

3.3.3.2.4 Results and discussion

All the samples had the correct number of hydrogen atoms present. This was determined by summing the integration parameters and comparing to the number of hydrogen atoms in the sample. The traces confirmed that the salts had formed in a 1:1 ratio and that they were over 90% pure, as the NMR traces had an acceptable signal to noise ratio. The parent drugs were also analysed and were found to be free of impurities. An example of a NMR trace is in appendix C.

3.4 Physicochemical characteristics

3.4.1 Introduction

This section is designed to gain an understanding of the physicochemical attributes of each model drug and salt in order to provide an explanation for variations in the behaviour of each salt form and to explore if there are any patterns in behaviour.

3.4.2 Differential scanning calorimetry (DSC) and Thermogravimetric analysis (TGA)

Determination of melting point is an important part of assessing solubility; theory suggests that an increase in melting point will result in a decrease in solubility. This is because as it takes more energy to break bonds and melt a material so it will take more energy to allow water molecules to break intermolecular bonds. It has been found that solubility and melting point are related and this section aims to describe the relationship between salts and melting point. Rubino (1989) discovered an inverse relationship when the logarithm of solubility for a range of sodium salts of drugs was plotted against melting point.

Perkin Elmer DSC uses a power-compensated system which incorporates separate heaters for both sample and reference. Sample and reference are maintained at the same temperature resulting in different amounts of heat being supplied to each part as appropriate. The difference in power supply to the heaters is monitored. Heating rates of 0.1 to 400 °C/minute are possible in 0.1 °C increments with a temperature range of -170-725 °C with the Diamond DSC controlled by Pyris software. Hyper-DSC is now possible using elevated heating rates (200-400 °C) to determine thermal events not visible at lower heating rates e.g. the detection and quantitation of amorphous material in crystalline samples (Saunders *et al.* 2004). Sample sizes are usually between 3-5 mg and for Hyper-DSC can be as little as 1 mg.

TGA utilises a thermobalance, which allows constant monitoring of sample weight as a function of temperature. This can involve heating or cooling a sample at a controlled rate or maintaining the sample at a fixed temperature. The sample is

contained in a furnace with a microbalance monitoring the change of weight over time or over a temperature range. The furnace normally operates between -40-400 °C and large sample sizes are required to give an adequate weight loss for measurement on the microbalance (10-20 mg). This technique is ideal for looking at solvates and hydrates, as in conjunction with DSC, can identify at what temperature the solvent evaporates and TGA can be used to calculate the molar ratio of material:water in a hydrate.

3.4.2.1 Materials

The salts used were made as detailed in section 2.2. The model drugs were obtained from as in section 2.2.1.

3.4.2.2 Equipment

A Perkin Elmer PYRIS Diamond DSC with an Intracooler 2P was used to analyse the samples and PYRIS software was used to interpret the results. Aluminium holed pans were used to encase the sample before analysis.

TGA was performed on a Thermal Analysis TGA 4 instrument owned by Bristol Myers Squibb, Moreton, Wirral, UK.

3.4.2.3 Method

The DSC methodology was as follows: Approximately 3 mg of sample was accurately weighed into the sample pan using a Kern 770 five decimal place balance and sealed in a press. Three samples were prepared of each material and analysed under the same conditions.

The program used a scan rate of 10 °C/min from 0 °C to a maximum of 250 °C or a temperature exceeding the melt, using nitrogen as the purge gas at 40 ml/min. The equipment was calibrated with an indium sample to ensure reliable results. The instrument method was identical for both DSC and TGA.

3.4.2.4 Results and discussion

Melting point information and enthalpy of fusion data are summarised in table 3.4 and 3.5 for the model drugs and their amine salts. DSC scans of selected materials are illustrated in figures 3.1 and 3.2. All other DSC scans are found in appendix C.

The data shows that on addition of an amine counterion to the model drug, a crystalline product is formed with a sharp melting point(s); the melting points of the salt forms are greater than for the parent.

For all homologous series of salts (gemfibrozil, etodolac, flurbiprofen and ibuprofen) there is a reduction in melting point and $\Delta HJ/g$ as chain length increases. The salts of gemfibrozil and ibuprofen have a lower melting point than the parent as chain length increases beyond 4 carbon units. The $\Delta HJ/g$ values have been calculated by the program by using the initial mass information and the energy measured. $\Delta HJ/g$ has been converted to kJ/mole and is the energy required to break the bonds and as this is a positive value the reaction is endothermic, in the traces this is indicated by a peak. $\Delta HkJ/mole$ gives an indication of the total energy required to break the crystal lattice, melting point reduces as chain length increases and $\Delta HkJ/mole$ reduces also. This result may be due to an increased chain length creating disorder in the crystal lattice making it break apart more easily.

Table 3.4 Melting points and enthalpies of fusion for the amine salts of etodolac and flurbiprofen determined using DSC. (n=3) Mp indicates Melting Point.

Etodolac and salts	Mp °C	Enthalpy of fusion kJ/mole	Flurbiprofen and salts	Mp °C	Enthalpy of fusion kJ/mole
Drug	151-153	29.4	Drug	115-117	24.7
Butylamine	148-155	25.2	Butylamine	139-141	23.6
Pentylamine	109-111	23.0	Pentylamine	93-96	10.7
Hexylamine	140-143	28.8	Hexylamine	87-91	27.5
Octylamine	111-113	27.6	Octylamine	103-104	33.8
Benzylamine	164-165	48.2	Benzylamine	136-138	38.9
Cyclohexylamine	199-203	28.8	Cyclohexylamine	197-201	47.8
Tert-butylamine	177-185	23.7	Tert-butylamine	193-198	46.7
AMP1	165-167	33.2	AMP1	154-157	33.6
AMP2	116-122	32.1	AMP2	123-126	36.4
Tris	159-161	58.2	Tris	150-152	39.4

Table 3.5 Melting points and enthalpies of fusion for the amine salts of gemfibrozil and ibuprofen determined using DSC (n=3).

Gemfibrozil and salts	Mp °C	Enthalpy of fusion kJ/mole	Ibuprofen and salts	Mp °C	Enthalpy of fusion kJ/mole
Drug	62-64	22.3	Drug	76-79	24.2
Butylamine	75-77	25.5	Butylamine	104-106	19.3
Pentylamine	78-80	22.1	Pentylamine	83-86	8.23
Hexylamine	70-72	22.7	Hexylamine	91-94	20.3
Octylamine	37-40	28.7	Octylamine	80-82	21.4
Benzylamine	91-93	20.9	Benzylamine	107-109	25.9
Cyclohexylamine	135-137	41.2	Cyclohexylamine	197-201	49.0
Tert-butylamine	141-146	24.7	Tert-butylamine	185-190	35.9
AMP1	119-122	52.0	AMP1	130-134	51.1
AMP2	104-106	28.7	AMP2	112-116	23.3
Tris	119-121	68.0	Tris	160-164	60.8

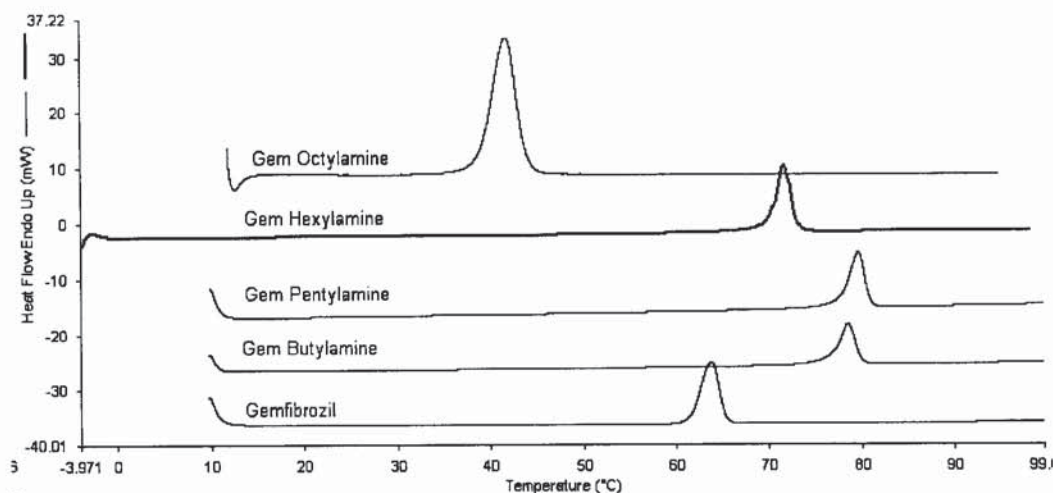


Figure 3.1 DSC scans for the homologous salts of the gemfibrozil series

DSC results for gemfibrozil benzylamine and ibuprofen benzylamine both display two peaks, figure 3.2 and 3.3. Ibuprofen benzylamine shows two merged peaks upon heating, the first occurs at about 110°C and the second peak at 120°C, figure 3.2 (2). When the same sample is re-heated under the same conditions a single peak is produced on the DSC trace at 109°C, figure 3.2 (1). The TGA of ibuprofen benzylamine shows that upon heating the weight of the material changed at a temperature corresponding to the onset of the endothermic event on the DSC scan (figure 3.3).

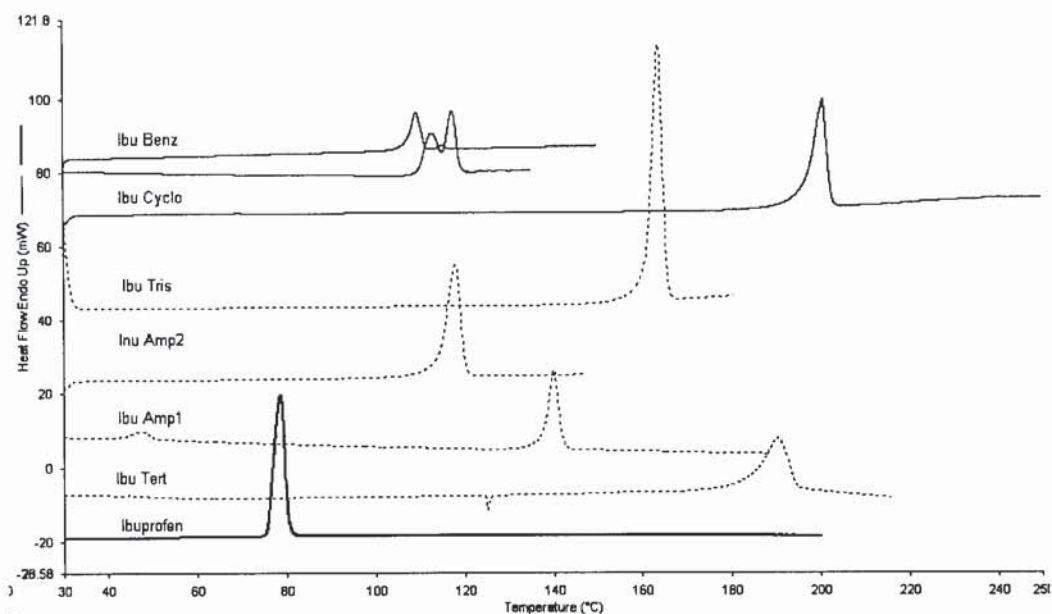


Figure 3.2 DSC scans of ibuprofen and its benzylamine, cyclohexylamine, tris, AMP2, AMP1 and tert-butylamine salts. Ibuprofen benzylamine upper scan is the second repeat of the run.

Sample: Ibuprofen Benzylamine
Size: 24.3700 mg
Method: 10degC to 200deg C

TGA

File: C:\...IbuBenz.001
Operator: Sarah David
Run Date: 29-Jul-03 13:05

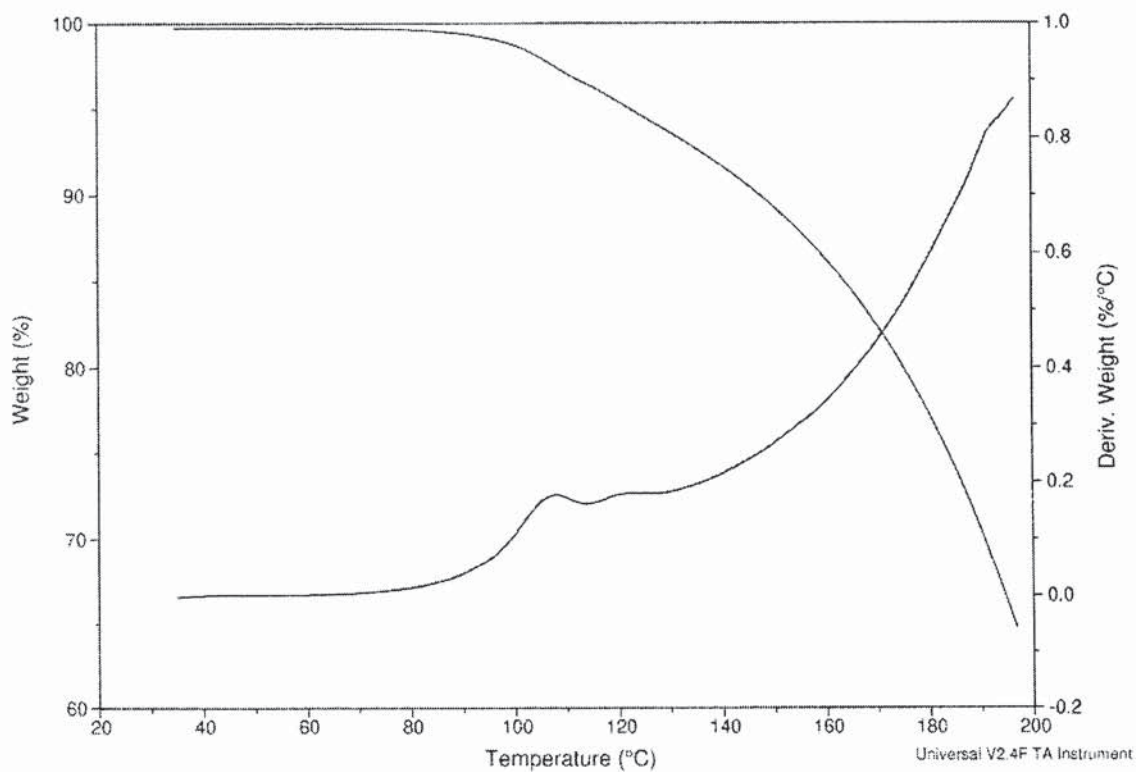


Figure 3.3 TGA of ibuprofen benzylamine

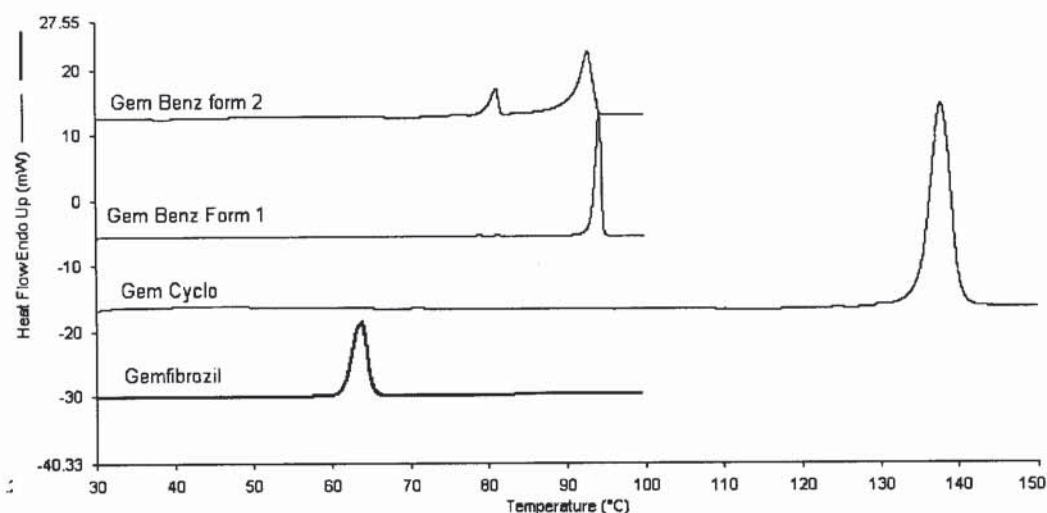


Figure 3.4 DSC scans for the cyclohexylamine and benzylamine salt of gemfibrozil showing the possible presence of a solvate (form 2).

The two forms of gemfibrozil benzylamine that are shown in figure 3.4 (forms 1 & 2) were made by the same salt formation process suggesting that the introduction of a benzylamine group may create disorder in the crystal structure resulting in polymorphism or a solvate could have been formed incorporating the solvent acetonitrile in the crystal lattice. The first peak occurs at about 80°C which is the boiling point of acetonitrile (81-82°C). TGA of this sample will confirm whether the peak is due to solvent, which would be identified by weight loss in the sample when the sample is heated. If this material is a polymorph the TGA will not show any weight loss upon heating. Production of polymorphs is common when crystallising salt forms and has previously been described by O'Connor and Corrigan (2001) who found pseudopolymorphism in AMP1 and benzylamine salts of diclofenac.

The cyclohexylamine salts of the model drugs all have high melting points, relative to the other salts, and have high ΔH kJ/mole values, because of their high melting points we would predict these powders to have low aqueous solubilities. The tert-butylamine salts of the drugs have high melting points relative to the parent drug and single sharp melting endotherms. The salts crystallise easily, the ΔH kJ/mole values for each salt are less than cyclohexylamine salts. These salts are therefore expected to have higher aqueous solubilities than cyclohexylamine salts, if there was a simple relationship between melting point and solubility.

The AMP1, AMP2 and tris salts are very different molecules because the number of OH groups varies in each counterion. Therefore the amount of hydrogen bonding present in the crystal lattice and the molecular weight varies from molecule to molecule. The AMP2 salts have lower melting points than the other substituted tert-butylamine salts (table 3.4 and 3.5) and generally have lower enthalpy values ($\Delta kJ/moles$). The AMP2 salts are therefore expected to have higher aqueous solubilities than AMP1 and tris salts. Etodolac AMP2 has a shoulder on its peak close to 100 °C (temperature range not shown, figure 3.5) and the TGA trace shows a weight loss at 100°C which corresponds to a loss of water from the sample. The weight loss was calculated and converted to moles of water and was found to correspond to formation of a monohydrate salt.

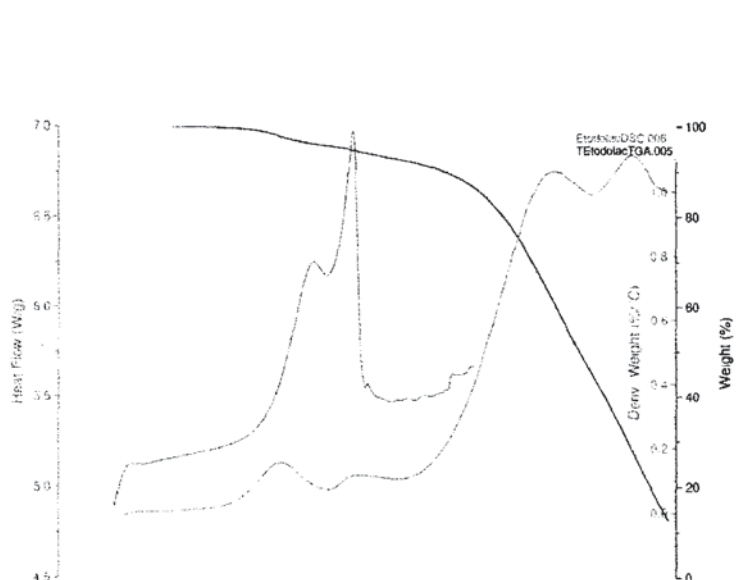


Figure 3.5 DSC (green) and TGA (blue) trace of etodolac AMP2 salt form. The derivative of the weight change is represented in red.

3.4.3 Calculation of Log P and Log D values

3.4.3.1 Introduction

Lipophilicity is an important parameter to consider when predicting water solubility of a particular compound. A highly lipophilic compound will have limited water solubility and will not interact with hydrophilic, polar molecules such as water. Log P and Log D are a way of describing a compound's lipophilicity, CLog P is a calculated parameter usually by a computer program, e.g. Hansch and Leo's CLog P. Log P is the octanol-water partition coefficient and log D is the measurement at a particular pH. Log P results can be related to solubility, however for solids solubility also depends on the energy required to break the crystal lattice. Bannerjee et al. (1980) have suggested the following empirical equation to relate solubility, melting point and log P:

$$\text{Log}P = 6.5 - 0.89(\log S) - 0.015mpt \quad \text{equation 3.1}$$

where S is the solubility in water in micromoles per litre.

It is therefore possible to have compounds with high Log P values which are still water soluble due to their low melting points. Similarly, it is possible to have a compound with a low solubility and a high melting point with a low Log P.

For formulation and dosage forms, injectable drugs ideally have Log P values below 0, for oral absorption medium lipophilicity is required (Log P 0-3), for transdermal absorption Log P's of 3-4 are suitable and if the Log P is above 4 there may be a toxic build up in fatty tissues (Banerjee et al., 1980).

3.4.3.2 Method

CLogP was calculated for all the model drugs, the counterions and the salts. BioByte Corp. (USA) supplied the ClogP version 4.0 software and required the use of SMILES (Simplified Molecular Input Line Entry System) notations of chemical formula.

SMILES is a way of re-writing a chemical formula without including hydrogen atoms e.g. the SMILES notation for butylamine is NCCC and the SMILES notation for

octylamine is therefore NCCCCCCCC. Using this notation, a chemical formula can be simplified for ease of calculation.

3.4.3.3 Results and discussion

ClogP V4.0 was used to calculate the octanol-water coefficients for the model drugs and the counterions used to form the salts (table 3.6). As chain-length increases, the lipophilicity of the counterion increases. The hydrophilic counterions (those containing OH) have negative ClogP values indicating their affinity for the aqueous phase. The benzylamine and cyclohexylamine counterions have similar lipophilicities and the values are between those of butylamine and pentylamine. Tert-butylamine has a low lipophilicity.

Table 3.6 Estimated ClogP values from the computer program ClogP V4.0.

Drug	CLogP	Counterion	CLogP	Counterion	ClogP
Etodolac	3.52	Butylamine	0.92	Tert-butylamine	0.59
Flurbiprofen	3.44	Pentylamine	1.45	AMP1	-0.59
Gemfibrozil	4.16	Hexylamine	1.98	AMP2	-0.59
Ibuprofen	3.68	Octylamine	3.04	Tris	-0.94
		Benzylamine	1.09	Cyclohexylamine	1.37

Using equation 3.1, it can be predicted that gemfibrozil should have a high solubility in water because it has a low melting point, but this is not the case in practice due to the acidic nature of the solution formed when gemfibrozil, which is a weak acid, dissolves in water.

From the CLogP data it is predicted that AMP1, AMP2 and tris salts would have the greatest aqueous solubilities and that the butylamine and tert-butylamine salts will have good aqueous solubilities because they have low LogP values. The rank order of diclofenac salt solubilities was found to be AMP1 > AMP2 > tert > tris by O'Connor and Corrigan (2001) whereas Anderson and Conradi (1985) found a solubility order of the flurbiprofen salts of the same counterions of AMP2 > tris \approx AMP1 > tert. The tert-butylamine salt has low aqueous solubility which is not as predicted by the LogP values. Unfortunately, looking at LogP values as a predictor of solubility is probably a

very simplistic approach as pH plays a major role in affecting solubility which cannot be predicted empirically at the moment.

3.4.4 Determination of pKa for the salt forms

The chemical and biological activity of pharmacologically active substances is dependent on the degree of ionisation of the molecule. Accurate knowledge of ionisation constants is very important to predict the solubility in different pH conditions and to examine the implications for absorption.

3.4.4.1 Method

The SPARC online programme calculates molecular properties by breaking molecular structures into functional units with known chemical properties. Known reactions are calculated and the impact on reactivity of appended molecular structures quantified by perturbation theory. The SPARC pKa calculator has been tested on 4338 pKa's for more than 3685 compounds spanning a range of over 31 pKa units (Hilal et al. 1995) with reported success.

The SPARC (SPARC performs automated reasoning in chemistry) online calculator was used to calculate the pKa values of the starting materials and the ionised salts. When entering the website, pKa determination is selected. It is important to select the single pKa determination from the options page and choose the appropriate conditions e.g. N as a base and maximum output. The online calculator requires SMILES notations for the insertion of chemical structures. However there is a facility on the webpage to draw the structure and by the click of a button it is converted to the appropriate SMILES notation.

SPARC is available from <http://ibmlc2.chem.uga.edu/sparc/index.cfm> and it a quick and easy way to predict pKa values. The website calculator has been used previously by Hilal et al. (1999) to successfully calculate the multiple ionisation sites of many compounds with values as reliable as experimental measurements.

3.4.4.2 Results

Table 3.7 Calculated pKa values using the SPARC online calculator for the model drugs and their counterions.

Carboxylic acids	SPARC pKa calc.	Counterions	SPARC pKa calc.
Etodolac	4.336	Butylamine- octylamine	10.333
Flurbiprofen	4.346	Benzylamine	9.353
Gemfibrozil	4.720	Cyclohexylamine	10.516
Ibuprofen	4.525	Tert-butylamine	10.516
Piroxicam	13.071	AMP1	9.195
Naproxen	4.463	AMP2	7.939
Indomethacin	4.497	Tris	6.437

Table 3.8 Calculated pKa values using the SPARC online calculator for etodolac and flurbiprofen and their amine salts.

Etodolac salts	pKa calc	Flurbiprofen	pKa calc
E butylamine to octylamine	0.894	F butylamine to octylamine	0.841
E benzylamine	-0.110	F benzylamine	-0.163
E cyclohexylamine	0.998	F cyclohexylamine	0.945
E tert-butylamine	1.135	F tert-butylamine	1.083
E AMP1	-1.647	F AMP1	-1.610
E AMP2	-2.928	F AMP2	-2.9804
E tris	-3.398	F tris	-3.451

Table 3.9 Calculated pKa values using the SPARC online calculator for ibuprofen and gemfibrozil their amine salts.

Ibuprofen salts	pKa calc	Gemfibrozil salts	pKa calc
I butylamine to octylamine	1.109	G butylamine to octylamine	0.985
I benzylamine	-0.105	G benzylamine	-0.019
I cyclohexylamine	1.213	G cyclohexylamine	1.089
I tert-butylamine	1.351	G tert-butylamine	1.226
I AMP1	-1.431	G AMP1	-1.556
I AMP2	-2.712	G AMP2	-2.836
I tris	-3.182	G tris	-3.307

The positive pKa values represent acidic compounds, whereas negative pKa values are hydrophilic molecules.

All of the homologous series of counterions (butylamine to octylamine) have the same pKa value. This is because the program assumes that the extension of the hydrocarbon chain has no impact on the charge distribution between the nitrogen and carbon atoms within the counterion. This is an incorrect assumption. It is well documented that for the alcoholic series methanol, propanol and hexanol the polarity of the molecule reduces as chain length increases. Oxygen is a very electronegative atom, nitrogen less so, and produces a polar bond when coupled to a non-polar hydrocarbon group. Methanol (CH_3OH) is a polar molecule, the alcohol ($-\text{OH}$) dominates the molecule and the hydrocarbon group is small, making it polar. Propanol is an equally polar and non-polar molecule, the alcohol still provides a polar bond but there are many more non-polar regions. Hexanol is mostly non-polar with some polar properties because of the increased hydrocarbon chain length; this has an impact on the dissociation ability of the molecule. The greater the chain length the weaker the acid or base. The strong acids and bases have polar bonds and are easily dissociated in solution, whereas the weaker acids and bases have large hydrocarbon groups attached with many non polar regions. Benzene rings are electron accepting so are structures containing them and are less likely to accept protons than corresponding aliphatic molecules so they are weaker bases. The cyclohexylamine ring system is a saturated system and electron donating so will impart greater basicity. As the hydrocarbon chain length increases the molecule becomes more hydrophobic and therefore more basic.

The hydrophilic series (tert-butylamine, AMP1, AMP2 and tert) becomes less electron donating (basic) as the number of hydroxyl groups increases. The increased number of oxygen atoms within the molecule draws electrostatic charge away from the nitrogen.

3.4.5 Surface area

3.4.5.1 Introduction

Surface area analysis of a solid is performed because it provides information on available void spaces on the surface of a solid, usually in powder form. In addition, the dissolution rate of a solid is partially determined by its surface area. Surface area

can dramatically affect the properties of a material; the smaller the particle size, the larger the surface area. If the surface area is large, the dissolution rate should be fast. Therefore to increase dissolution rate, milling is often used to reduce particle size. Spray freezing into liquid (SFL) has been developed to produce micronized powders to enhance the dissolution of drugs. SFL was used by Hu *et al.* (2003) to significantly enhance the dissolution of carbamazepine, a poorly water soluble drug. Methods to reduce particle size often make the material amorphous which can improve solubility but the material may undergo uncontrolled crystallisation.

The most reproducible method to measure surface area is to adsorb a monolayer of a condensable, inert gas (usually nitrogen or krypton), mixed with an inert non-condensable, carrier gas (usually helium) onto the surface of the powder at a reduced temperature and then desorbing the gas at room temperature. The sorption isotherms obtained in this technique are interpreted using the equations developed by Braunauer, Emmett and Teller and this technique is referred to as the BET method. Surface area is measured in m^2/g . Information has been provided by the Gemini 2360 instructions.

Other methods that are commonly used to measure the internal pores of a solid include the use of mercury. Mercury porosimetry measures pore size distribution by the capillary rise phenomenon and mercury intrusion can be used to calculate surface area by filling the voids at a known pressure. Differential vapour sorption (DVS) can also be used to measure surface area.

The Gemini 2360 Analyser only uses pure nitrogen as the analysis gas and is able to maintain a constant pressure over the sample, while varying the rate of gas delivery to match adsorption rate. This allows surface areas as low as $0.01 \text{ m}^2/\text{g}$ to be easily determined.

Four samples were chosen for surface area measurement. These were: ibuprofen, ibuprofen butylamine, ibuprofen octylamine and ibuprofen AMP2. It was only possible to analyse a small number of samples as sample preparation can take up to four days because the samples have to be completely dry and purged with nitrogen gas. Sample preparation time is individual to a material and can vary between 2-4 days.

The equipment was located at Bristol Myers Squibb, Moreton, Wirral. However it was possible to identify four interesting samples to analyse, those with high, medium and low solubility including the parent compound. This would allow solubility to be related to surface area for the samples.

3.4.5.2 Materials and experimental

All materials were used as detailed in section 2.2. A Gemini 2360 Analyser was used to calculate the surface area of the materials. Nitrogen gas was supplied in-house at Bristol Myers Squibb, Moreton, Wirral.

3.4.5.3 Method

A calibration was performed with alumina, supplied by Gemini Instruments. A sample of 1.5471 g was degassed for 2 h at 300 °C at a degassing flow rate of approximately 100 ml/min. The surface area was measured under a saturation pressure of 772.04 mm Hg over a relative pressure range of 0.06-0.5 mm Hg and under evacuation conditions of 500 mm Hg/min over 3 minutes. Five measurements of the volume of gas adsorbed were collected at different pressures and used to calculate the surface area. The surface area report is displayed in table 3.9.

Ibuprofen and ibuprofen butylamine samples of approximately 1 g were heated in sample tubes at 50 °C and degassed with nitrogen gas for 29 h before analysis on the Gemini 2360 Analyser under the same conditions as for calibration. Ibuprofen octylamine and ibuprofen AMP2 were degassed at 50 °C for 25 h prior to analysis. The analysis was performed twice on each sample

3.4.5.4 Results and discussion

The results of BET multipoint surface area analysis of the samples are displayed in table 3.10, below.

The surface area measurements confirm that the material with the highest solubility in water has the highest surface area, ibuprofen butylamine and the material with the lowest solubility (ibuprofen) has the lowest surface area value. Ibuprofen AMP2 has a surface area of 0.8 m²/g, which is not as high as ibuprofen butylamine yet has a solubility far exceeding ibuprofen butylamine. This result may be explained by the

possible surface activity properties of ibuprofen AMP2 which influences the solubility more than surface area (see section 5).

An increase in surface area will influence the dissolution rate of a drug according to the Noyes-Whitney equation. The smaller the particle size the greater the effective surface area exhibited by a given mass of drug, and the higher the dissolution rate. Digoxin, tolbutamide, aspirin and naproxen have undergone particle size reduction techniques and this has improved the dissolution so that the bioavailability has been enhanced. The relative bioavailability of danazol has been increased 400% by administering particles in the nano- rather than micron size range (Aulton, 2002).

Table 3.10 Surface area and saturated water solubility measurements of ibuprofen, ibuprofen butylamine, ibuprofen octylamine and ibuprofen AMP2. Solubilities are mean; \pm SD

	Surface area m ² /g	Saturated water solubility mg/ml
Ibuprofen	0.1672, 0.1639	0.071 \pm 0.002
I butylamine	1.7350, 1.5298	162.66 \pm 8.645
I octylamine	0.5926, 0.5796	1.65 \pm 0.548
I AMP2	0.8018, 0.8032	+200

The interpretation of these results is difficult as extent of solubility and dissolution is not simply controlled by surface area but by many other factors such as pH, hydrophilicity and melting point.

3.4.6 Dynamic vapour sorption (DVS)

3.4.6.1 Introduction

DVS enables an easy and accurate measurement of moisture and vapour sorption. The DVS instrument used was made by Surface Measurement Systems and provides a rapid, automated, programmable and accurate measurement of gravimetric moisture and organic vapour uptake in solid materials. It uses a very small sample size and a dynamic flow of humidified gas means that moisture sorption can be measured in a few hours.

The instrument consists of temperature-controlled chambers for the sample and reference pans connected to a microbalance module. Dry gas is introduced at a controlled rate and a vapour generator module regulates the humidity that passes into the reference and sample chambers. The experiment can be performed at a constant humidity or under changing temperature and humidity. DVS can be used with organic vapours to look at organic vapour isotherms, surface studies of hydrophilic substances, BET surface area, average surface energy and heat of sorption.

This technique is ideal for the confirmation of hydrates together with other techniques such as DSC and TGA (Hodson, 1996), hygroscopicity and for carrying out accelerated stability testing of raw materials at elevated temperature and humidity.

Three materials were selected to be tested. These were; etodolac butylamine, etodolac AMP2 and ibuprofen benzylamine. Etodolac butylamine was selected because of its elevated water solubility and etodolac AMP2 and ibuprofen benzylamine were chosen because of multiple peaks on their DSC profiles. Both these compounds were suspected of being hydrates because of additional peaks, not attributable to melting, around 100°C. The TGA profile of each compound shows a loss in weight around 100°C, which could be bound water or bound solvent. DVS should be able to determine whether the material is a hydrate or a solvate.

Ten other materials were tested from the hydrophilic series to investigate the water sorption characteristics of the model drugs and their amine salts as hydrophilicity increases: flurbiprofen, flurbiprofen tris, AMP2, AMP1 and tert-butylamine plus gemfibrozil, gemfibrozil tris, AMP2, AMP1 and tert-butylamine.

3.4.6.2 Materials and Experimental

A DVS-1 was used at Bristol Myers Squibb, Moreton, Wirral manufactured by Surface Measurement Systems. It has a 1.5 g capacity and a working temperature range of 5-45 °C. Commonly sample sizes of approximately 10 mg were used. The software was used to analyse the samples at 20 °C over 0-100% humidity, which was increased by increments of 10% after the equilibration of sample mass. The

experiment was set to equilibrate the mass at 0% humidity before increasing the humidity surrounding the sample to 100% humidity and then reducing the humidity to 0%. The duration of the experiment was determined by the time taken for the material's mass to equilibrate at a particular humidity; this can vary from 12-24 hours. The selected drugs and their salts were prepared as detailed in section 2.2.

3.4.6.3 Results and discussion

The results of the DVS study are displayed in table 3.11, below. The samples did not lose or gain a large amount of water over the period of the experiment. Etodolac AMP2 lost some weight when the humidity was reduced to 0%. This can be attributed to water that was calculated from the DSC and TGA experiments suggesting that etodolac AMP2 could be a monohydrate salt. The area below the dotted line on the DVS graph of etodolac AMP2 indicates loss of weight during the DVS experiment see figure 3.5.

Table 3.11 DVS analysis of a selection of model drugs and salts from 0-100% humidity over time.

Substance	Change in Mass (%)	Substance	Change in Mass (%)
Flurbiprofen	0.042	Gemfibrozil	0.04
F tris	0.2	G tris	0.37
F AMP2	1.30	G AMP2	0.05
F AMP1	0.25	G AMP1	2.00
F tert-butylamine	0.20	G tert-butylamine	0.13
E butylamine	0.20	I benzylamine	0.08
E AMP2	-0.05		

Ibuprofen benzylamine did not lose any weight when the surrounding humidity was reduced to 0%, this indicates that water is not present in the molecule and that any loss on heating detected with TGA is due to solvent, see figure 3.6. Ibuprofen benzylamine is therefore not a hydrate but a solvate. Residual acetonitrile, held within its structure, could be bound to the salt causing it to be released at a temperature higher than its boiling point (81-82 °C). Further investigation would be required to confirm which solvent is present in the ibuprofen benzylamine structure.

There was very little surface absorption of water with the other salts even though tris itself is hygroscopic. The largest change in mass was observed with gemfibrozil AMP1 and flurbiprofen AMP2 which show a slight hysteresis and over 1% change in mass over the humidity range. The salts would potentially be unstable at high humidities so should be kept at below 40% relative humidity. The remainder of the salts are quite stable to humidity which is shown by the limited hysteresis observed in the change in mass vs humidity graphs; none of these salts tested are hygroscopic which can be a common problem with salt formation (figures 3.6 to 3.8).

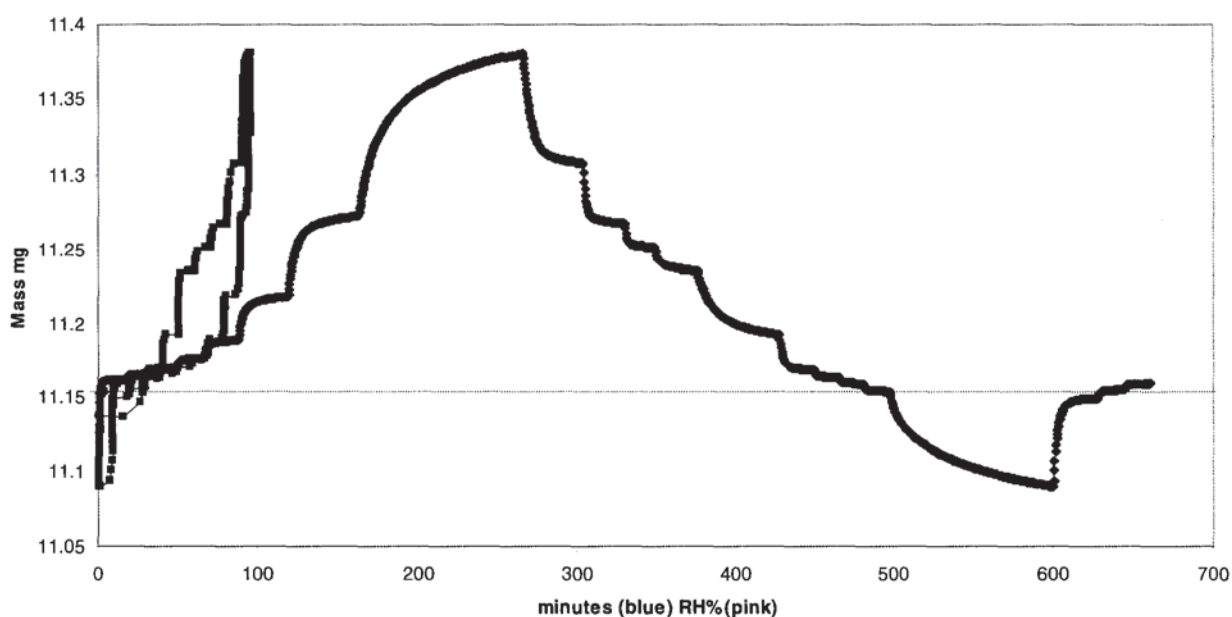


Figure 3.6 DVS data for etodolac AMP2 representing weight change over time and RH%

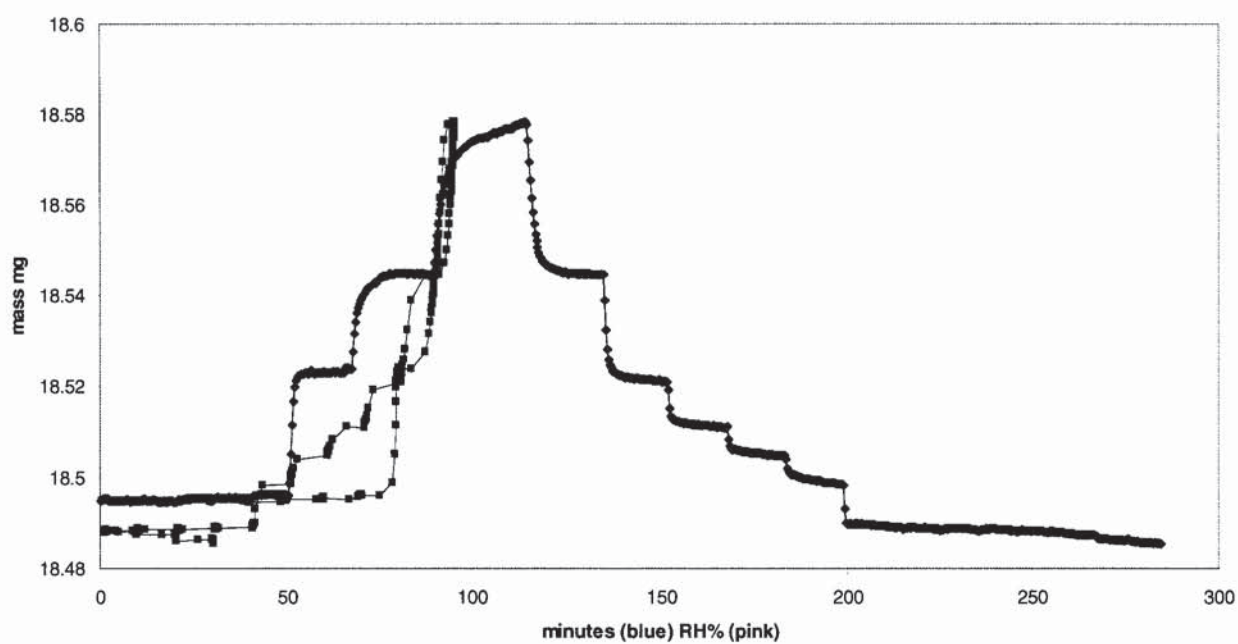


Figure 3.7 DVS data for ibuprofen benzylamine representing weight change over time and RH%

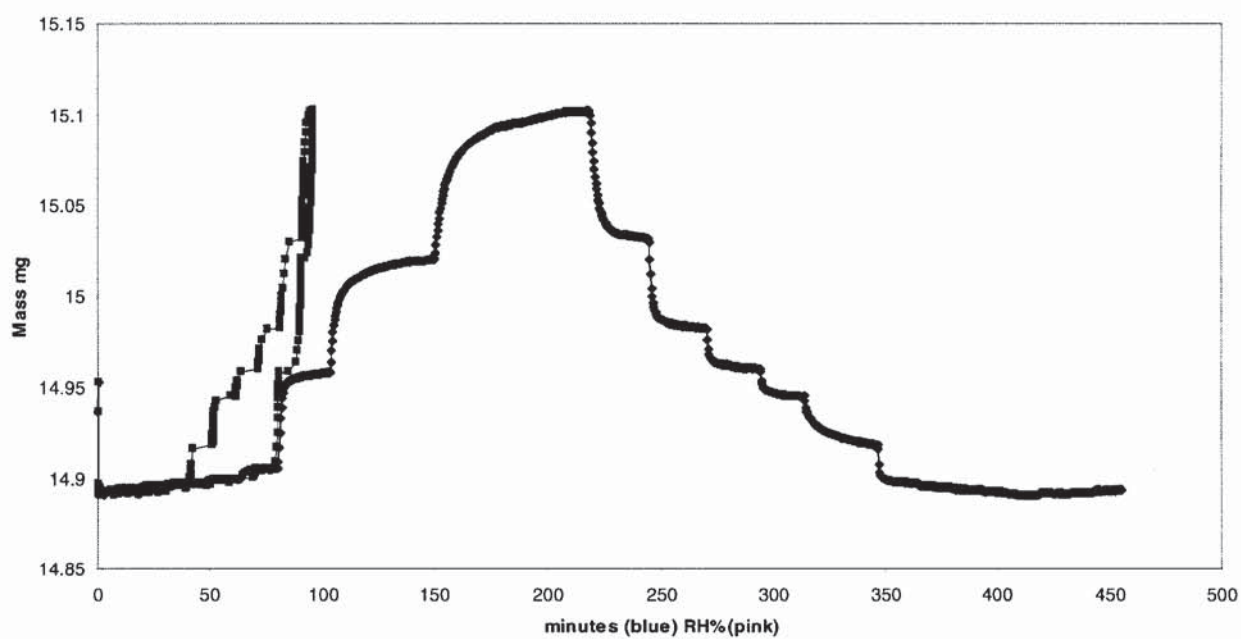


Figure 3.8 DVS data for etodolac butylamine representing change in weight over time and RH%

3.5 Physicochemical studies

3.5.1 Introduction

In order to understand the solubility and its influence on absorption processes, it is essential to understand the physicochemical properties of the materials under investigation. The aim of the previous section was to characterise the solid-state properties of the samples whereas this section was designed to explore the dissolution and solubility of the drugs and their salt forms.

The dependence of solubility on pH is discussed in depth in section 4 and it is imperative to understand the effect of pH on solubility of a particular drug before trying to modify its properties. Therefore, it was important to generate the pH-solubility profiles of all the drugs used.

The next step was to measure the saturated solubility of the prepared salts in water to determine whether solubility was increased by salt formation and to observe if there were any pH changes that could affect solubility. Solubility experiments were also performed at fixed pH to investigate if pH alone was the driving force of solubility enhancement.

Dissolution of the model drugs will be the rate-limiting step for drug absorption because they are classified as BCS class II (Amidon *et al.* 1995). Therefore the dissolution process is a very significant factor in influencing absorption and the potential for increasing the dissolution rate could lead to changing the classification of a drug/salt to BCS class I.

The aims of the dissolution experiments were to:

- Characterise the dissolution process using powdered samples in a specially constructed basket
- Study the effect of different pH conditions on dissolution of the powder samples
- Devise a suitable experiment to measure Intrinsic Dissolution Rate (IDR)

3.5.1.1 Theoretical considerations of the dissolution process

The dissolution process is often described by the Noyes-Whitney equation:

$$\frac{dm}{dt} = kA (C_s - C) \quad \text{equation 3.2}$$

where m is the mass of solute passed into the solution at time t , dm/dt represents the dissolution rate, A is the surface area of undissolved solid in contact with the solvent, C_s is the saturated concentration of the solute at a set temperature, C is the solute concentration at time t and k is the generalised first-order rate constant (IDR rate constant). When considering the Noyes-Whitney and interfacial barrier models, k is a generalised constant.

Higuchi et al. (1958) first proposed the diffusion layer theory; Mooney et al. (1980a) further developed the model and applied Fick's Laws of diffusion to calculate the pH values across the diffusion layer as dissolution occurs and to describe the initial dissolution rates of three carboxylic acids. In a second paper, they investigated the effect of buffer on the dissolution rate and concluded that reporting of acid dissolution rates is meaningless without reference to buffer pH and buffer concentration (Mooney et al., 1980b). Auinins et al. (1985) continued the theme and tested the model on three acidic drugs; they concluded that boundary layer thickness cannot be accurately calculated and this caused inaccuracies in the model.

The diffusion layer model (figure 3.9) assumes that a thin film of saturated solution of concentration C_s exists at the interface of the dissolving solid and diffusion medium. The dissolution rate is controlled by the diffusion of solute molecules from the saturated solution in the diffusion layer to the bulk solution. The concentration of the bulk solution is denoted by C_b , within the stagnant diffusion layer there is a concentration gradient from $x=0$ where the concentration is greatest (saturated) to $x=h$, where the concentration is the same as the bulk solution.

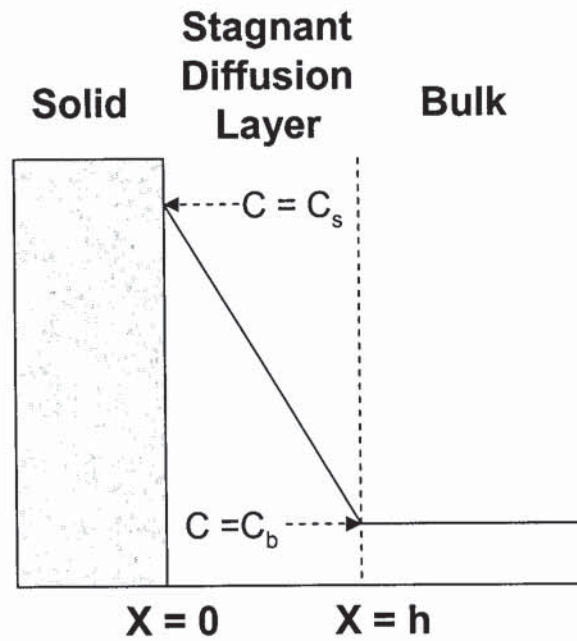


Figure 3.9 Diffusion layer model of drug diffusion

The Nernst-Brunner diffusion layer form of the Noyes Whitney equation (equation 3.2) defines the rate of dissolution as:

$$J = \frac{dm}{A \cdot dt} = \frac{D}{h} (C_s - C_b) \quad \text{equation 3.3}$$

where, J is flux which is defined as the amount of material m dissolved, and, therefore transported across the diffusion layer, in unit time per unit surface area A of the dissolving solid. D is the diffusion coefficient (equation 3.4). The boundary layer is affected by the hydrodynamic conditions, *i.e.* rate of stirring or shaking; size, shape and position of stirrer; volume of dissolution fluid; size and shape of container and viscosity of dissolution medium (Aulton, 1988; Macheras et al., 1995).

The diffusion coefficient can be described by the equation:

$$D = \frac{RT}{6Nr\pi\eta} \quad \text{equation 3.4}$$

where R is the universal gas constant, T is the absolute temperature, N is Avogadro's constant, η is the kinematic viscosity and r is the radius of the molecule in solution. From equations 3.2 and 3.3, the IDR rate constant, k is proportional to a change in drug concentration, surface area, concentration difference ($C_s - C$) and changes in the boundary layer.

Using the theoretical diffusion layer model, it is clear that dissolution volume can affect dissolution rate. In the stomach gastric emptying occurs which constantly varies the stomach volume, and allows the drug to dissolve in an infinitely dilute solution. This is best modelled in *in-vitro* simulations by using 'sink' conditions where the maximum value of C is a tenth of C_s . This reduces the variable ($C_s - C$), in equation 3.2 to the constant C_s (Macheras et al., 1995).

The Nernst-Brunner equation can be reduced under sink conditions to:

$$J \approx \frac{D}{h} C_s \quad \text{equation 3.5}$$

The surface area of the undissolved solid in contact with the dissolution medium is easily controlled during IDR experiments and can be removed from the equation 3.2 in order to simplify it. However, during the powder dissolution experiments, the surface area (A) of the powdered samples was not controlled, although the particles were ground to an observable homogeneity.

3.5.1.1 The theory of salt dissolution

The solubility of a weak acid can be improved by salt formation because this is because the basic moiety can affect the pH of the micro-environment of the drug. For weak acids the pH of the surrounding medium can hugely affect the saturated solubility, as demonstrated by the equation 3.6:

$$S = S_o + \frac{S_o K_a}{[H_3O^+]} \quad \text{equation 3.6}$$

where S is the solubility at the experimental pH and S_o is the intrinsic solubility. In the stomach contents, the pH can vary from approximately 2-4, depending on the fed and

fasted state or location and if the weak acid has a low pK_a (e.g. gemfibrozil pK_a 4.72) then dissolution will be limited by low solubility.

If a salt is formed, the pH of the micro-environment of the drug is buffered by the presence of basic ions. This creates an intermediary pH in the boundary layer of the micro-environment around the drug in which it can dissolve. Once the drug diffuses out of the boundary layer, it rapidly precipitates as a fine solid in the stomach contents as the pH is low. The drug will rapidly dissolve in the favourable pH of the intestine when emptied from the stomach and consequently will be absorbed (Macheras *et al.*, 1995). Theory states that salts do not provide a higher solubility at a given pH, because of the buffering capacity of the ionised form of the drug and the salt.

Higuchi *et al.* (1958) presented the simultaneous chemical reaction and diffusion (SCRD) model for the dissolution of benzoic acid into basic solution. The authors provided predictive equations for the IDR or flux. Higuchi *et al.* (1964) also reported an equation for the initial dissolution rate of the sodium salt of a weak acid dissolving in acidic medium, where at a low bulk pH, the self buffering capacity of the diffusion layer of the salt is overcome by the bulk pH and dissolution is low. Mooney *et al.* (1981) investigated dissolution kinetics of carboxylic acids into unbuffered media. The authors presented an extension to the SCRD model to represent the concentration of hydrogen ions at the surface of the solid. Their study concluded that the self buffering capacity of the dissolving acid increases with acid strength but can decrease with increasing pH of the bulk solution; this was attributed to an increase in $[OH^-]$ in the bulk but is probably due to the common-ion effect and the presence of an increased concentration of inorganic ion e.g. Na^+ , K^+ (see chapter 5). Aunins *et al.* (1985) extended the SCRD model to dissolution of carboxylic acids in buffered systems. They concluded that buffer capacity influences the pH of the boundary layer and hence affects dissolution. Buffer capacity is therefore an important parameter to consider when reporting dissolution rates.

3.5.1.2 The theory of salt solubility

Salts are amphoteric species containing both acidic and basic functional groups; they can exist as an uncharged species as both acidic and basic groups are ionised, termed zwitterions if present on the same molecule. Ionisation must be complete to give a stable salt form; if ionisation is not complete then the result is a mixture of two species which is unstable. To ensure stable salt, or ionic bond formation, the pKa difference between acid and base must be 4 units and the acid or base cannot be strong or the ionised state will be preferential (Stahl and Wermuth, 2002).

The process of dissolution is governed by the breaking of intermolecular interactions in the solid, the separation of solute molecules and the ability of the solvent molecules to enter the crystal lattice and form new interactions with the solute. The intermolecular bonds in a salt include ionic interactions, H-bonds and Van der Waals forces. Drug salts often contain strong electrophilic, or electron-withdrawing groups, together with large hydrophobic regions to create ion-dipole interactions in polar solvents, often water.

For salts the attractive force, F , between oppositely charged particles or ions is expressed by Coulomb's law:

$$F = \frac{q^+ \cdot q^-}{D \cdot d^2} \quad \text{equation 3.7}$$

where q^+ and q^- represent the electric charges on the particles or ions, d is the distance between them and D is the dielectric constant of the surrounding medium.

In solution the ions may dissociate which causes the ions to separate to give:



If the ions do not completely dissociate in solution then the equilibrium is said to be due to ion-pair formation. The ion-pair equilibrium is expressed as:



The association constant, K , is given by:

$$K = \frac{a_{AB}}{a_{A^-} \cdot a_{B^+}} \quad \text{equation 3.10}$$

where a_{AB} , a_{A^-} and a_{B^+} are the activities of the corresponding species. As K increases the potential for absorption of A-B increases, which can occur with hydrophobic interactions. Passive diffusion does not involve ion-pairs but the neutralising action of the ion-pair favours membrane permeation.

The enthalpy of solution ΔH_{sol} describes the energy of interactions as a solute dissolves, but the standard free energy, ΔG^θ , is related to solubility, C_s , by:

$$\Delta G_{sol}^\theta = -RT \ln C_s \quad \text{equation 3.11}$$

where R is the gas constant and T is the absolute temperature. The free energy is the net useful energy available for the reaction resulting from the total energy for the reaction minus energy lost to intermolecular force activity (friction). According to the Van't Hoff equation, the logarithm of the equilibrium constant (K_s) (e.g., solubility product) is a linear function of the reciprocal of the absolute temperature (K_0), shown by equation 3.12:

$$\ln K_s = \ln K_0 - \frac{\Delta H_{sol}}{RT} \quad \text{equation 3.12}$$

3.5.2 pH solubility profile of model drugs

3.5.2.1 Introduction

The pH solubility profile of a weakly acidic compound has two regions, Phase I and Phase II. In Phase I the total solubility is shown in equations 3.13 and 3.14:

$$S = [HA] + [A^-] \quad \text{equation 3.13}$$

$$S = S_o \left(1 + \frac{K_a}{[H^+]} \right) \quad \text{equation 3.14}$$

Where S is the total solubility at any given pH, S_o is the intrinsic solubility of the free acid, [HA] and [A] represent concentrations of the undissociated and dissociated forms, respectively, in solution, and K_a is the acid dissociation constant defined as equation 3.15:

$$K_a = \frac{[H^+].[A^-]}{[HA]} \quad \text{equation 3.15}$$

As the pK_a is approached and exceeded *i.e.* between pH 5-9 there is a rapid and continuous increase in solubility as predicted by equation 3.16:

$$pH - pK_a = \log \left\{ \frac{S - S_o}{S_o} \right\} \quad \text{equation 3.16}$$

The total solubility in Phase II is described as equation 3.17 and 3.18:

$$S = \left(1 + \frac{[H^+]}{K_a} \right) \sqrt{K_{sp}} \quad \text{equation 3.17}$$

$$K_{sp} = [X^+].[A^-] \quad \text{equation 3.18}$$

Where K_{sp} is the solubility product of the salt (Stahl and Wermuth, 2002).

This common ion effect where the pH solubility curve is split into two distinct phases has been previously reported by Anderson and Flora (1996) and observed for

flurbiprofen by Anderson and Conradi (1985) and for diclofenac acid (O'Connor and Corrigan, April 2001).

3.5.2.1 Materials

Model drugs were purchased as detailed in section 2.2.1. Hydrochloric acid, sodium hydroxide, potassium di-hydrogen orthophosphate, di-sodium hydrogen phosphate, orthophosphoric acid were purchased from Sigma-Aldrich (Poole, UK). All materials were of analytical or pharmaceutical grade as appropriate. Double distilled water was generated in-house using a Fison's Fi-Streem still.

3.5.2.2 Equipment

A Variomag electronic multipoint magnetic stirrer set at 500 rpm was used for sample preparation. HPLC equipment was used as detailed in section 2.1.1.2.

3.5.2.3 Methods

The saturated solubilities of etodolac, gemfibrozil, flurbiprofen and ibuprofen were determined using phosphate buffers in the pH range 5-9. The composition of the buffers is detailed in Appendix 3.4. Approximately 500 mg of drug were added to 20 ml of buffer, each experiment was performed in triplicate. The samples were stirred for at least 3 days under ambient conditions, during this time the vials were checked for solid and the pH was monitored. If the pH required altering, 0.1 M NaOH or 0.1 M phosphoric acid was added accordingly, dropwise to return the pH to the starting condition. If necessary, more drug was added to the samples if all the solid dissolved. Once the pH had stabilised and excess solid was present in all samples, 10 ml was removed with a plastic disposable syringe and filtered through a 25 mm diameter PTFE 0.45 μ m syringe filter, discarding the first 5 drops. Dilutions were made as appropriate with a micropipette and volumetric flasks, using solvent mix (acetonitrile:water 65:35) to dilute the samples. The samples were analysed by HPLC as detailed in section 2.2.

3.5.2.4 Results and discussion

The SPARC on-line calculator (<http://ibmlc2.chem.uga.edu/sparc/>) program calculates that etodolac and flurbiprofen have very similar pKa values (table 3.12) and that gemfibrozil has the highest pKa and that ibuprofen has pKa between that of

gemfibrozil and flurbiprofen. This information would suggest etodolac more soluble at a particular pH due to a greater degree of ionisation and gemfibrozil to be the least soluble at a particular pH.

Table 3.12 SPARC calculation of pK_a for the model drugs

Drug	SPARC pK _a calculation	Literature values
Etodolac	4.336	4.65
Flurbiprofen	4.346	4.22
Gemfibrozil	4.720	4.70
Ibuprofen	4.523	4.4, 5.2

The pK_a for each weak acid was calculated from the experimental solubility data. Equation 3.14, the solubility of a weak acid, was re-arranged to the equation of a straight line:

$$S = S_o + S_o \cdot K_a \cdot \frac{1}{[H^+]} \quad \text{equation 3.19}$$

Where, S is the solubility (y value) S_o is the intrinsic solubility (intercept) and S_o·K_a is the gradient. The pK_a can be calculated from the gradient.

The calculated pK_a values for each weak acid and the linear regression fit (R²) are listed in table 3.13.

Table 3.13 Table to indicate the calculated pK_a values for the weak acids used and their regression fit to theory.

Drug	Calculated pK _a	Regression fit
Etodolac	7.16	0.963
Flurbiprofen	4.52	0.934
Gemfibrozil	5.20	0.999
Ibuprofen	6.00	0.9998

Shaw (2001) reported an average solubility for ibuprofen of 0.05 mg/ml over the pH range 1-4. This value compares well, together with the whole solubility profile, with the experimental values reported in table 3.14. The pK_a calculation using the experimental data gives a good fit to theory ($r^2 = 0.9998$) yet it has an unexpected high pK_a value of 6.

The pK_a values calculated from the experimental data are higher than have been reported. Etodolac, calculated pK_a 7.14 and ibuprofen, calculated pK_a 6.0 are unrealistic values for weak carboxylic acids. Flurbiprofen and gemfibrozil have calculated pK_a values that are similar to literature. Phase I of the pH solubility curve was used in the calculation of pK_a for flurbiprofen. Experimental errors in measurement of accurate pH values and obtaining insufficient data points can help explain the inaccurate results.

Etodolac, gemfibrozil and ibuprofen have pH-solubility curves that follow equation 3.7 well ($r^2=0.963 - 0.9998$) (figures 3.11 to 13) , flurbiprofen (figure 3.10) has two phases in its pH solubility profile, after approximately pH 6 the overall solubility reduces as $[OH^-]$ increases. If a salt is formed above pH 6 then it will be the sodium salt as sodium hydroxide is used as the alkali. Therefore, excess Na^+ ions lead to the sodium salt of the weak acid forming, which has a lower solubility than the free acid and it precipitates out of solution. Bogardus and Blackwood (1979) noted that the salt and free form can exist in the solid state in equilibrium with the saturated solution. Therefore if the precipitate is collected it would contain both the free acid, flurbiprofen and the salt, flurbiprofen sodium. This phenomenon is called the common ion effect and is explained further in Chapter 4.

Table 3.14 The pH/solubility relationship for flurbiprofen and gemfibrozil in phosphate buffer solutions. Results are the mean of 3 replicates \pm SD.

Flurbiprofen		Gemfibrozil	
Buffer pH	Solubility mg/ml	Buffer pH	Solubility mg/ml
5.10	0.089 \pm 0.011	4.10	0.0007 \pm 0.0001
5.89	0.370 \pm 0.020	5.00	0.0023 \pm 0.0009
5.50	2.834 \pm 0.047	5.50	0.0032 \pm 0.0006
6.63	4.067 \pm 0.040	6.00	0.0137 \pm 0.0008
6.67	4.459 \pm 0.029	6.50	0.0381 \pm 0.0005
6.69	4.484 \pm 0.044	7.00	0.0973 \pm 0.0028
7.20	6.684 \pm 0.008	8.00	2.9630 \pm 0.0807
8.00	6.809 \pm 0.301	9.00	4.8723 \pm 0.2653
9.64	6.531 \pm 0.412		

Table 3.15 The pH/solubility relationship for etodolac and ibuprofen in phosphate buffer solution. Results are the mean of 3 replicates \pm SD.

Etodolac		Ibuprofen	
Buffer pH	Solubility mg/ml	Buffer pH	Solubility mg/ml
4.94	0.085 \pm 0.133	4.17	0.054 \pm 0.004
5.97	2.114 \pm 0.399	4.51	0.077 \pm 0.012
7.01	15.075 \pm 1.926	5.03	0.176 \pm 0.013
7.52	27.345 \pm 1.930	5.45	0.258 \pm 0.082
7.93	51.830 \pm 2.309	6.10	1.624 \pm 0.284
		6.94	10.758 \pm 0.461

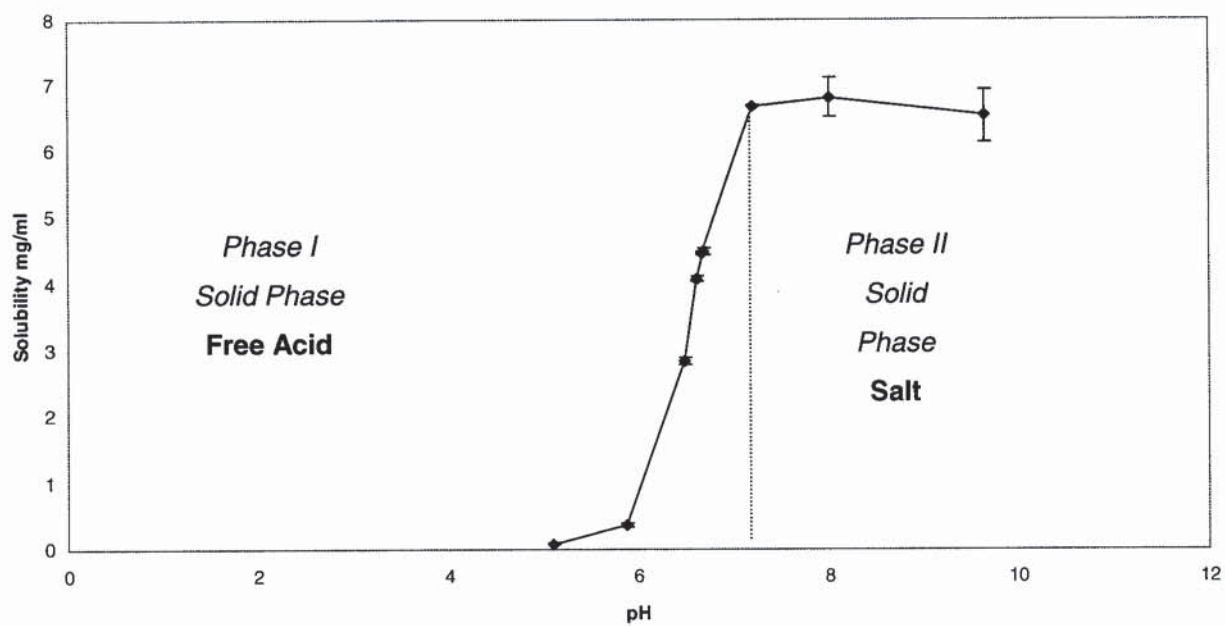


Figure 3.10 The solubility/pH profile for flurbiprofen n=3; mean \pm SD.

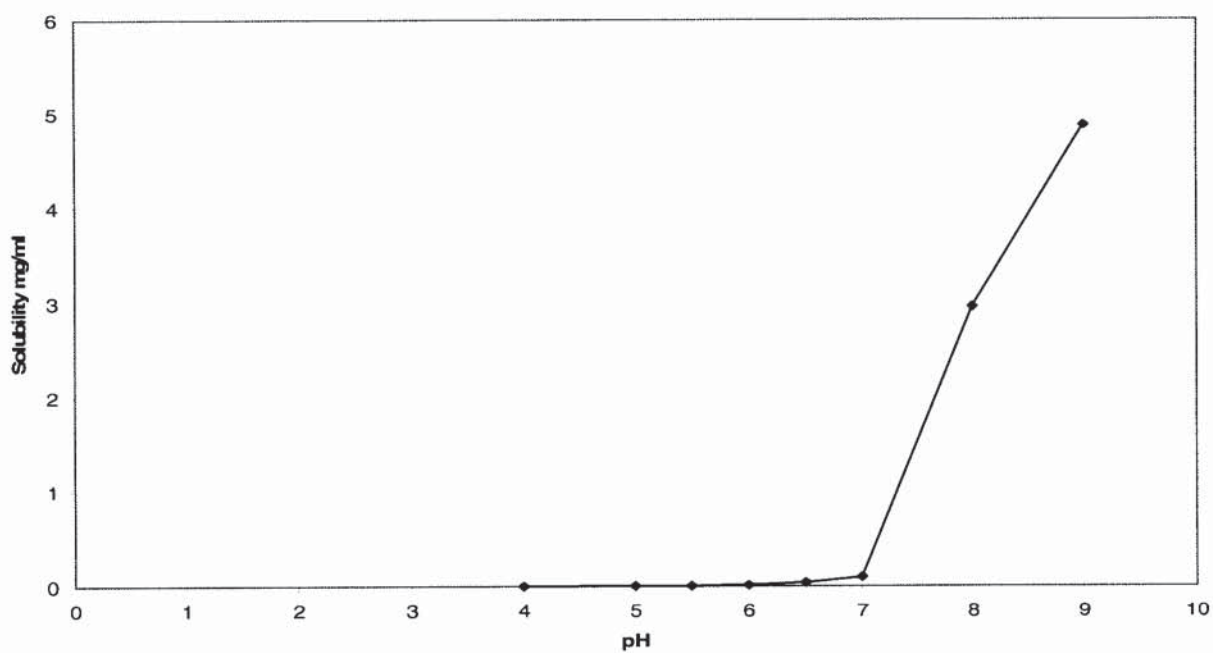


Figure 3.11 The solubility/pH profile for gemfibrozil n=3; mean \pm SD.

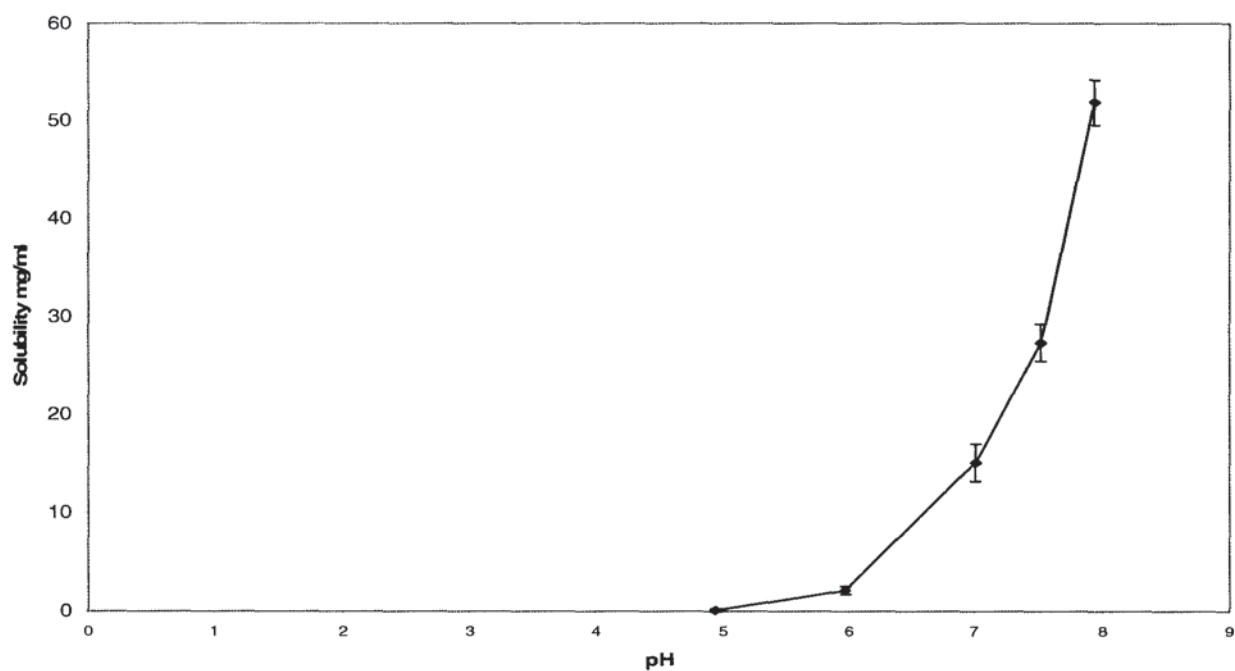


Figure 3.12 The solubility/pH profile for etodolac n=3; mean \pm SD.

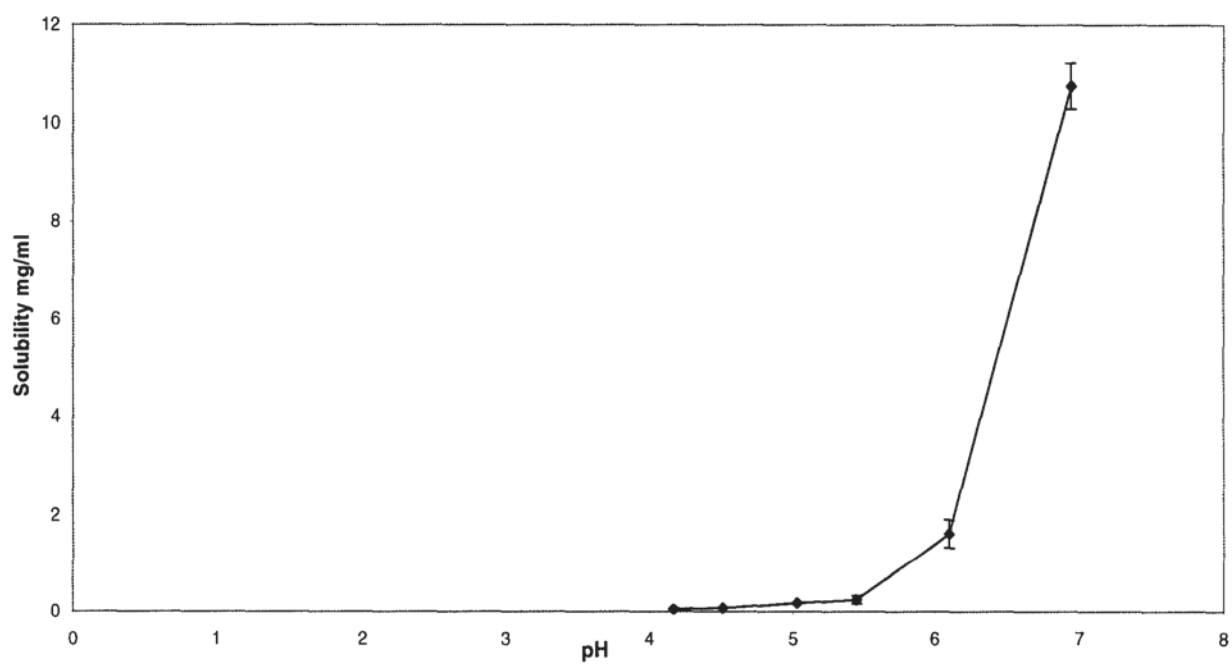


Figure 3.13 The solubility/pH profile for ibuprofen n=3; mean \pm SD.

3.5.3 Saturated solubility of model drug and salt in water

3.5.3.1. Materials and Experimental

All materials were used as in section 2.2. A Variomag electronic multipoint magnetic stirrer set at 500 rpm was used for sample preparation. HPLC equipment was used as detailed in section 2.1.1.2.

3.5.3.2 Methods

The saturated aqueous solubilities of model drugs and prepared salts were determined under ambient conditions. Excess solid was added to 15 ml of water and stirred for at least 24-48 hours. The experiment was performed in triplicate. After this time the pH was measured and 10 ml was extracted with a plastic disposable syringe. The sample was filtered through a 0.45 μm PTFE syringe filter and diluted, if necessary, with solvent mix (acetonitrile: water 65:35) using pipettes and appropriate volumetric flasks. The samples were analysed by HPLC.

3.5.3.3 Results and discussion

The measured saturated aqueous solubilities are in tables 3.16 to 3.18 and figures 3.13 and 3.14. They illustrate that solubility of the model drug is increased in all cases by salt formation, the degree of enhancement dependant on model drug and counterion. Each counterion increased model drug aqueous solubility from a minimum of 3.5-fold, for ibuprofen benzylamine to a maximum of 2801-fold, for ibuprofen AMP2.

The molar saturated aqueous solubility of gemfibrozil is markedly lower than for the other drugs: etodolac, flurbiprofen and ibuprofen (table 3.16). Generally, the results from the studies are discussed in mg/ml although it is more accurate when comparing the results to use moles/l (M). When the results are converted to moles/l (M) the same rank order is observed with comparative increase factors (tables 3.17 and 3.18). The results in these studies are assessed in terms of overall rank order; therefore it was sufficient to discuss and present the results in mg/ml.

Table 3.16 Aqueous solubilities of the drugs and their amine salts as molar concentrations.
Results are calculated from mean values

	Etodolac and salt Molar solubility (M)	Gemfibrozil and salt Molar solubility (M)	Flurbiprofen and salt Molar solubility (M)	Ibuprofen and salt Molar solubility (M)
Drug	7.72×10^{-4}	8.79×10^{-5}	1.35×10^{-4}	3.45×10^{-4}
Butyl	0.489	0.111	5.99×10^{-4}	0.583
Pentyl	0.0394	0.0172	0.0227	0.0424
Hexyl	0.0151	0.0106	0.00811	0.0200
Octyl	3.69×10^{-3}	2.32×10^{-3}	1.72×10^{-3}	4.93×10^{-3}
Benz	8.01×10^{-3}	7.45×10^{-3}	8.12×10^{-43}	7.99×10^{-4}
Cyclo	0.0126	9.94×10^{-3}	1.08×10^{-3}	9.84×10^{-5}
Tert	0.0435	0.0243	8.74×10^{-3}	0.180
AMP1	0.199	0.0353	0.0348	0.458
AMP2	0.510	0.0219	0.0255	0.643
Tris	0.248	0.0228	0.0304	0.0274

Considering the homologous series of salts (figure 3.14):

In general there is a solubility enhancement order for salts of all drugs, from highest to lowest (i.e. butylamine>pentylamine>hexylamine>octylamine). This is reflected by the reducing increase factor as the chain length increases. As the chain length increases the lipophilicity and hydrophobicity of the counterion increases and solubility reduces. If this data is coupled with the melting point information from the DSC (section 3.4.2) then a trend is found with solubility and melting point, that as melting point reduces, solubility is also reduced. This contradicts the attractive notion that as melting point reduces solubility increases due to the reduced energy required to break the crystal lattice. This simple theory does not fit because salts are complex molecules containing covalent, ionic bonds and many different types of attractive intermolecular forces that require disruption for dissolution to occur. As chain length increases the lipophilicity and oiliness increases and this seems to be the driving force for solubility in this series.

Table 3.17 The saturated aqueous solubilities, corresponding pH values and the solubility increase factor of the amine salts of etodolac and gemfibrozil. * indicates measured solubility value. Results are the mean of 3 replicates \pm SD.

Material	Etodolac			Gemfibrozil		
	Solubility mg/ml	Measured pH	Increase factor	Solubility mg/ml	Measured pH	Increase factor
Drug	0.222 \pm 0.097	4.42	-	0.022 \pm 0.008	5.40	-
Butylamine	17.62 \pm 0.21	6.78	79.1	35.93 \pm 1.81	8.70	1649.6
Pentylamine	14.75 \pm 0.05	6.84	66.2	5.76 \pm 0.09	8.10	265.38
Hexylamine	5.86 \pm 0.16	6.79	26.3	3.73 \pm 0.06	7.80	171.14
Octylamine	1.53 \pm 0.01	6.42	6.9	0.88 \pm 0.01	7.50	40.2
Benzylamine	3.16 \pm 0.03	6.97	14.2	2.66 \pm 0.03	8.60	122.2
Cyclohexylamine	4.87 \pm 0.04	7.30	21.9	3.47 \pm 0.18	7.10	159.0
Tert-butylamine	15.69 \pm 0.50	7.34	70.4	7.86 \pm 0.27	7.60	357.3
AMP1	74.65 \pm 3.77	8.68	334.9	11.76 \pm 1.53	7.70	534.6
AMP2	N/A *		897.3	30.25 \pm 0.99	7.70	1375
Tris	101.03 \pm 0.86	7.26	453.3	8.46 \pm 0.49	7.50	384.6

Table 3.18 The saturated aqueous solubilities, corresponding pH values and the solubility increase factor of the amine salts of flurbiprofen and ibuprofen. * indicates measured solubility. Results are the mean of 3 replicates \pm SD.

Material	Flurbiprofen			Ibuprofen		
	Solubility mg/ml	Measured pH	Increase factor	Solubility mg/ml	Measured pH	Increase factor
Drug	0.033 \pm 0.014	4.20	-	0.071 \pm 0.002	3.67	-
propylamine	13.16 \pm 0.341	7.43	398.8			
butylamine	5.39 \pm 0.220	7.2	162.5	162.66 \pm 8.645	8.37	2278.2
pentylamine	7.17 \pm 0.357	7.30	216.4	12.42 \pm 0.081	7.64	174.0
hexylamine	2.60 \pm 0.069	6.44	78.3	6.15 \pm 0.471	7.73	86.2
octylamine	0.56 \pm 0.009	6.50	17.0	1.65 \pm 0.548	7.19	23.1
benzylamine	2.85 \pm 0.198	7.00	86.0	0.25 \pm 0.196	7.35	3.5
cyclohexylamine	0.37 \pm 0.149	7.56	11.4	1.03 \pm 0.034	6.43	14.5
tert-butylamine	2.77 \pm 0.083	6.00	83.6	5.02 \pm 0.048	6.53	70.3
AMP1	8.94 \pm 1.430	6.70	270.9	135.00 \pm 28.058	8.21	1900.8
AMP2	11.56 \pm 1.244	6.70	350.3	N/A*		2801.1
Tris	11.16 \pm 2.351	6.8	338.2	8.97 \pm 0.156	6.67	125.6

Benzylamine and cyclohexylamine are very closely related structurally; they are both of similar size differing only because cyclohexylamine has a saturated ring and in benzylamine, the ring is unsaturated. Each salt has an increased solubility compared to the parent drug but cyclohexylamine gives the greater enhancement of solubility in all cases. The enhancement of solubility is in the range of 3.5-158-fold; the cyclohexylamine and benzylamine are not as effective at improving solubility as the butylamine or the hydrophilic counterions (AMP1, AMP2 and tris). Cyclohexylamine and benzylamine salts are easy to crystallise and both have high melting points, indicating good stability. Cyclohexylamine salts have higher melting points and are slightly more lipophilic than the benzylamine salts so these parameters are not controlling solubility.

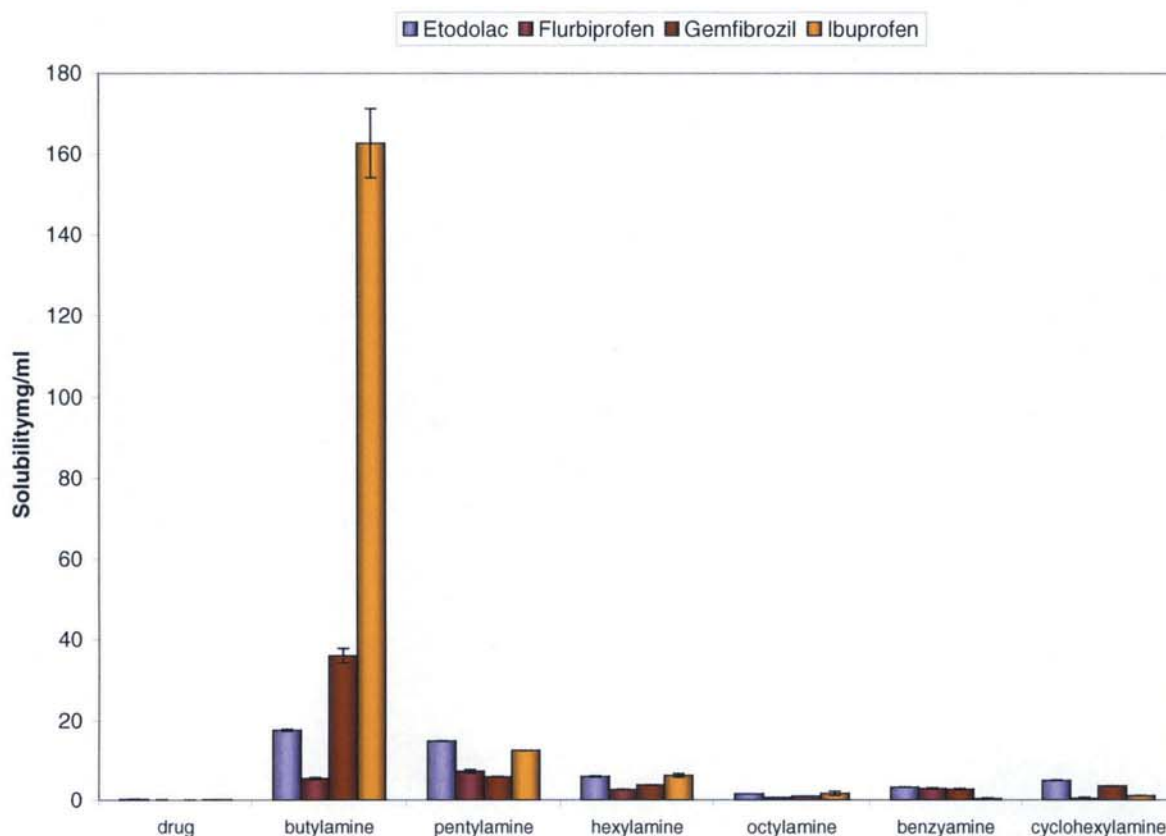


Figure 3,14 The saturated aqueous solubility of etodolac, flurbiprofen, gemfibrozil and ibuprofen and their amine salts. (n=3; mean \pm SD)

The hydrophilic series used consisted of tert-butylamine, AMP1, AMP2 and tris salts. They are termed 'hydrophilic' because of the increasing number of hydroxyl groups

within the molecules, from zero to three. Figure 3.15 demonstrates the effect of the hydrophilic counterions on the model drugs. The tert-butylamine counterion results in a 70-357-fold increase in solubility for the range of drugs. The addition of a single hydroxyl group increases the solubility of the parent molecule from 271-fold to 1901-fold; which is a substantial improvement in solubility compared to the tert-butylamine salts. As additional hydroxyl groups are added to the counterion (AMP2 salts), there is a large increase in solubility, from 349-2801 fold, an increase factor similar to that of the butylamine counterion. There is no further improvement in solubility as additional hydroxyl groups (tris) are added. This result was also reported by Anderson and Conradi (1985) with a range of flurbiprofen salts and O'Connor and Corrigan (2001) using diclofenac salts, they both used the tert-butylamine, AMP1, AMP2 and tris counterions. As the number of hydrophilic groups increases the hydrophilicity increases and this was predicted to improve solubility, this is true for the addition of one or two hydroxyl groups. As the number of hydroxyl groups increases, the potential for hydrogen bonding increases. It is possible that the tris salt structures form complex intermolecular forces which are more difficult to break, resulting in inhibited dissolution.

For two salts within this study; etodolac AMP2 and ibuprofen AMP2, it was not possible to obtain a saturated aqueous solution. For these samples a measured solubility was used to demonstrate the effect of the AMP2 counterion on solubility; with the concentration increasing to beyond 200 mg/ml, "foaming" was observed. These materials were predicted to demonstrate surfactant-like properties (Chapter 5).

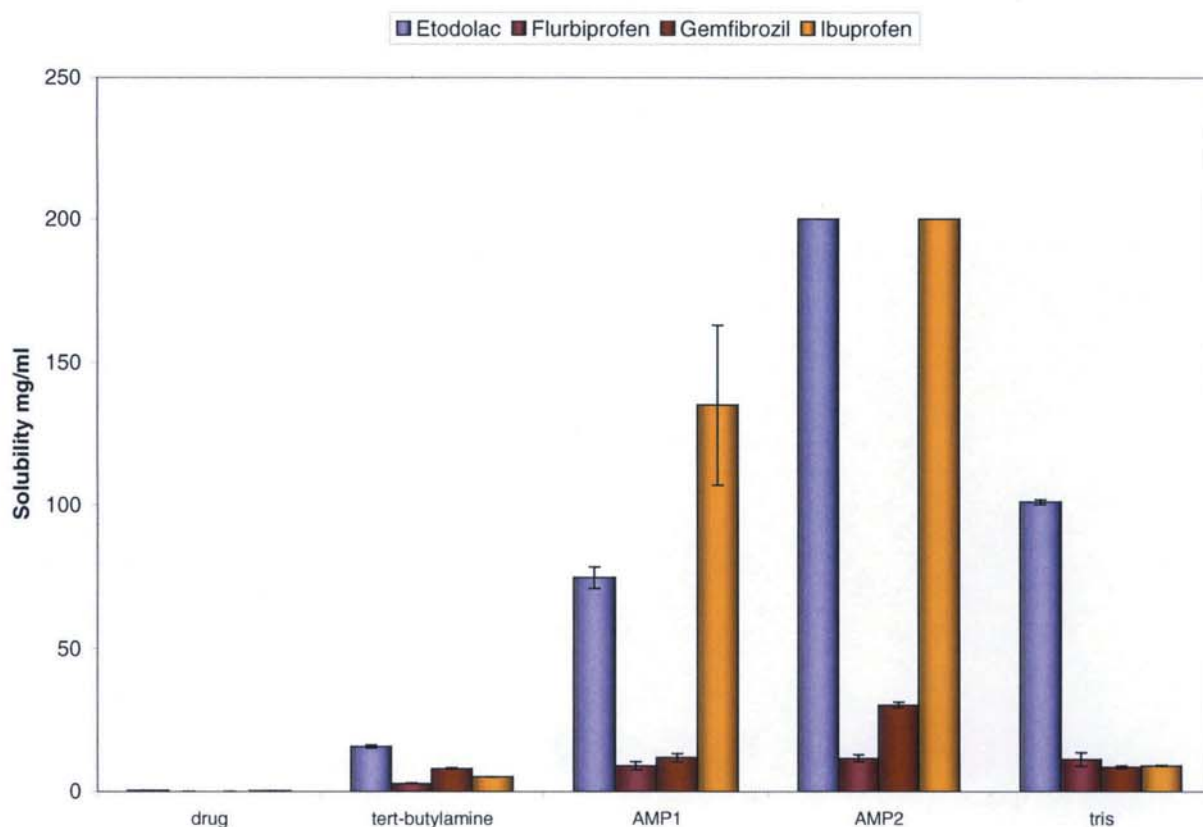


Figure 3.15 The saturated aqueous solubilities of etodolac, flurbiprofen, gemfibrozil and ibuprofen and their hydrophilic amine salt. (n=3; mean \pm SD)

3.4.3.4 Relating solubility to physicochemical characteristics

3.4.3.4.1 pH-solubility relationships

The butylamine counterion consistently increases the solubility of the parent compound by the greatest extent, and a trend can be seen within the homologous series (butylamine-octylamine) that solubility is reduced as chain length increases. The butylamine counterion also has the ability to increase the pH of the saturated solution to over 8 for ibuprofen and gemfibrozil and to around pH 7 for flurbiprofen and etodolac, whereas the pH of saturated solutions containing the longer-chained counterions is lower. The increase in pH appears to be dependent on the nature of the model drug not power of the amine counterion. However, the increase in solubility observed with the gemfibrozil butylamine salt far exceeds the predicted solubility from the pH solubility profile (table 3.19) at the pH of the saturated solution.

Table 3.19 The saturated aqueous solubility and measured pH values against the solubility data from the pH-solubility profiles of each drug, etodolac, flurbiprofen, gemfibrozil and ibuprofen.

	Aqueous solubility of the butylamine salt (pH solubility curve)		Saturated aqueous solubility of the butylamine salt	
	Buffer pH	mg/ml	pH of solution	mg/ml
Etodolac	7.01	15.08	6.78	17.62
Flurbiprofen	7.20	6.68	7.20	5.39
Gemfibrozil	9.00	4.87	8.70	35.93
Ibuprofen	8.00	No data	8.37	162.66

The pH of the saturated solutions of each salt is an indication of the pH of the boundary layer when the salt dissolves. As the butylamine counterion confers the highest pH solution it has the highest solubility, it is the stronger base of all the amine counterions because the molecule is small and the basic charge is spread evenly over the surface of the molecule. As the chain length increases through the series the basic charge has a larger area to spread over and becomes weaker.

Although the question remains; can salts improve solubility and dissolution in low pH conditions where the drug would be expected to precipitate out?

For ibuprofen and etodolac AMP2 salts, (table 3.16 and 3.17) the pH of the saturated solution has no influence on solubility, therefore other mechanisms must be responsible for the massive increase in solubility observed, (Chapter 5).

Rubino (1989) looked at the solubility and solid state properties of a range of sodium salts of drugs. The solid phase after equilibrium with water was collected and discovered to be a hydrate; the solubility was inversely related to the molar amounts of water in the crystal. No comment was made about the prediction of potential hydrate formation as a means of improving solubility. Although Rubino (1989) found that in-situ hydrate formation affects solubility, if the starting material is a hydrate (etodolac AMP2) then enhanced solubility is observed. Therefore the enhanced solubility of etodolac AMP2 could be because it is a monohydrate although it is likely other mechanisms are also involved (Chapter 5)

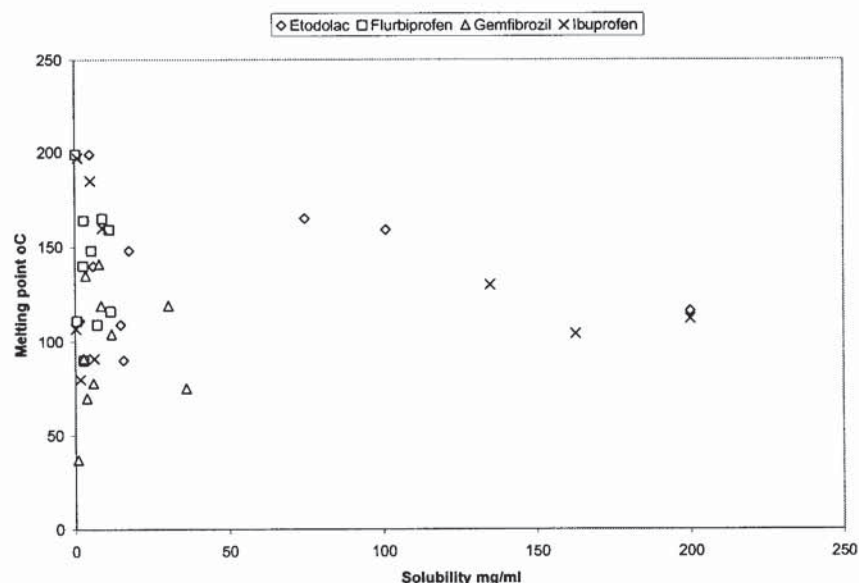
O'Connor and Corrigan (2001b) showed for a range of diclofenac salts including benzylamine, tert-butylamine, AMP1, AMP2 and tris, that there was a linear log-log relationship between $[H^+]$ and salt solubility. Solubility was related to pH for a basic drug by Ledwidge (1997). In this study the pH of the saturated solution was plotted against the logarithm of salt concentration for each of the model drug salt series and a linear relationship for etodolac ($R^2=0.7049$ $n=10$), flurbiprofen ($R^2=0.45$ $n=10$), gemfibrozil ($R^2=0.6922$ $n=10$) and ibuprofen ($R^2=0.7049$ $n=10$) was observed.

3.5.3.4.2. Relationships between salt melting points and solubility

It has been observed that salt melting point has an inverse linear relationship with the logarithm of salt solubility for a series of secondary amine hydrochloride salts ($n=8$) (Thomas and Rubino, 1996). Ledwidge reported a similar relationship for a series of salts of an experimental basic drug CEL50 ($n=7$). A direct relationship between the inverse of the melting point and the logarithm of the solubility for a range of salts of a basic anti-malarial drug was observed by Agharakar *et al.*, 1976. Anderson and Conradi (1985) reported a non-linear relationship between the salt melting point and $\log K_{sp}$ (stoichiometric solubility) for a series of flurbiprofen salts ($n=6$). O'Connor and Corrigan (2001b) observed a trend between salt melting point and the logarithm of the solubility ($n=8$) and between the inverse of the melting point and the logarithm of the solubility ($n=8$) for a selection of amine salts of diclofenac.

Conversely, Gu and Strickley (1987) concluded that no simple solubility-melting point relationship could be established for tris(hydroxymethyl)aminomethane salts of four anti-inflammatory drugs.

Figure 3.16 Relationship between melting point and solubility for a range of amine salts for the drugs etodolac, flurbiprofen, gemfibrozil and ibuprofen.



Within the range of amine salts studied here (etodolac ($n=10$), flurbiprofen ($n=11$), gemfibrozil ($n=10$) and ibuprofen ($n=10$)), no relationship was found between salt melting point and solubility (figure 3.16).

This suggests, together with experimental results from Gu and Strickley (1987) that melting point relationships are complex when considering salts, which are a combination of covalent bonds, ionic bonds and intermolecular forces. Whereas the melting points of covalently bonded molecules can be related to aqueous solubility, once another molecule is added by ionic bonds this alters the melting point characteristics in an unpredictable way.

3.5.4 Contact-angle measurements

3.5.4.1 Introduction

Camtel Instruments LTD performed two experiments at their head office in Royston which investigated the contact angle of water when it was dropped on a powder sample of model drug or salt. Gemfibrozil was selected because of its low aqueous solubility (0.022 mg/ml) and gemfibrozil butylamine was selected because of its high solubility (35.94 mg/ml). A drop shape analyser was used to measure the surface tension and contact angle with video-based analysis.

The sessile drop technique has been used for estimating the surface energy of pharmaceutical powders (Ahfat et al., 2000). However, traditionally powders required compression into disks or compacts; this approach is not ideal because of variation in porosity and changes in the surface energy. Neumann and Good (1979) reported that the presence of pores in the surface of the compact leads to sessile drop penetration over time. Experiments with sulphathiazole showed that if compacts retain their properties on compression, reliable surface energies can be determined by video microscopy (Muster and Prestidge, 2002).

Muster and Prestidge (2002) used video microscopy to evaluate wetting of compacts which is how the Camtel apparatus measures the contact angle, based on Young's theory and the interfacial tensions of the solid-liquid. Once the surface tension is known, which can be calculated from the drop weight method (Adamson, 1990), contact angle can be easily measured and observed with a video with high magnification.

It is clear to see that the production of compacts is undesirable because many powders are difficult to compress and may laminate or produce uneven surfaces on which the liquid drop will land. A new method of measuring the contact angle and wettability of pharmaceutical powders involves letting an aqueous droplet fall onto a thin film of powdered sample. This process is videoed by time lapse photography and the contact angles on either side of the droplet are measured over time.

3.5.4.2 Materials

Gemfibrozil was supplied by DiPharma (Italy) and gemfibrozil butylamine was made in-house by the method detailed in section 2.2.

3.5.4.3 Equipment

An FTA-100 series Drop Shape Analyser was used to measure both contact angles and surface tension by capturing snapshots or movies of the droplet. Contact angles can be measured from 0-180°; low angle images may be difficult to measure although this can be achieved manually.

3.5.5.4. Method

A thin film of powder was placed in the sample holder and a drop of water was introduced to the sample by pressing a button or turning a knob to dispense. The software automatically analyses the drop shape and computes the contact angle. The experiment was performed twice for each material.

3.5.4.5 Results and discussion

The contact angle of gemfibrozil butylamine dramatically reduced over time from around 80° to 14° over about 0.4 seconds (figure 3.17). Gemfibrozil butylamine is very hydrophilic and wets easily, this is confirmed by its high aqueous solubility. A DVD included in an envelope on the inside cover of this thesis for a video of the contact angle measurement over time. It requires Real Player viewer to open the document.

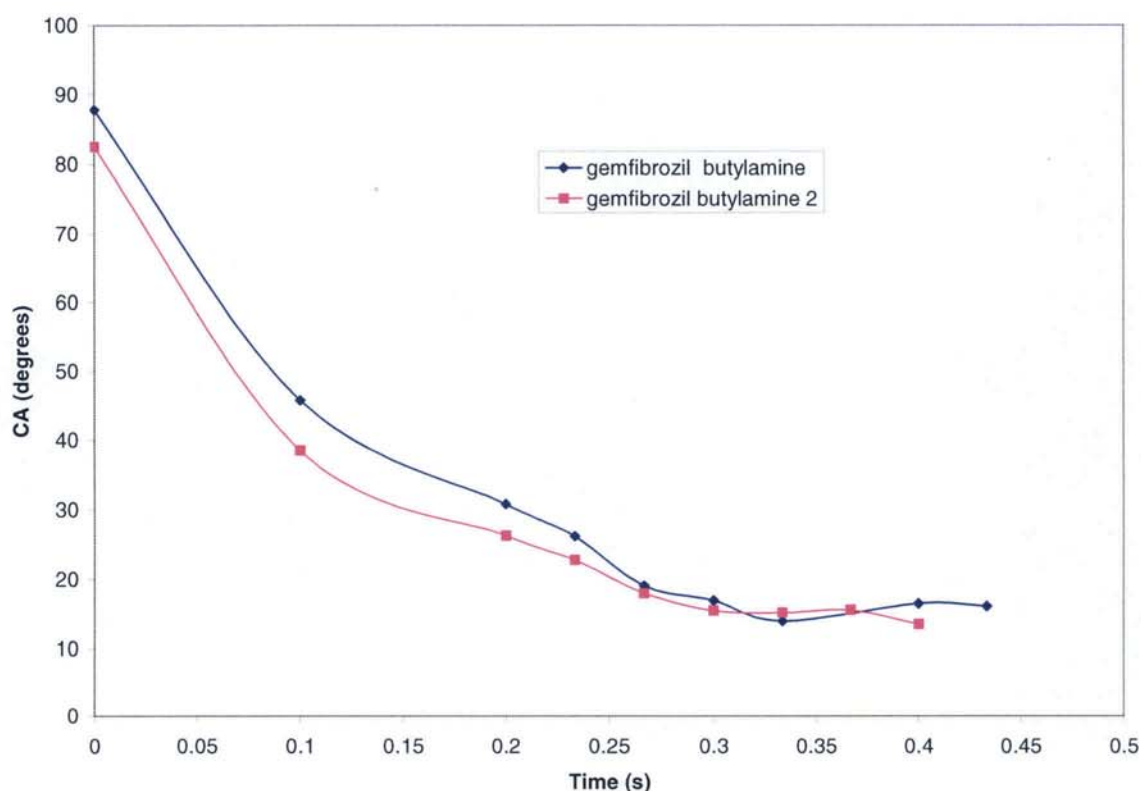


Figure 3.17 Contact angle (CA) measurements for gemfibrozil butylamine (n=2) in seconds (s).

Gemfibrozil was observed for 60 seconds and over this time the contact angle remained relatively constant (figure 3.18). The contact angle was 121° at the start of the experiment and was 105° at the end of the 60 seconds, a substantially reduced change than for gemfibrozil butylamine. The movie of this experiment shows the

water droplet remains on top of the powder for the duration of the experiment, whereas for gemfibrozil butylamine, the droplet is absorbed into the powder. Gemfibrozil is determined to be hydrophobic with this experiment in accordance with its low solubility in water (0.022 mg/ml).

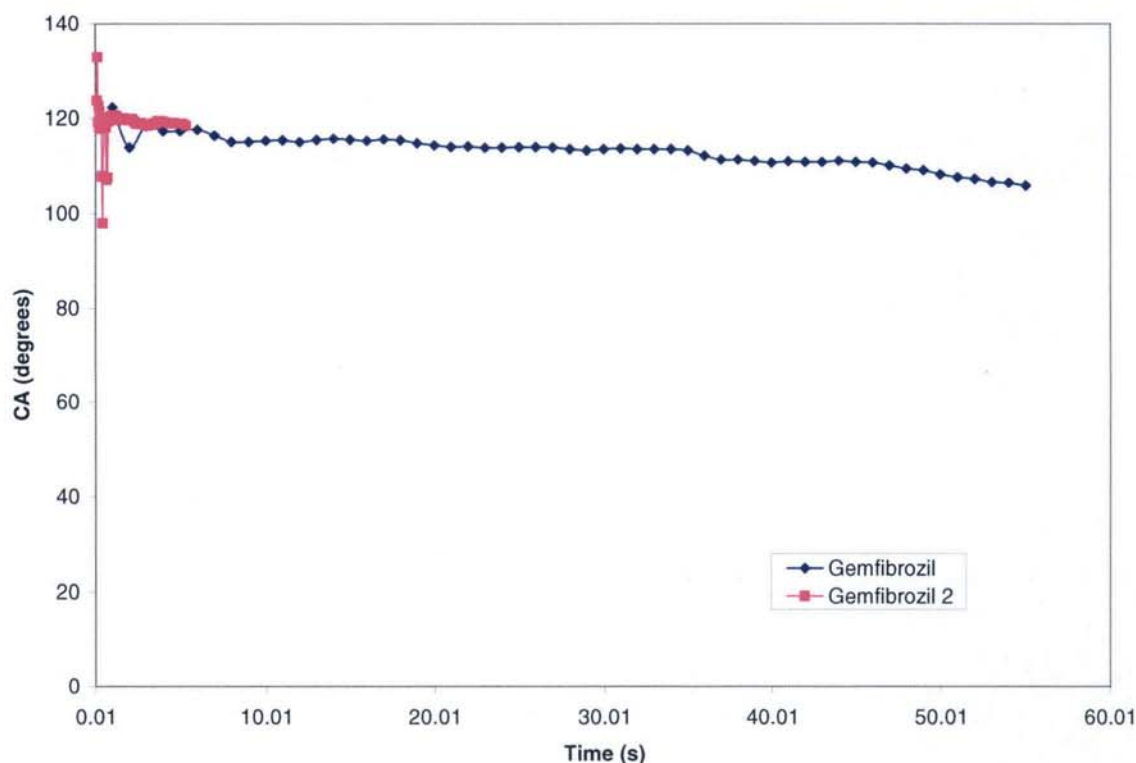


Figure 3.17 Contact angle (CA) measurements for gemfibrozil (n=2) in seconds (s).

The results of these experiments confirm that gemfibrozil is poorly wettable and consequently has a low water solubility and the salt gemfibrozil butylamine is very easily wettable and also has a high water solubility. It is difficult to draw any further conclusions because of the small data set and ideally experiments would have been repeated at least three times to achieve a definitive result. It would have been beneficial to analyse all of the salts to see if the contact angles, or wettability results were related to solubility.

3.5.5 Estimation of solubility using the SPARC on-line calculator

The SPARC online calculator was used to calculate the approximate theoretical solubility of the drugs and salts used in the previous experiments. The calculator has successfully been used previously by Letinski *et al.* (2002) for the structure-property model predictions of solubility with alcohols and diesters. The paper describes

experimental data for aliphatic alcohols and phthalate and adipate diesters using a slow stir water solubility test method and compares them with calculated predictions. Due to unreliable solubility data because of emulsion formation and phase separation, two quantitative structure property models SPARC (Kariakhoff et al. 1991) and WSKOWWIN (Meylan et al. 1996) together with a novel solubility method which avoided such problems were used to calculate the water solubility range of the selected alcohols and diesters. The SPARC model estimates agreed more closely with the measured values than the WSKOWWIN model. The SPARC data was found to fit the experimental data better, from a linear regression of the data. The SPARC model uses molecular properties to calculate an estimated solubility whereas the WSKOWWIN model requires octanol/water partition coefficient data to estimate solubility.

The SPARC model was therefore chosen to estimate the aqueous solubility of the drug and salts used in the following experiments.

3.5.5.1 Method

The SPARC online calculator can be found at <http://ibmlc2.chem.uga.edu/SPARC/> and at the home page selection of Properties, then Options and Solubility leads to the online calculator. A calculation is performed by selecting SMILES and input of the molecules structure using the SMILES abbreviated form and click on Calculate. SPARC requires the melting point of the molecule to calculate the water solubility in mg/l.

3.5.5.2 Results

The results from the calculator clearly do not agree with the experimental values by at least 1000-fold for the salts (table 3.20 and 3.21). The estimated solubilities of the drugs are closer to experimental but still approximately 10-fold different for etodolac. The drug with the highest estimated solubility is ibuprofen but etodolac has the highest experimental solubility

Table 3.20 SPARC versus measured aqueous solubilities (mg/ml) of etodolac and flurbiprofen salts (n=3; mean; \pm SD) under ambient conditions.

Material	SPARC solubility	Actual solubility	Material	SPARC solubility	Actual solubility
Etodolac	0.0292	0.222 \pm 0.097	Flurbiprofen	0.0177	0.033 \pm 0.014
E butylamine	0.00609	17.62 \pm 0.208	F butylamine	0.0000353	5.39 \pm 0.220
E pentylamine	0.00345	14.75 \pm 0.054	F pentylamine	0.0000235	7.17 \pm 0.357
E hexylamine	0.000782	5.86 \pm 0.161	F hexylamine	0.0000119	2.60 \pm 0.069
E octylamine	0.000119	1.53 \pm 0.007	F octylamine	0.00000443	0.56 \pm 0.009
E benzylamine	0.00146	3.16 \pm 0.028	F benzylamine	0.0000435	2.85 \pm 0.198
E cyclohexylamine	0.00406	4.87 \pm 0.038	F cyclohexylamine	0.0000828	0.37 \pm 0.149
E tert butylamine	0.0308	15.69 \pm 0.497	F tert butylamine	0.000245	2.77 \pm 0.083
E AMP1	0.144	74.65 \pm 3.774	F AMP1	0.00800	8.94 \pm 1.430
E AMP2	1.882	N/A	F AMP2	0.144	11.56 \pm 1.244
E tris	1.048	101.03 \pm 0.855	F tris	0.341	11.16 \pm 2.351

Table 3.21 SPARC versus measured aqueous solubilities (mg/ml) of ibuprofen and gemfibrozil salts (n=3; mean; \pm SD) under ambient conditions.

Material	SPARC solubility	Actual solubility	Material	SPARC solubility	Actual solubility
Gemfibrozil	0.00932	0.022 \pm 0.008	Ibuprofen	0.113	0.071 \pm 0.002
G butylamine	0.0000285	35.93 \pm 1.808	I butylamine	0.00115	162.66 \pm 8.645
G pentylamine	0.00000943	5.76 \pm 0.092	I pentylamine	0.000483	12.42 \pm 0.081
G hexylamine	0.00000678	3.73 \pm 0.064	I hexylamine	0.000162	6.15 \pm 0.471
G octylamine	0.00000470	0.88 \pm 0.006	I octylamine	0.0000628	1.65 \pm 0.548
G benzylamine	0.0000323	2.66 \pm 0.033	I benzylamine	0.000476	0.25 \pm 0.196
G cyclohexylamine	0.0000825	3.47 \pm 0.179	I cyclohexylamine	0.000676	1.03 \pm 0.034
G tert butylamine	0.000110	7.86 \pm 0.268	I tert butylamine	0.00100	5.02 \pm 0.048
G AMP1	0.00522	11.76 \pm 1.527	I AMP1	0.0629	135.00 \pm 28.058
G AMP2	0.0512	7.76 \pm 0.989	I AMP2	0.889	N/A
G tris	0.104	8.46 \pm 0.494	I tris	1.180	8.97 \pm 0.156

3.5.6 Salt solubility in buffer

3.4.6.1 Introduction

The aim of this section was to investigate the solubility of the model drugs and a selection of their amine salts at a fixed pH. This was carried out to minimise any pH effects that can be a driving force for increasing solubility. In these experiments pH was not controlled but measured after the solution equilibrated after 48 hours (section 3.4.3). Phosphate buffer (pH 6) was used because it is approximately 2 pH units above the pK_a of the model drugs and a similar degree of ionisation should therefore be present in all the samples. This provided two points on the pH solubility curve for each salt investigated and so a pH-solubility curve could be derived from the results; this could be used to predict the aqueous solubilities of the salts at a particular pH. The butylamine, hexylamine and AMP1 salts of all model drugs were tested and the AMP2 salts of etodolac and ibuprofen.

3.4.6.2. Materials and Experimental

All materials were used as in section 2.2. Double distilled water was generated in-house using a Fison's Fi-Streem still.

A Variomag electronic multipoint magnetic stirrer set at 500 rpm was used for sample preparation. HPLC equipment was used as detailed in section 2.1.1.2. The composition of the buffers are detailed in Appendix 1.

3.4.6.3 Methods

The saturated aqueous solubilities of model drugs and prepared salts were determined at pH 6 under ambient conditions. Excess solid was added to 15 ml of water together with a small magnetic flea and stirred for at least 48 hours; the experiment was performed in triplicate. After 48 hours the pH was recorded and 10 ml was extracted with a plastic disposable syringe. The sample was filtered through a 0.45 μm PTFE syringe filter and diluted, if necessary, with solvent mix (acetonitrile: water 65:35) using micropipettes and appropriate volumetric flasks. Calibration standards were made to cover the range of solubilities detected. The samples were analysed by HPLC.

3.4.6.4 Results and discussion

The results from the saturated aqueous solubilities of model drugs and a selection of amine salts at pH 6 are detailed in table 3.22 and 3.23, below. The results are further displayed in figures 3.18 to 3.19 in the form of bar charts for ease of visualisation.

Table 3.22 Solubility of the butylamine, hexylamine and AMP1 salts of etodolac and flurbiprofen, including etodolac AMP2 in pH 6 buffer. (n=3; mean \pm SD)

Material	Solubility mg/ml	pH	Material	Solubility mg/ml	pH
Etodolac	2.11 \pm 0.399	5.97	Flurbiprofen	0.480 \pm 0.038	5.80
E butylamine	2.52 \pm 0.357	6.15	F butylamine	0.735 \pm 0.102	5.93
E hexylamine	1.32 \pm 0.223	5.75	F hexylamine	0.955 \pm 0.086	6.40
E AMP1	2.19 \pm 0.156	6.12	F AMP1	0.569 \pm 0.159	5.88
E AMP2	2.51 \pm 0.346	6.22			

Table 3.23 Solubility of the butylamine, hexylamine and AMP1 salts of gemfibrozil and ibuprofen, including ibuprofen AMP2 in pH 6 buffer. (n=3; mean \pm SD)

Material	Solubility mg/ml	pH	Material	Solubility mg/ml	pH
Gemfibrozil	0.038 \pm 0.058	6.50	Ibuprofen	1.62 \pm 0.284	6.10
G butylamine	0.263 \pm 0.020	6.48	I butylamine	1.33 \pm 0.130	5.89
G hexylamine	0.475 \pm 0.020	6.62	I hexylamine	1.93 \pm 0.041	6.35
G AMP1	0.232 \pm 0.056	6.28	I AMP1	1.58 \pm 0.110	6.05
			I AMP2	4.71 \pm 0.034	6.55

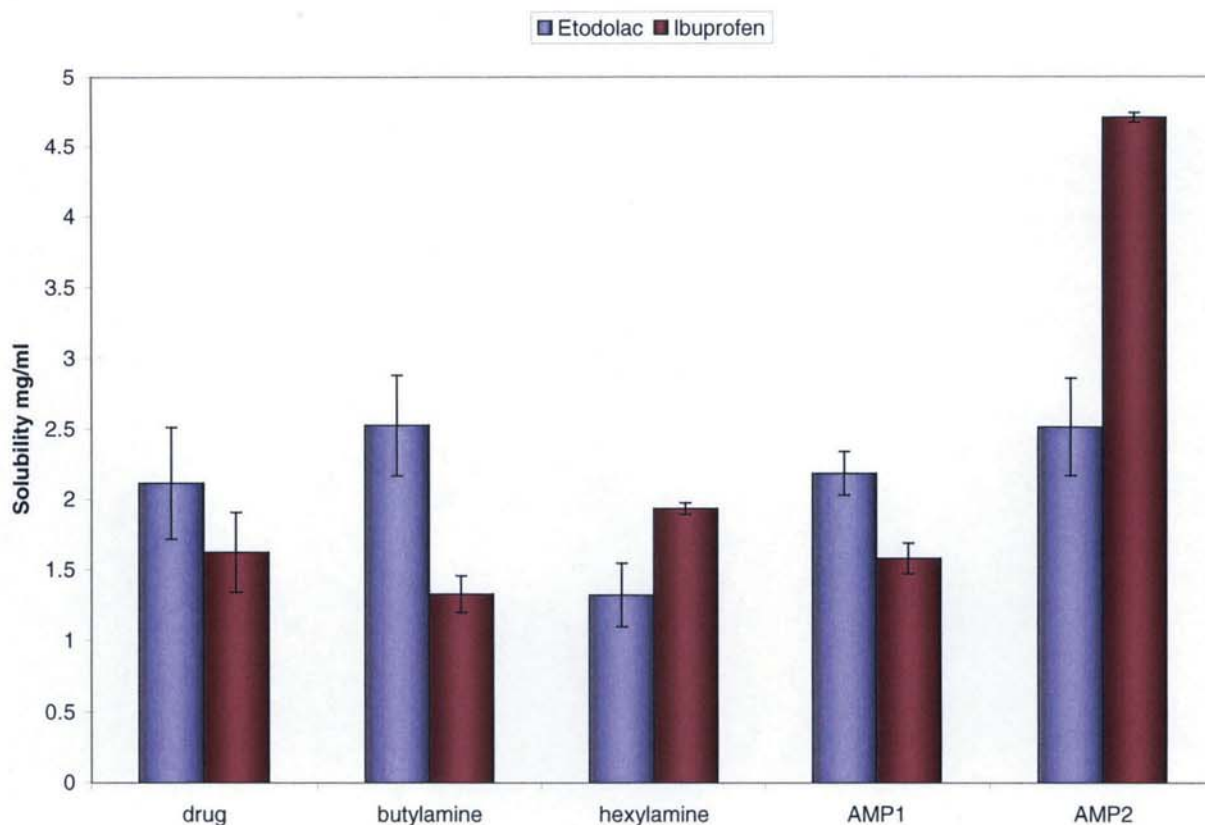


Figure 3.18 Aqueous solubilities of the butylamine, hexylamine, AMP1 and AMP2 salts of etodolac and ibuprofen in pH 6 buffer (n=3; mean \pm SD).

The results show that when the solutions are left to equilibrate at room temperature for at least 48 hours in buffer solution only a small increase in solubility is observed and in some cases, it can result in a reduction in solubility compared to the parent compound.

The etodolac salt series show no increase in solubility for each salt and the hexylamine counterion reduces the solubility. The ibuprofen salt series show no increase in solubility except the AMP2 counterion which shows a 2.9-fold increase in solubility, but this result could be due to the elevated solution pH compared to parent.

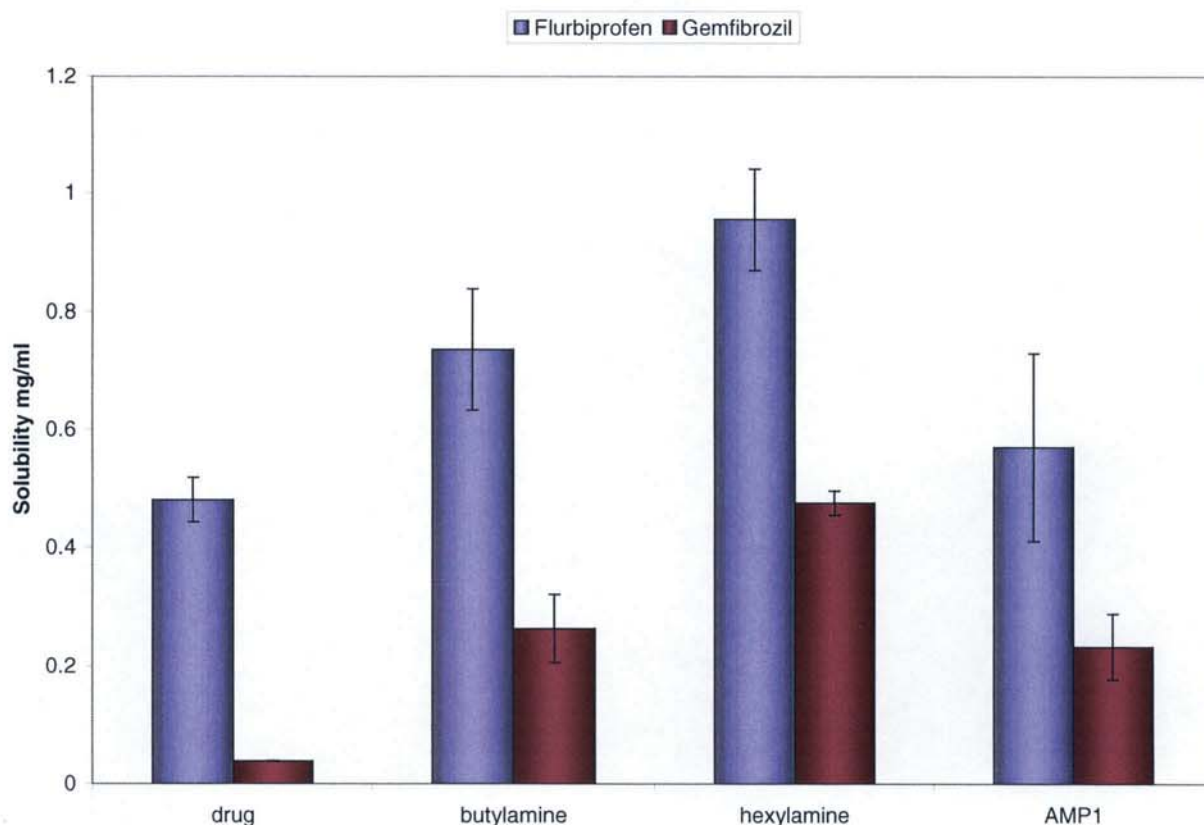


Figure 3.19 Aqueous solubilities of the butylamine, hexylamine amine salts of flurbiprofen and gemfibrozil at pH 6 (n=3; mean \pm SD).

Flurbiprofen salts show an increase in solubility compared to the parent (figure 3.19). The maximum increase was for the hexylamine counterion. A two-fold-increase in solubility at pH 6.4 was measured compared to the parent at pH 5, the elevated solubility was due to pH. The salts of gemfibrozil show improved solubility compared to parent. The pH range is only 6.3 to 6.5 in all the experiments. The salts produced an increase in solubility of between 6.1- and 12.5-fold compared to parent, the hexylamine salt having the greatest solubility. The gemfibrozil salts gave the best improvement in solubility at pH 6. The butylamine salt does not generally give an increased solubility at pH 6, as seen in section 3.5.3 and that in these experiments the hexylamine salts can increase the solubility more extensively for flurbiprofen and gemfibrozil at pH 6.

From these data, it can be concluded that the increased solubilities observed in section 3.5.3 are due to the counterion affecting the pH of the solution. When pH is not controlled in any way (*i.e.* when no buffer is used), the diffusion layer model

proposes that the pH of the saturated solution represents the pH of the theoretical diffusion layer surrounding the salt as it dissolves. When using a buffer at pH 6 the diffusion layer is saturated with a solution of controlled pH, so inhibiting the dissolution of the drug-salt within the diffusion layer. This explains why the solubility is not elevated for all of the salts formed.

3.5.7 Dissolution

3.5.7.1 Introduction

The dissolution methods were based on the official USP paddle and basket apparatus. Apparatus 1 includes a cylindrical vessel with hemispherical bottom and a nominal capacity of 1 litre, made of glass contained in a secure assembly where it is heated to a temperature of $37^{\circ}\text{C} \pm 0.5^{\circ}\text{C}$. The shaft is positioned along the vertical axis of the vessel and a cylindrical mesh basket is attached, as described in the USP 26. The shaft rotates at a speed of $100 \text{ rpm} \pm 4\%$. The distance between the inside bottom of the vessel and the basket is maintained at $25 \pm 2 \text{ mm}$ during the test.

Apparatus 2 uses the assembly from Apparatus 1, except that a paddle formed from a blade and a shaft is used as the stirring element, as described in the USP 26. The paddle and shaft may be coated in an inert material and held at $25 \pm 2 \text{ mm}$ above the bottom of the vessel throughout the test. The dosage unit is allowed to sink to the bottom of the vessel before rotation of the blade is started, usually at 50 rpm.

Dissolution media composition is commonly phosphate buffers of pH 6.8 to 7.6. The BP monograph for gemfibrozil tablets states a dissolution medium of pH 7.6 to be used in a volume of 900 ml. There is no BP test for flurbiprofen tablets so a pH of dissolution medium of pH 7.2 for gemfibrozil and pH 6.8 for flurbiprofen was chosen by ourselves to ensure good solubility and similar degrees of ionisation (pK_a of 4.6 and 4.2 respectively, SPARC online calculator) and a dissolution volume of 1000 ml was used for all experiments.

3.4.7.2 Statistical Analysis

Dissolution curves

The f_2 test is a logarithmic transformation of the sum-squared error of differences between the test T_t and the reference products R_t over all time points, n (Moore and Flanner, 1996)(equation 3.20).

$$f_2 = 50 \log \left\{ \left[1 + \left(\frac{1}{n} \right) \sum_{t=1}^n w_t (R_t - T_t)^2 \right]^{-0.5} \bullet 100 \right\} \quad \text{equation 3.20}$$

where w_t is an optional weight factor.

The FDA has recommended the use of the f_2 test to discriminate between test and reference dissolution profiles, in the document FDA Guidance for Industry, Waiver of *in-vivo* bioavailability and bioequivalence studies for immediate release solid oral dosage forms based on a biopharmaceutics classification system (August 2000). The f_2 test is a similarity factor test that measures the similarity in percent (%) of dissolution between the two curves. This method is suitable to compare dissolution profiles when more than three or four dissolution time points are available and can only be applied if the difference between R_t and T_t is less than 100.

The FDA suggested that two dissolution profiles are considered similar when the f_2 value is between 50 and 100. To allow the use of mean data, the coefficient of variation should not be more than 20% at the earlier time points (e.g. 10 minutes) and should be no more than 10% at other time points. From the context of these guidances it is generally interpreted that f_2 should be calculated from cumulative percent dissolved.

The f_2 test is insensitive to the shape of the dissolution profiles and cannot take into account unequal spacing between sampling time points. It is impossible to evaluate false positive and false negative results based on f_2 as the similarity factor is a sample statistic and cannot be used to prove a statistical hypothesis. It has also been suggested that the similarity factor is too liberal in concluding similarity between dissolution profiles (Liu and Chow, 1996; Liu *et al.*, 1997). It is unlikely to achieve a

value of 100 as, in practice, batch to batch variation generates slightly different dissolution profiles although the clinical effect is unaffected. Gohel and Panchal (2002) recommend a lower acceptance limit of 60 and propose an amended equation to calculate similarity between dissolution curves.

The similarities between dissolution curves can also be assessed by other statistical analysis such as the difference factor (f_1) (Moore and Flanner, 1996) and the Rescigno index (ζ_1 and ζ_2) (Rescigno, 1992). Alternatively an ANOVA one-way analysis of variance could be performed on the differences of release at dissolution time points. As with all statistical methods, there are advantages and limitations and the acceptance limit criteria can always be questioned. For the purpose of this thesis, the f_2 test has been selected as the statistical method of choice, because it is recommended by the FDA.

For the experimental data in this section a separate classification has been created in order to differentiate retarded dissolution and enhanced dissolution. Four categories have been formed and given a sign indicating the effect on dissolution which is based on their f_2 value, see table 3.24. The dissolution profiles of the salts were compared to the parent compound and the effect on the dissolution profile was given a classification, as described in table 3.24

Table 3.24 F_2 fit factors for classification of dissolution curves into categories.

Sign	Classification	f_2 value
++	Significant enhancement of dissolution	0-25
+	Moderate enhancement of dissolution	25-50
No sign	No effect on dissolution	50-100
-	Dissolution inhibition	25-50
--	No measurable dissolution	0-25

3.5.7.3 Powder dissolution

The aim of these series of experiments was to investigate the controlled powder dissolution of the model drugs and a selection of their amine salts over a range of pH. The primary objective was to study the effect of pH on the solubility and dissolution of the salts and to determine which salt had the greatest ability to alter its immediate microenvironment and therefore improve dissolution.

Powder dissolution was performed at pH 7.2 for flurbiprofen, gemfibrozil and its salts. Additionally, buffer solutions were prepared one pH unit above the pK_a of the model drug to be investigated e.g. etodolac and its salts were analysed at pH 5.2, flurbiprofen and its salts at pH 5.2, gemfibrozil at pH 5.6 and ibuprofen at pH 5.5. These conditions were used to ensure that the same degree of ionisation was maintained throughout the study and so that the free acid had a solubility adequate for detection.

3.5.7.4 Dissolution at pH 7.2

3.5.7.4.1 Materials

All materials were used as in section 2.2. Potassium dihydrogenorthophosphate, disodium hydrogenorthophosphate, orthophosphoric acid, sodium hydroxide were supplied by Sigma-Aldrich (Poole, UK). All materials were of analytical grade.

3.5.7.4.2 Equipment

The dissolution equipment consisted of a Hanson SRII 6-flask dissolution test station, equipped with 1 litre round bottomed flasks and wax-covered baskets conforming to Apparatus 1-USP regulations. The mesh baskets were covered with paraffin prior to use, as described in section 3.4.5.1 and used by Shaw (2001). Sampling was performed manually by extracting 2 ml of dissolution medium with a disposable syringe from the sample tube and placing 0.5-1 ml in hplc vials; the remaining solution was returned to the vessel. Analysis was performed by hplc as described in section 2.1. The calibration data was used to calculate the amount of drug released during dissolution.

3.5.7.4.3 Method

6 litres of phosphate buffer pH 7.2 was prepared as detailed in the appendix. 100 mg \pm 3 mg of model drug or salt were weighed in the wax-covered baskets. The baskets were gently tapped to give an even level of powder until it was below the upper limit of the paraffin coated mesh. 1 litre of dissolution medium was placed in the glass dissolution flasks and warmed to 37.5 ± 0.5 °C. The mesh baskets and sampling rods were slowly lowered into the dissolution flasks to the positions specified by the USP and then the rotational motor was set at 100rpm.

All dissolution experiments were conducted over 90 minutes and sample time points were at 10, 20, 30, 50, 70, 90 minutes. More data points were taken at the start of the experiment because most of the dissolution was expected to occur within the first 30 minutes. As the data was collected manually considerable dexterity and organisation was required to ensure all the samples were taken within 20 seconds of each other to reduce any variations in that could occur when sampling. Each experiment was performed in triplicate to enable sound statistical analysis. Calibration standards of 0.1, 0.75, 0.5, 0.25, 0.1 and 0.01 mg/ml were used to generate a standard curve used to calculate unknown concentrations of dissolution samples.

3.5.7.4.4 Results and discussion

The f_2 test was used to analyse the dissolution data; a difference of >50 from the reference is usual to show similarity of dissolution profiles. This rule was used to judge whether the differences were significant. All f_2 values were calculated using pure drug as the reference and averaging the data from all of the replicates. The f_2 values calculated for flurbiprofen and gemfibrozil are detailed in table 3.25 and 3.26 below. They indicate that at pH 7.2 salt formation can show both retardation and enhancement of dissolution compared to the parent drug.

Table 3.25 f_2 fit factor results for the powder dissolution of flurbiprofen and a selection of its amine salts at pH 7.2

Flurbiprofen	F_2 fit factor value	f_2 fit factor classification
F cyclohexylamine	-- 22.2	Different
F tert-butylamine	- 35.3	Different
F hexylamine	59.3	Similar
F benzylamine	59.4	Similar
F AMP1	+ 30.9	Different
F AMP2	+ 38.9	Different
F tris	+ 42.1	Different

Table 3.26 f_2 fit factor results for the powder dissolution of gemfibrozil and a selection of its amine salts at pH 7.2

Gemfibrozil	f_2 fit factor value	f_2 fit factor classification
G butylamine	++ 12.9	Different
G AMP1	++ 12.1	Different
G AMP2	++ 16.3	Different
G tris	++ 23.3	Different
G cyclohexylamine	++ 24.5	Different
G benzylamine	+ 33.1	Different
G hexylamine	+ 49.4	Different

3.5.7.4.4.1 Flurbiprofen

The results show that dissolution is similar with flurbiprofen hexylamine, benzylamine and the parent drug and that dissolution is retarded with the salts cyclohexylamine and tert-butylamine at pH 7.2. In fact, the formation of the cyclohexylamine salt severely retards dissolution at pH 7.2 whereas the tert-butylamine moderately retards dissolution. This result is contrary to the solubility experiments in section 3.5.3 that show that solubility was enhanced by salt formation in all cases.

Retardation of dissolution occurs for two salts because the solubility of flurbiprofen at pH 7.2 is approximately 6.68 mg/ml (section 3.5.3) which is greater than the

saturated water solubilities of the salts: tert-butylamine 2.77 mg/ml (pH 6.0) and cyclohexylamine 0.37 (pH 7.6), (see section 3.5.3). The aqueous solubility of these salts is less than that of flurbiprofen at pH 7.2, for flurbiprofen hexylamine the solubility was 2.60 mg/ml (pH 6.4) and for flurbiprofen benzylamine 2.85 mg/ml (pH 7.0) and they would be expected to have reduced dissolution compared to the drug. However, there is no difference in dissolution rate at pH 7.2 between flurbiprofen and the salts hexylamine and benzylamine. Hydrodynamic effects and different wetting properties of the salts may assist the dissolution of these salts.

Dissolution of flurbiprofen was moderately enhanced by the hydrophilic salts with a dissolution enhancement order of AMP1>AMP2>tris which is opposite to the solubility order found from the saturated solubility experiments in section 3.5.3 which was AMP2~tris>AMP1. The solubilities of these salts were 11.6, 11.1 and 8.9 mg/ml respectively at pH approximately 6.7, whereas the solubility of flurbiprofen is 4.5 mg/ml. The dissolution of the salts was expected to be higher at this pH, but differences in particle wetting and particle sizes can affect dissolution rates.

The dissolution profiles of flurbiprofen and its salts are displayed in figures 3.20 and 3.21. Figure 3.21 shows that the dissolution of the AMP1, AMP2 and tris salts give a moderate enhancement in dissolution at pH 7.2. Figure 3.20 shows that flurbiprofen dissolution was not enhanced by the amine salts; it was retarded by the tert-butylamine and hexylamine salt forms.

Results are presented as % of drug dissolved over time, in minutes. Because the dissolution experiments used a standard basket content of 100 mg they were equivalent in weight but not equivalent in moles so molecular weight was not considered. This results in a maximum of approximately 63 to 79 % release of drug if each salt fully dissolves in the dissolution media.

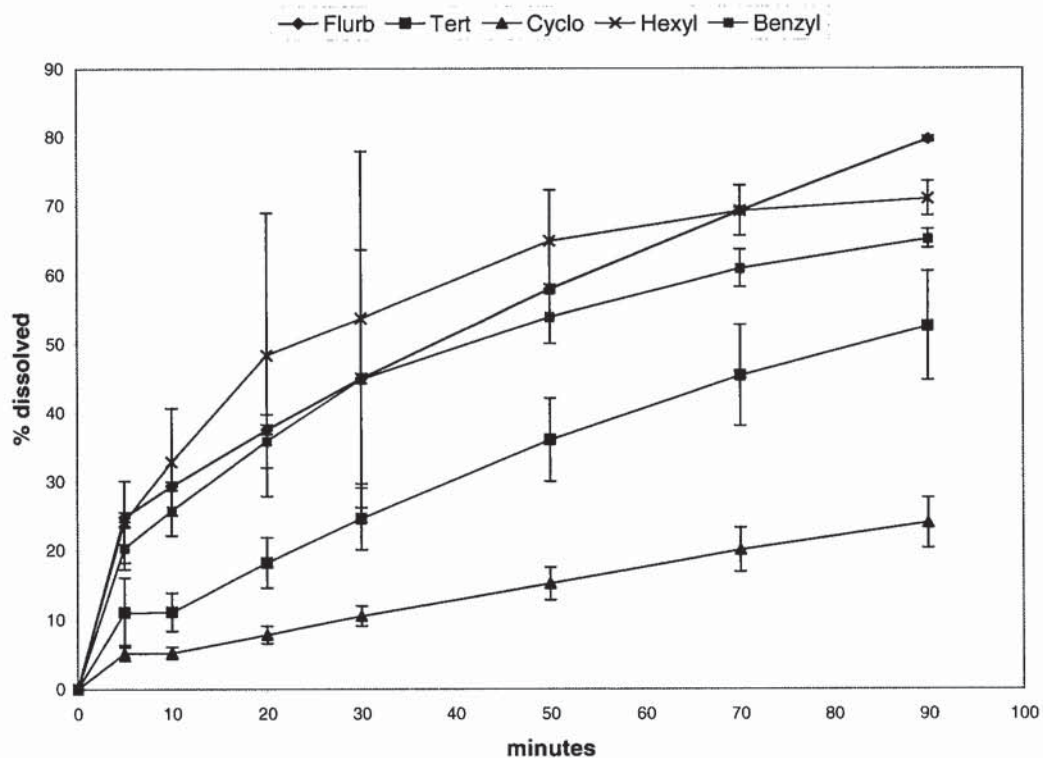


Figure 3.20 The powder dissolution of flurbiprofen and its benzylamine, cyclohexylamine, hexylamine and tert-butylamine salts at pH 7.2. (n=6; mean \pm SD)

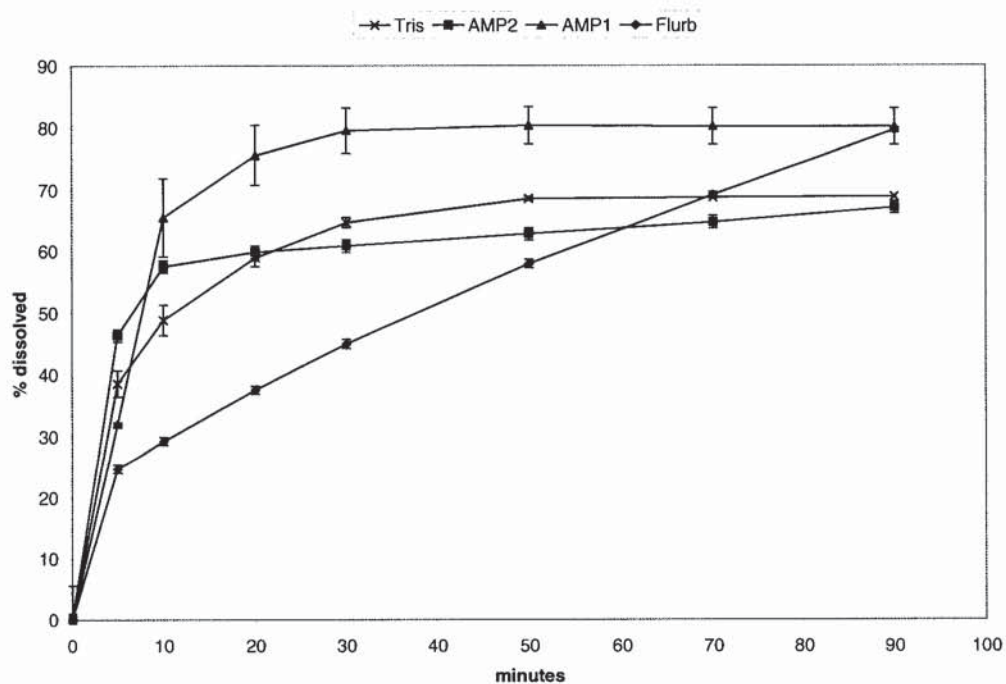


Figure 3.21 The powder dissolution of flurbiprofen and its AMP1, AMP2 and tris salts at pH 7.2. (n=6; mean \pm SD)

3.5.7.4.4.2 Gemfibrozil

The dissolution of gemfibrozil was enhanced for all salts, see table 3.27. The benzylamine and hexylamine salts enhanced dissolution moderately, whereas the butylamine, AMP1, AMP2, tris and cyclohexylamine salts greatly enhanced dissolution. The order from greatest enhancement to least enhancement was butylamine>AMP1>AMP2>tris>cyclohexylamine>benzylamine>hexylamine and the solubility order was observed to be butylamine (35.9 mg/ml)>AMP1>tris>AMP2>hexylamine>cyclohexylamine>benzylamine (2.66 mg/ml) at variable pH; the solubility of gemfibrozil at pH 7 was 0.10 mg/ml (section 3.5.3).

Table 3.27 f_2 fit factor results for the powder dissolution of gemfibrozil and a selection of its amine salts at pH 7.2

Gemfibrozil	f_2 fit factor value	f_2 fit factor classification
G butylamine	++ 12.9	Different
G AMP1	++ 12.1	Different
G AMP2	++ 16.3	Different
G tris	++ 23.3	Different
G cyclohexylamine	++ 24.5	Different
G benzylamine	+ 33.1	Different
G hexylamine	+ 49.4	Different

Therefore the solubilities of all the salts are much higher than the model drug itself at pH 7.2 and this enhancement in solubility accounts for the enhancements in dissolution seen in this experiment (figure 3.22, 3.23). The solubility order differs slightly from the dissolution order probably because of pH and hydrodynamic effects. Gemfibrozil butylamine undergoes complete dissolution in 10 minutes at pH 7.2 which confirms that the salt has the highest solubility.

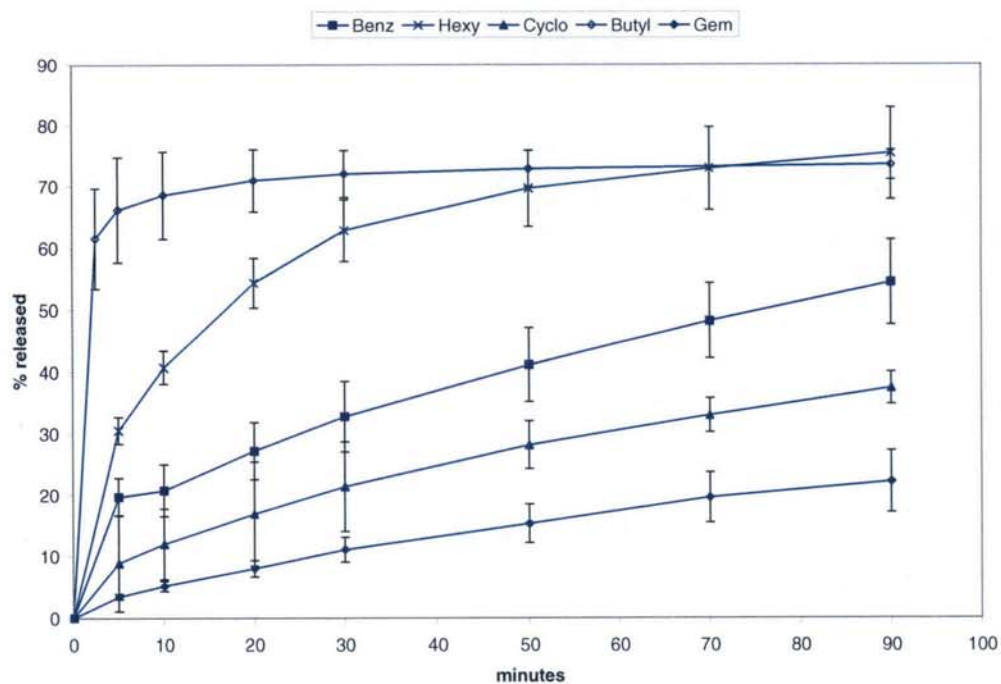


Figure 3.22 The powder dissolution of gemfibrozil and its butylamine, benzylamine, hexylamine and cyclohexylamine salts at pH 7.2. (n=6; mean \pm SD)

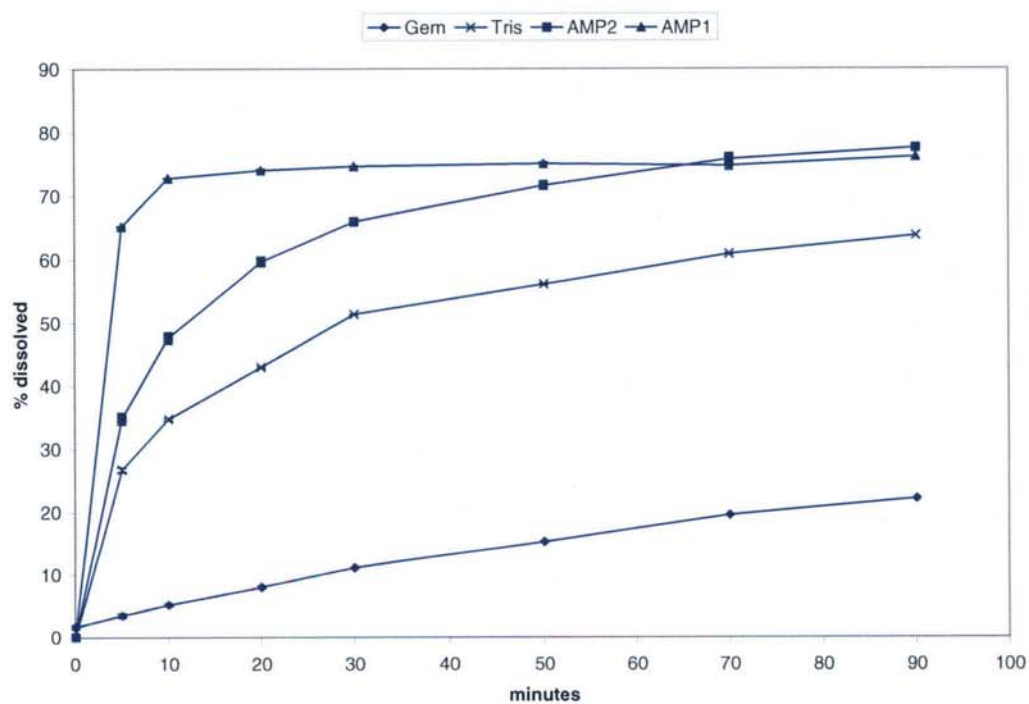


Figure 3.23 The powder dissolution of gemfibrozil and its tris, AMP1 and AMP2 salts. (n=6; mean \pm SD)

The flurbiprofen and gemfibrozil experiments were performed at pH 7.2 which is a favourable pH for dissolution of flurbiprofen. However, because gemfibrozil has a lower pK_a and solubility at pH 7.2, enhancement of solubility was possible. To fully understand the effect of salts on dissolution it would be beneficial to look at dissolution at a lower pH to see if dissolution is still enhanced and to perform the dissolution at a pH where the dissociation of ionised species is constant for all model drugs.

3.5.7.5 Dissolution at pH 5

Dissolution was performed at one pH unit above the pK_a for each of the model drugs, so *i.e.* etodolac pH 5.2, flurbiprofen pH 5.2, ibuprofen pH 5.5 and gemfibrozil pH 5.6. This pH was selected to complement the results of the aqueous solubility in buffer at pH 6 experiments (section 3.4.4) and observe the effect of pH on dissolution.

3.5.7.5.1 Materials

All materials that were used for these experiments were identical to section 3.4.6.2.1.

3.5.7.6.2 Equipment

Section 3.4.6.2.1

3.5.7.6.3 Method

The method of dissolution was identical to section 3.4.6.2.3 however sample size was 200 ± 2 mg of salt leading to calibration standards of 0.2, 0.15, 0.1, 0.05, 0.01 and 0.001 mg/ml being used.

Powders for dissolution were pre-sieved through 710 μ m steel sieves to remove any large aggregates.

3.5.7.6.4 Results and discussion

Tables 3.28 to 3.31 list the f_2 values for the model drugs and a selection of their amine salts, and their dissolution profiles are shown in figures 3.24-3.27.

Butylamine, hexylamine and AMP1 salts and each model drug were investigated at a $pK_a + 1$; for gemfibrozil the AMP2 and tris salts were also studied.

Table 3.28 f_2 fit factor results for the powder dissolution of etodolac and its butylamine, hexylamine and AMP1 amine salts at pH 5.2

Etodolac	f_2 fit factor value	F_2 fit factor classification
E butylamine	++ 16.7	Different
E hexylamine	++ 17.8	Different
E AMP1	++ 11.5	Different

Table 3.29 f_2 fit factor results for the powder dissolution of flurbiprofen and its butylamine, hexylamine and AMP1 amine salts at pH 5.2

Flurbiprofen	f_2 fit factor value	f_2 fit factor classification
F butylamine	67.8	Similar
F hexylamine	+ 36.0	Different
F AMP1	57.5	Similar

Table 3.30 f_2 fit factor results for the powder dissolution of gemfibrozil and a selection of its amine salts at pH 5.6

Gemfibrozil	F_2 fit factor value	f_2 fit factor classification
G butylamine	++ 4.21	Different
G AMP1	++ 26.7	Different
G AMP2	++ 19.8	Different
G tris	+ 49.7	Different
G hexylamine	68.5	Similar

Table 3.31 f_2 fit factor results for the powder dissolution of ibuprofen and its butylamine, hexylamine and AMP1 amine salts at pH 5.5

Ibuprofen	F_2 fit factor value	f_2 fit factor classification
I butylamine	+ 28.3	Different
I hexylamine	69.6	Similar
I AMP1	++ 17.1	Different

Dissolution of etodolac was enhanced by the formation of all the selected salts. The dissolution of flurbiprofen was enhanced by the formation of the hexylamine salt only, butylamine and AMP1 had similar dissolution to flurbiprofen. All gemfibrozil salts enhanced dissolution except the hexylamine salt which had similar dissolution to gemfibrozil. Ibuprofen butylamine and ibuprofen AMP1 enhanced the dissolution of ibuprofen; the hexylamine salt had similar dissolution to ibuprofen.

The salts of etodolac markedly enhance the dissolution of etodolac at pH 5.2, (figure 3.24) complete dissolution (approximately 60-70% release) of the salts occurs after 30 minutes. The saturated aqueous solubility of etodolac is about 0.085 mg/ml at pH 4.97 yet, at pH 5.2 the solubility of etodolac AMP1 is at least 0.16 mg/ml. The experiment could be re-run with excess of 200 mg of salt to investigate whether the solubility of the salts is elevated compared to etodolac upon dissolution at pH 5.2. The measured solubility of etodolac AMP1 at pH 5.2 is comparable to the solubility of etodolac at pH 5.2 from the pH solubility profile (section 3.5.2) therefore it is not possible to conclude that the salts have improved the solubility of etodolac from this data.

The increase in dissolution is explained by the boundary layer theory. Dissolution is enhanced because the salt provides a microenvironment around each dissolving particle of intermediary pH. The pH of this diffusion layer is equal to the pH of the saturated solubility of the salt as determined by Serajuddin and Jarowski (1985), and, it can be hypothesised that the greater the ability of the counterion to alter the pH of the diffusion layer, the more successful the salt at enhancing dissolution. Etodolac butylamine, hexylamine and AMP1 all enhance dissolution to similar degrees and so alter the pH of the diffusion layer to promote dissolution; this results in enhanced dissolution.

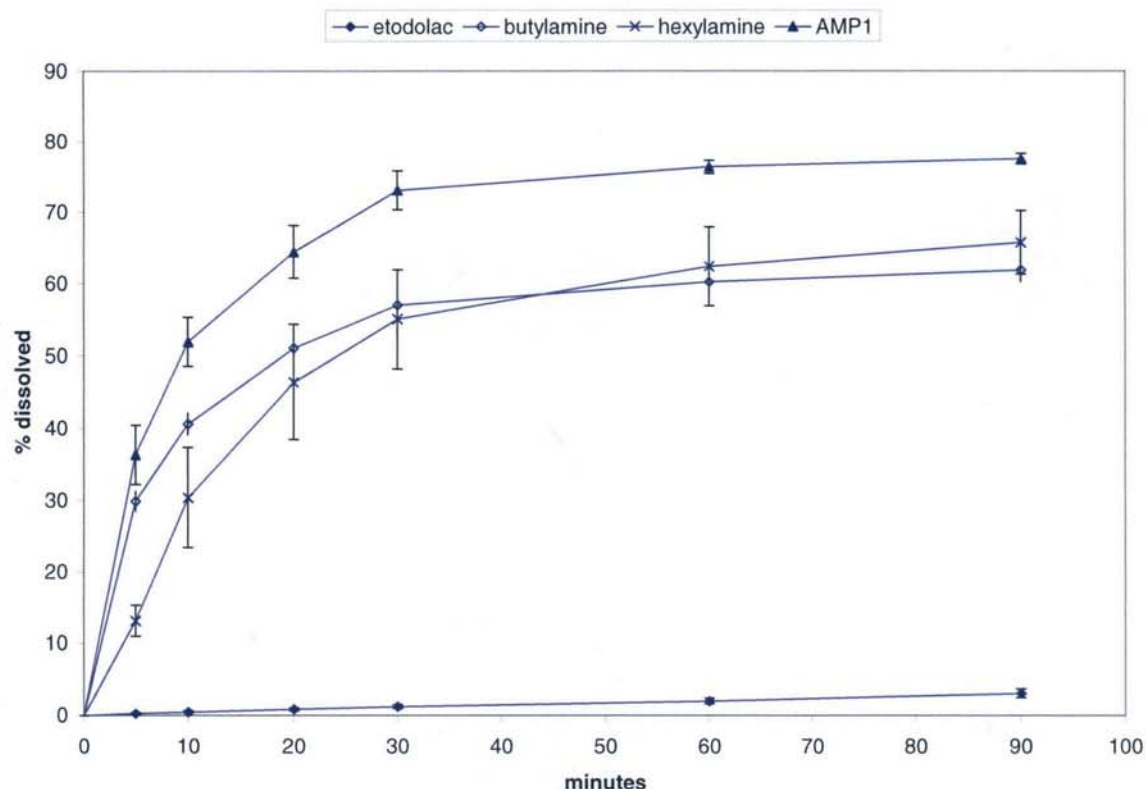


Figure 3.24 Powder dissolution of etodolac and its butylamine, hexylamine and AMP1 salts at pH 5.2. (n=3; mean \pm SD)

Flurbiprofen and its butylamine, hexylamine and AMP1 salts show slow dissolution at pH 5.2. Although the dissolution curve (figure 3.25) suggests that all the salts improve the dissolution compared with the model drug, the statistical analysis shows that only flurbiprofen hexylamine has a different dissolution profile than flurbiprofen, the two other curves are similar to flurbiprofen. This result can cause the validity of the f_2 test to be questioned because the profiles seem to be quite different, but the dissolution is variable in these samples.

Flurbiprofen hexylamine markedly improves the dissolution to a concentration of 0.06 mg/ml and is still increasing after 90 minutes. The aqueous solubility of flurbiprofen at pH 5.10 is 0.089 mg/ml, so although dissolution rate is enhanced overall solubility is not enhanced.

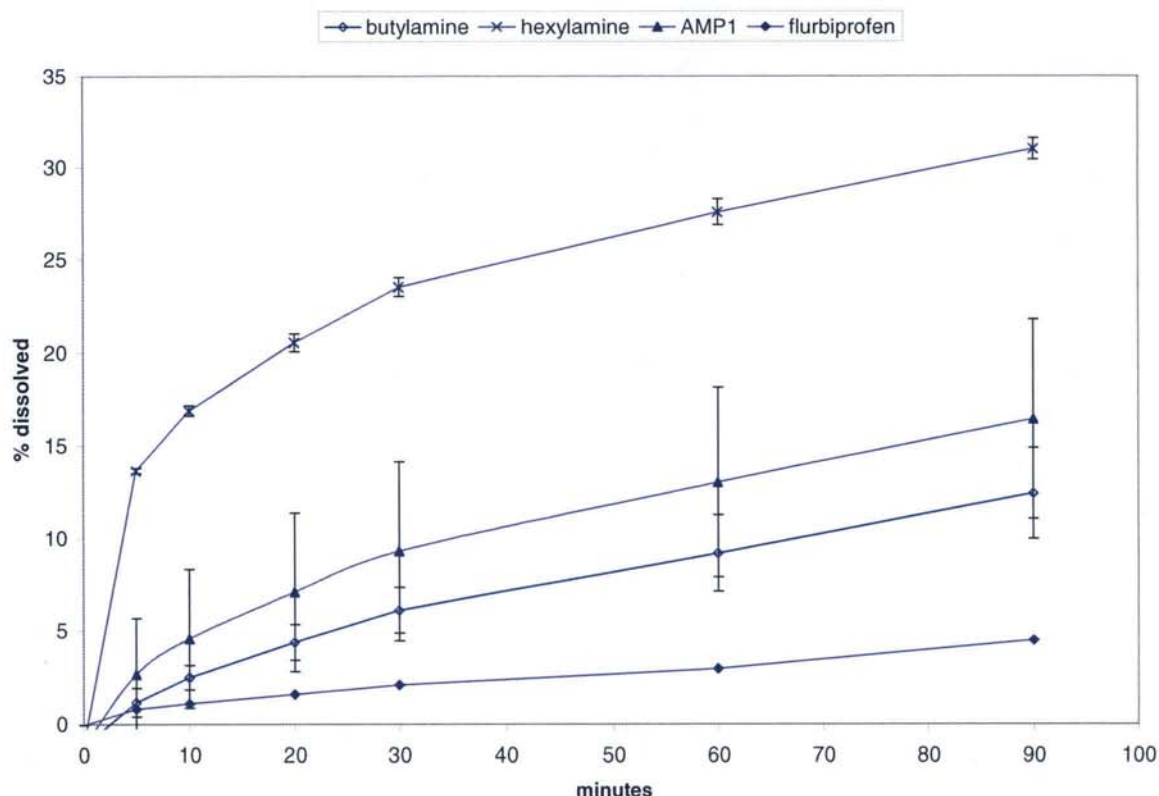


Figure 3.25 Powder dissolution of flurbiprofen and its butylamine, hexylamine and AMP1 salts at pH 5.2. (n=3; mean \pm SD)

Gemfibrozil undergoes almost no dissolution at pH 5.6 (figure 3.26) and has an aqueous solubility of 0.0032 mg/ml at pH 5.5. Gemfibrozil hexylamine has similar dissolution to gemfibrozil at pH 5.6. Gemfibrozil AMP1 and gemfibrozil butylamine undergo complete dissolution at pH 5.6 to an overall concentration of 0.186 mg/ml which far exceeds the saturated solubility of gemfibrozil at pH 5.5 by 58-fold. In this example, the actual solubility of the model drug has been increased by salt formation together with increased dissolution. This result indicates that as dissolution occurs the salt provides a microenvironment of elevated pH so that gemfibrozil dissolves in the diffusion layer and does not precipitate as ion-pair theory suggests. Gemfibrozil may remain dissolved in the diffusion layer which is maintained by the base, or as gemfibrozil diffuses through the diffusion layer it may remain associated with the base so that once in the dissolution medium it does not precipitate out. This is contrary to theory which suggests that as an ion-pair dissolves, it dissociates into ions that are free to move in the solution because there is no ionic association

between the acid and base therefore the ions may exist as an ion pair in solution (Stahl and Wermuth, 2002).

However, in water ions occur as H_3O^+ as this conformation is thermodynamically favourable, water is covalently bonded but H_3O^+ exists as an ion-pair in solution. It has been shown that the non ideal properties of strong electrolytes in aqueous solutions is due to partial dissociation and hydration (Heyrovska, 1996). Heyrovoska looked at the dissociation of a common electrolyte NaCl and proposed a number of equations to describe this event. Recent x-ray diffraction studies have demonstrated the presence of about 30% ion pairs in $NaCl_{(aq)}$ (Ohtaki and Fukushima, 1992 and Ohtaki, 1993). This provides strong support to the hypothesis of partial dissociation of ion pairs in aqueous solutions, which is demonstrated by equation 3.21 which represents the equilibrium of a saturated solution of a salt in aqueous solution, using sodium chloride as an example:



Where $\alpha < (\text{or} =) 1$ is the degree of dissociation, $m[(1-\alpha)+2\alpha]=im$ is the total number of moles of solute and i is the van't Hoff factor.

It is therefore possible that a proportion of salt molecules exist as ion-pairs in aqueous solution and that there is a dynamic equilibrium in the dissolution medium. If the pH of the medium is unfavourable for dissolution, the equilibrium may shift producing more ion-pairs. Therefore there are less free ions are present in a lowered pH environment in which the acid may precipitate out. This leads to an enhancement in solubility and dissolution.

The remainder of the gemfibrozil salts including AMP2 and tris also enhance dissolution but not to the same extent as the butylamine salt. This may be because the butylamine salt has a greater ability to increase the pH of the diffusion layer allowing for complete dissolution of the salt at pH 5.6.

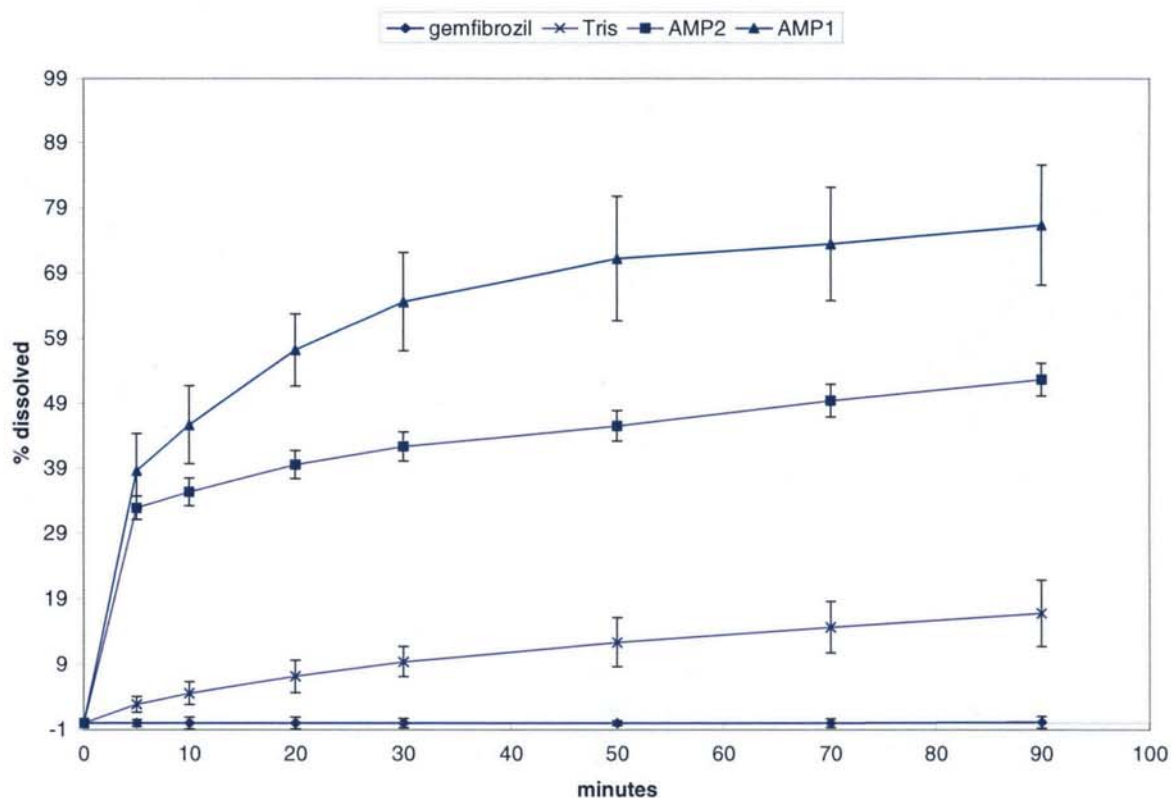


Figure 3.26 Powder dissolution of gemfibrozil and its tris, AMP2 and AMP1 salts at pH 5.6.
(n=6; mean \pm SD)

Ibuprofen exhibits similar dissolution as the hexylamine salt at pH 5.5 (figure 3.31) but both AMP1 and butylamine increase the dissolution of at pH 5.5. AMP1 markedly improves the dissolution (60% dissolved over 90 minutes) and butylamine moderately improves the dissolution (40% dissolved over 90 minutes). Ibuprofen has an aqueous solubility of 0.258 mg/ml at this pH and would be expected to completely dissolve in the dissolution media, this does not occur over 90 minutes, in fact only 6% dissolves in this time. The saturated aqueous solubility results show both AMP1 and butylamine ibuprofen salts are above 100 mg/ml and therefore have enhanced dissolution compared to ibuprofen. The solubility at fixed pH experiments suggest that these salts do not have an elevated solubility but enhance dissolution.

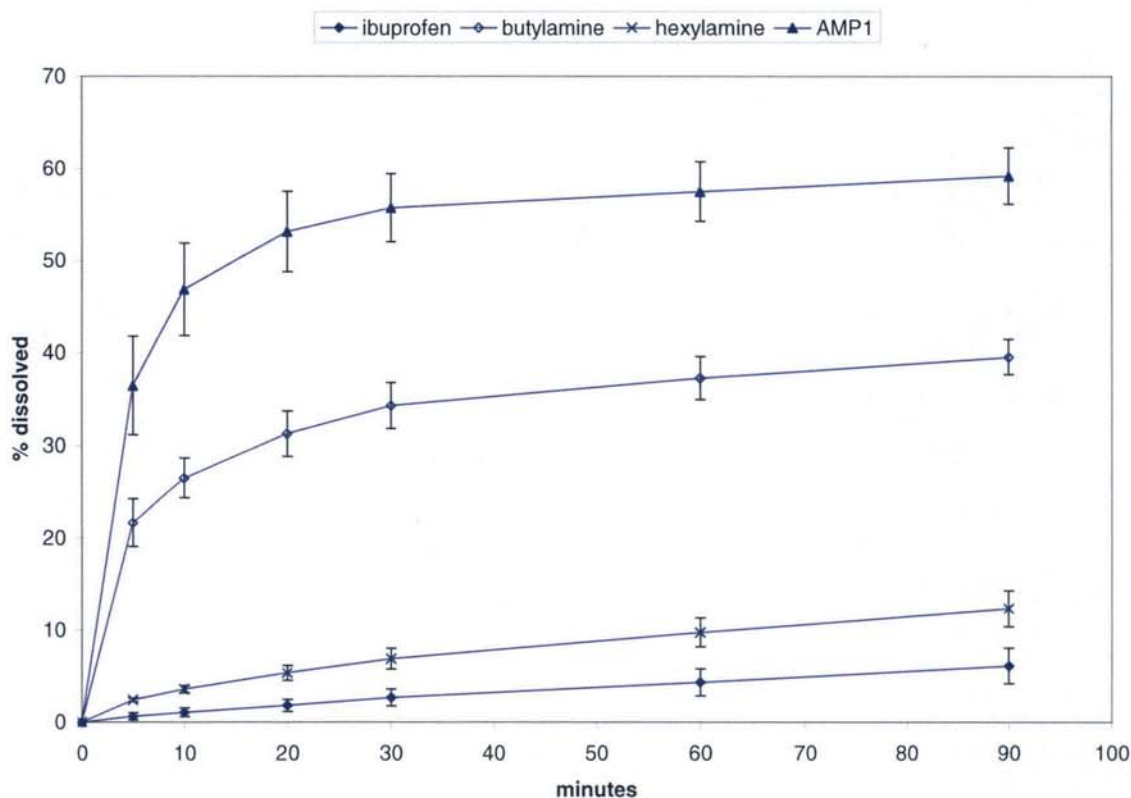


Figure 3.27 Powder dissolution of ibuprofen and its butylamine, hexylamine and AMP1 salts at pH 5.4. (n=6; mean \pm SD)

3.5.8 Intrinsic Dissolution of salt forms

Intrinsic dissolution experiments were designed to ensure dissolution fluid viscosity, rotational speed of the sample and surface area were maintained constant throughout the experiment and that the experiment was performed under sink conditions ($C_s > C$). Under these conditions, the rate of diffusion is directly proportional to the saturated concentration of the drug in solution, if dissolution is controlled solely by diffusion.

Intrinsic dissolution rate (IDR) is given by:

$$IDR = K_1 C_s \quad (\text{mg/ml/min})$$

equation 3.22

K_1 is the IDR constant and C_s the saturated solubility (Aulton, 2002).

IDR differs from conventional dissolution measurements from dosage forms where disintegration of the dosage form occurs first, which exposes an uncontrolled surface area for dissolution. During IDR measurement, formulation effects are eliminated and surface area remains constant throughout which allows measurement of the intrinsic properties of the drug or salt as a function of the dissolution media.

A compressed disk of material is usually made by slow compression of drug in a 13 mm IR disc punch and die, set at a high compaction pressure and long dwell time to ensure minimum porosity and maximum compression. Aulton (2002) describes the disk being fixed to the holder of the rotating basket apparatus with molten paraffin wax so that it is completely coated. The lower circular face should be cleared of residual wax, exposing one face of the disk for introduction into the dissolution media. The coated disk is rotated at 100 rpm in 1000 ml of fluid 20 mm from the base of a flat bottomed dissolution flask, the amount of drug release is measured over time and the IDR is calculated as the slope of the line. This method of disk preparation for IDR measurement is not ideal as many indentations could be introduced to the face of the disk when removing the wax thus not providing a constant surface area.

IDR apparatus are available commercially from e.g. International Crystal Laboratories that consists of a die in which the cylindrical compacts can be prepared, when disassembled one face of the compact is exposed. The compact remains in part of the die which can be dropped into the dissolution vessel when required. This method will reduce some of the lamination problems that can affect disk preparation. It was not possible to use this technology in the experiments as it was too expensive.

Shaw (2001) developed an alternative method of IDR measurement that used poly tetra-fluoroethylene (PTFE) disk holders, conventional round bottomed 1000 ml dissolution flasks and a USP paddle as the stirring device. Disks of 13 mm were compressed using a conventional IR press for 1-10 minutes with a compression of 7000 kg for ibuprofen. PTFE holders were manufactured to fit the disk which were fixed with paraffin wax.

Disk preparation for a selection of model drugs and their salts was found to be difficult as on ejection from the die many of the materials exhibited lamination effects. Dwell time and applied pressure had to be varied to optimise disk preparation. The PTFE holders were modified by the addition of a weight to the bottom of the holder to ensure that the face of the disk always faced the paddle when placed in the dissolution media (figure 3.28).

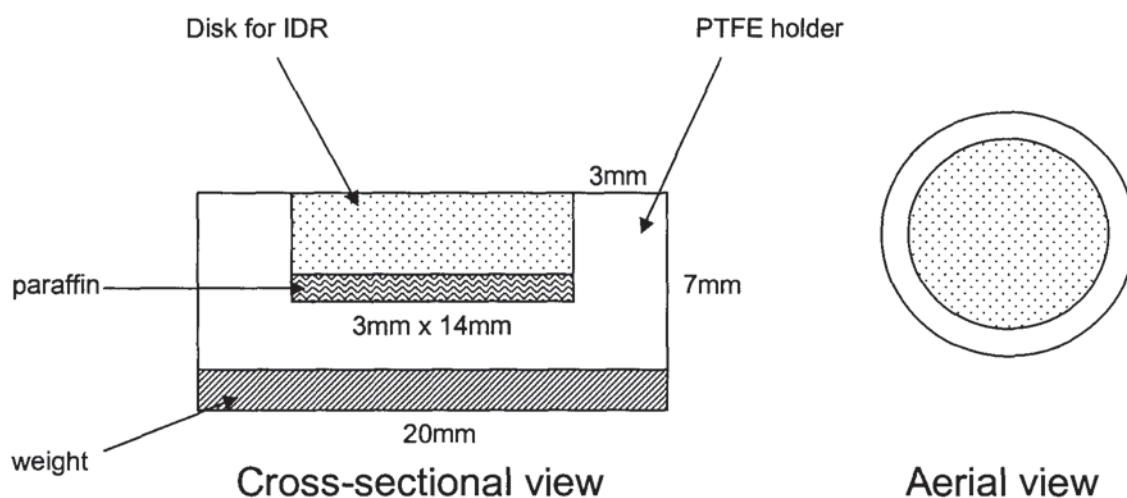


Figure 3.28 Diagram of PTFE disk holders used in IDR experiments, not to scale.

Classically disks or tablets can be produced to characterise intrinsic dissolution rates, however this method introduces many variables which can complicate the analysis of pure drug dissolution. The majority of drugs are poorly compressible so excipients are commonly used to improve the compression properties of the drug under investigation. Piroxicam has been found to produce fragile disks that exhibit fragmentation upon dissolution (Yu *et al.* 2004). Excipients can also affect the dissolution behaviour of the compact, modified gum karaya has been found to enhance dissolution of a poorly soluble drug, nimodipine (Murali Mohan Babu *et al.* 2001). Interactions may occur between drug and excipients leading to altered dissolution profiles, O'Dowd and Corrigan (1999) investigated the dissolution kinetics

of three component compacts and concluded that enhancement in dissolution was due to complexation between ingredients.

Dissolution behaviour is also determined by the porous layer that develops at the surface of a two component compressed disk as dissolution occurs. The structure of this porous layer will be affected by the properties of the two components of the compact, including their solubility, particle size, packing arrangement and percolation. Percolation theory considers the situation where pores form in the compact as dissolution occurs. These are of sufficient size to allow the generation of networks allowing solvent to penetrate and increase the contact area. Healy and Corrigan (1996) found that excipient particle size plays a critical role in determining percolation and thus dissolution rate.

Whilst excipient selection in tablet production is very important, the presence of an excipient introduces many variables that are beyond the scope of this thesis. As the aim of this work is to look at the solubility and dissolution of salts, the effect of excipients is not considered here.

The process of compaction may alter the properties of the ingredients within the tablets as a high amount of energy is required to form the compacts. Hendriksen (1990) developed a method for powder dissolution using weighed samples that were rapidly tipped from a glass vial onto the surface of the stirred dissolution medium. There are several disadvantages to this method including co-ordinating addition of all the samples at the same time, rate and location in the vessel and wetting problems that may occur because the powder may sit on the surface of the media. Shaw (2001) developed a novel method for powder dissolution by dipping the USP baskets into molten paraffin wax so that the basket was covered up to 1cm from the base. Powder was then accurately weighed in the basket so that the powder level was below the sealant line. The basket rotational speed was optimised at 100 rpm; this reduced powder disruption in the basket and allowed good mixing conditions. Dash *et al.* (1988) noted that the USP basket method was not as discriminating as the USP paddle method however Shaw (2001) demonstrated that the method had sufficient sensitivity for the study requirements. This method was chosen to investigate the dissolution characteristics of the model drugs and salts under controlled pH

conditions. Dissolution experiments were performed at a pH of one unit above the pKa for a selection of model drugs and their salts and at a higher pH, to simulate intestinal conditions.

3.5.8.1 Materials

See section 3.4.6.1

3.5.8.2 Equipment

See section 3.4.6.2

3.5.8.3 Method

Tablets were prepared using flurbiprofen, flurbiprofen benzylamine, flurbiprofen tert-butylamine, flurbiprofen cyclohexylamine, gemfibrozil, gemfibrozil butylamine, gemfibrozil benzylamine and gemfibrozil tert-butylamine. Compressed tablets of drug and salt were made using a Specac KBr press and 13mm die which was based on the method described by Shaw (2001). The tablets were made using a pressure of 7 tonnes on a powder of weight $0.01 \text{ moles} \pm 2 \text{ mg}$ with a 5 minute dwell time and a 24 hour recovery time. At least 3 replicates were made of each model drug and salt. The tablets were carefully attached to the PTFE holders so that no paraffin was present on the face of the tablet. The dissolution medium was prepared using pH 6.8 for the flurbiprofen experiments and pH 7.2 for the gemfibrozil experiments.

Samples were extracted using disposable 5 ml syringes and 0.5 ml placed in hplc vials, the remainder returned to the dissolution chamber. Samples were taken at regular time points: 5, 10, 20, 30, 50, (70) and 90 minutes.

3.5.8.4 Results and discussion

The main requirement for a dissolution method designed to determine IDRs is that a significant part of the profile is linear, indicating that a fixed surface area of drug is exposed to the dissolution medium and the stirring conditions are not causing a turbulent flow. f_2 data from the IDR experiments are displayed in table 3.30 and 3.31 and their dissolution profiles in figures 3.29 and 3.30.

The model drugs were difficult to compress; often they underwent lamination effects when ejecting from the die so that flakes from the surface of the faces were lost, exposing rough surfaces. These effects were reduced by reducing the pressure and dwell time and consequently many tablets were made and appropriate ones chosen for the experiments. Ultimately lamination effects could not be eliminated and may be a source of error. The tert-butylamine, benzylamine and cyclohexylamine salts compressed well to form smooth complete tablets that were always made with ease. Gemfibrozil butylamine salt had a tendency to stick to the smooth faces of the die and consequently it was difficult to separate the die faces from the tablet. This was carried out with a scalpel to ensure the faces of the tablets were not damaged and that this source of error was kept to a minimum. In an effort to reduce the sticking, each face of the die was painted with 10% w/v magnesium stearate suspension in ethanol. The lubricating suspension was left to evaporate before the die was constructed and powder inserted. Extreme care was required to avoid disturbing the coating during construction of the die. Determination of IDR requires a constant surface area, the effects of lamination and stickiness may have increased the surface area for the salt forms and resulted in inaccurate IDR rates.

The IDR profiles for both flurbiprofen and gemfibrozil and its salts show linear profiles which indicate that an IDR can be measured with success. The exception is gemfibrozil butylamine which completely dissolves within 30 minutes and therefore data was not used to calculate IDR because the profile was not linear. The IDR (in $\text{mg}/\text{min}/\text{cm}^2$) for both drugs and their salts was calculated by dividing the gradient obtained from each linear profile by the surface area (1.327 cm^2) of the exposed drug. The data is summarised in tables 3.32 and 3.33. The calculated correlation coefficients demonstrate good linearity for the IDR rate of the flurbiprofen and gemfibrozil salts, with R^2 values of 0.99. It is interesting to note that the IDR order found during this experiment mirrors the order of solubility *i.e.* which is flurbiprofen benzylamine>tert-butylamine>cyclohexylamine. The correlation of solubility to dissolution was not found in the powder dissolution experiments, probably because particle size, surface area and hydrodynamic conditions were variable.

Table 3.32 IDR results for flurbiprofen and its cyclohexylamine, tert-butylamine and benzylamine salts, n=3.

Material	IDR (mg/min/cm ²)	Correlation coefficient R ²
Flurbiprofen	0.00062	0.9886
F cyclohexylamine	0.00013	0.9945
F tert-butylamine	0.00046	0.9998
F benzylamine	0.00057	0.9998

Table 3.33 IDR results for gemfibrozil and its butylamine, tert-butylamine and benzylamine salts. n=3.

Material	IDR (mg/min/cm ²)	Correlation coefficient R ²
Gemfibrozil	0.00032	0.9991
G butylamine	-	-
G tert-butylamine	0.00089	0.9976
G benzylamine	0.00041	0.9985

The IDR rates demonstrate very low dissolution rates, the highest being 0.00089 mg/min/cm² and the lowest being 0.00013 mg/min/cm². Shaw (2001) found IDR rates at 70 rpm for paracetamol as 2.62 mg/min/cm² and ibuprofen as 0.3537 mg/min/cm² using USP buffer pH 6.8. The IDR measurements for flurbiprofen and gemfibrozil were performed at similar pH and stirrer speed of 100 rpm so IDR was expected to be similar to that of ibuprofen.

Flurbiprofen salts demonstrate similar dissolution to flurbiprofen or retardation of dissolution at pH 6.8. The experiment was carried out at pH 6.8 in order to maintain a constant degree of ionisation between the gemfibrozil (pK_a 4.7) and flurbiprofen (pK_a 4.3) experiments because there is a 0.4 difference in pK_a. Salt formation does not improve the dissolution characteristics of flurbiprofen. The IDR of flurbiprofen is twice that of gemfibrozil and has reasonable dissolution at a high pH so the benefits of salt formation are not seen at this pH.

Table 3.34 The f_2 fit values for the intrinsic disk dissolution of flurbiprofen and its benzylamine, cyclohexylamine and tert-butylamine salts at pH 6.8.

Flurbiprofen	f_2 fit factor value	f_2 fit factor classification
F benzylamine	64.8	Similar
F tert-butylamine	-47.3	Different
F cyclohexylamine	-25.9	Different

Flurbiprofen, benzylamine salt and tert-butylamine salt IDR resulted in large standard deviations (figure 3.29) indicating a variability in the results. These errors are probably due to the uneven surface of the face of the tablet due to lamination effects. Lamination was minimised as much as possible in the preparation procedure but it seems the effects were highly significant. It is therefore difficult to rely on the statistical f_2 evaluation of the data for these salts as each fit value is compared to the model drug itself, which has large errors.

The salts of gemfibrozil show the largest enhancement of dissolution, observed for gemfibrozil butylamine, which has a fit factor of (++)12.4) which shows marked enhancement in dissolution. The other gemfibrozil salts do not result in a different dissolution to gemfibrozil, however gemfibrozil tert-butylamine gives a 2.8-fold increase in dissolution although this is not statistically significant according to the f_2 test.

The IDR order is the same as the saturated solubility order found in section 3.5.3, which is gemfibrozil butylamine>tert-butylamine>hexylamine>gemfibrozil.

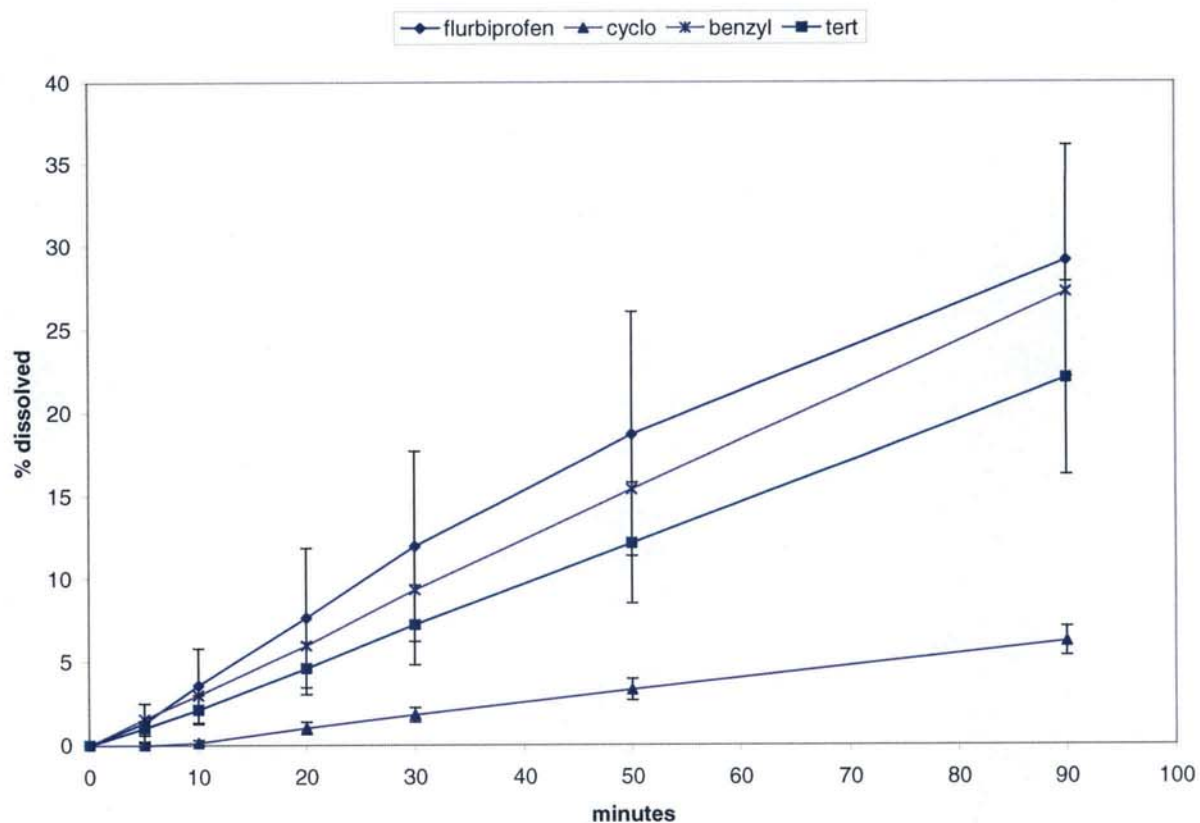


Figure 3.29 Intrinsic disk dissolution of flurbiprofen and its benzylamine, cyclohexylamine and tert-butylamine salts at pH 6.8. Results are the mean of 3 replicates and \pm SD.

Table 3.35 The f_2 fit values for the intrinsic disk dissolution of gemfibrozil and its benzylamine, cyclohexylamine and tert-butylamine salts at pH 7.2.

Gemfibrozil	f_2 fit factor value	F_2 fit factor similarity
G benzylamine	83.6	Similar
G tert-butylamine	53.4	Similar
G butylamine	++ 12.4	Different

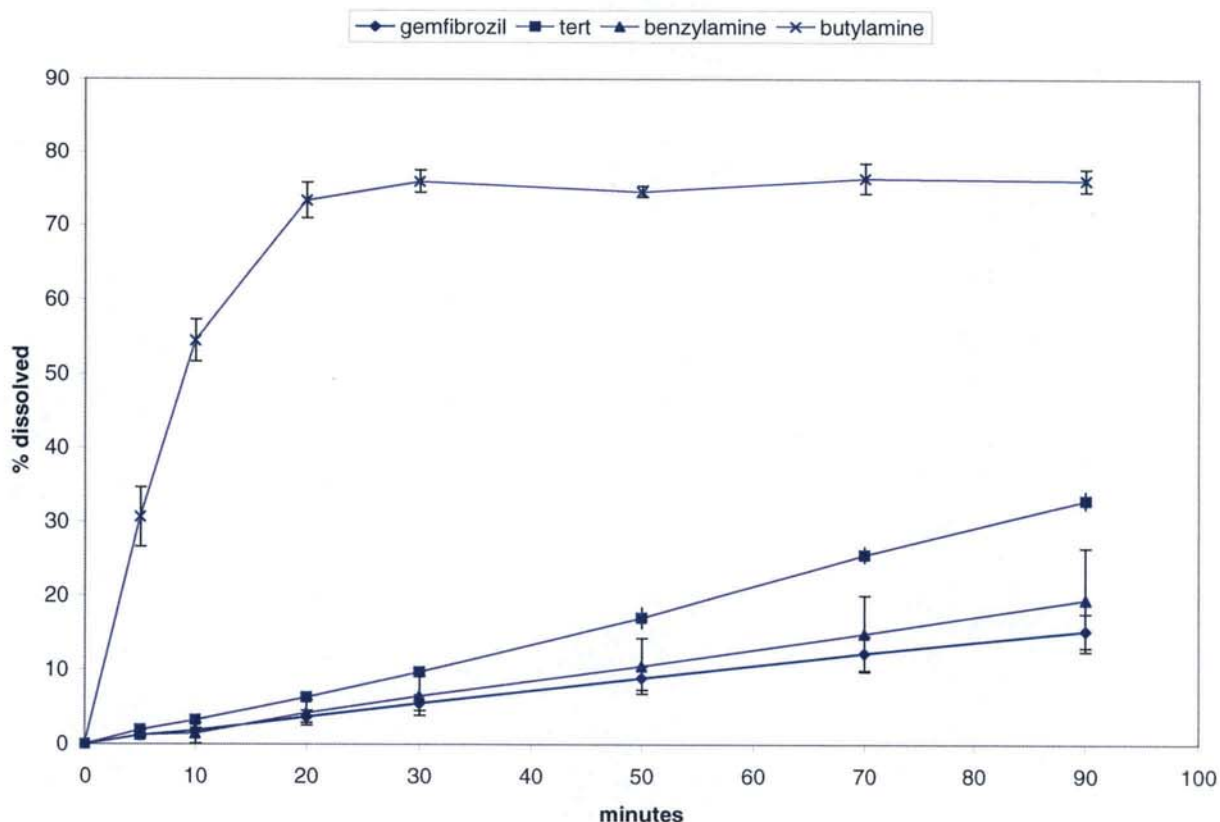


Figure 3.30 Intrinsic disk dissolution of gemfibrozil and its butylamine, benzylamine and tert-butylamine salts at pH 7.2. Results are the mean of 3 replicates and \pm SD.

3.5.8.5 Conclusions

From the IDR experiments it can be concluded that dissolution characteristics can be related to saturated water solubility data and that a rank dissolution order can be elucidated from solubility data. (There is not enough data from the IDR experiments to directly relate solubility to dissolution, ideally it would be beneficial to look at the salts of etodolac and ibuprofen also)

The dissolution data is more difficult to interpret as dissolution at a high pH results in retardation of dissolution for flurbiprofen salts because flurbiprofen itself has a high solubility at that pH. The solubility order for the hydrophilic counterions is consistently AMP1>AMP2>tris for both flurbiprofen and gemfibrozil at pH 7.2 and pH 5.6, which confirms the hypothesis that additional hydrophilic groups (OH) do not improve aqueous solubility. In this case, the saturated aqueous solubility order was not the same as the rank dissolution rates.

When the pH of the dissolution media was lowered to one pH unit above the pK_a , enhancement of dissolution was seen for all examples of model drug and selected salts. Gemfibrozil salts enhanced the overall solubility and dissolution rates due to the buffering capacity of the basic component of the salt, in the microenvironment of the diffusion layer surrounding each dissolving particle.

The AMP1 and butylamine salts consistently improved dissolution and the hexylamine salt caused the greatest enhancement in dissolution for the flurbiprofen series. This behaviour cannot be predicted from the physicochemical data measured or the solubility.

Chapter 4 The Common Ion Effect

4.1 Introduction

4.1.1 Salting-in and salting-out

The solubility of a non-electrolyte in water can either be increased or decreased by the addition of an electrolyte. When the solubility is increased it is known as salting-in; if it is reduced it is known as salting-out.

Salting-out commonly occurs when inorganic ions are added to the solution. There is a reduction in solubility observed as the added electrolyte ions interact with water molecules, and thus reduce the amount of water available for dissolution of the non-electrolyte. The greater the degree of hydration of the ions, the more the solubility of the non-electrolyte is reduced by the added ions. For example if the effect of equivalent amounts of lithium chloride, sodium chloride, potassium chloride, rubidium chloride and cesium chloride are considered, then lithium would decrease the solubility to the greatest extent as the salting-out effect decreases as the alkali metal becomes larger. Lithium is the smallest ion and has the greatest density of positive charge *per* unit of surface area and is the most extensively hydrated, whereas cesium is hydrated the least. Salting-out is encountered frequently and commonly affects the solubility of proteins in the presence of inorganic ions. Arakawa and Timasheff (1984) identified that the mechanism of protein salting-out by divalent cation salts was controlled by the balance between hydration and salt binding.

The salting-in effect occurs when either the salts of various organic acids or organic-substituted ammonium salts are added to aqueous solutions of non-electrolytes. The solubility increases as the concentration of the salt is increased. Arakawa and Timasheff (1987) discovered the salting-in effect of glycine and sodium chloride towards β -lactoglobulin. The improved solubility of β -lactoglobulin in solutions containing sodium chloride and glycine was due to the binding of electrolytes is due to a large dipole moment on the surface of the protein around neutral pH.

4.1.2 Common-ion effect

The phenomenon of decreasing solubility due to the presence of one of the ions in solution is known as the common-ion effect. When the solute phase consists of two or more species, for example for an ionisable inorganic salt, the solution phase contains discrete ions:



The equilibrium constant (K_{eq}) is the relationship between the solid and saturated solution phases, as defined by the Law of Mass Action:

$$K_{eq} = \frac{\alpha_{A(solution)} \cdot \alpha_{B(solution)}}{\alpha_{AB(solid)}} \quad \text{equation 4.2}$$

where $\alpha_{A(solution)}$, $\alpha_{B(solution)}$ and $\alpha_{AB(solid)}$ are the activities of A and B in solution, which can be substituted with concentrations for very dilute solutions. The activity of the solid is defined as unity and equation 4.2 becomes:

$$K_{sp} = C_A C_B \quad \text{equation 4.3}$$

where C_A and C_B are the concentrations of A and B in solution. In this situation K_{eq} becomes K_{sp} , the solubility product.

The presence of inorganic and organic ions present as excipients or within the dissolution media can reduce the solubility and the dissolution rate (Serajuddin *et al.*, 1987) of the salt forms of drugs by the common ion effect. Anderson and Conradi (1985) observed that the aqueous solubilities of the salts of acidic drugs varied depending on the cation or base used to prepare the salts. The pH-solubility curve for weak acids commonly shows an increase in solubility as the pH rises, but the ions present in

buffered solutions appeared to lower the aqueous solubility of the weak acid, e.g. flurbiprofen.

The common-ion effect has been recognised as an important phenomenon that lowers the expected solubility of weak acids. Serajuddin *et al.* (1987) investigated the dissolution of an organic acid in different concentrations of NaCl medium. It was shown that the dissolution rate was affected by the concentration of NaCl in the buffered dissolution medium and the presence of NaCl reduced the solubility in water. They concluded that selection of appropriate dissolution medium was necessary to discount the common ion effect and that comparisons of studies were only possible with similar strength buffer systems.

Section 3.5.2 shows the pH-solubility profiles for a selection of weakly acidic compounds, etodolac, flurbiprofen, gemfibrozil and ibuprofen. Most of these compounds, with pKa's of around 4, exhibit model pH-solubility profiles where solubility rises as pH increases according to the solubility of a weak acid equation (equation 3.7).

Flurbiprofen and its pH-solubility curve has been documented by Anderson and Conradi (1985) and Anderson and Flora (1996). They describe a pH-solubility curve that is split into two regions; the first region (pH<7.3) where the free acid is present and Region II (pH>7.3) where the sodium salt is formed. This two region solubility system has been observed also with diclofenac by O'Connor and Corrigan (2001a) and Ledwidge and Corrigan (1998). Common ion effects have also been reported for other drug-salt systems using basic drugs by Bogardus (1982) who looked at common ion equilibria with hydrochloride salts and Serajuddin and Jarowski (1985) who studied pharmaceutical acids and their sodium salts.

The solubility range is generally estimated to be 4 log units between the uncharged and ionised acid before the common ion effect becomes apparent and a solubility maximum is reached, whereas the solubility range of bases is approximated to be 4 log units (Avdeef, 2001, 2003). However many have found exceptions to these generalisations

and concluded that the common ion effect is substance specific and it is a difficult mechanism to predict or generalise on (Streng *et al.*, 1984; Anderson and Conradi, 1985). Bergstrom *et al.*, (2004) investigated the solubility of a large number of basic drugs at a range of pH values in phosphate buffer. They found that the drugs had lower solubilities in the phosphate buffer than other solvents and this was attributed to salting out effects (Arakawa and Timasheff, 1984; Kalil *et al.*, 2000; Ni and Yalkowsky, 2003) and as many of 36% of compounds showed a solubility range of 1-2 log units. 24% displayed a solubility range of 2.5-3.5 log units, indicating a varied response to the common ion. Streng *et al.* (1984) found that the solubility of terfenadine was seven times higher in the presence of lactic acid compared to phosphoric acid.

Thus the use of the Henderson-Hasselbach (HH) equation to calculate solubility can give values that are very different from experimental observations and that the estimation of parameters using the HH equation, *e.g.* calculation of solubility, lipophilicity, and pH-dependent permeability can lead to inaccurate results. This may help to explain the poor performance of software packages that calculate solubility which do not take into consideration the common ion effect. Bergstrom *et al.* (2004) also made the point that solubility data found in the literature is often determined at different pH values, using different solvents, temperatures and end points. If the experiments are performed at different ionic strengths then this may have a huge impact on the aqueous solubility due to the common ion effect. The solubility slope which is predicted by the HH equation to be -1 log unit/pH unit for cationic drugs, varied from -0.5 to -8.6. The large variation in slope demonstrates the variable response of each compound and was attributed to dimers or aggregates such as micelles. Formation of complexes has also been attributed to larger slopes than -1 (Dittert *et al.*, 1964). Bergstrom neglected to consider that the HH equation was probably inappropriate to use in his set of experiments because each compound's solubilities were all affected by salting out. The HH equation was designed to describe compounds that were not affected by this phenomenon. It would have been better to look at solubility as a function of ionic concentration together with pH, as solubility is controlled by the presence of the common ion and not only pH.

The common-ion effect occurs because, as the solution is made more alkaline, the pH rises due to the addition of sodium hydroxide, a strong alkali. As more and more sodium ions saturate the solution, the free acid is ionised in solution and due to the equilibrium shifting prefers to form an association with sodium. The subsequent sodium salt form has a reduced solubility in the aqueous environment and precipitates out, reducing the overall solubility.

This section investigates what occurs when the pH rises above 7, especially with flurbiprofen and to explain why the solubility falls as the pH increases in Region II of the pH solubility curve. A systematic approach to studying Region II was developed which included a range of NSAIDs to determine which drugs exhibited a depression in solubility as pH increased.

Experiments were designed in three stages:

Stage 1 - Solubility screen to identify an NSAID that would be susceptible to the common ion effect.

Stage 2 – Investigate the saturated solubility of each NSAID in increasing concentrations of sodium hydroxide solution. This was done to mimic what actually happens as pH increases and models what occurs in Region II. In Region II, not only does pH increase, but the concentration of sodium and hydroxide ions increases as pH rises.

Stage 3 – Identify an optimum concentration of saturated NSAID in sodium hydroxide solution. To this solution, small amounts of sodium chloride were added to observe the effect of added sodium ions on the solubility of the NSAID, to explain the pH-solubility curves observed with flurbiprofen. The results of this experiment would confirm that the common ion effect was responsible for the reduction in solubility as the pH increased above 7.

Seven NSAIDs were tested which were: etodolac, flurbiprofen, gemfibrozil, ibuprofen, indomethacin, naproxen and piroxicam.

4.2 Experimental

4.2.1 Materials

Diclofenac, indomethacin, naproxen, piroxicam and sodium hydroxide were obtained from Aldrich (Poole, UK). Etodolac, flurbiprofen, gemfibrozil and ibuprofen were obtained as detailed in section 2.2. Standard 1 M sodium hydroxide solution was obtained from Fisher Scientific, Loughborough, UK. Double distilled water was generated in-house using a Fisons Fi-streem still.

4.2.2 Equipment

A Variomag multipoint stirrer was used for sample preparation, set at 500 rpm. HPLC equipment and methods were used as detailed in section 2.1.

4.2.3 Method

4.2.3.1 Solubility screen in 2 M sodium hydroxide

A solubility screen was devised to measure the solubility of the selected NSAIDs in 2 M sodium hydroxide solution. 20 ml of 2 M sodium hydroxide solution was accurately measured into 40 ml glass sample vials. A small magnetic flea was placed in each vial and excess powdered NSAID was added to the solution until saturated. The vials in which a precipitate formed easily were identified as being affected by common ions and those materials were used in further experiments. These are identified in section 4.2.4.

4.2.3.2 Solubility of NSAID in sodium hydroxide

Solutions of 2, 1.5, 1, 0.5 and 0.1 M sodium hydroxide were prepared and 10 ml of each was accurately pipetted into 40 ml glass sample vials containing a small magnetic flea. Solid was added incrementally to each solution until a precipitate formed and was maintained for the duration of the experiment. The vials were stirred on a magnetic stirrer for 24-48 h to allow for equilibration; after this time the samples were analysed. 5 ml was extracted from each vial with a disposable syringe and filtered through 0.45 μ m 2.5 cm diameter PTFE syringe filters. The filtrate was then analysed by HPLC, to determine the concentration of NSAID. The experiments were performed under ambient conditions and in triplicate.

Additionally concentrations of 1.1, 1.2, 1.3, 1.4 M sodium hydroxide were prepared and the saturated solubility of naproxen was obtained at each concentration.

4.2.3.3 The effect of added NaCl on a saturated solution of NSAID in sodium hydroxide 200 ml of 0.1 M sodium hydroxide was placed in a beaker with a magnetic flea and flurbiprofen was added until a saturated solution formed; this was repeated for piroxicam. Naproxen was added to 75 ml of 1 M sodium hydroxide solution and stirred with the aid of a magnetic flea. The saturated suspensions were left stirring for 12 h to ensure equilibrium was established. Additional powder was added if no precipitate was present. The experiments were performed under ambient conditions and in triplicate.

The solutions were pre-filtered through Whatman ashless paper filters with pore size 12 μm under vacuum using a Buchner funnel and flask. The filtrate was collected and re-filtered through 0.4 μm cellulose 250 ml bottle top filters under vacuum to remove excess solid. The filtrate was then measured into 40 ml sample vials with small magnetic fleas according to table 4.1. Sodium chloride was added to the vials as detailed in table 4.1. The vials were mixed for at least 30 minutes before 5 ml was extracted with a disposable syringe and filtered through 0.45 μm PTFE syringe filters, supplied by Chromosexpress. The filtrate was diluted if necessary and analysed by HPLC.

Table 4.1 Table detailing sample volume and additional sodium chloride to investigate the common ion effect on saturated NSAID solutions.

Material	Volume (ml)	mMoles of drug	mg added of sodium chloride	Overall concentration mmols/ml of NSAID
Flurbiprofen, piroxicam	10	0.5	29.3	0.05
Naproxen	5	0.5	30	0.1
Flurbiprofen, piroxicam	10	1	58.5	0.1
Naproxen	5	1	60	0.2
Flurbiprofen, piroxicam	10	1.5	87.8	0.15
Naproxen	5	1.5	90	0.3
Flurbiprofen, piroxicam	10	2	119	0.2
Naproxen	5	2	120	0.4
Flurbiprofen, piroxicam	10	3	175.5	0.3
Flurbiprofen, piroxicam	10	4	234	0.4
Naproxen	5	4	240	0.8
Flurbiprofen, piroxicam	10	5	292.5	0.5

4.2.4 Results and Discussion

4.2.4.1 Solubility screen in 2 M sodium hydroxide

Table 4.2 The behaviour of selected NSAIDs in 2M sodium hydroxide solution.

NSAID	Solubility in 2M sodium hydroxide
Etodolac	Unlimited
Indomethacin	Unlimited
Ibuprofen	Unlimited
Gemfibrozil	Unlimited
Flurbiprofen	Limited
Naproxen	Limited
Piroxicam	Limited

Table 4.2 confirms the NSAIDs affected by the common ion effect *i.e.* those materials that had 'limited' solubility in 2 M sodium hydroxide solution were used in subsequent solubility experiments.

4.2.4.2 NSAID solubility in increasing concentrations sodium hydroxide

The saturated solubility of flurbiprofen and piroxicam decreased as the molar concentration of sodium hydroxide solution increased from 0.1 M to 2 M. The reduction in solubility followed an exponential decline of good regressional fit; for flurbiprofen the fit is $R^2=0.8809$ and for piroxicam it is $R^2=0.976$ (figures 4.1 and 4.2).

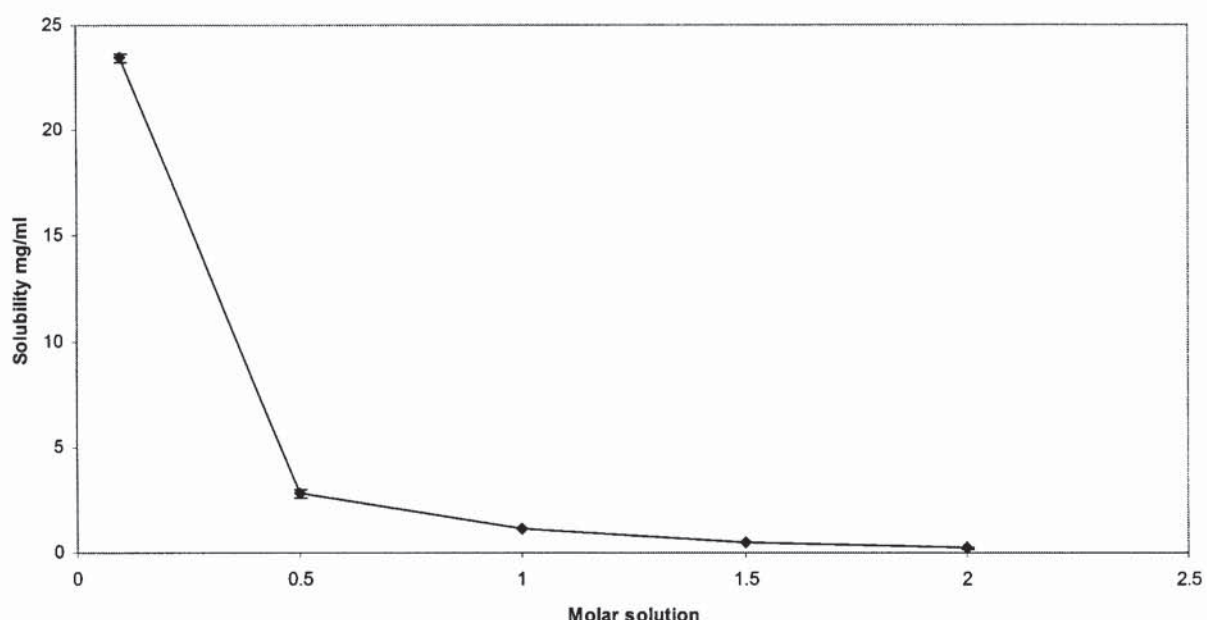


Figure 4.1 The solubility of flurbiprofen in sodium hydroxide solution, from 0.1-2M. Logarithmic regression fit of $R^2= 0.8809$. (n=3; mean \pm SD).

The saturated solubility of flurbiprofen fell from 24.06 mg/ml at 0.1 M to 1.15 mg/ml at 2 M sodium hydroxide (figure 4.1); the standard deviations are small at these concentrations. Figure 4.3 shows that the solubility of piroxicam decreases from 34.90 mg/ml in 0.1 M to 1.10 mg/ml in 2 M sodium hydroxide; again variation is small.

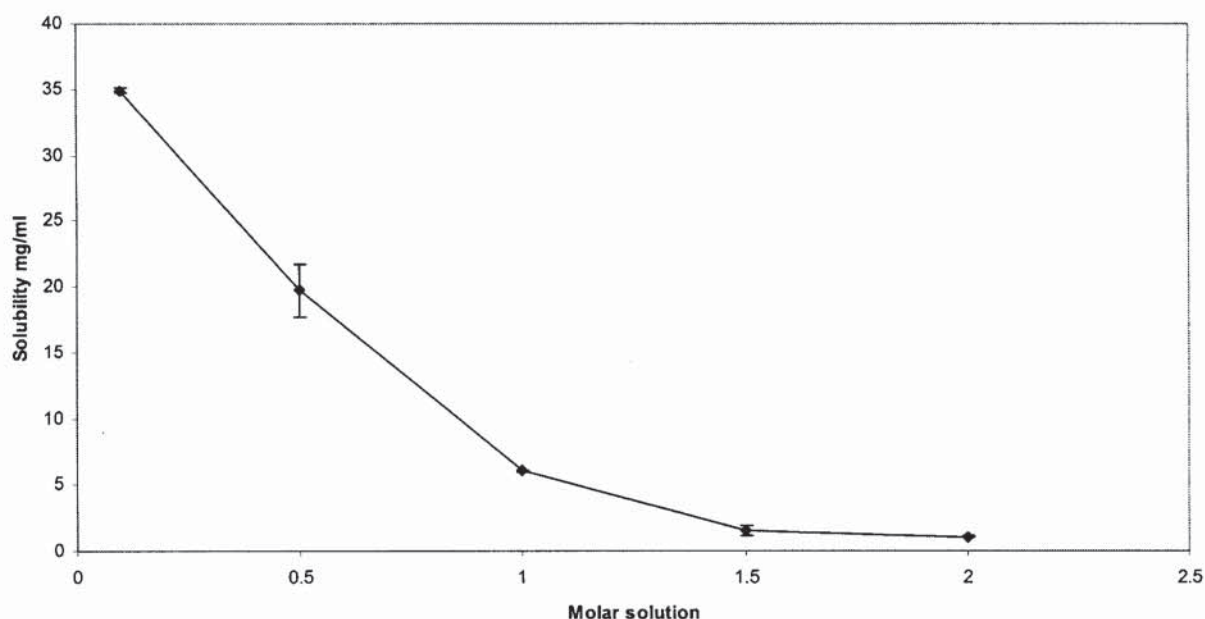


Figure 4.2 The solubility of piroxicam in sodium hydroxide solution, from 0.1-2M. (n=3; mean \pm SD). The curve has a logarithmic fit of $R^2=0.976$.

Naproxen solubility increased up to a concentration of 1 M sodium hydroxide and then decreased as the concentration increased above 1 M (figure 4.3). The solubility increased from 23.66 mg/ml in 0.1 M NaOH to 124.21 mg/ml in 1 M NaOH and then reduced to 4.69 mg/ml in 2 M NaOH. In order to minimise errors in the concentrations of sodium hydroxide used, standard sodium hydroxide solutions were purchased and serial diluted in further experiments. The solubility of naproxen in 1 M standard sodium hydroxide was found to be 186.81mg/ml, higher than found previously. The new solubility value was identified as the true concentration as standard solutions were used and Class A volumetric flasks were used for all volume measurements and calibrated pipettes.

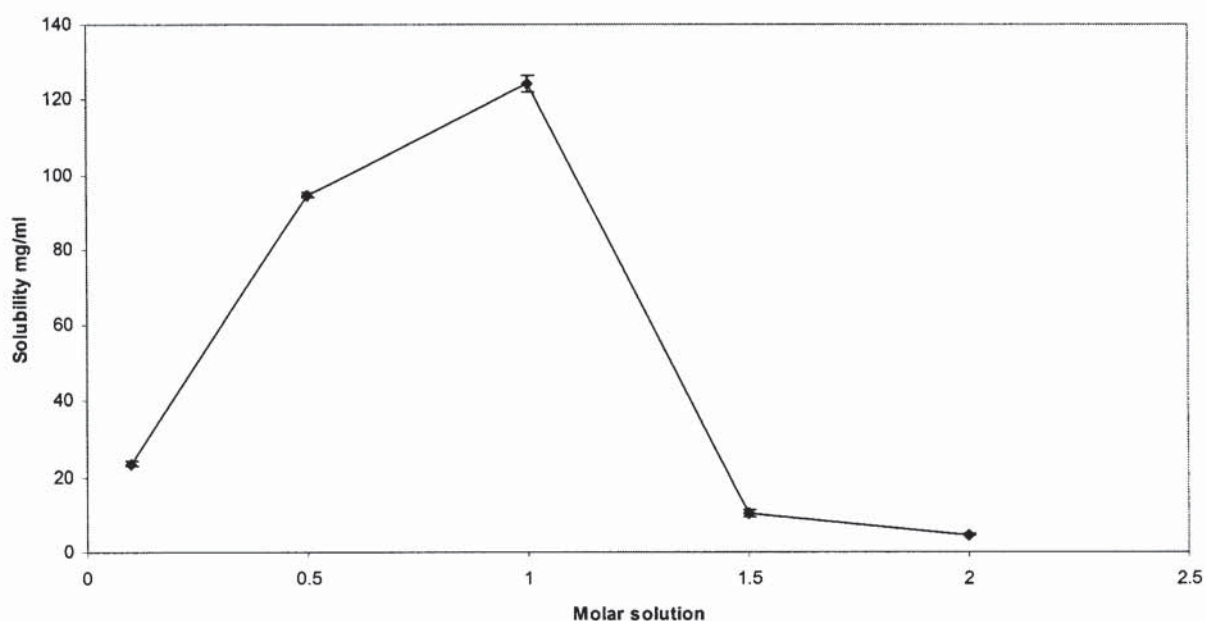


Figure 4.3 The solubility of naproxen in sodium hydroxide solution, from 0.1-2M. (n=3; mean \pm SD).

The solubility of naproxen was explored in more depth between 1 M and 2 M sodium hydroxide and the results are shown in figure 4.4. Between 1 M and 2 M sodium hydroxide, a reduction in solubility is seen as observed with flurbiprofen and piroxicam. The reduction in solubility occurs from 1.1 M and follows an exponential decline in concentration with a fit of $R^2=0.919$.

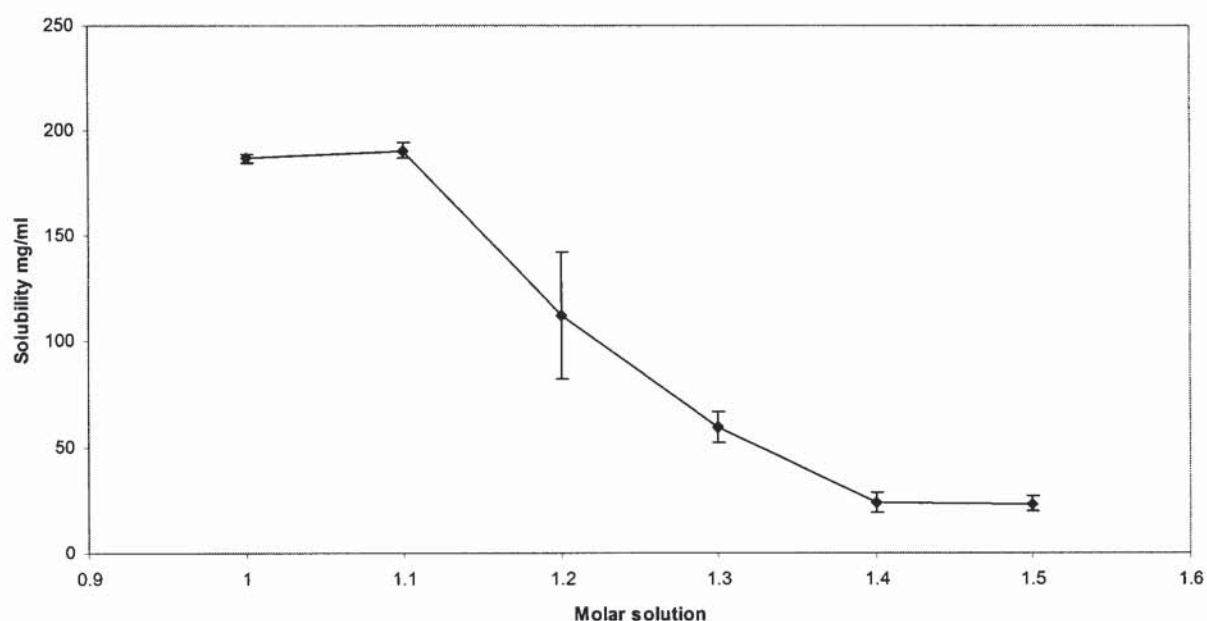


Figure 4.4 The solubility of naproxen in sodium hydroxide solution, from 1-1.5M. The curve has a logarithmic regression fit of $R^2=0.919$ after 1.1M. (n=3; mean \pm SD).

The results show that as the concentration of sodium hydroxide increases, solubility falls exponentially. This may be due to the increasing concentration of Na^+ present in solution, which leads to the formation the sodium salt of the NSAID and this has a lower solubility than the free acid. The sodium salt precipitates out as the solution is swamped by Na^+ and the equilibrium in equation 4.1 shifts to the left. As further Na^+ ions are added the amount of NaA increases.



Stage 3 of the experiment was designed to prove that the solubility of the NSAIDs is directly affected by sodium ions which reduce the solubility and that the common ion effect is responsible.

4.2.4.3 The effect of added NaCl on a saturated solution of NSAID in sodium hydroxide
The results for each drug are displayed in figures 4.5, 4.6 and 4.7. Each shows an exponential reduction in solubility as increasing amounts of sodium chloride were added to the solution.

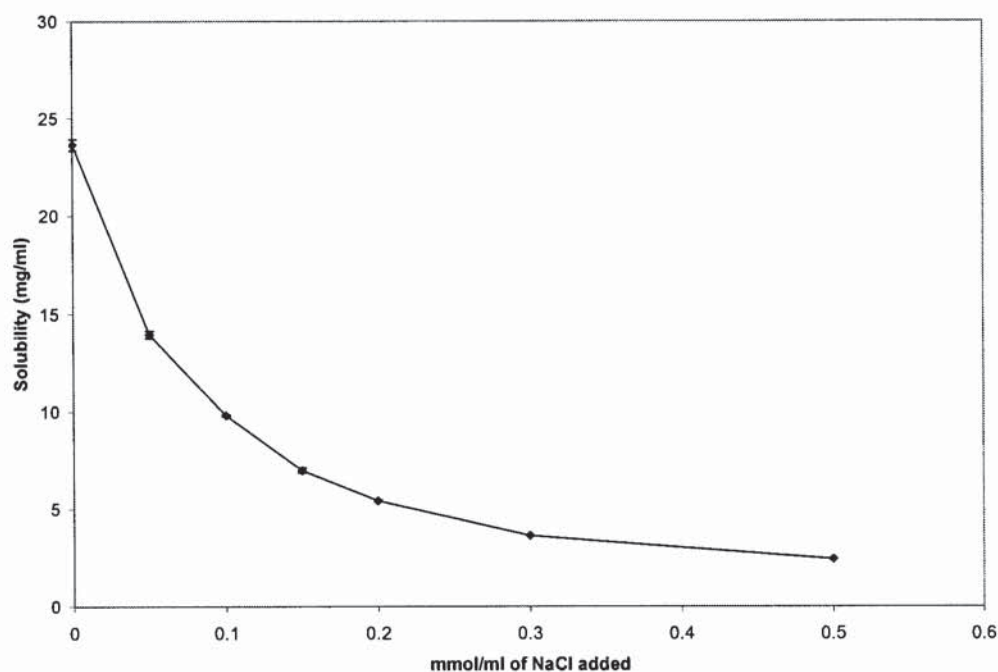


Figure 4.5 The effect of added sodium chloride on the solubility of flurbiprofen in 0.1 M sodium hydroxide solution. (n=3; mean \pm SD). It has a exponential regression fit of $R^2=0.9884$.

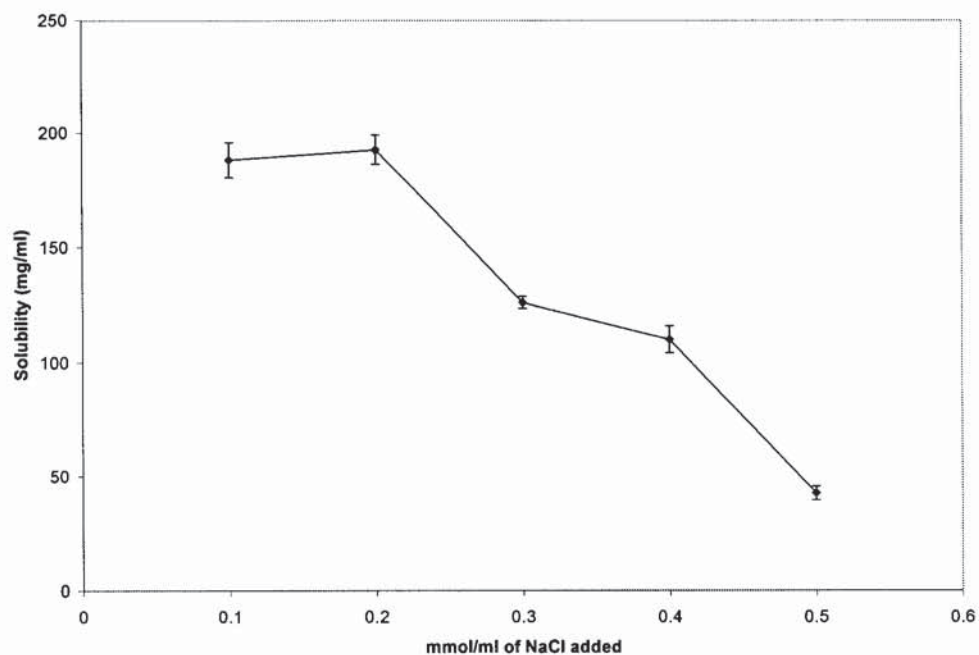


Figure 4.6 The effect of added sodium chloride on the solubility of naproxen in 1M sodium hydroxide solution. (n=3; mean \pm SD). It has an exponential regression fit of $R^2=0.9431$ for the sloping part of the curve, from 0.2 to 0.5 mmol/ml.

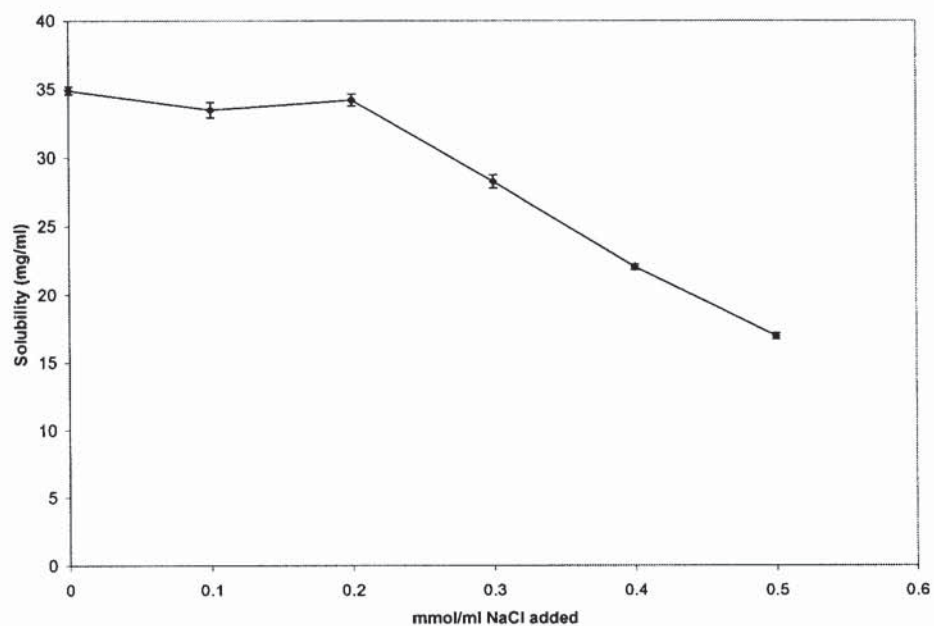


Figure 4.7 The effect of added sodium chloride on the solubility of piroxicam in 0.1M sodium hydroxide solution. (n=3; mean \pm SD). It has an exponential regression fit of $R^2=0.9884$ for the sloping part of the curve, from 0.2-0.5mmol/ml.

Each NSAID has a good logarithmic regression fit to each curve, from $R^2=0.9884$ for piroxicam to $R^2=0.9431$ for naproxen; piroxicam may have a better fit due to a fewer number of data points. More data points were collected for flurbiprofen resulting in a more reliable result. It was more difficult to perform this experiment with piroxicam and naproxen as when sodium chloride was added at lower concentrations there was a transient precipitate present in the sample. It was difficult to decide when the appropriate time was to take the sample. When left to equilibrate for at least 30 minutes, there was a plateau region before the solubility reduces on addition of sodium chloride, because after 30 minutes the precipitate re-dissolved. When large amounts of sodium were present the suspension became very viscous and it was difficult to extract the sample in sufficient quantities to analyse. These problems required the experiment to be repeated several times in order to minimise errors.

Figures 4.5, 4.6 and 4.7 show that the selected NSAIDs have solubilities that are affected by common-ions. Both Anderson and Flora (1996) and Anderson and Conradi (1985) identified a plateau in flurbiprofen solubility as pH increased, and they displayed it graphically as solubility (M) versus pH. Serajuddin and Jarowski (1984) observed a reduction in theophylline solubility as pH increased, displayed as solubility (mg/ml) versus pH. The reduction in solubility is due to the addition of sodium ions not hydroxide ions and it is inaccurate to display the reduction in solubility as a function of pH. As pH increases, solubility would increase due to the presence of hydroxide ions, however because sodium hydroxide is added the sodium saturates the system and it is impossible to eliminate sodium or a similar ion from the system. If potassium hydroxide was used a similar effect would be expected, but the potassium salts would have different solubilities.

Thomas and Rubino (1994) studied a range of hydrochloride salts of beta-blocking drugs and their solubility and salting-out relationships. It was reported that some, not all, salts exhibited salting-out in the presence of sodium chloride and Setchenow plots were used to analyse the data. The Setchenow equation was originally used as a means to

characterise and quantify salting-out for a non-electrolyte solute in the presence of strong electrolytes although Bogardus (1982) concluded that the Steschenow treatment was inappropriate for description of common-ion equilibria of hydrochloride salts because self-association of the drug cannot be detected. Data analysis based on solubility product equilibrium theory was deemed a more satisfactory approach as detection of self-association is not usually a problem since the apparent K_{sp} , calculated as the product of solubility and chloride concentrations, will not be constant.

The Setchenow equation:

$$\log \frac{M_o}{M} = K_s C \quad \text{equation 4.2}$$

where M_o/M is the ratio of the hydrochloride salt solubility in water/sodium chloride solution, C is the molar concentration of sodium chloride and K_s is the salting out constant. It remains to be clear whether this treatment is ideal for acidic drugs and their salts because the methodology in these experiments was very different.

The results were linearised in an attempt to determine a rank order of susceptibility to the common ion effect. Results from the addition of sodium chloride experiments were plotted as log of the concentration of solubility (mg/ml) against sodium chloride added (log(mmol/ml)) and the results are displayed in figure 4.8.

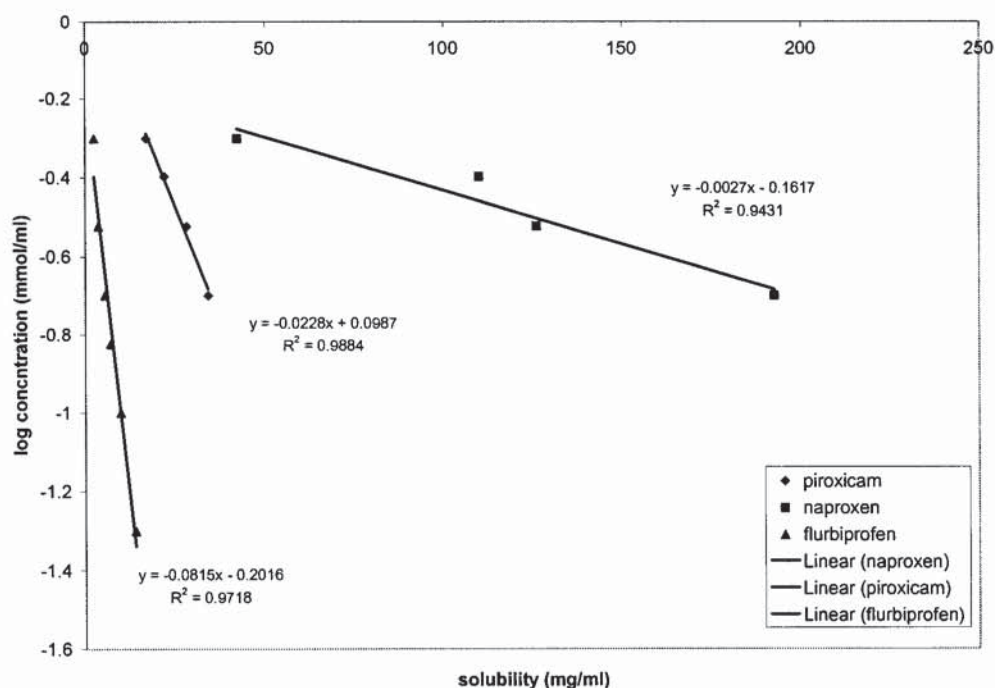


Figure 4.8 Plots of solubility (mg/ml) against log concentration (mmol/ml) sodium chloride added for flurbiprofen (0.1 M sodium hydroxide), piroxicam (0.1 M sodium hydroxide) and naproxen (1 M sodium hydroxide) in sodium hydroxide solutions, actual concentrations in brackets. Only data from the linear portion of the graph is shown, (n=3; mean \pm SD). A multiple linear regression was performed on the data and equations of the line and R² values are displayed.

A multiple linear regression was performed on the data for flurbiprofen, piroxicam and naproxen and the constant K from the slope of the linear portion of the plots. The materials have a good linear regression fit values of R²= 0.9718 for flurbiprofen, 0.9431 for naproxen and 0.9884 for piroxicam. Unfortunately only four data points were available for analysis for naproxen and piroxicam and more data points could be generated from the linear part of the graph. Due to difficulties performing these experiments (described previously), this was not possible.

Thomas and Rubino (1996) also attempted to determine why there is some structural specificity in the determination of sensitivity of the compounds to the common-ion effect. Compounds that exhibited salting-out had ring substituents that were relatively small and the aromatic rings tend to be planar. The presence of larger, bulkier groups that

could hinder close stacking was observed to decrease susceptibility. It was concluded that hydrophobic ring overlap may enhance the stability of the hydrochloride complexes, and formation of such complexes may facilitate precipitation of the hydrochloride salts in the presence of excess chloride ion. Serajuddin *et al.* (1987) concluded that aggregation occurs in a stacking arrangement for ring type structures. This may explain why flurbiprofen which has two joined aromatic rings, allows twisting of the planar rings that may assist stacking and overlap of hydrophobic rings and facilitate the precipitation of Na⁺ complexes. Piroxicam and naproxen (for structures see appendix A.1) both have two aromatic rings and may also facilitate the precipitation of Na⁺ complexes.

Thomas and Rubino (1996) observed that materials with one aromatic ring show little or no salting out, so gemfibrozil and ibuprofen should show no salting out effects and this is true for this study. Etodolac and indomethacin contain indole rings together with aromatic rings and these do not show salting-out effects, as observed in table 4.2.

Thomas and Rubino (1996) also discovered there was a direct relationship between log P and a salting-out constant which was found from the gradient of a plot of solubility against log concentration, but this relationship is not apparent for this data set. Naproxen has the highest salting out constant and a Log P value of 3.22 and flurbiprofen has the lowest salting out constant and a Log P value of 3.44; piroxicam has a Log P value of 1.8. Although this is based on three samples, drug structure and association in solution was seen to determine the salting-out behaviour of the selected examples.

4.2.5 Further work: examination of crystal structure

The assumption is that aggregation of the sodium salt of a weak acid is due to physicochemical processes that may allow sodium to destabilise the aqueous drug molecule to allow precipitation of the solid salt. It is presumed that the formation of this solid is a thermodynamic process, so the system reaches a state of minimum free energy. DSC and elemental analysis could be performed on a dried precipitate to confirm the presence of a sodium salt. Examination of the crystal lattice therefore may

provide an understanding of the thermodynamic processes involved in precipitation and determining the crystal structure of the sodium salts of e.g. flurbiprofen and etodolac sodium, may show differences in packing which can explain the behaviour. If it is possible to distinguish why flurbiprofen or naproxen sodium precipitate rather than etodolac sodium, then it can be determined why some weak acids are affected by salting-out and others not.

Further experiments could be done to observe the progression of precipitation with added sodium. This could be measured by ssNMR, solution calorimetry and surface tension.

Chapter 5 Surface active characteristics of drug-salt systems

5.1 Introduction

5.1.1 Amphipathic compounds

Surfactants or surface-active compounds are molecules that have the ability to accumulate at phase boundary surfaces and alter the chemistry of the interface. Amphiphiles are surface-active compounds that have two distinct regions in their chemical structure; they contain hydrophobic and hydrophilic regions. The hydrophobic components are commonly hydrocarbon chains or ring systems containing either saturated or unsaturated bonds. The hydrophilic regions can be anionic, cationic or non-ionic. Common surfactants and their classification are listed in table 5.1.

Table 5.1 Classification of surfactants

<i>Anionic</i>	<i>Hydrophobic moiety</i>	<i>Hydrophilic moiety</i>
Sodium stearate	$\text{CH}_3(\text{CH}_2)_{16}-$	$-\text{COO}^-\text{Na}^+$
Sodium dodecyl sulphate	$\text{CH}_3(\text{CH}_2)_{11}-$	$-\text{SO}_4^-\text{Na}^+$
Sodium dodecyl benzene sulphonate	$\text{CH}_3(\text{CH}_2)_{11}\text{C}_6-$	$-\text{SO}_3^-\text{Na}^+$
<i>Cationic</i>		
Hexadecyltrimethylammonium bromide	$\text{CH}_3(\text{CH}_2)_{15}-$	$-(\text{CH}_3)_3\text{N}^+\text{Br}^-$
<i>Non-ionic</i>		
Heptaoxyethylene monoethylamine ethylamine	$\text{CH}_3(\text{CH}_2)_{15}-$	$-(\text{OCH}_2\text{CH}_2)_7\text{OH}$

The dual nature and structure of these molecules accounts for their unique behaviour and allows them to adsorb to a solution/air interface thus being surface-active. The hydrophobic region of the molecule escapes from the hostile aqueous environment by protruding into the vapour phase. Similarly emulsions can be formed by surfactant accumulation at oil/water interfaces, with the separate regions protruding into each phase, leaving the hydrophilic group in contact with the aqueous phase.

In this way surfactants can lower the surface tension of water by accumulating at the surface and affecting the arrangement of water molecules at the surface. Each surfactant molecule squeezes between water molecules and disrupts the surface tension; this occurs to achieve a minimum free energy state. Since the intermolecular attraction between water molecules and non-polar groups is less than between two water molecules, the surface tension is lowered.

The Gibbs adsorption equation describes the equilibrium between the surfactant molecules at the surface or interface and the molecules in the bulk solution and is written

$$d\gamma = -S_{xs}dT - C_{xs}d\mu \quad \text{equation 5.1}$$

where S_{xs} is the surface excess entropy, C_{xs} is the surface excess concentration, T is the temperature, μ is the chemical potential and γ is the surface energy.

Figure 5.1 shows a typical plot of surface tension against log concentration for an aqueous solution of a model surfactant. Surface tension falls rapidly and then stabilises and becomes constant as concentration is increased. As the surfactant molecules saturate the surface of the solvent, the increased numbers of surfactant molecules arrange themselves in an alternative manner. Micelles form when the surface is saturated with surfactant molecules (figure 5.2) where a collection of surfactant molecules spontaneously form the most stable conformation and the hydrophilic moiety is in contact with the solvent and forms the external surface. The internal part of the micelle contains the hydrophobic section of the amphiphile.

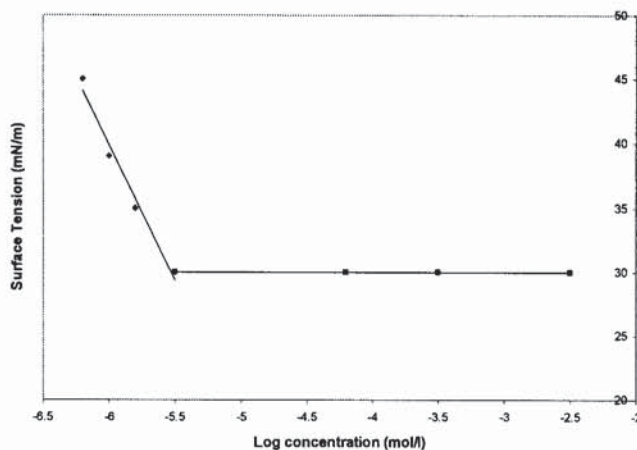


Figure 5.1 Surface tension versus log concentration plots for a model compound illustrating typical surfactant behaviour (schematic).

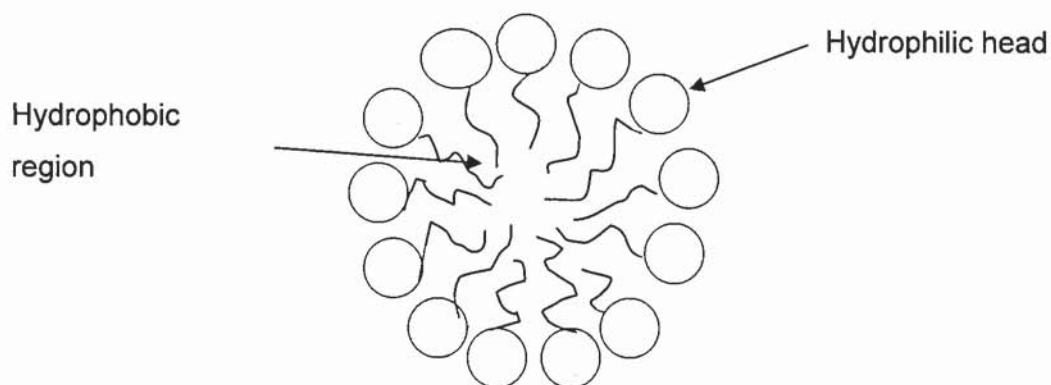


Figure 5.2 Schematic diagram of the conformation of a typical micelle

Micelles are formed at higher concentrations because the surfactant molecules prefer to associate together to shield the hydrophobic portion of the amphiphile. At this point, there is no further reduction in surface tension as more micelles are formed and agglomerate as surfactant concentration increases. The surface excess concentration of surfactant molecules remains approximately the same and further increases in surfactant concentration do not result in any further change in surface tension. The intercept of the two linear parts of the lines is termed the critical micelle concentration (CMC).

Amphipatic compounds are very useful to pharmaceutical scientists as they can be utilised in many ways. Surface-active drugs or surfactants can be used to disrupt membranes to improve the delivery of more insoluble drugs. They can also be used to solubilize slightly soluble drugs and to prevent them from degradation, also, the stability of the drug in micelles can be altered favourably or unfavourably by the presence of surface active agents. In this way, surface active agents including drugs and other molecules can be used to improve formulations to enhance drug delivery.

5.1.2 Factors affecting the CMC

Addition of electrolytes can alter the mode of association of surface-active materials; hence the CMC can be altered. Other factors such as temperature, ionic strength and pH can also affect the CMC. Consideration of these parameters and their possible effects is important when designing experiments with surface-active materials.

5.1.2.1 The effect of chain length

The surface activity of a particular surfactant depends on the structure of the hydrophilic and hydrophobic portions. In a homologous series of surfactants, an increase in hydrocarbon chain length can strongly affect the CMC; for example, the CMC of dodecyl β -D-glucoside is 132-times lower than that of octyl β -D-glucoside; i.e. the CMC decreases by a factor of 3.4 per methylene group (Shinoda *et al.*, 1961). This effect occurs because, as the non-polar portion increases in size, there is more disruption at the interface and micelles form more readily. It is well known that the CMC is strongly dependent on chain length while the type of hydrophilic group has only a minor effect. For example, adding one CH(OH) unit to $R_8OCH_2-CH_2OH$, leads to an increase in CMC by a factor of 1.18 (Shinoda *et al.*, 1959), table 5.2.

Table 5.2 CMC values of singly dispersed anionic^a and non-ionic surfactants (Shinoda et al., 1996). ^aAttwood and Florence (1983).

Surfactant	CMC mM
R ₈ OH	3.8
R ₈ OCH ₂ CH ₂ OH	4.9
R ₈ OCH ₂ CH(OH)CH ₂ OH	5.8
Octyl glycoside	25.0
R ₈ OH	0.23
Decyl glycoside	2.2
Dodecyl glycoside	0.19
SLS ^a	8.3

5.1.3.2 The effect of added electrolytes

The effects of electrolytes on micelles are an important consideration as physiological conditions contain many electrolytes which could affect the activity of the micelles and hence alter the intended action of the micelle. Micelle formation, or CMC, can be affected by the addition of electrolytes, for example addition of increasing concentrations of electrolyte to a solution of trimeprazine tartrate causes the micellar radius to increase (Attwood *et al.*, 1996). The CMC of phenothiazine micelles decreases and aggregation number increases with increasing electrolyte concentration. Aggregation number is the number of molecules that are associated together to form a micelle. At higher salt concentrations, a spherical-to-rod transition occurs. Similar behaviour has been observed for solutions of conventional surfactants in high electrolyte concentrations where spherical micelles have transformed into polydisperse rod-like micelles (Attwood, 1995). Micelle formation of block copolymer surfactants is encouraged as temperature increases, the aggregation number increases as there is a decrease in polarity as the temperature increases (Alexandridis and Hatton, 1995).

5.1.3.3 The effect of hydrophilicity on micelle formation

Micellar amphiphiles have hydrophobic groups consisting of hydrocarbon chains. Increases in chain length result in a decrease in CMC. Many drugs that are surface-active form small, tightly packed micelles in aqueous solution (Florence and Attwood, 1998). CMC was observed to decrease with an increase in hydrophobicity for a

series of diphenylmethane drugs which was characterised by an increase in aggregation number (Attwood, 1976).

5.1.3.4 The effect of pH

The variation in physiological pH along the gastro-intestinal tract is an important consideration when designing and delivering drugs for specific purposes. Changes in pH can affect the ionisation of molecules and will alter the absorption characteristics of a delivery system. The solution pH can affect the micellisation of drugs and for a series of piperazine-containing drugs the CMC was increased and the aggregation number decreased with decreasing pH, due to protonation of the second nitrogen atom of the drug's piperazine ring (Attwood and Natarajan, 1981).

5.1.3.5 Studying the micellisation process

Micelle formation has been extensively studied and has been envisioned as a stepwise process: as the CMC is reached, aggregation occurs and micelles form. Micelles are characterised by physicochemical parameters such as the CMC, aggregation number (N) which is the number of surfactant molecules present in the micelle, particle size and hydrophilic-lipophilic balance (HLB). These parameters are usually not sufficient to describe a very complex aggregation of molecules, *e.g.* micelles are often polydisperse and often average size is usually used to represent the distribution. Also micelles are assumed to be spherical but cylindrical shaped micelles have been described by Fendler (1983). Micelles are also highly dynamic structures and can rotate about their molecular axis (Ernandes *et al.*, 1977) and diffuse laterally along the micellar surface (Liang *et al.*, 1993). In comparison with other aggregates, such as bilayers, micelles are loosely packed and less stable (Frezzatti *et al.*, 1986).

5.1.4 Surface activity of drugs

Surface activity at the air/solution interface has been reported for a wide variety of drugs which include phenothiazine drugs (Attwood *et al.*, 1996 & 1997), benzodiazepines (Attwood *et al.*, 1993), tranquilisers and analgesics (Attwood *et al.*,

1980), peptides (Hwang and Vogel, 1998), antibiotics and tricyclic depressants (Atherton and Barry, 1985, Attwood *et al.*, 1995, Sarmiento *et al.*, 1997), antihistamines (Causon *et al.*, 1981), anticholinergics (Yokoyama *et al.*, 1994), beta-blockers (Ruso *et al.*, 1999), local anaesthetics (Attwood and Fletcher 1986), non-steroidal ant-inflammatory drugs (Rades and Muller-Goymann, 1997) and anti-cancer drugs (King *et al.*, 1989) (table 5.3).

Surface-active drugs associate in two ways (table 5.3); by closed association and by open association (Attwood, 1995). The hydrophobic groups of most drugs are aromatic and if these have a high degree of flexibility, then as a consequence, these drugs may resemble surfactants in their association behaviour. Those drugs with rigid aromatic ring systems have a charge-bearing moiety, *e.g.* N attached directly to the hydrophobic ring system (Attwood, 1995). Although reports using micellar systems to deliver drugs are widespread, *e.g.* cytotoxics delivered in liposomes or the use of surfactants to solubilise or enhance the permeation of poorly soluble drugs, the use of surfactants as drugs is less widespread. Long chain surfactants containing quaternary ammonium or pyridinium ions as headgroups have been used as bactericidal or bacteriostatic agents (Kopecki, 1996). Trimethyl alkylammonium compounds with alkyl chains ranging from two to 16 carbons have shown long lasting and almost irreversible anaesthetic activity that increases with increasing chain length (Scurlock and Curtis, 1981). However, neurotoxic effects render these compounds unacceptable for clinical use. The potential role of surfactants as drugs as drug delivery systems has yet to be realised.

Table 5.3 Micellar properties of some non-peptide surface active drugs in water

Class	Drug	CMC (M)
Analgesics	Dextropropoxyphene	1.0×10^{-1}
Antibiotics	Penicillin G	2.5×10^{-1}
Anticholinergics	Adiphenine.HCl	8.2×10^{-2}
Antifungal polyenes	Nystatin	3.0×10^{-1}
Antihistamines	Diphenhydramine.HCl	9.0×10^{-2}
β -blockers	Acetobutolol.HCl	1.7×10^{-1}
General anaesthetics	Thiopental	7.0×10^{-3}
Local anaesthetics	Tetracaine.HCl	1.3×10^{-1}
Phenothiazines	Chlorpromazine.HCl	1.9×10^{-2}
Tranquilizers	Flupenthixol	8.5×10^{-3}
Tricyclic antidepressants	Amitriptyline.HCl	3.6×10^{-2}

5.1.4.1 Closed Association

Flexible hydrophobic groups are common in drugs that form stable micelles in solution, e.g. drugs with a diphenylmethane structure (see figure 5.3 diphenhydramine). A plot of light scattering ratio against concentration shows a well defined change in gradient at a critical concentration, which is commonly identified as the CMC. Alternatively surface tension, vapour pressure, osmometry and conductivity can be measured as a function of concentration. All yield inflection points at critical concentrations equivalent to the CMC of a typical surfactant system. Figure 5.4 illustrates a typical drug micelle.

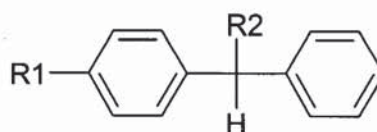


Figure 5.3 Structure of typical diphenylmethane derivatives. Diphenhydramine R1= $\text{OCH}_2\text{CH}_2\text{N}^+\text{H}(\text{CH}_3)_2$ R2= H

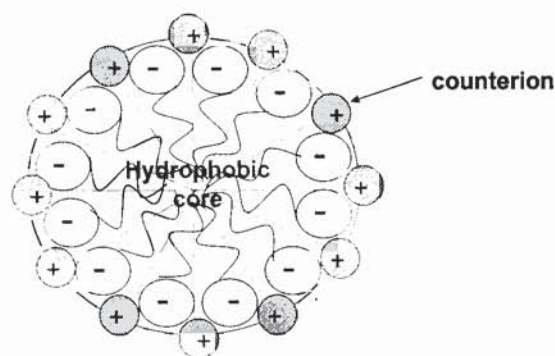


Figure 5.4 Schematic representation of a typical micelle of ionic surfactant molecules

5.1.4.2 Open Association

Drugs containing tricyclic, rigid hydrophobic ring structures do not form micelles but associate in a continuous or open pattern characterised by a lack of concentration dependency and absence of CMC (Attwood, 1995). These structures generally have a large group attached to the ring system, e.g. chlordiazepoxide has two charge bearing N atoms present within the aromatic rings of the molecule and propranolol, methantheline and pavartrine have ester groups substituted directly on to the ring system. The continuous association is attributed to the delocalisation of charge on the hydrophobic ring system; see figure 5.5 for structures.

Association of these types of molecules usually starts at low concentrations and the aggregates grow by a stepwise addition of monomers, consequently the aggregates continually increase in size rather than attain an equilibrium size as in micellisation. The aggregation number is commonly used to describe the micellisation process and represents the number of surfactant molecules in a typical micelle.

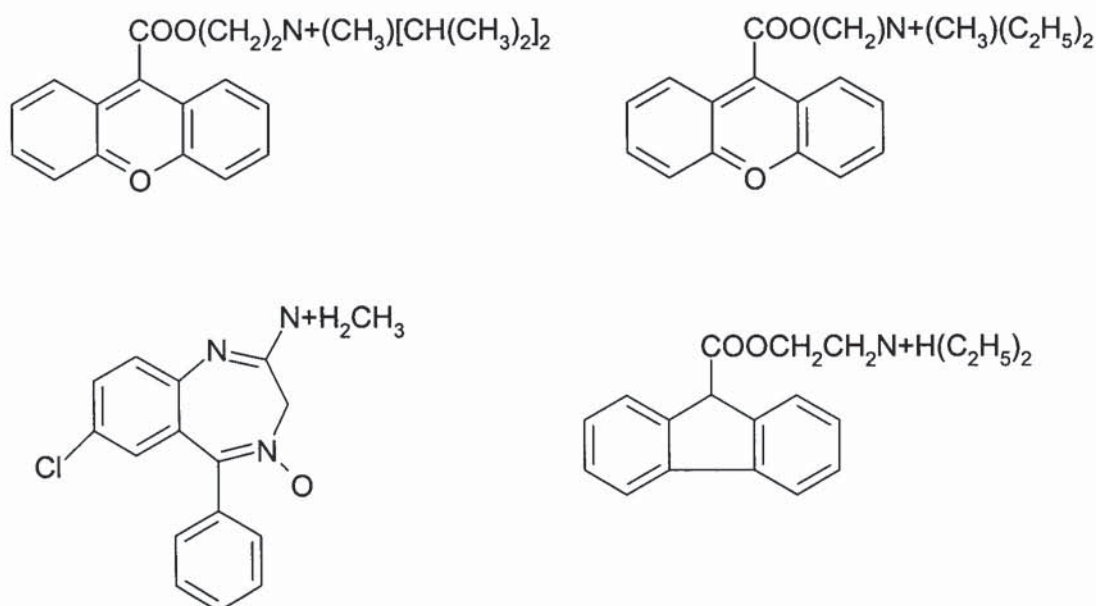


Figure 5.5 Structures of drugs that exhibit continuous association patterns in aqueous solution: Upper left: propantheline, upper right: methantheline, lower right: pavadrine and lower left: chlordiazepoxide.

5.1.4.3 Previous studies on surface-active drug systems

Antidepressants, such as amitriptyline, clomipramine, imipramine and nortriptyline have tricyclic hydrophobic moieties and typically form micelles in solution. Attwood *et al.* (1995) studied two structurally related antidepressants, clomipramine and imipramine (figure 5.6) and concluded that micellisation was affected by ionisation and temperature. A change in a substituent of one of the hydrophobic aromatic rings can create differences in the packing characteristics within micelles of clomipramine and imipramine (Sarmiento *et al.*, 1997). Clomipramine has a chlorine atom attached to an aromatic ring which is large and bulky and reduces the CMC when compared to imipramine which has a small hydrogen atom at the same location. Imipramine and clomipramine (figure 5.6) were found to form tightly-packed, stacked aggregates rather than typical surfactant micelles. This was confirmed by calculating the free space in the interior or apparent molar volume and calculating the adiabatic and apparent molar compressibility of the drugs.

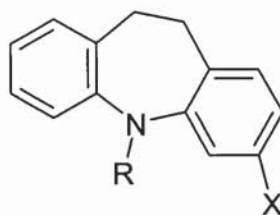


Figure 5.6 Structure of clomipramine $R = \text{CH}_2\text{CH}_2\text{CH}_2\text{N}(\text{CH}_3)_2$ $X = \text{Cl}$ and imipramine $R = \text{CH}_2\text{CH}_2\text{CH}_2\text{N}(\text{CH}_3)_2$ $X = \text{H}$

The phenothiazine tranquillisers such as promazine, chlorpromazine, promethazine and trimeprazine have been found to aggregate in a micelle-like manner. The drugs were observed to form pre-micellar aggregates which subsequently grow with further increases in drug concentration by the stepwise addition of monomers (Attwood *et al.*, 1990a, Attwood *et al.*, 1990b). NMR studies suggest that convex-concave vertical stacking of the phenothiazine molecules occurs within the micelles, with alkyl side chains on alternate sides of the stack (Attwood *et al.*, 1994). In the presence of electrolytes, micelle size increased as the concentration of drug rose above the CMC.

Trimeprazine and promethazine were studied by Attwood *et al.* (1996) because of their structural similarity; trimeprazine has one additional CH_3 attached to the phenothiazine ring system (figure 5.7). However trimeprazine is available commercially as the tartrate salt and promethazine as the hydrochloride salt. The tartrate counterion is influential in determining the mode of association of trimeprazine even at low concentrations. The association of trimeprazine tartrate remains micellar in contrast to that of promethazine hydrochloride, which is characterised by a change to open association as electrolyte is added. This suggests that there is a large difference in the degree of involvement of the ionised counterion with the micellar structure and that micelles are predominantly formed with the tartrate rather than the chloride counterions. The mechanism for preferred micelle formation with organic counterions has been attributed to the hydrophobic bonding between the micellar surface and the counterion by Mysels and Princen (1959). Conversely the mode of association of the antihistaminic drug tripeleennamine

changes from closed to open when the chloride ion is replaced by the maleate ion (Attwood and Udeala, 1976). No explanation was suggested for this result.

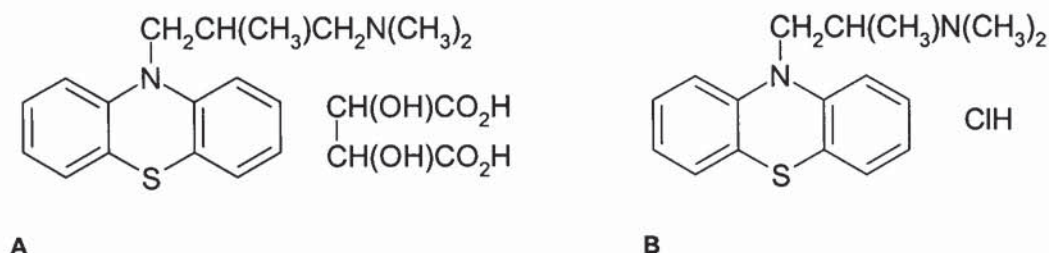


Figure 5.7 Structures of trimeprazine tartrate (A) and promethazine hydrochloride (B).

The association of chlordiazepoxide hydrochloride, flurazepam hydrochloride and diltiazem hydrochloride were studied by Attwood et al. (1993). Chlordiazepoxide hydrochloride aggregates by stepwise addition of monomers exhibiting continuous association, as expected from its structure (see figure 5.5). Flurazepam and diltiazem hydrochloride form small micelles of typical aggregation number ≤ 5 in water.

The sodium salts of two NSAIDs, fenoprofen and diclofenac, have been studied and display self association properties (Rades and Muller-Goymann, 1997; Ledwidge and Corrigan, 1998). Fenoprofen sodium association has been studied by NMR, photon correlation spectroscopy (PCS) and transmission electron spectroscopy (TES) and the differences in chemical shift of the two phenyl rings of fenoprofen sodium suggest that the micelles have a bilayer, or partially overlapping bilayer structure. PCS and TEM support the assumption that disc-like micelles are formed by fenoprofen sodium, although this could not accurately be determined (Rades and Muller-Goymann, 1997). It was not possible to detect a definitive CMC.

Ledwidge and Corrigan (1998) studied the sodium and N-(2-hydroxyethyl)pyrrolidine (HEP) salts of diclofenac and observed CMCs of 25 and 20 mM respectively. A definitive CMC measurement was possible for the HEP salt only, confirming micelle formation. The sodium salt was assumed to aggregate by open association. The presence of the hydrocarbon side chain was deemed responsible for micelle formation.

Khalil *et al.* (2000) investigated the aqueous solubility of diclofenac diethylamine (DDEA) in the presence of polymers and surfactants compared with diclofenac sodium. They discovered that DDEA was capable of forming micelles at peak solubility and that micelle association was affected by electrolytes in solution; with precipitation occurring at high salt concentrations. Solubility was enhanced by all co-solvents except glycerol which converted diclofenac into the less soluble hydrate form. Significant deviations from the log-linear solubility equation were found with the co-solvent systems. The common ion effect was responsible for precipitation of diclofenac acid in electrolyte solutions.

5.1.4.4 The effect of the counterion on micelle formation

The counterion associated with the charged group of ionic surfactants, particularly salts of drugs that are ionised in water, has a significant effect on the micellar properties. Generally the more weakly hydrated the counterion, the larger the micelles formed by the surfactant. For example small micelles are formed with the hydrochloride salts which are expected to be easily hydrated (aggregation number ≤ 5) of flurazepam and diltiazem (Attwood *et al.*, (1993) whereas micelles of tartrate salts can be much larger (aggregation number ≥ 50) (Attwood *et al.*, 1996). Hydrogen and chloride ions have a high density of positive charge *per* unit of surface area and therefore will be extensively hydrated. A greater depression in CMC and a greater increase in micellar size is noted with organic counterions, such as maleates, than with inorganic ones and has been attributed to the hydrophobic bonding between the micellar surface and the counterion (Mysels and Princen, 1959).

5.1.5 Surface activity effects of amphiphilic drug-membrane interactions

Surface-active drugs can also interact with membranes because of their hydrophobic and hydrophilic regions. They can exert a variety of effects at the molecular level from changes in lipid organisation to channel formation, induction of lipid flip-flop and of bi-phasic behaviour. Lipid flip-flop is induced by amphotericin B, bi-phasic drugs include local anaesthetics and tranquillisers (Schreier *et al.*, 2000). These effects

correlate with cell shape changes, membrane vesiculation, disruption and finally solubilisation. Chlorpromazine induces solubilisation of membrane proteins thus disruption of the lipid bilayer (Schreier *et al.*, 2000). Many drugs utilise these characteristics to exert their effects, for example antimicrobial peptides bind to lipid membranes and this is their mechanism of antimicrobial action (Schreier *et al.*, 2000). Some drugs cause cell lysis which is very similar to that of classical detergents, leading to a low therapeutic index which would require careful dosage e.g. antipsychotics and local anaesthetics (Macheiros *et al.*, 1998, 2000).

5.2 Experimental

Saturated aqueous solubilities of ibuprofen AMP2 and etodolac AMP2 (section 3.5) were very high in water and did not reach a saturation point under the conditions used. A tendency to foam was observed and this suggested that the solutions were behaving like detergents and that the salts themselves were surface-active.

Etodolac AMP2 and ibuprofen AMP2 were further investigated to examine their surface active properties and to determine their method of aggregation. This was studied by measuring the surface tension as a function of concentration and by dynamic light scattering measurements. A selection of other salts was examined by dynamic light scattering as micelle formation has been suggested as a possible mechanism of salt solubilisation behaviour in aqueous solution (O'Connor and Corrigan, 2001a).

5.2.1 Materials

All drugs were obtained as detailed in section 2.1 and the salts were made according to the method in section 3.2. Double distilled water was generated in house with a Fison's Fi-Streem still.

5.2.2 Equipment

The surface tension system consisted of a Camtel CDCA-100 Dynamic Contact Angle Tensiometer. The tensiometer was automated and data was collected by the instrument software. Wilhelmy plate geometry was used to measure the surface

tension of the solutions. A Wilhelmy plate was used in preference to a DuNouy ring as it is a direct measurement of surface tension. The Wilhelmy method uses a thin plate of perimeter about 40 mm which is lowered to the surface of a liquid and the downward force directed to the plate is measured. Surface tension is directly calculated from the force divided by the perimeter of the plate.

For the method to be valid the plate must be completely wetted before the measurement to ensure that the contact angle between the plate and the liquid is zero. If this is not true then the Wilhelmy method is not valid. The position of the plate must be correct, the lower end of the plate must be on the same level as the surface of the liquid, otherwise the buoyancy effect must be calculated separately.

Using the DuNouy ring one must use correction factors which take account the dimensions of the ring (the perimeter, ring wire thickness and the effect of the opposite inner sides of the ring to the measurement) therefore the Wilhelmy plate was preferred.

A Brookhaven ZetaPlus Zeta Potential Analyser together with a Brookhaven ZetaPlus Particle sizing option allowing particle sizing by photon correlation spectroscopy, using a 15 mW static laser. The Brookhaven uses Quasi Elastic Light Scattering to determine particle size and assumes that the particles are spherical in shape. Particles are commonly polydisperse and when a distribution of sizes is present, the effective diameter measured is an average diameter which is weighted by the intensity of light scattered by each particle.

5.2.3 Surface Tension determination

5.2.3.1 Method

The CDCA-100 was used with a small sample container which held a sample volume of 5 ml. It was programmed to measure the surface tension every second for a maximum of 5 minutes. The machine automatically raised the platform to the Wilhelmy plate and held it at the surface of the liquid and measured the surface tension as a function of time.

Aqueous solutions were prepared using etodolac AMP2 and ibuprofen AMP2 of at least 5 ml of concentrations 1, 2.5, 5, 10, 15, 20, 25, 50, 75 100 mg/ml. These solutions were tested individually for 5 minutes and one solution of etodolac and one of ibuprofen were tested for at least 30 minutes to observe whether there were any changes over extended times. Three readings were collected at 50, 100 and 150 minutes for each concentration and plotted as a function of the concentration, in moles/L or mg/ml.

Saturated solutions of the model drugs and their butylamine, hexylamine, AMP1 and AMP2 salts were prepared by allowing excess solid to dissolve in 20 ml of double distilled water for 24 hours. The samples were filtered through 0.45 μ m 13mm PTFE syringe filters and the filtrate analysed by HPLC to determine the concentration. The saturated solutions were serially diluted to produce at least 4 samples for surface tension measurement.

5.2.3.2 Results and Discussion

The surface tension of aqueous solutions of etodolac and ibuprofen AMP2 are displayed in figure 5.8.

CMC is usually calculated from a plot of surface tension (γ) against log concentration, the discontinuity on the line is usually termed the critical micelle concentration, i.e. the concentration at which micelles first form in a solution. The CMC has been calculated for etodolac and ibuprofen AMP2 as shown in figures 5.9 and 5.10.

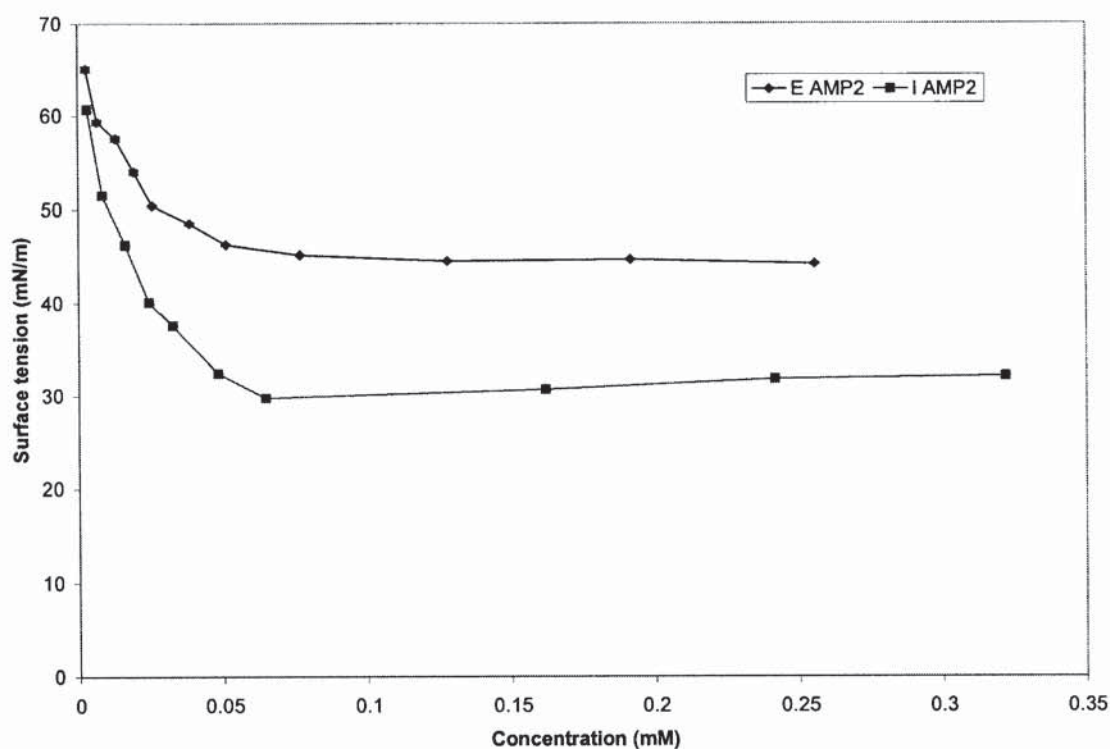


Figure 5.8 Surface tension measurements against concentration of aqueous solutions of etodolac AMP2 and ibuprofen AMP2. (n=3; mean \pm SD).

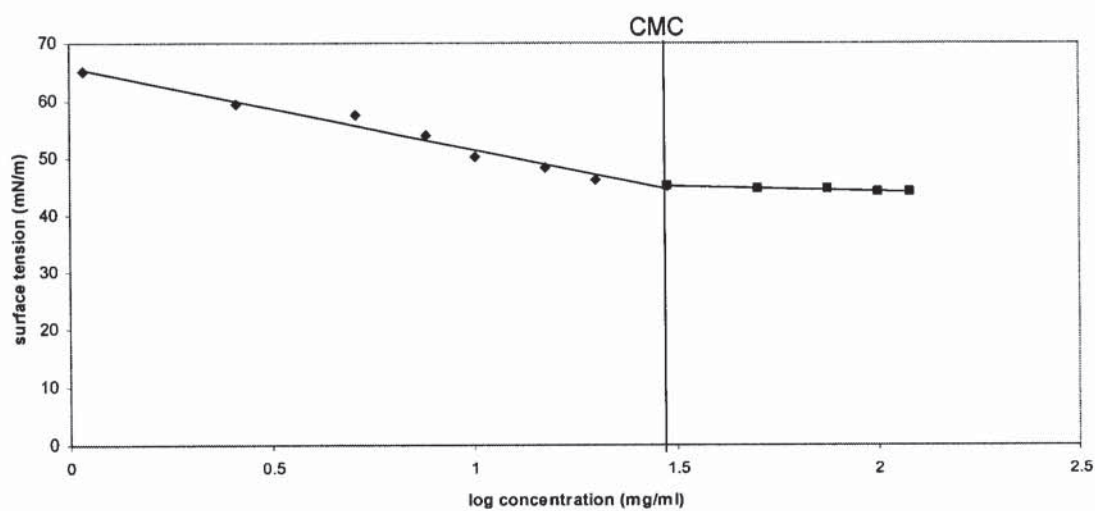


Figure 5.9 Surface tension versus log concentration (mg/ml) for aqueous solutions of ibuprofen AMP2 used to calculate the CMC.

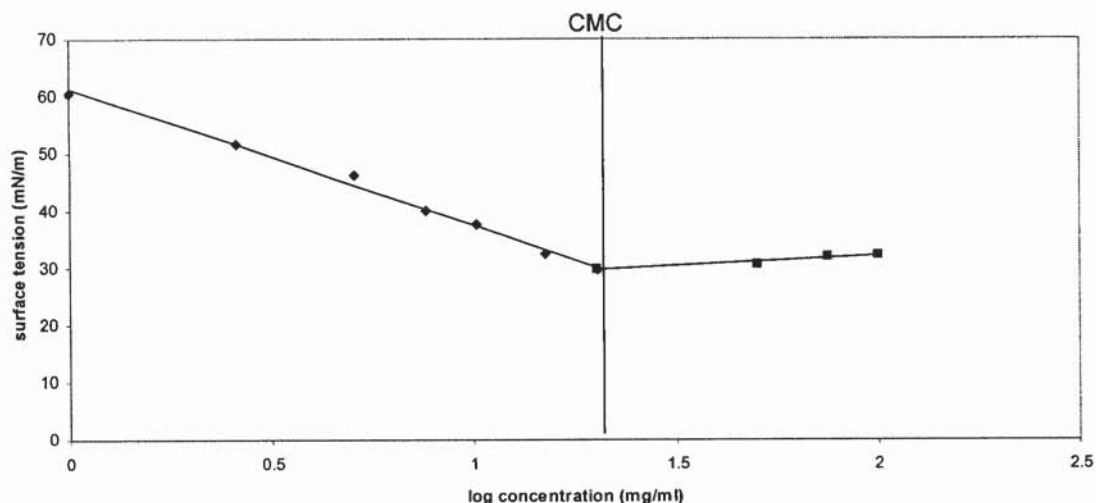


Figure 5.10 Surface tension versus log concentration (mg/ml) for aqueous solutions of etodolac AMP2 used to calculate the CMC.

The CMC's are estimated as 7.65×10^{-2} mM (30 mg/ml) for etodolac and 6.43×10^{-2} mM (20 mg/ml) for ibuprofen. The CMC is the point when the surface of the liquid is saturated with molecules and micelles begin to form to allow the attainment of a minimum free energy state. As the concentration increases after the CMC, micelles spontaneously form as more surfactant is added and there is no further change in surface tension over the measured concentration range.

The surface tension measurements for the model drugs and their amine salts are listed in table 5.4. Some materials show CMC like characteristics and so behave like classical surfactants having a clear discontinuity on the surface tension against concentration plot. These materials would be expected to form micelles in solution. Other materials only depress the surface tension and would be expected to exhibit continuous association.

Table 5.4 Summary of the solution properties of etodolac, flurbiprofen, gemfibrozil, ibuprofen and their butylamine, hexylamine, AMP1 and AMP2 salts. * indicates solution concentration of 100 mg/ml.

Material	Concentration of saturated aqueous solution (mM)	Surface tension (mN/m)	Mode of association
Etodolac	7.74×10^{-4}	63.3	Continuous
E butyl	4.17×10^{-2}	63.3	Continuous
E hexyl	1.55×10^{-2}	42.1	Continuous
E AMP1	1.50×10^{-1}	39.6	Micellar
E AMP2*	2.55×10^{-1}	44.3	Micellar
Flurbiprofen	1.23×10^{-4}	69.7	Continuous
F butyl	1.58×10^{-2}	48.6	Continuous
F hexyl	7.20×10^{-3}	41.5	Continuous
F AMP1	2.70×10^{-2}	49.1	Continuous
F AMP2	2.87×10^{-2}	49.2	Continuous
Ibuprofen	3.40×10^{-4}	53.6	Continuous
I butyl	3.58×10^{-1}	31.7	Micellar
I hexyl	1.95×10^{-2}	26.8	Continuous
I AMP1	3.39×10^{-1}	32.1	Micellar
I AMP2*	3.21×10^{-1}	32.1	Micellar
Gemfibrozil	8.80×10^{-5}	64.4	Continuous
G butyl	9.29×10^{-2}	36.6	Micellar
G hexyl	1.14×10^{-2}	35.5	Continuous
G AMP1	2.95×10^{-2}	37.8	Micellar
G AMP2	8.45×10^{-2}	38.0	Micellar

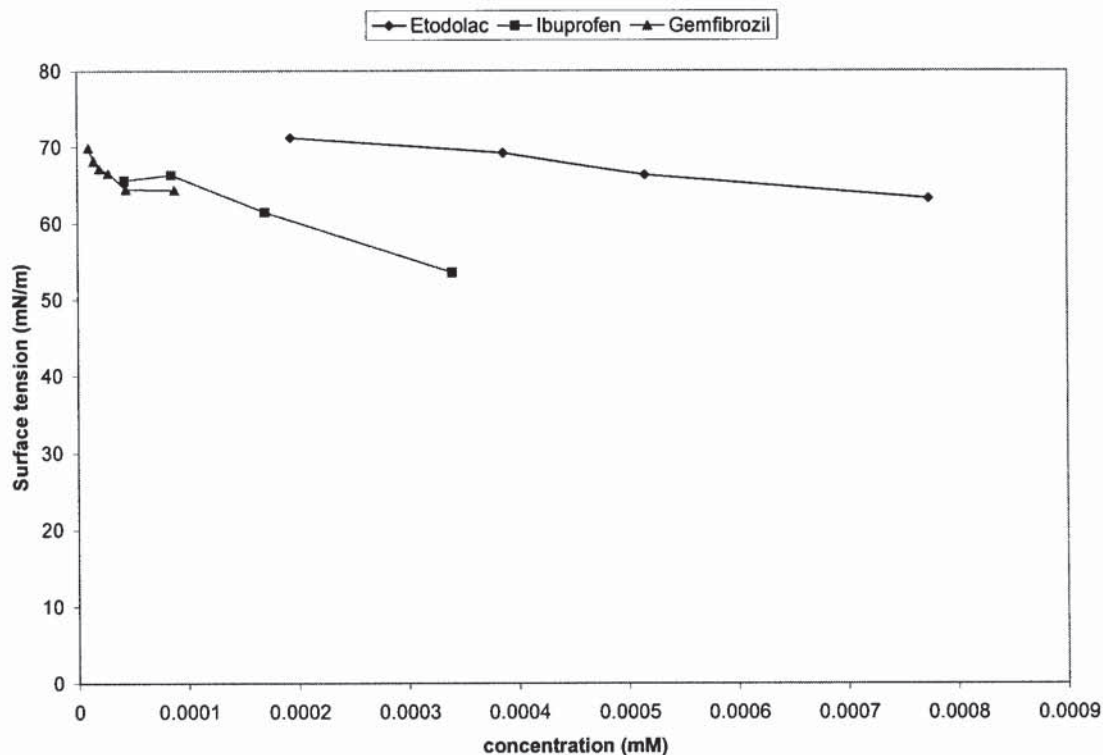


Figure 5.11 Surface tension of aqueous solutions of ibuprofen, etodolac and gemfibrozil. (n=3; mean \pm SD).

Figure 5.11 illustrates the effect of concentration on surface tension for the parent drugs. As concentration increases, the surface tension is lowered in a linear fashion. Ibuprofen causes the greatest depression in the surface tension of water from 71.9 to 53.6 mN/m² at a concentration of 0.07 mg/ml; etodolac is the most soluble salt yet has a surface tension of 63.3 mN/m² in an aqueous solution of 0.222 mg/ml. Flurbiprofen aqueous solution has a surface tension of 69.7 mN/m² at 0.030 mg/ml (data not shown on graph), which is very close to the surface tension of water 71.9 mN/m².

NSAID drugs have been recognised as weak surfactants by their ability to lower the surface tension of water. Agrawal *et al.* (2004) found that nimesulide lowered the surface tension of water to a minimum of 61 mN/m² and concluded that solubilisation may be due to weak ionic interactions in aqueous solution or molecular aggregation. These molecules were assumed to aggregate by open association because no CMC

was detected. Al-Saidan (2004) found that enhanced skin permeation was due to the ionic surfactant action of ibuprofen.

The drug molecules have structures that contain polar carboxylic acid functional groups and hydrophobic benzene rings. Molecules like these are termed ambiphilic, as they have both hydrophilic and hydrophobic regions. The polar carboxylic acid functions interact with water to dissolve and therefore have the ability to alter the tension of water at the surface, so surface activity is expected of these types of molecules. They do not behave like typical surfactants because there is no CMC detected. Alteration of the surface tension is another mechanism that these types of molecules may use to aid dissolution.

The butylamine and hexylamine aqueous salt solutions of the model drugs all lower the surface tension of water. The effect of concentration on surface tension is displayed in figure 5.12 for all the aqueous butylamine salt solutions. The data show an indication of a CMC from the curves but surface tension does not remain constant as concentration increases beyond this value like typical surfactants. The addition of the butylamine counterion lowers the surface tension of water approximately 20 units more than the drug alone. Ibuprofen butylamine depresses the surface tension of water to 31.65 mN/m^2 , which is the lowest surface tension value, and hence it is the most powerful surface active salt. Ibuprofen butylamine also has the greatest aqueous solubility of 100 mg/ml; the reason for this may be related to its surface activity. The data suggests that some of the salts may aggregate in closed association by producing micelles because there is a well defined curve in surface tension as concentration increases, for gemfibrozil and ibuprofen butylamine.

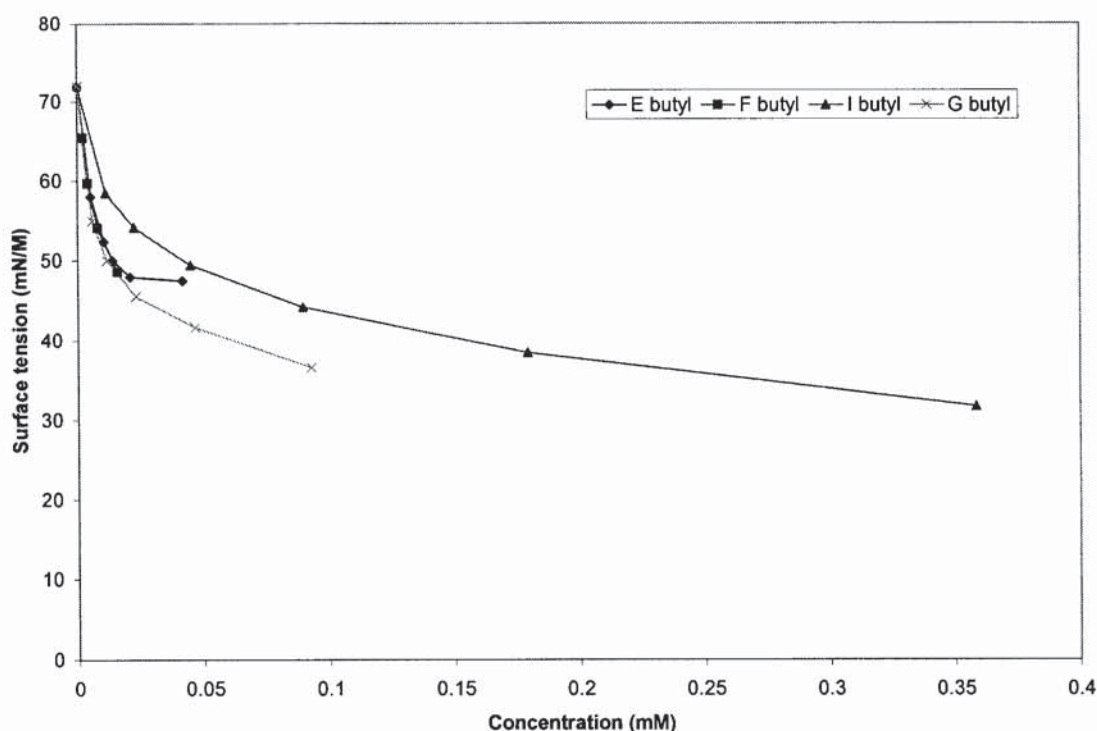


Figure 5.12 Surface tension measurements of a function of concentration for the aqueous solutions of the butylamine salts of etodolac, flurbiprofen, gemfibrozil and ibuprofen. (n=3; mean \pm SD) last point indicates the concentration of a saturated aqueous solution.

The surface tension measurements for the hexylamine salts of the parent drugs are displayed in figure 5.13. The salts studied all reduce the surface tension of water. As chain length increases to 6C (hexylamine salts), there is a greater depression in surface tension and enhancement in surface activity. The reduction in surface tension as the chain length increases from 4 to 6C and is between 1 and 20 units, with etodolac salts having the greatest effect on surface tension (table 5.4). The solubilities of the salts are not increased by a reduction in surface tension as the hexylamine salts have lower aqueous solubilities than the butylamine salts (section 3.5.3). Therefore a reduction in surface tension does not improve solubility. Closed association is not likely because surface tension continues to reduce as concentration increases and there are no visible CMCs.

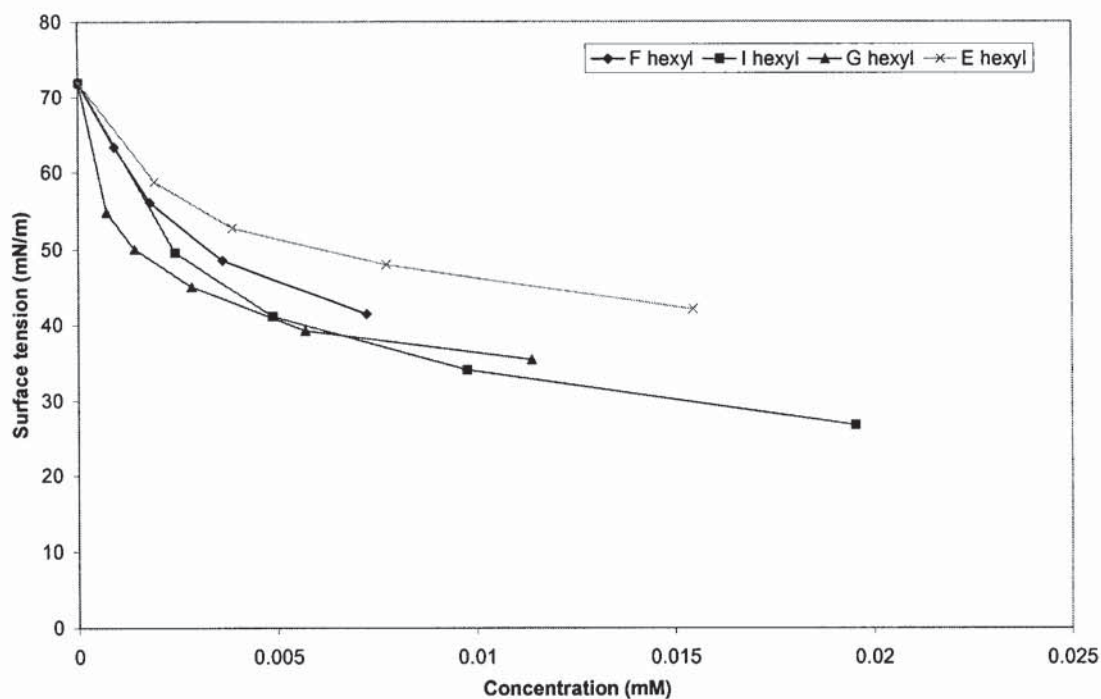


Figure 5.13 Surface tension measurements as a function of concentration for the aqueous solutions of the hexylamine salts of etodolac, flurbiprofen, gemfibrozil and ibuprofen. ($n=3$; mean \pm SD).

The AMP1 salts of etodolac and ibuprofen display surface activity (figure 5.14), with the depression in surface tension similar to that of the butylamine counterion, about 20 units below the drug itself. The depression in surface tension as concentration increases is similar for AMP1 and AMP2 salts, although the maximum solubility for each material varies. The AMP1 and AMP2 salts of etodolac and ibuprofen display a clear inflection point on the curve and are expected to form micelles as the concentration increases above the CMC.

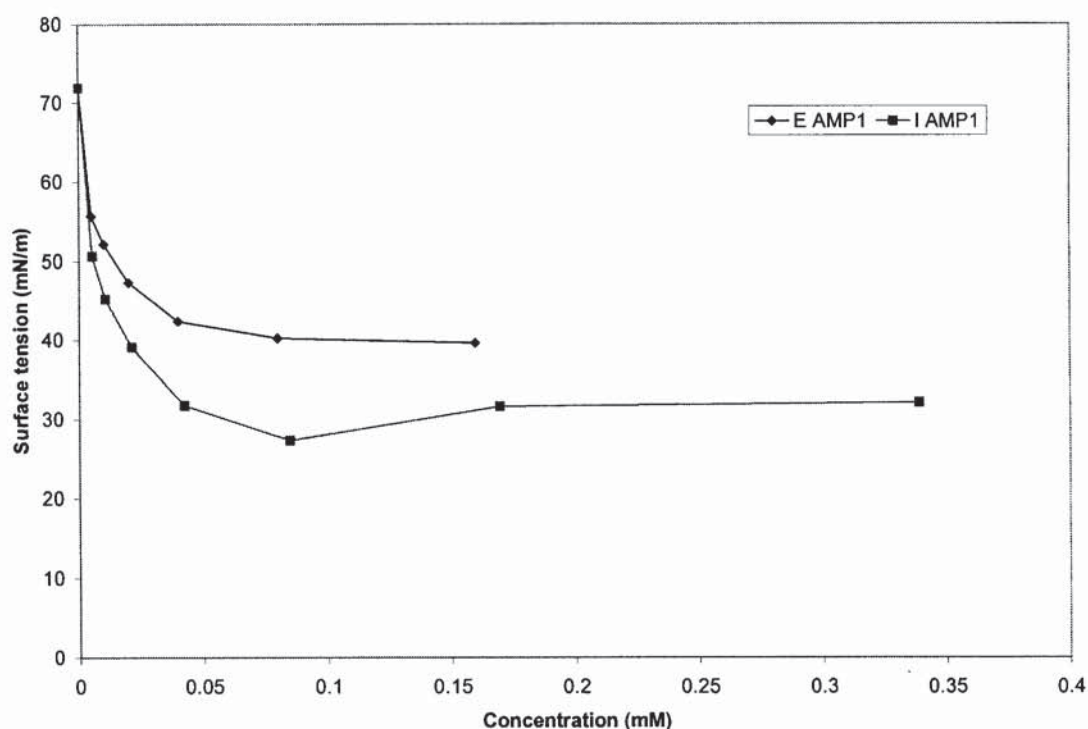


Figure 5.14 Surface tension measurements as a function of concentration for an aqueous solution of the AMP1 salts of etodolac and ibuprofen. (n=3; mean; \pm SD).

The saturated aqueous solubility for ibuprofen AMP1 (135.00 mg/ml) is greater than etodolac AMP1 (74.65 mg/ml); this may be because it is more surface active as it depresses the tension of water the most. The CMC has been calculated to be approximately 2.92×10^{-2} mM (11 mg/ml) for etodolac AMP1 at a surface tension of 41.95 mN/m. The CMC for ibuprofen AMP1 has been calculated as approximately 2.43×10^{-2} mM (7 mg/ml) at a surface tension of 32.06 mN/m.

The AMP1 and AMP2 salts of flurbiprofen show the least surface activity of all the AMP salts. Results are similar for both forms therefore the increased solubility of the AMP2 flurbiprofen salt is not due to an altered surface tension (figure 5.15). A CMC was not calculated for the flurbiprofen AMP1 and AMP2 data sets as the inflection point is not well defined.

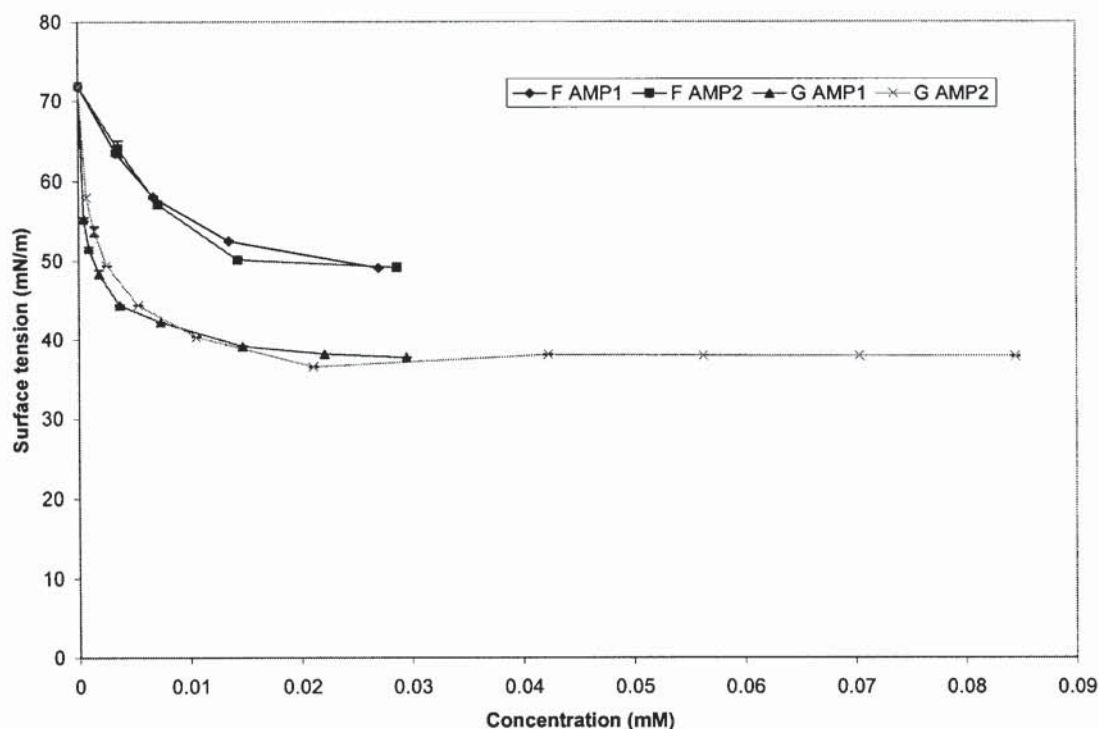


Figure 5.15 Surface tension measurements for the aqueous solution of gemfibrozil AMP1, AMP2 and flurbiprofen AMP1, AMP2. (n=3; \pm SD).

The CMC for gemfibrozil AMP2 was calculated as approximately 6.33×10^{-3} mM (2.14 mg/ml), figure 5.15. A CMC was not calculated for gemfibrozil AMP1 as there was not a clear inflection point. Micellisation is likely to occur with gemfibrozil AMP2 salts.

5.2.3.3 Conclusions

All the carboxylic acid drugs studied are surface-active because they lower the surface tension of water. The addition of an amine counterion to form salts, results in a more surface-active material that has an improved aqueous solubility than the drug itself, see section 3.3. As chain length of the counterion increases, surface activity increases but solubility is not clearly related to surface-activity, for these materials open association is likely as a clearly defined CMC was not observed. The AMP counterions have a similar effect on the surface tension as the butylamine counterion, however the AMP counterions have defined CMCs and are more likely to aggregate

in a closed association, *i.e.* micelles are more likely to form. The presence of the hydroxyl groups aids micellar association and aggregation. The elevated increase in solubility of ibuprofen and etodolac AMP2 salts is not just due to increased surface activity as these solutions are no more surface active than the AMP1 salts.

5.2.4 Photon Correlation Spectroscopy (PCS)

PCS was performed using a Brookhaven ZetaPlus 90Plus which measures particle size by light scattering. Dynamic Light Scattering (also called PCS) provides a fast, simple method for submicron particle sizing. Random intensity fluctuations in scattered laser light arising from the Brownian motion of colloidal particles are analysed to give either a simple mean size and polydispersity (distribution width) or complete distribution data even for multimodal distributions. The 90Plus is suitable for routine measurements of particle size distributions from about 2 nm to 5 microns in virtually any liquid. It is a self-contained unit which incorporates a powerful 30mW diode laser and dual angle - 15° and 90° - detection system.

5.2.4.1 Method

Experiment 1: Etodolac and ibuprofen AMP2

Aqueous solutions of 1, 2.5, 5, 7.5, 10, 25, 50, 75 and 100 mg/ml of etodolac AMP2 and ibuprofen AMP2 were used as detailed in section 5.2.3.

Experiment 2: Amine salt solutions

The amine salts of etodolac, gemfibrozil, flurbiprofen and gemfibrozil were used, which included the counterions butylamine, hexylamine, AMP1 and AMP2. Saturated aqueous solutions of each salt were prepared as in section 5.2.3 and subsequent diluted samples were used directly after surface-tension measurements. Each sample was filtered through 0.2 µm PTFE syringe filters prior to analysis and approximately 2 ml was placed in a clear sided 10 mm, 4.5 ml BI-SCP cuvette supplied by Brookhaven. The instrument was set to collect data for one minute and to repeat five times; after each minute the average particle size was calculated. The dust filter was turned on.

5.2.4.2 Results and Discussion

Experiment 1: Etodolac and ibuprofen AMP2

The results from particle sizing by photon correlation spectroscopy are shown in figure 5.16.

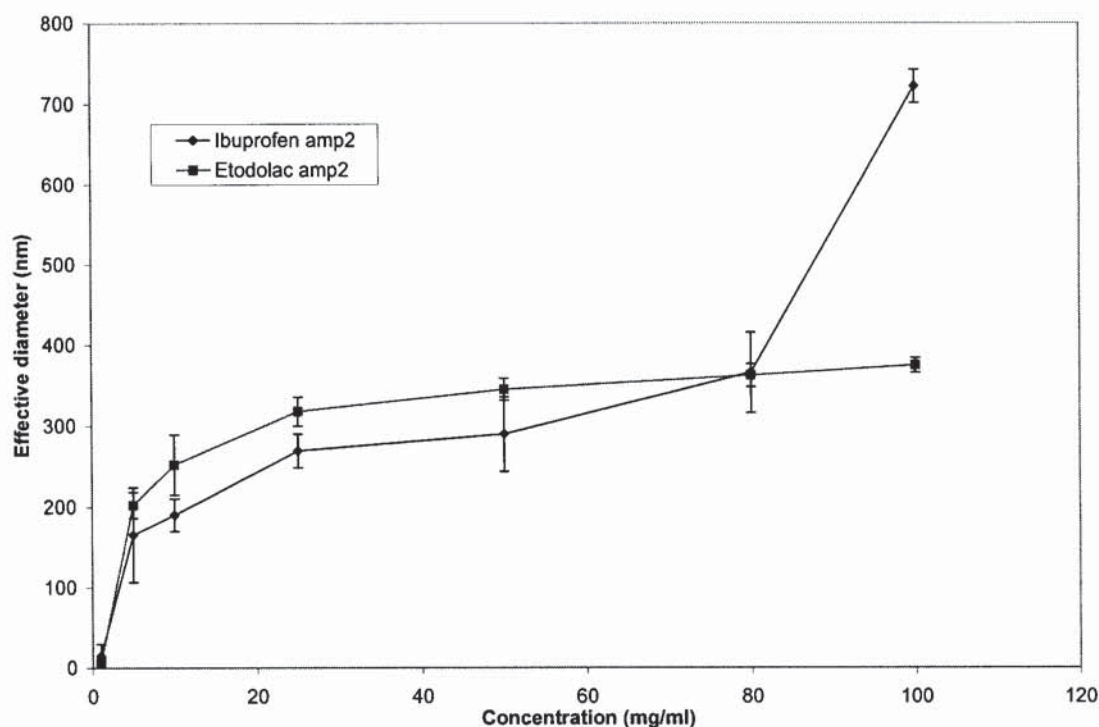


Figure 5.16 Plot of micelle effective diameter (nm) against concentration (mg/ml) for etodolac and ibuprofen AMP2 using photon correlation spectroscopy.

The results from 1 mg/ml solutions of etodolac and ibuprofen AMP2 show that there were no detected micelles or particles present; this was considered the control. Both etodolac and ibuprofen AMP2 show evidence of micelle formation above 5 mg/ml where the particle size was averaged to be 202.6 and 165.6 nm, respectively. As the concentration rises above 5 mg/ml there is a rise in particle size which is consistent with aggregation and confirms a closed association. There are very large aggregates being detected above 80 mg/ml for ibuprofen AMP2. These aggregates are around 700 nm which is unusual for a single micelle therefore the micelles could be aggregating to produce larger particles.

PCS evidence of micelle formation at 5 mg/ml is not consistent with the CMC values that were calculated for etodolac AMP2 (30 mg/ml) and ibuprofen AMP2 (20 mg/ml). The PCS results suggest that micelle formation occurs at a concentration far below the CMC, this is known as pre-micellar aggregation. These aggregates subsequently grow with further increase of drug concentration by the stepwise addition of monomers (Atwood *et al.*, 1990a, Attwood *et al.*, 1990b). These salts are surface-active and micelle-forming well below the CMC value. There is evidence to suggest that the CMC is the saturation point where there is no further increase in micelle size and aggregation follows this point characterised by a plateau in the size measurements by PCS of etodolac AMP2. Ibuprofen is characterised by an increase in particle size up to the CMC (20 mg/ml) where micelle size is constant (plateau region) until aggregation occurs above 80 mg/ml where there is a steep rise in particle size.

The mean micelle size of etodolac AMP2 increases from 202.6 to 374.4 nm from 5-100 mg/ml and follows a consistent growth pattern characterised by a gentle sloping line. Ibuprofen AMP2 has micelles that grow from 165.6 to 721.5 nm, a larger growth than etodolac AMP2. Above 80 mg/ml there is a sudden growth in the micelles which would indicate that the micelles had agglomerated to form much larger particles. There is good reproducibility in the results indicating that spherical micelles were detected. If the results had a large standard deviation, cylindrical shaped aggregates may be expected.

Experiment 2: Amine salt solutions

A selection of amine salts was investigated to determine if there was evidence of micelle formation in aqueous solution because of their surface-active nature indicated by surface tension measurements. The results for salt solubility and photon correlation spectroscopy particle sizing are shown in table 5.5.

Table 5.5 Effective particle size (nm) measured by PCS and aqueous solubility data (mg/ml) for the AMP1, butylamine and hexylamine salts of etodolac, flurbiprofen, gemfibrozil and ibuprofen.

Material	Effective particle diameter (nm) \pm SD	Aqueous solubility mg/ml \pm SD
Etodolac	0	0.222 \pm 0.1
E AMP1	145.9 \pm 1.9	30.0 \pm 3.8
E butylamine	0	17.62 \pm 0.2
E hexylamine	0	5.86 \pm 0.2
Flurbiprofen	0	0.033 \pm 0.01
F AMP2	0	> 200
F AMP1	0	8.94 \pm 1.4
F butylamine	0	5.39 \pm 0.2
F hexylamine	0	2.60 \pm 0.1
Gemfibrozil	0	0.022 \pm 0.01
G AMP2	135.0 \pm 80.2	> 200
G AMP1	247 \pm 2.7	11.76 \pm 1.5
G butylamine	230 \pm 13.8	35.93 \pm 1.8
G hexylamine	0	3.73 \pm 0.1
Ibuprofen	0	0.07 \pm 0.001
I AMP1	220 \pm 10.2	135.00 \pm 28.1
I butylamine	217.0 \pm 27.4	162.66 \pm 8.7
I hexylamine	0	6.15 \pm 0.5

Results are the mean of five replicates \pm SD for PCS and three replicates for solubility.

None of the drug solutions show evidence of micellisation. This confirms that they do not aggregate while being surface-active and they are more likely to favour a stacking arrangement in solution. Gemfibrozil and ibuprofen butylamine are the only alkyl hydrocarbon salts that display evidence of micellisation, see figure 5.17. They both produce micelles of around 200 nm size and as solution concentration increases, the average particle size reduces possibly due to disruption or a conformational change of the micelles. Both ibuprofen and gemfibrozil butylamine have small variations in the particle sizes indicating spherical particles. Flurbiprofen and etodolac butylamine salts solutions do not show any evidence of micellisation by PCS analysis; these materials are surface active and have lower aqueous solubilities than ibuprofen and

gemfibrozil butylamine. The ability to form micelles may enhance solubility; evidence for this will be required from further experiments, which is beyond the scope of this chapter.

The hexylamine salt solutions of all the drugs do not show any evidence of micellisation. They are slightly more surface-active than the shorter-chained butylamine counterions so would be expected to form micelles. The slightly longer chain may inhibit micelle formation due to an increasing flexibility. This result is expected as it mirrors what was observed by Attwood *et al.* (1976) that an increasing chain length on the counterion results converts closed to open association in solution. The result confirms that additional flexibility reduces the CMC but inhibits micelle formation.

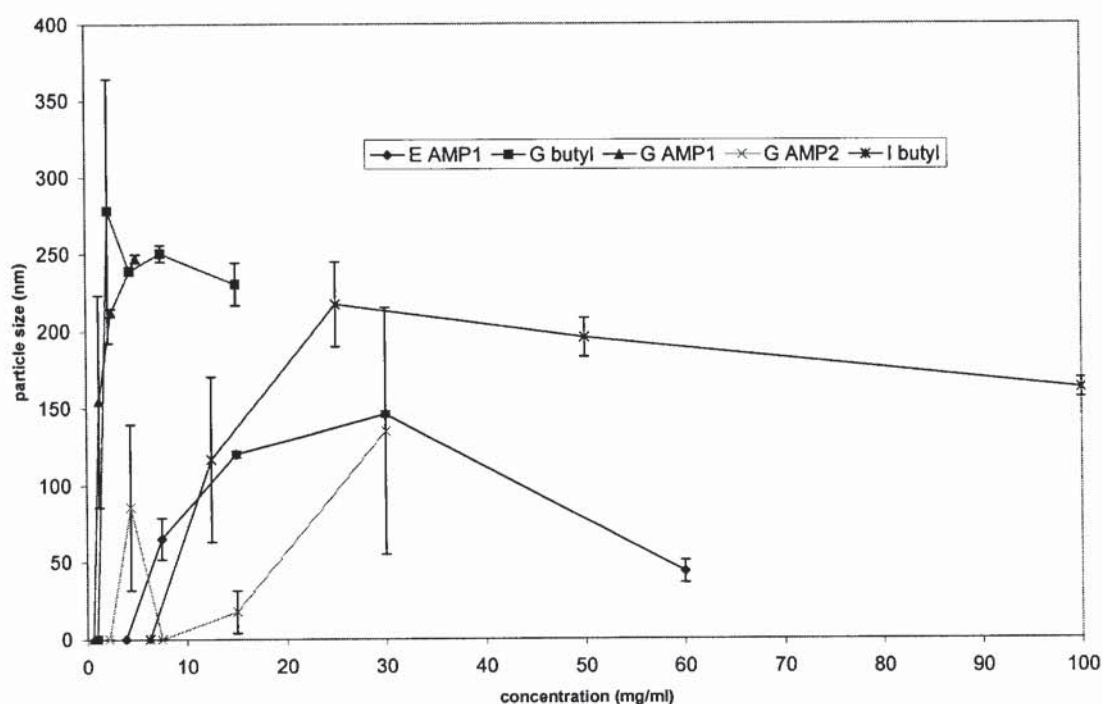


Figure 5.17 Particle size versus concentration for the salts showing evidence of micellisation as determined by PCS. (n=3; mean \pm SD).

The AMP1 salts of etodolac, ibuprofen and gemfibrozil show evidence of micellisation. Gemfibrozil AMP2 shows evidence of agglomeration in solution but there is a large variation in the size of the particles measured by PCS so micellisation cannot be confirmed. The size of the aggregates varies from 17.6 to 135 nm, which may indicate there are rod-like micelles present. Evidence suggests that flurbiprofen AMP1 does not form micelles; therefore it may associate by stacking. The micellisation of AMP1 salts starts with association of small particles which increase in size by stepwise addition of molecules to the micelle as concentration increases. As concentration increases, the micelles, in general, reduce in size, which is unexpected as micelles usually form super-aggregates as concentration increases. Further experiments would be required with a more powerful laser to fully characterise the micelle suspensions.

5.2.4.3 Conclusions

The addition of a short chained (4C) or a hydroxyl-containing (AMP1, AMP2) amine counterion is preferred for micelle formation in solution. These micelles are spherical and of 100-250 nm in size. As chain length of the counterion increases, micelle formation is inhibited because of the increasing flexibility of the chain. The exact structure of the micelles is not known but can be investigated by NMR or by using PCS with a powerful laser. NMR has been used to characterize fenoprofen micelles, in which an upfield shift of the phenyl proton signals in the NMR measurements is observed to indicate micelle formation. From differences in the chemical shift of the two phenyl rings of fenoprofen sodium it was concluded that the micelles have a bilayer or partially overlapping bilayer structure (Rades and Muller-Goymann, 1997). Further studies by NMR on the micelles formed in these experiments would be required to confirm the conformation of the salt micelles.

The interaction between the hydroxyl groups and water is conducive to micelle formation and contributes to the surfactant properties of the salts. There is evidence of pre-CMC micellisation in all salts; this suggests that the CMC is not the initialisation of micellisation but the concentration that represents saturation of the surface with surface active material. Flurbiprofen and its salts are surface-active but do not form micelles; this could be due to the flexible nature of the two benzene rings

which can twist about a central axis and promote stacking (see chapter 6). Further studies using computer modeling could be used to identify the structures that would preferentially aggregate by closed or open association.

Chapter 6 X-ray Crystallography

6.1 Introduction

6.1.1 Using Single Crystals

In 1912 Max von Laue of Germany discovered that a beam of X-rays could be diffracted, or scattered from a crystal in an orderly way. A crystal is composed of molecules that are arranged in a regular repeating array in three dimensions. The molecules can be described as being layered into planes, and stacks of planes in a crystal can reflect X-rays. The directions of the diffracted beams result from the size of the unit cell which is the smallest repeating unit of the crystal. The intensities of the diffracted beams depend on the arrangement of the atoms in each unit. The goal of X-ray diffraction analysis is to determine the atomic arrangement that accounts for the observed diffraction pattern.

In many laboratory applications, the X-rays are generated in a high voltage sealed tube source using either a molybdenum or copper anode. These X-rays are directed towards the face of the crystal. The diffraction beams are collected and measured by a detector (e.g. ionisation chamber). The crystal is rotated in order to collect diffracted beams at different angles. When one beam (figure 6.1) is recorded at a time there is no problem recording the angles (i.e. indexing) because the crystal orientation and angle is known. When many beams can be recorded at the same time (e.g. on a photographic plate, figure 6.1) each beam must be identified. Modern instruments replace the film with an image plate which can be read with a laser scanner, or apply television technology with a charged-coupled device (CCD) detector. The benefit of this is faster data measurement.

Symmetry in the crystal allows for easy elucidation of the structure from the diffraction pattern. A screw axis, which combines rotation about the axis with translation by a fraction of the unit cell length, or a glide plane, which combines reflection in the plane with translation, can be identified by noting regular absences in diffracted-wave orders. The presence or absence of centres of symmetry and simple rotations or reflections can be determined by a statistical survey of intensities. Such

symmetry elements interact to determine the space group, for which there are a total of 230 possibilities. The possible number of structures is limited by geometry in a symmetrical compound, which facilitates the elucidation of the structure. Optically active molecules, those with a chiral centre, can have two forms; standard X-ray measurements cannot distinguish them, but their exact phase can be identified by measuring “anomalous scattering” of X-rays. The X-ray patterns will be identical but one will have shifted relative to the other. The reflected waves differ in phase only, the angle of which can be 0 – 360° . However, if there is a centre of symmetry in the unit cell, either because the molecule itself has a centre of symmetry or because both left- and right-handed enantiomers are present, this can reduce to 0° or 180° .

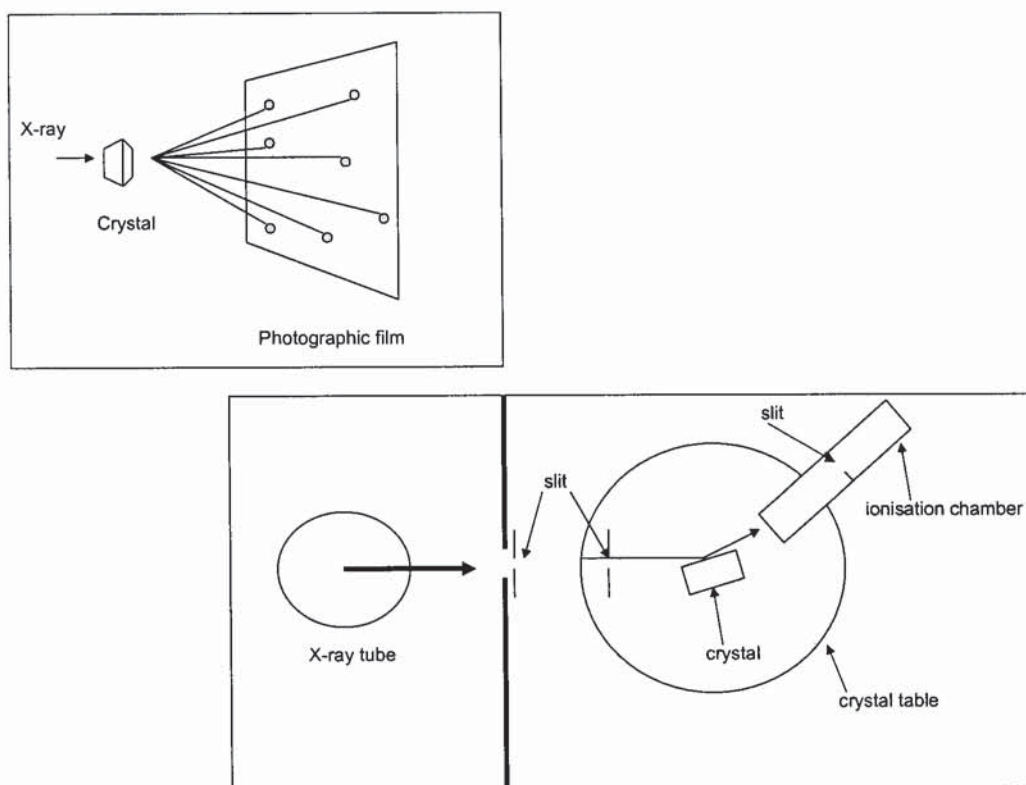


Figure 6.1 Above: Photographic imaging of crystals using X rays. Below: Ionisation spectrometer used by W. H. Bragg to conduct the first investigations of the X-ray spectra.

The first organic structures, naphthalene and anthracene, had been outlined by W. H. Bragg in 1922. Vitamin B-12 represented the biggest challenge to scientists as it had 181 atoms in the molecule and took D. Hodgkin of Oxford 8 years to solve its structure. She was awarded the Nobel Prize in 1964 as well as deserved

acknowledgement of her achievement. At that time it was hard to imagine solving more complex structures, although 20 years later, methodology was finally improved to solve the structure of proteins. In 1958 J. C. Kendrew solved the crystal structure of myoglobin, which has 2,500 atoms in its molecule. Since then a library of over 300,000 organic and metal-organic molecules has been stored in the Cambridge Structural Database, September 2003. Other rapidly expanding databases cover protein and inorganic structures.

Modern X-ray diffraction uses the same principles as had been used by Bragg in 1922, although computers are now an essential part of solving crystal structures. Computers are necessary to allow the measurements of 100,000 or 200,000 intensities and the recording of the positions of the crystal and recorder accurately. The information is automatically turned into an electron density sheet which the operator, aided by peak search software, has to translate into an atomic arrangement.

The process of solving a crystal structure using X-rays starts with growing a crystal of sufficient size and quality for X-ray diffraction. Most organic molecules can be crystallised from a volatile organic solvent in which it is soluble, e.g. ethanol, methanol, propanol, chloroform. Proteins and oligonucleotides may require alternative solvents, and the vapour diffusion method or the sparse matrix screening approaches, which allow for the crystallisation of even the smallest amount of protein or RNA (Holbrook, 1998).

Miller indices help the identification of stacks of planes. The Miller indices are calculated from the intercepts of the first plane out from the origin, which is taken as the reference plane. Its reciprocal intercepts in three dimensions give Miller indices of h , k , l .

The electrons of each atom scatter X-rays. These scattered X-rays interfere constructively or destructively to produce the diffraction pattern, a process which is far too complicated to analyse. Fortunately it is mathematically equivalent to reflection from stacks of planes in the crystal. The condition for constructive

interference of rays reflected from successive planes in a stack is given by Bragg's Law, also known as the Bragg equation:

$$n\lambda = 2d \sin \theta \quad \text{equation 6.1}$$

where n = integer; λ = wavelength; d = distance between planes and θ = glancing angle of incidence and reflection. Given n and λ for the experimental setup, the spacing d can be calculated from the angle θ at which a particular set of planes gives a reflection. Tables of Miller indices and d -spacings are used for identification of crystals.

X-rays scattered by atoms that lie nearly on planes will combine strongly, while atoms that are slightly diffused on a plane reflect weakly. The intensities of the reflections from atoms aligned on planes give information about the three-dimensional structure of the crystal. The X-ray waves are characterised by amplitude (square root of intensity), phase and wavelength; by knowing each parameter we can calculate the electron density in the crystal and locate the atoms by the Fourier transformation algorithm, described by Hao *et al.* (1996). The phases cannot normally be measured. Phase determination of single crystal X-ray data is most conveniently performed by direct methods which predict a consistent set of phases starting from a systematic or random guess. Vector methods, which include the Patterson method or the isomorphous replacement method, provide an alternative. Fourier transformation of the measured data with phases set to zero yields a map showing vectors between atoms, interpretable if there are a few heavy atoms that stand out from the others, which is useful for large molecules e.g. proteins or receptors.

For proteins a heavy atom e.g. bromide, cobalt, lead is often required to be chemically inserted because these atoms have a high density of electrons and their scattered X-rays are more intense. If one or more heavy atoms are in the unit cell, its position(s) can be determined by differences in intensities compared to the original and so the phase may be calculated (Bragg, 1968). Structure refinement is required to elucidate the exact structure. According to the Cambridge Structural Database 76% of all organic and organometallic compounds crystallise in only five space groups, and 90% of all organic and organometallic crystal structures belong to the 17

most common space groups. This greatly facilitates solving crystal structures of complex molecules such as proteins (Cambridge Crystallographic Data Centre, 1999).

The crystal must be of sufficient quality and stability to diffract X-rays, and it is required to be around 0.4 mm in size for mounting on a conventional X-ray diffractometer. If the crystal is bigger, parts of it may not receive the incoming X-ray beam; and if it is smaller, the diffracted beams become weak and hard to measure accurately. If the crystal is much smaller than 0.4 mm, unless a heavy atom is present (atomic number >17) the crystal may need to be analysed by synchrotron radiation. Synchrotron radiation is emitted by an accelerated beam of electrons circulating in a vacuum chamber as it passes through a device called a wiggler or undulator. Whereas X-rays produced conventionally by bombarding a metal target with an electron beam are limited by the ability of the target to withstand the heating effect, the absence of impacts in a synchrotron allows the radiation to be very intense and far more powerful than conventional X-rays. Synchrotron radiation can be directed on small crystals, or highly flawed crystals unsuitable for conventional single crystal X-ray diffraction, for example metastable polymorphic forms, solvates and hydrates. The synchrotron has been used in the pharmaceutical area for characterising lipid drug carrier systems (Westesen *et al.* 1993). Synchrotron radiation was preferred in this case as conventional X-ray analysis took 8-24 hours; the synchrotron was quicker and more efficient. The structure of the chemotherapeutic drug Taxol[®] which induced microtubules to adopt structure in solution has also been successfully solved using synchrotron X-ray scattering by Andreu *et al.* (1992).

6.1.2 Crystal growth

The crystal is required to have a uniform internal structure, and certain crystallisation procedures are implemented to prepare good quality crystals. Slow cooling of saturated solutions, slow diffusion of a non-solvent liquid or vapour into a saturated solution, diffusion of reacting solution and seeding to obtain larger crystals can be used to form suitable crystals (Jones, 1981; Threlfall, 1995; Guillory, 1999; Mullin, 2001). Polymorphic forms can be grown by crystallisation from different solvents at different temperatures, sublimation, crystallisation from the melt, pH adjustment or

addition of non-solvents. The crystals grown may not be of sufficient size but can be used as a seed for further crystal growth.

6.1.3 Powder diffraction

X-ray powder diffraction can analyse polycrystalline powders that are unsuitable for single crystal crystallography even with synchrotron radiation. The equipment used is very similar to the single crystal diffractometer. However, instead of a crystal, a powder sample is exposed to the X-rays. Sample preparation should ideally create a statistically infinite amount of randomly oriented powder with crystalline sample size less than 10 μm . Sample preparation is the most critical factor influencing the quality of the analytical data. Copper (Cu) tubes with the wavelength of the strongest radiation ($K\alpha$) approximately 1.54 angstroms (\AA) are most commonly used for X-ray powder diffraction. The radiation produced by this source includes $K\alpha_1$, $K\alpha_2$ and $K\beta$. The $K\beta$ is removed via a filter and the $K\alpha_1$ radiation is generally used for analytical work with the effects of $K\alpha_2$ being removed during data processing.

Powder diffraction is used by pharmaceutical scientists to identify microcrystalline samples and to distinguish between materials. A molecule's powder diffraction pattern is unique because its crystal structure is also unique. In this way the diffraction pattern can be used as a fingerprint of that molecule. An amorphous solid does not contain an ordered arrangement of atoms and when X-rays are directed on a sample there are no crystal planes to diffract the rays. Thus, powder X-ray diffraction is ideal for identifying polymorphs and assessing crystallinity.

Many solids are not suitable for structural characterisation by single crystal diffraction as they are not of sufficient size, quality or stability. In these cases it is possible to try crystal structure determination from powder diffraction data. The unit cell determination is based by analysing the position of each diffraction peak. Symmetry or space group assignment, structure solution and structure refinement are controlled by the intensity of the peaks. Structure refinement is carried out with the Rietveld refinement technique (Rietveld, 1968), which is now used routinely. The most difficult part of structure determination is finding the structure solution for the powder diffraction data. There are two ways that the structure solution can be found; these are the 'traditional' and 'direct-space' approach.

The 'traditional' approach involves using peak intensities as individual reflections and then solving the crystal structure from direct methods and Patterson methods that are used in single crystal diffraction. However, it is difficult to obtain a powder diffraction pattern that does not contain peak overlap and intensity values are unreliable. Individual reflections are difficult to identify from the powder diffraction. Developing reliable procedures for peak extraction is one of the areas of focus to advance this approach.

On the other hand, in the 'direct-space' approach, a number of structures are generated independently of the experimental powder diffraction data. For each trial structure a powder diffraction pattern is generated and compared with the experimental pattern. The theoretical and experimental powder diffraction patterns are compared via a least-squares fit of the data to give an *R*-factor (Harris and Tremayne, 1996). The strategy is to find a structure with the lowest *R*-factor, using Monte-Carlo (David *et al.*, 1998), simulated annealing or genetic algorithms (Harris *et al.*, 1998). Developments in direct space techniques have been described by Turner *et al.* (2002) and Habershon *et al.* (2002) which will help to understand the events leading to correct structure solution.

6.1.4 *Ab initio* crystal structure prediction

Molecular packing analysis using molecular mechanics can also be used to predict the structure of crystals using powerful computer programs (Holden *et al.*, 1993; Gavezzotti, 1997; Williams, 2002). Cerius² (Chemical Simulation Software Package, Accelrys Inc., San Diego, CA, USA) is a commercial package that incorporates a polymorph predictor based on molecular structure. The package generates thousands of possible positions and orientations of the molecule in the crystal structure and then energetically minimises the structures with a force field. Cerius² has been successfully used to study possible polymorphs and crystal structure of pharmaceutical molecules by Payne *et al.* (1999 a, b). Molecular packing analysis using Polymorph Predictor¹⁸ has been used together with powder diffraction data by Kiang *et al.* (2003) to resolve the structure of rofecoxib.

The potentials of each of the atoms can be calculated from first principles if the molecule contains fewer than 50 atoms (Ko and Fink, 2002). As many organic pharmaceutical molecules exceed 50 atoms, more complex mathematical parametric expressions are used. Determination of the conformation of a symmetrical, rigid molecule is relatively straightforward, but increasing the flexibility of the molecule or the number of degrees of freedom makes the determination of the correct conformation more complicated (Mooij *et al.* 2000). It is hoped that the generation of accurate crystal structures of complex molecules can be achieved by *ab initio* methods in the future so experimental data from single crystal or powder diffraction data will not be required. In the short term the combination of crystal structure prediction with powder diffraction techniques can determine the correct structure when either of the methods on its own may fail.

6.1.5 Relating crystal structure to physicochemical characteristics and mechanical properties; the future: growing crystals with specific properties.

Single crystal X-ray crystallography has been used successfully to obtain the crystal structure of organic molecules for nearly a century. Powder X-ray diffraction and *ab initio* methods of obtaining crystal structures are emerging fields; there is much work to be done on understanding and improving both concepts to obtain accurate crystal structures and to understand the intermolecular interactions involved in crystal packing. Although the nature and behaviour of bonds between molecules are well understood, it is still difficult to comprehend the special arrangement of such forces (Braga and Fabrizia, 1999).

Payne *et al.* (1996) estimated the Young's Modulus of aspirin from its crystal structure by molecular modelling. The structure was obtained experimentally from single crystal X-ray diffraction data and the modulus calculated for the crystal using the Dreiding force field. The predicted modulus of aspirin was 0.1 unit away from the experimental Young's Modulus value. Roberts *et al.* (1999) successfully predicted the mechanical properties of polymorphs of sulphathiazole and carbamazepine using the atom-atom potential model applied to lattice dynamics, as long as crystal morphology is considered when interpreting the results. So, it has been demonstrated that a

mixture of experimental and *ab initio* techniques can be used to look at the mechanical properties of a small selection of pharmaceutically active compounds. The potential application in pharmacy would be the design and growth of crystals with improved mechanical properties to help the formulation scientist produce improved dosage forms.

Crystal engineering is the design and synthesis of crystals in which the arrangement of the constituent molecules is controlled so as to elicit one or more desired functional properties from the crystal (Datta and Grant, 2004). If it is possible to predict a property, then it is possible to control the crystal structure of molecules with pre-determined properties (Panunto *et al.* 1987). Crystal design considers the chemical and geometrical aspects of the crystal and the long range, anisotropic interactions and hydrogen bonds, medium range isotropic interactions responsible for gross shapes, and close packing effects. Crystal engineering has successfully been exploited in the synthesis of porous solids, clay-like materials and ion exchange materials for separation and catalysis (Desiraju, 2003). As crystal engineering moves from structure design to property design, its applicability to pharmaceutical design will increase.

6.2 Single crystal X-ray crystallography: experimental work

6.2.1 Crystal growth

Crystal growth was by slow evaporation of a concentrated solution of the required salt in ethanol, methanol and propan-1-ol. The crystals were viewed under 8x magnification using a light microscope equipped with polarising filters that could be crossed. If the crystal was of sufficient size (0.4 mm diameter) and of sufficient quality then it was mounted on a goniometer head.

Flurbiprofen salts were used for crystal growth; the butylamine, hexylamine, benzylamine and cyclohexylamine salts were grown.

The crystals of each salt occurred as white needles; most crystals were small yet had shiny faces and sharp extinction under the polarising microscope. These samples would have only been suitable for irradiation on a synchrotron, not a conventional

source. Flurbiprofen cyclohexylamine formed crystals of a suitable size for single crystal X-ray diffraction. These crystals were long and needle-like, with a 'wood-grain' appearance and a more gradual onset of extinction when rotated between crossed polarisers, suggesting a mosaic of smaller crystals. The selected crystal was 0.5 x 0.07 x 0.05 mm. A length slightly greater than the diameter of the uniformly intense portion of the X-ray beam was deliberately chosen to compensate for the narrow diameter.

6.2.2 Structure determination and refinement

Structure determination and refinement was performed by Dr Carl Schwalbe at Aston University.

The space group was found to be $P2_1/n$ with cell dimensions $a = 15.0930(17)$, $b = 6.2822(11)$, $c = 19.8741(33)$ Å, $\beta = 91.235(11)^\circ$. Intensity data were collected at 294 K on the Enraf-Nonius CAD4 diffractometer. Because of the small volume and weak diffracting power of the crystal, only 964 of the 3321 reflections collected were considered observed ($F > 4\sigma$).

6.2.2.1 Method of structure determination and refinement.

Phase determination with direct methods (SHELXS) revealed nearly the entire structure but suggested disorder of the methyl group and the fluorine atom. Despite the problems of weak data and disorder, refinement proceeded smoothly. All fully and partially occupied phenyl, cyclohexyl and methyl H atoms were placed in calculated positions. No assumption was made about the state of protonation, as a difference electron density map revealed three credible peaks attached to the cyclohexylammonium N atom and none near the carboxylate O atoms. Final refinement reduced $R(\text{obs})$ to a respectable 0.0706, but $wR2$ for all data was 0.2238. Estimated standard deviations in bond distances were typically 0.007-0.009 Å.

6.2.2.2 Redetermination from data collected with synchrotron radiation.

A much higher-quality data set was kindly collected by Dr. Simon Teat on Station 9.8 at the Daresbury Synchrotron Radiation Source. A crystal of dimensions 0.34 x 0.04 x 0.03 mm was used for data collection, and the temperature was lowered to 150 K to improve the signal-to-noise ratio. The space group remained $P2_1/n$ with cell dimensions now $a = 14.7991(5)$, $b = 6.3014(2)$, $c = 19.7845(7)$ Å, $\beta = 91.273(2)^\circ$.

With X-rays of wavelength 0.6934 Å a total of 28,903 reflections were collected, which after averaging of equivalent data yielded 5,530 independent reflections. After similar treatment of hydrogen atoms and final refinement as before $R(\text{obs})$ reached 0.0523 and $wR2$ was 0.1429 with typical estimated standard deviations for bond distances 0.002 Å. Where numerical results are discussed in subsequent sections, they will be taken from the low-temperature synchrotron data.

6.2.3 Results and Conclusions

6.2.3.1 Description of the structure.

Both benzene rings show a high degree of planarity, with a $44.15(5)^\circ$ twist between them. The fluorophenyl ring has two-fold rotational disorder providing two alternative sites for the fluorine atom with occupancy 0.675 and 0.325. The methyl group is also disordered over two almost equally occupied positions (figure 6.2) with occupancy, 0.523 : 0.477 and no apparent coupling with the choice of fluorine site. All three cyclohexylammonium H atoms are involved in hydrogen bonding to a carboxylate O atom; thus O1 accepts two hydrogen bonds while O2 accepts one. Successive hydrogen bonds efficiently form narrow hydrophilic domains, while cyclohexane rings overlaying benzene rings create broad hydrophobic domains, as shown in figure 6.2 and 6.3 revealing different aspects of the same structure.

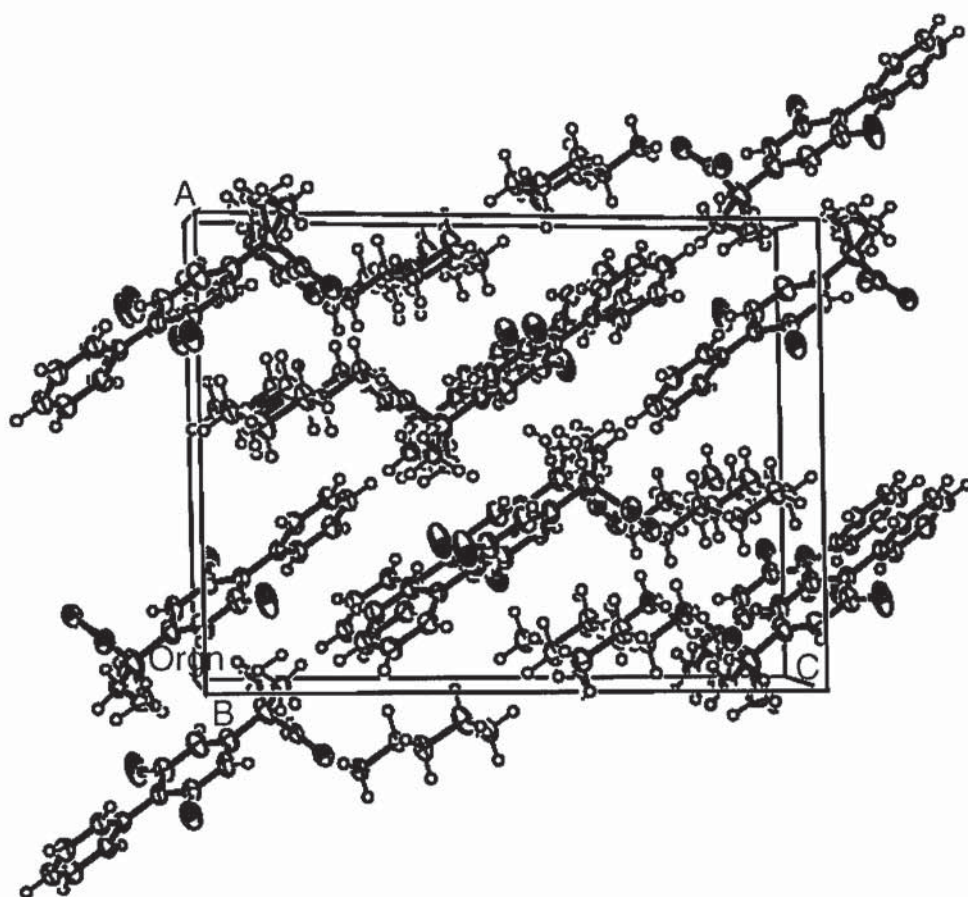


Figure 6.2 Crystal structure of flurbiprofen cyclohexylamine

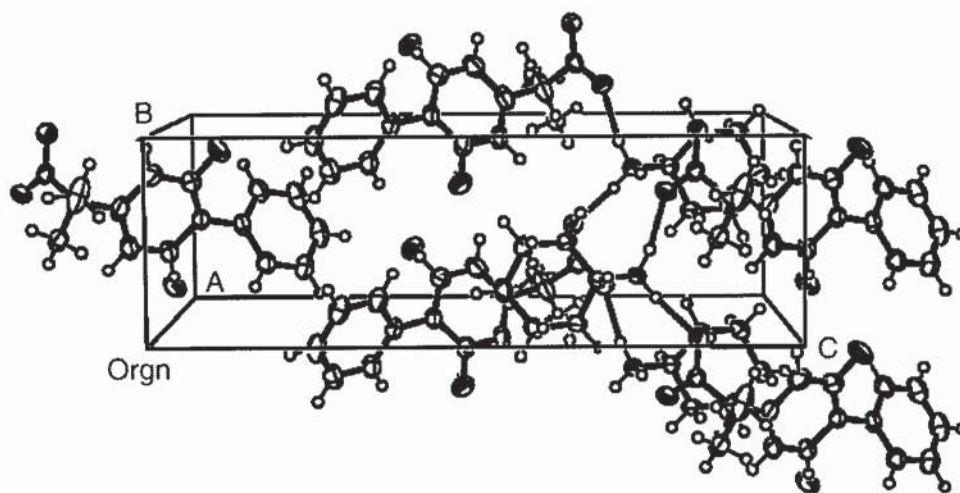


Figure 6.3 Crystal structure of flurbiprofen cyclohexylamine

6.2.3.2 Relationship of crystal structure to solubility

Several studies have related aqueous solubility to physicochemical characteristics (Thomas and Rubino, 1996; O'Connor and Corrigan, 2001; Parshad *et al.*, 2002). Each study has failed to identify a single parameter that can be used to predict aqueous solubility. This is because the intermolecular forces involved in salts of organic molecules are complex and have not been extensively studied by X-ray crystallographic analysis. One study investigating the aqueous solubility of salts of benzylamine derivatives using single crystal diffraction suggested that a reduced number of hydrogen bonds caused the apparent higher solubility (Parshad *et al.*, 2004). The aqueous solubility was expected to be influenced by competition between the free energy of hydration of the ions and the crystal lattice energy. The solubility was driven by the number of ionic hydrogen bonds, a reduced number leading to a decreased crystal lattice energy. Parshad *et al.* (2004) concluded that further studies involving energy considerations of hydrogen bonds and non-specific interactions would be required to account for solubility differences in terms of hydrogen bond patterns and crystal packing characteristics.

Flurbiprofen cyclohexylamine has low aqueous solubility (0.37 mg/ml) so knowledge and understanding of the crystal structure of the salt may help to explain its aqueous solubility. The narrow hydrophilic domains in the crystal structure contain hydrogen bonds; surrounded by hydrophobic domains of overlapping benzene and cyclohexane rings that may protect the hydrogen bonds from polar water molecules that are required for dissolution. The hydrophobic domains may repulse water molecules and make the hydrogen bonds relatively inaccessible.

More crystal structures are required to examine the relationship between salt solubility and crystal structure. Unfortunately the other salt crystals were too small to be analysed by single crystal X-ray diffraction and synchrotron radiation was not available to solve the crystal structures of the other salts.

6.3 Structure determination using powder diffraction data: experimental work

6.3.1 Introduction

Prof. K. D. M. Harris at Cardiff University (formerly at Birmingham University) was approached with the purpose of setting up a collaboration to solve the crystal structures of the amine salts from X-ray powder diffraction. Dr Eugene Cheung performed the practical analysis, structure determination and refinement on all the salts analysed.

6.3.2 Experimental

Gemfibrozil and flurbiprofen salts were analysed by Dr Cheung at Cardiff; these included the butylamine, hexylamine, octylamine, AMP1, AMP2 and tris salts of each drug.

The samples were ground in a pestle and mortar to reduce the particle size and to ensure random orientation of the crystals. This was particularly difficult with electrostatic powders when material was in short supply. As each salt was made in-house, there was a limited quantity of material available for analysis. The sample was mounted between Sellotape[®] and placed in the diffractometer, the data was recorded on a Siemens D5000 powder X-ray diffractometer with germanium monochromated CuK α -1 radiation.

DSC data was recorded on each sample prior to sending to Dr Cheung to ensure the correct crystal form was present (see section 3.4.2). Gemfibrozil octylamine and flurbiprofen butylamine were re-crystallised slowly from ethanol to ensure the desired crystal form existed.

Powder patterns were indexed using:

ITO (Visser, 1969)

TREOR (Werner et al., 1985)

DICVOL (Lour and Vargas, 1982 and Boultif and Lour, 1991)

Structure solution was carried out using a genetic algorithm as implemented in the program EAGER. EAGER has been developed by Harris, K.D.M., Johnson, R.L., Cheung, E.Y., Habershon, S., Turner, G.W., Hanson, A.J., Cardiff University, 2004

(an extended version of the program GAPSS, Harris, K.D.M., Johnson, R.L., Kariuki, B.M, University of Birmingham, 1997).

Structures were then refined using the Rietveld method in the program GSAS (Larson and Von Dreele, 2000).

6.3.3 Results

6.3.3.1 Gemfibrozil

The single crystal of gemfibrozil was obtained from the powder diffraction pattern and the unit cell dimensions were found to be:

Cell length a	14.84
Cell length b	7.32
Cell length c	30.68
Cell volume	3013.32

Gemfibrozil has a long thin unit cell and is therefore likely to form needle-like crystals. It does not form dimers, the crystal lattice is connected in the y-axis (b) by hydrogen bonds. All the oxygen's of the carboxylic function are involved in hydrogen bonding, forming a channel of hydrogen bonds. Benzene rings form a ladder arrangement loosely held together. The hydrogen bonds are only in the y-axis and slipping of planes may be mechanically inhibited by rigid benzene rings in the b direction. Slip may be accommodated in the z plane (c), figure 6.4.

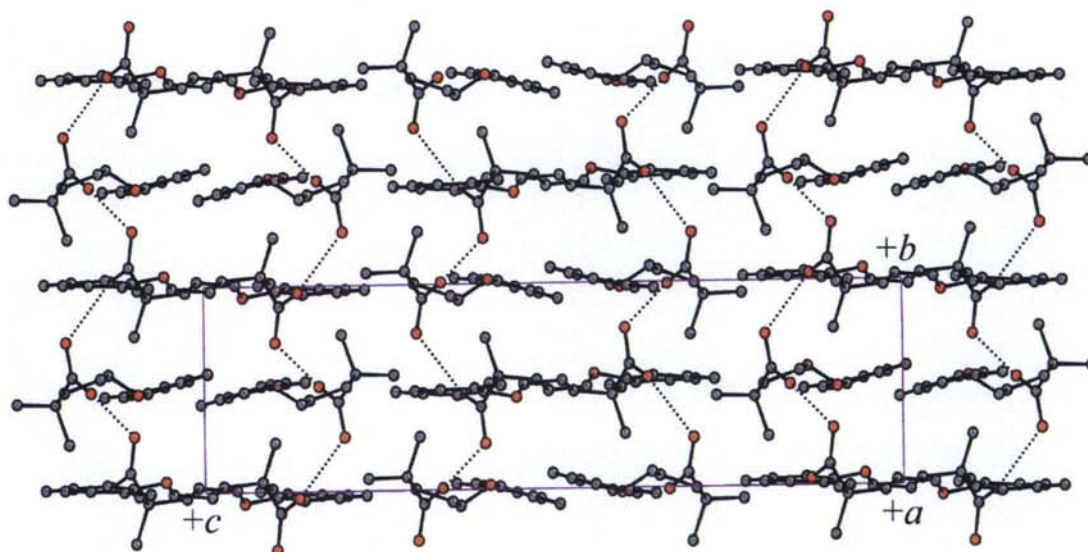


Figure 6.4 The crystal structure and unit cell of gemfibrozil

The shape of the unit cell is as follows:

Cell angle alpha	30.68
Cell angle beta	115.30
Cell angle gamma	90.0
R factor	0.0209

6.3.3.2 Gemfibrozil butylamine

The single crystal of gemfibrozil butylamine was obtained from the powder diffraction pattern and the unit cell dimensions were found to be:

Cell length a	12.64
Cell length b	6.17
Cell length c	26.00
Cell volume	2024.06

The unit cell has similar dimensions to gemfibrozil, although the smaller cell volume results in a denser crystal structure. The hydrogen bonds are arranged in channels (figure 6.5) with all oxygen atoms involved in hydrogen bonding, leaving none free to form extra bonds. The crystal structure is characterised by a ladder of benzene rings not associated by bonds but forming a hydrophobic domain. Slip would not be possible on the y plane because the rigid benzene rings would interfere with any

mechanical processes. Hydrogen bonds hold the crystal lattice strongly in one direction only, weak bonds in between the layers of hydrogen bonds may allow slip.

Each butylamine counterion is represented by multiple atoms which attempts to indicate the level of disorder present in the molecule.

The shape of the unit cell is:

Cell angle alpha	90.00
Cell angle beta	93.30
Cell angle gamma	90.0
R factor	0.0445

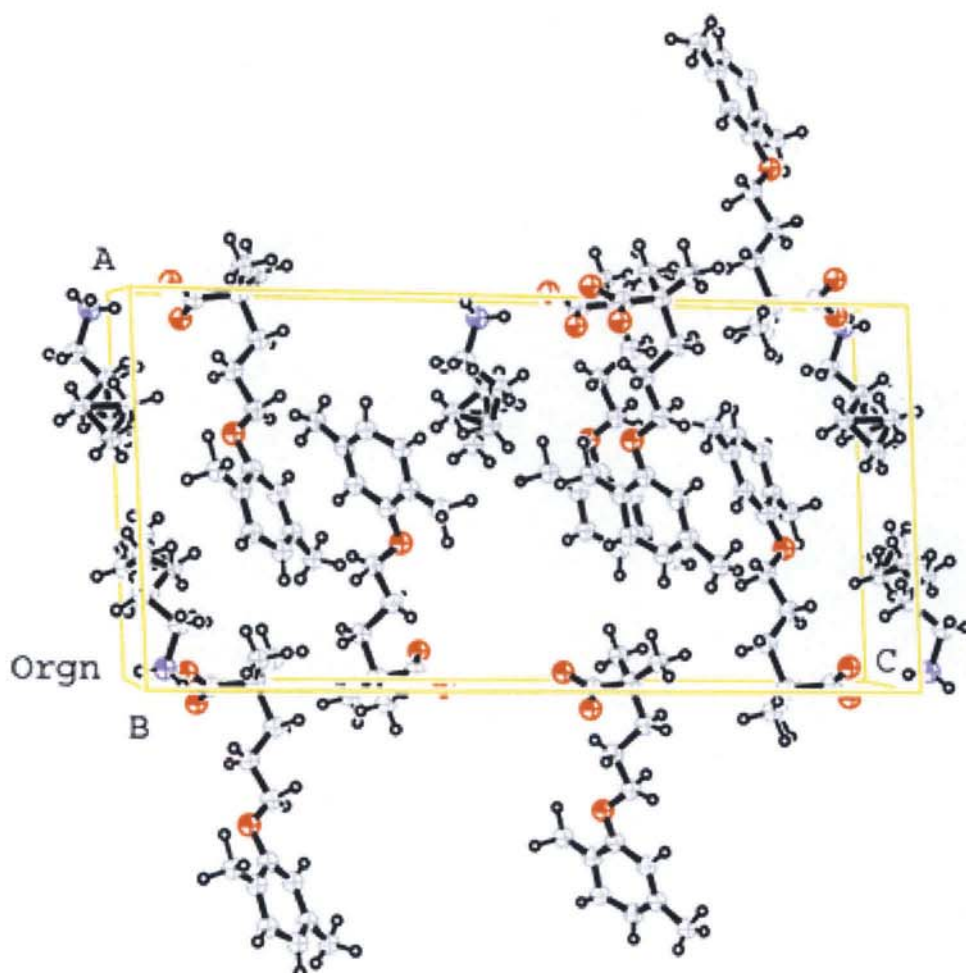


Figure 6.5 The unit cell of gemfibrozil butylamine

6.3.3.3 Gemfibrozil pentylamine

The single crystal of gemfibrozil pentylamine was obtained from the powder diffraction pattern and the unit cell dimensions were found to be:

Cell length a	6.50
Cell length b	10.22
Cell length c	16.99
Cell volume	1071.11

The unit cell has become denser as the unit cell volume has reduced and the unit cell is a different size compared to gemfibrozil butylamine. The unit cell has shortened along the a- and c-axis and lengthened along the b-axis. The arrangement of the molecules and hydrogen bonds remains unchanged within in the unit cell compared to gemfibrozil butylamine (figure 6.6 and 6.7). Each pentylamine counterion is situated within the channel of hydrogen bonds and each molecule has a degree of disorder which is illustrated by multiple atoms in the figure. Gemfibrozil pentylamine has a greater degree of disorder than gemfibrozil butylamine.

The shape of the unit cell is:

Cell angle alpha	75.26
Cell angle beta	81.62
Cell angle gamma	80.79
R factor	0.0354

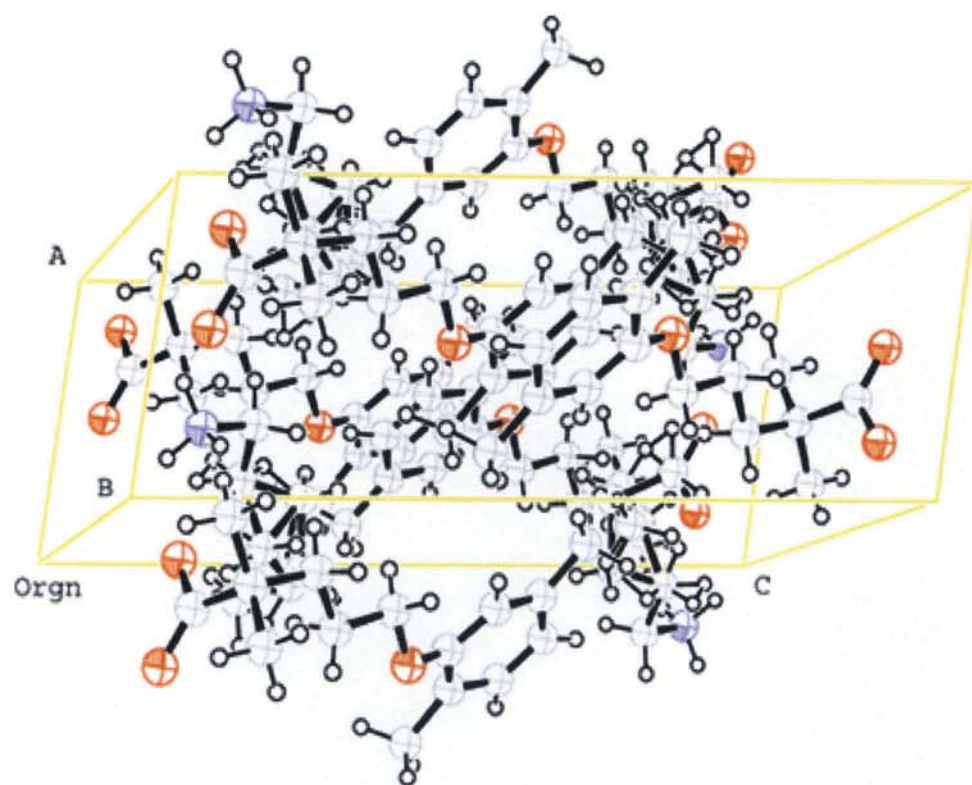


Figure 6.6 The unit cell of gemfibrozil Pentylamine.

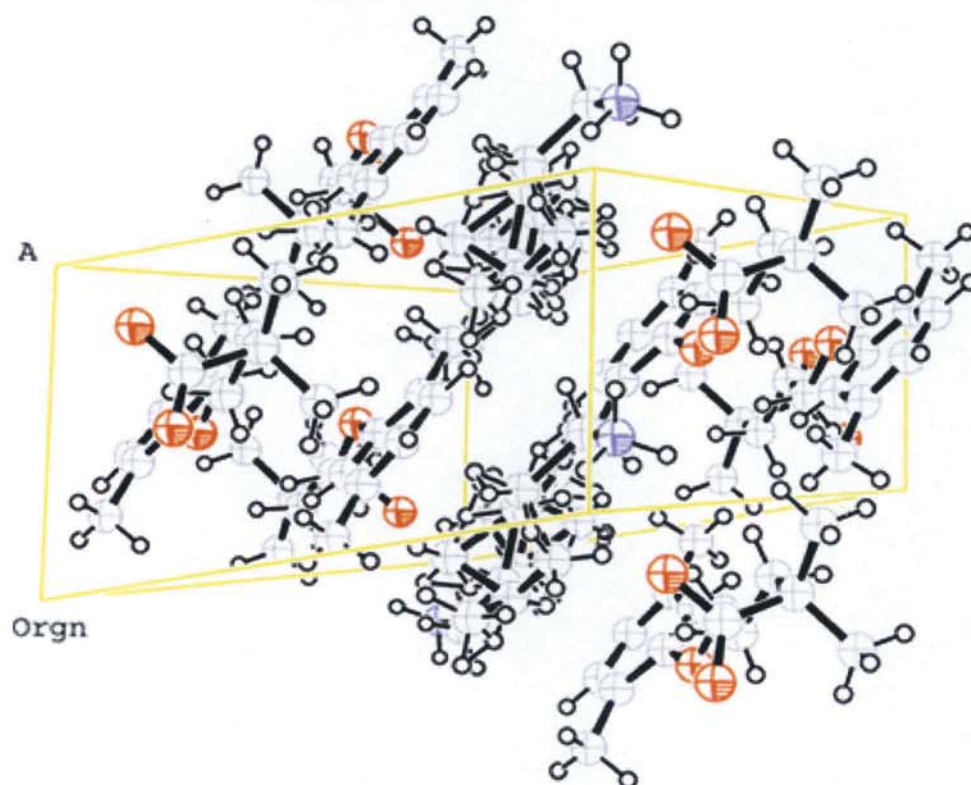


Figure 6.7 Unit cell of gemfibrozil pentylamine re-oriented for ease of visualisation

6.3.3.4 Gemfibrozil hexylamine

The crystal of gemfibrozil hexylamine was obtained from the powder diffraction pattern and the unit cell dimensions were found to be:

Cell length a	6.65
Cell length b	13.41
Cell length c	13.42
Cell volume	1123.61

The unit cell dimensions are very similar to gemfibrozil pentylamine, the crystal structure is illustrated in figure 6.8. The addition of a carbon atom to the counterion does not make a significant difference to the crystal packing. The degree of disorder of the counterion is slightly increased due to the degrees of freedom increasing as the length of the chain extends.

The shape of the unit cell is:

Cell angle alpha	75.23
Cell angle beta	75.99
Cell angle gamma	84.47
R factor	0.0377

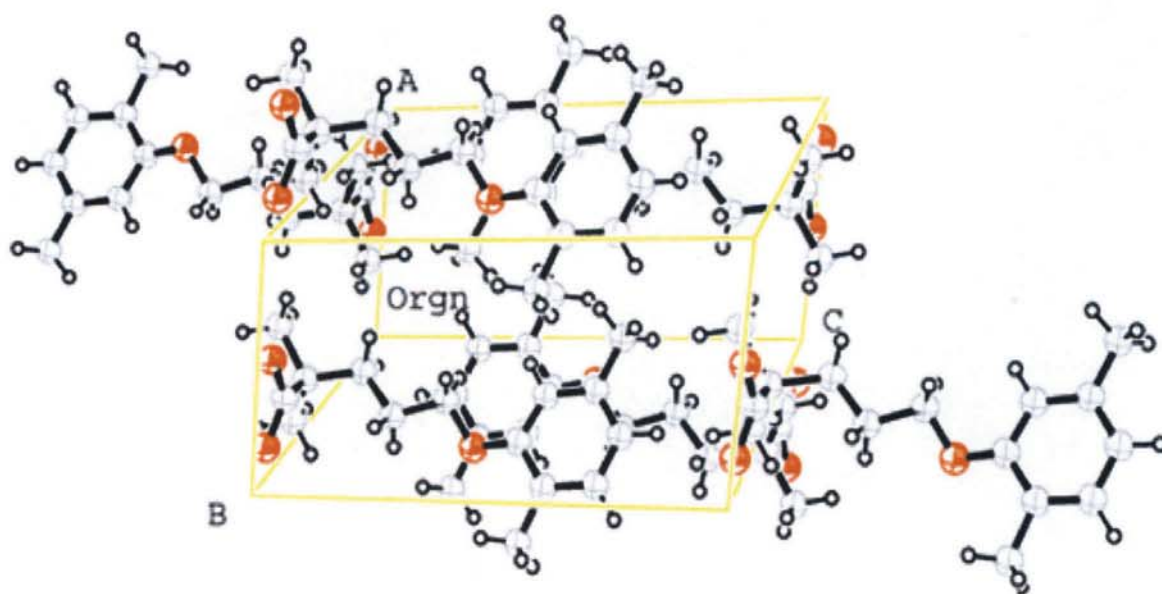


Figure 6.8 The unit cell of gemfibrozil hexylamine

6.3.3.5 Gemfibrozil AMP2

The crystal structure of gemfibrozil AMP2 was obtained from the powder diffraction pattern and the unit cell dimensions, in angstroms were found to be:

Cell length a	27.08
Cell length b	6.32
Cell length c	22.89
Cell volume	3918.02

The unit cell is very short on the y-axis, whereas the x- and z-axis are similar in length (figure 6.9). Each nitrogen atom on the counterion donates hydrogen bonds to two oxygen atoms of gemfibrozil and one oxygen on another AMP2 molecule. The unit cell volume much larger than for gemfibrozil or the other salts. Hydrogen bonds are formed along all the axis. Three dimensional hydrogen bonds form a strong crystal lattice. The arrangement of the crystal lattice may promote strong inter-particle bonding and should promote compressibility (see section 7.3.4.3). There is an additional hydroxyl group on the counterion which is available for additional hydrogen bonding if the molecules become close enough, e.g. upon compression.

The shape of the unit cell is:

Cell angle alpha	90.0
Cell angle beta	92.28
Cell angle gamma	90.0
R factor	0.0358

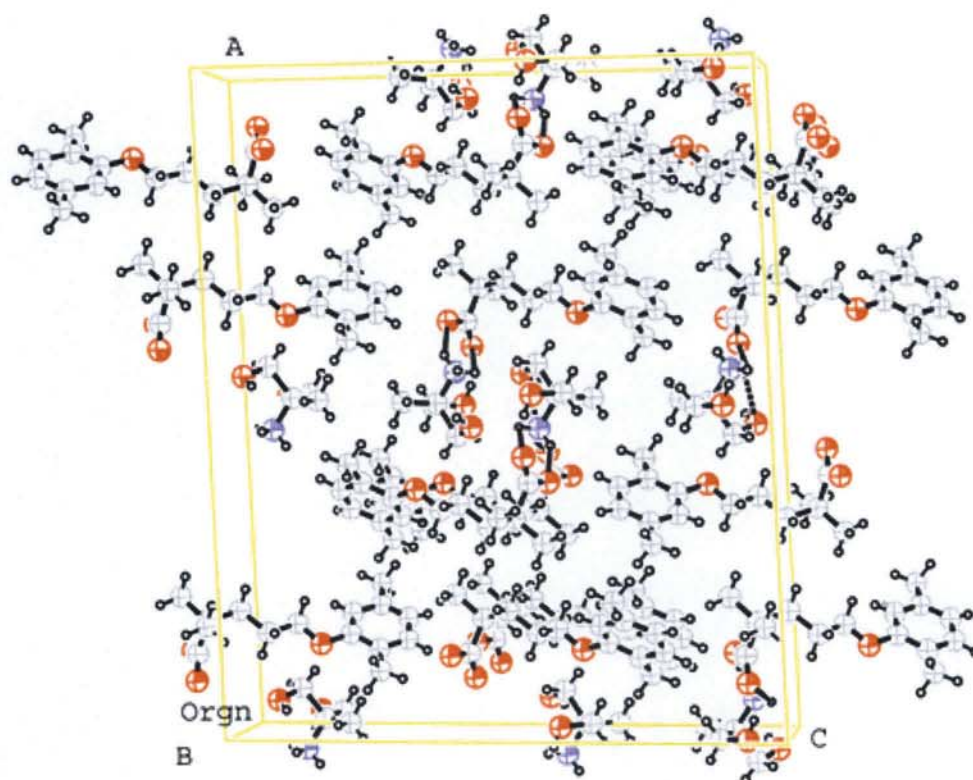


Figure 6.9 The unit cell of gemfibrozil AMP2

6.3.3.6 Gemfibrozil Tris

The crystal structure of gemfibrozil tris was obtained from the powder diffraction pattern and the unit cell dimensions were found to be:

Cell length a	18.50
Cell length b	10.04
Cell length c	11.00
Cell volume	2024.94

The unit cell axis are similar lengths so the unit cell is a square and the cell volume is similar to gemfibrozil. Hydrogen bonds form along the y-axis (figure 6.10), each nitrogen donates a hydrogen to an oxygen on the tris counterion. The benzene rings of gemfibrozil lie on top of each other forming hydrophobic regions which are loosely associated; channels of hydrogen bonds lie in-between the hydrophobic regions. On compression bonds are strong in the x- and y- direction: 4 hydrogen bonds in x-direction and 2 hydrogen bonds in y-direction (see section 7.3.4.3). All nitrogen and

oxygen atoms are involved in hydrogen bonding so there is no more potential for new bonds to form.

The shape of the unit cell is:

Cell angle alpha	90.0
Cell angle beta	97.37
Cell angle gamma	90.0
R factor	0.0299

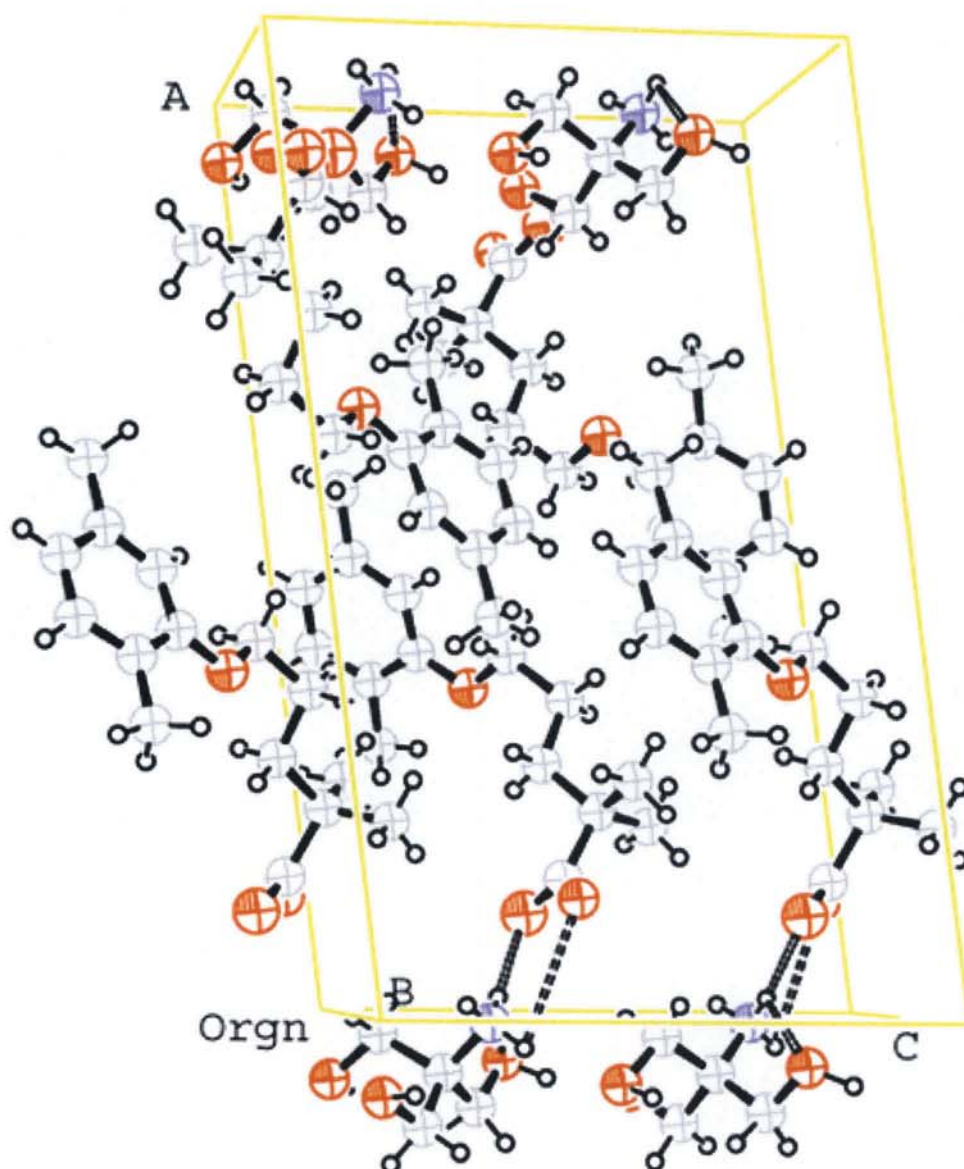


Figure 6.10 The unit cell for gemfibrozil tris

6.3.4 Discussion

The arrangement of molecules and hydrogen bonds in the crystal structure is similar in the homologous alkyl series. Although only gemfibrozil AMP2 and tris have been investigated from the hydrophilic counterion series the crystal structures are quite different. This is to be expected as the counterion varies in the number of hydroxyl groups present and the potential for hydrogen bonding will therefore vary. Knowledge of the complete series: tert, AMP1, AMP2 and tris salt forms of gemfibrozil would provide additional structural information. Acquiring the single crystal for gemfibrozil tert-butylamine and gemfibrozil AMP1 would complete the series. It would provide useful information about the presence and arrangement of the hydrogen bonds that may be related to solubility or mechanical properties.

Future studies to solve the crystal structures of the salts of flurbiprofen would be valuable to compare the hydrogen bonding motifs within the hydrophilic salt series. Differences or similarities between the crystal structures may help to explain the solubility differences. Further information regarding compression characteristics of powders and the relationship between hydrogen bonding and Young's modulus could be further investigated

Chapter 7 Mechanical Properties of Salts

7.1 Introduction

7.1.1 Summary

The purpose of this chapter is to investigate the compression characteristics by mechanical testing of compacts of 100% drug and salt. Powder compacts were made of drug and salt at different porosities in the form of disks and wafers. Discs were made in a 13 mm IR die and press, the shape of the die was found to promote lamination. The discs were assessed in terms of tensile strength on a QTS-25 texture analyser, and the force required to cause failure was recorded. The QTS-25 was found to have insufficient accuracy and reproducibility to analyse the discs satisfactorily. Wafers were made using a specially constructed die of 7 x 20 x 1 mm, this allowed the production of wafers of different porosity. It was possible to make wafers of all powdered material, however not all wafers were suitable for mechanical testing as lamination and adherence of powder to the die surfaces produced deformed wafers. The mechanical properties of wafers were tested on a Hounsfield Universal Testing Machine with a 5 N load cell and a bespoke manufactured miniature 3-point bend jig. Young's modulus of elasticity (E) was calculated from the measured force and displacement data.

The data was assessed and compared in terms of Young's Modulus and observed characteristics. The effect of counterion on the mechanical properties of the parent drug was investigated *i.e.* the effect of: chain length, increasing hydrophilicity and whether saturated or unsaturated counterions impact on mechanical properties of the salt form. An attempt was made to relate crystal structure to mechanical properties of the drug and salt powders.

7.1.2 The Process of Compression

Compression is the process of applying pressure to a material. Generally to form tablets by compression, a measured mixture of drug and excipient are compressed between an upper and lower punch at a specified pressure for a set time. The intact tablet is ejected from the die as a suitable dosage form. The mechanical events that

describe the process are: particle rearrangement, deformation at points of contact, fragmentation, bonding, decompression and ejection (Parrott, 1990).

7.1.2.1 Particle Rearrangement

The powder or granules flow in the die cavity as the pressure increases, the smaller particles filling void spaces between the larger ones. Granulation aims to produce spherical particles that are assumed to require less particle rearrangement as they tend to assume close packing as the pressure increases in the die and flow easily. On the other hand irregular particles will require more particle rearrangement to achieve a preferred orientation as compression occurs, for these particles flow is poor. Di Martino *et al.* (2001) discovered that spray drying acetazolamide improved the compression properties compared with polymorphic forms I and II due to an increased particle rearrangement due to spherical habit.

7.1.2.2 Deformation

Deformation occurs when a stress (force) is applied to a material. If after the stress is applied the material returns to its original shape, the deformation is termed elastic. If the material does not recover from the release of the stress, plastic deformation is said to occur. When the particles are packed closely, further compression may result in deformation at the points of contact. Everett Hiestand (1985) was the first to develop a model for bond deformation, it assumes spherical particles. It also assumes that attraction forces arise from dispersion forces, and that compression follows Hertz' equation for elastic deformation. A bonding index is calculated from the particle size, indentation hardness and the solid fraction. A large value for the bonding index (tensile strength/indentation hardness) is representative of plastic deformation. Johansson and Alderborn (2001) investigated the compression behaviour of microcrystalline cellulose and determined that permanent deformation was the main mechanism of compression. Deformation may involve a change of shape for the granule but as the particles are being brought closer together, more contact zones develop where inter-granular bonds are established (Johansson *et al.*, 1995; Nicklasson *et al.*, 1999a)

7.1.2.3 Fragmentation

Higher pressures in the die induce stresses within the particles which form cracks and result in fragmentation. Fragmentation induces densification and provides additional surfaces for bonding. Nicklasson et al. (1999b) prepared pellets with microcrystalline cellulose and dicalcium phosphate dehydrate. They found unlubricated pellets showed fragmentation; the breakdown of the pellet into smaller aggregates. Materials that have low deformation, *i.e.* that are brittle, are likely to fracture during compression inducing flaws in the compact. In some materials fragmentation does not occur and the stresses are relieved by plastic deformation. This is when the particles slide over each other to relieve stress (viscoelastic flow). Such deformation produces new surfaces for bonding.

7.1.2.4 Bonding

Tablet bonding refers to an attraction of particles to each other, not chemical bonds. In a tablet the particles are compressed together, there are no intermolecular forces such as H-bonds or Van Der Waals forces holding the particles together because they are not close enough to each other. The incidence of H-bonds in pharmaceutical tablets is expected to be small (Hiestand, 1997). Thermodynamically the attraction between particles forming interfacial contact areas, bonding, is the lower free energy state and as repulsion requires work (Coffin-Beach and Hollenbeck, 1983) therefore bonding is an exothermic process. Compaction is the process of fracturing, deforming and sliding of particles so that they fit close enough together that the attraction between each particle is inherent. Hiestand (1991) and Hiestand and Smith (1991) developed a theoretical model to describe tablet bonding and tested it experimentally. One model was for brittle mechanisms at higher compression forces and the other for plastic deformation at lower compression forces. The authors found that because many parameters could not be measured it was not the ideal model. Bond strength can be measured by tensile strength rather than indentation hardness because the compacts are fractured. Tensile strength is measured in force/unit area over a cross section so that stress is measured. It is the maximum force that produces fracture.

Melting-solidification caused by tablet compaction is a possible bonding mechanism but is only possible if the melting point is very close to room temperature. Friction could cause melting to occur that would result in entrapped air which would cause fracture upon ejection. This is a highly unlikely mechanism of tablet bonding as the pressures and volume changes involved in compression are not sufficient to produce melting. Many organic materials decompose upon melting and plastic deformation occurs at low pressures (Hiestand, 1997).

The compaction process produces increased strength by particle fracture and packing rearrangement; the powder bed is sheared and the particles are deformed (plastic deformation). Short-range dispersion interactions dominate in a compact as the particle contact produced by compression form a 'bridge', the spaces between particles has been eliminated.

7.1.2.5 Decompression and Ejection

The success or failure to produce an intact tablet depends on the decompression and ejection of the tablet from the die. As pressure is removed, the compact relies on elastic recovery to prevent capping or lamination. Capping occurs as the tablet is ejected, the lateral pressure is relieved yet the strain remains from the walls of the die. The tablet surface is separated from the main tablet body producing fragments. The fragments are commonly hard, brittle and dense indicating they may have been strongly bonded to the tablet. Capping occurs unless shear stress is relieved by plastic deformation. It has been demonstrated that if decompression occurs simultaneously in all directions then capping is reduced or eliminated.

Stress relaxation of plastic deformation is time dependent. Slow stress relaxation in the die can cause cracks to develop in the tablet, slower operational speeds will reduce the problem.

7.1.2.6 The Heckel Plot

For the compressional process, Heckel (1961) proposed equation 7.1:

$$-\ln(1 - D) = K.P + A \quad \text{equation 7.1}$$

in which P is the compaction pressure and D is the relative density, ρ_c/ρ_t , of the compact. The material constant, K , is the slope of the linear portion of the Heckel plot and measures plasticity of the material. The reciprocal of K is termed the mean yield pressure, P_y (Hersey and Rees, 1971), which is three times the yield strength of the material.

The Heckel relationship may be written in terms of relative density ρ_{rel} rather than volume (equation 7.2)

$$\log \frac{1}{1 - \rho_{rel}} = \frac{KP}{2.303} + A \quad \text{equation 7.2}$$

in which P is the applied pressure, and K and A are constants. The Heckel constant, K , has been related to the reciprocal of the mean yield pressure, which is the minimum pressure required to cause deformation of the material undergoing compression. A large value of the Heckel constant indicates that plastic deformation occurs at low pressures. The Heckel plot allows the identification of the mechanism of bonding. If the plot is linear, plastic deformation is the main mechanism for bonding. If the plot is non-linear then fragmentation occurs during compression.

A Heckel analysis is carried out on a tablet machine that is transformed to an analytical instrument allowing the measurement of pressures and volumes. It is suitable for measuring small amounts of powder which is ideal in a pharmaceutical product development setting where limited quantities are available for formulation work. Heckel plots are commonly used as the shape of the curve gives information about fragmentation, plasticity and time dependency of the compression behaviour with an eccentric press.

Rue and Rees (1978) investigated the limitations of the Heckel relationship and found that large differences in the shape of the curve can be obtained with different users. York (1979) considered experimental variables in the Heckel analysis and discovered that different experimental set-ups could produce a variation in the shape of the curve. Sonnergaard (1999) questioned the general validity of the Heckel

equation as differences between published Heckel parameters are obtained from 'at pressure' data or using the 'in-die' method. Krumme et al. (2000) analysed experimental results of the Heckel plots and developed computerised procedures for the characterisation of tableting properties using an eccentric press. They concluded that Heckel analysis should not be used as absolute values, although theory would suggest otherwise, but should be used as a guide. Accuracy of the analysis is determined by powder height measurement and the method of determination of true density. The porosity should be corrected for compensation of the solid fraction. Heckle plots are a non-linear transformation of compression data therefore signal errors may be enlarged by the calculations and become critical.

Heckel analysis is a commonly used and recognised method of characterising the compression properties of powders. Although the limitations described above suggest user variability the method can give useful information to enable the formulation of robust dosage forms.

7.1.2.7 Tablet Indices

Hiestand (1991) proposed a theory that describes the processes involved in tablet bonding using measurements on specially prepared compacts. The compacts were tested for strength as this provides the simplest method of characterising mechanical properties. Tensile strength (σ_T) was measured by the transverse compression of a square compact, the strain rate accurately determined on the machine. The maximum tensile strength was measured before fracture. For the experiment to be valid, there must be no macroscopic defects that could distort the result, e.g. lamination, capping or cracking. Compacts do not have uniform porosity due to the density differences and pressure distributions on compression, this leads to potential inaccuracies in measurements. Indentation Hardness can be expressed by an instantaneous value on impact (H_0) or a longer indenter dwell time (H_{30}). A flawless compact is required for this test as any defects would be exaggerated by the impact of the indenter. Stress until fracture is measured in kN/cm^3 .

The bonding index (BI) is described by equation 7.3:

$$BI = \frac{\delta_T}{H_0} \quad \text{equation 7.3}$$

As it compares indentation hardness to tensile strength it should indicate the relative survival, during decompression, of the areas of true contact that were established during compression. H_{30} is considered the best case scenario as slow strain rates and long dwell times improve plastic deformation whereas H_0 will represent a value most representative to a real tableting situation. Each value is useful as a large difference between values could indicate that tableting speed influences performance.

The Brittle Fracture Index (BFI) is the strength of a compact when a macroscopic defect is present. The macroscopic defect enhances brittle behaviour; the defect must be large in comparison with the pores within the compact which causes brittle fracture even when interparticle bonding is a ductile process. The compact will fail at a lower stress rate as the defect propagates crack formation due to increased stress on that area. For materials that are able to relieve stress by plastic deformation, the crack stress will be near to the non-defect value. In these materials, stress is absorbed more efficiently throughout the compact as the load is increased. The ratio of the strength of tablets with and without a hole is termed the BFI.

Brittle Fracture Index (BFI) proposed by Hiestand (1977) is described in equation 7.4:

$$BFI = \frac{1}{2} \left[\frac{\delta_T}{\delta_{Th}} - 1 \right] \quad \text{equation 7.4}$$

Where δ_T is the tensile strength and δ_{Th} is the tensile strength of the compact with the hole.

A BFI below 0.2 indicates that there will be no problem with fracture during tableting unless the bonding is very weak. If the BFI is greater than 0.8, brittle properties result in fracture problems when tableting. As the BFI was originally designed for use on

large square compacts with a central hole, Roberts and Rowe (1986) modified and extended the use of the BFI to cylindrical compacts of tablet sized dimensions to represent more realistic tableting conditions. Roberts and Rowe (1985) also criticised the use of large cubic compacts, used by Hiestand, which were claimed to avoid the formation of cracks and flaws inside the specimens to improve reproducibility. Roberts and Rowe (1985) used conventional cylindrical disks and showed this did not affect the values for BFI for a given material. They also found a strong dependence on porosity on the BFI.

Podczek and Newton (2002) investigated the impact of the correct calculations on the BFI as a concept by converting breaking loads of tablets with a central hole into true tensile and compressive strength values. They found that using Hiestand's raw data produced negative values for corrected tensile strength values, which compromised the validity of his approach. The BFI values also change with porosity, so the BFI is not a material constant as Hiestand suggests. Hiestand's theory is based on assuming a stress concentration at the hole of the compact and a stress concentration factor of 3 should be used for simplicity. Podczek and Newton produced stress concentration factors of between 5.5 and 6 for MCC which is clearly out of the range that Hiestand suggests. Thus the Hiestand approach of calculating a BFI cannot be supported on a theoretical and experimental basis.

The Strain Index (SI) is obtained from dynamic indentation hardness experiments. It is calculated from indentation hardness and Young's modulus of the material and Poisson's ratio and represents the elastic recovery following compression of a compact (equation 7.5).

The Strain Index (SI)

$$SI = \frac{H_o}{E'} \quad \text{equation 7.5}$$

where E' is the reduced elastic modulus ($E/(1-\nu^2)$) where ν is the Poisson's ratio. Poisson's ratio, ν , is the negative of the ratio of the lateral strain to uniaxial strain, in axial loading.

Hiestand describes the use of a square compact requiring large volumes of powder, using triaxial compression to reduce the number of fracture lines that would form due to decompression from uniaxial compression. Triaxial compression allows constant pressure to be maintained on each surface of the compact, reducing lamination and capping. The indenter used was a 2.54 cm diameter steel sphere orientated in the centre of a 19.05 mm square compact of 9.5 mm thickness. Porosity was calculated from true density measurements and the tablet dimensions, where an average of five readings was used directly before the experiment.

7.2.2.8 Leuenberger theory of powder compression

Leuenberger (1983) developed another approach to powder compression that examined the behaviour of the compact over a wide range of porosities. Tensile strength testing (δ_T) and indentation hardness (H_0) were performed on the compacts. The derived equations resulted from studying the physics of flow in a powder bed upon compaction. Compression of powders occurs in stages, over which the physics can vary, so finding a single model that represents each stage is difficult. It has been shown that within a broad density range there exists more than one linear region in such a semi-logarithmic hardness plot (Holman and Leuenberger, 1988). Tablet bonding is determined by process parameters as well as the formulation, as brittle and plastic substances compress in different ways. Tablets show a heterogeneity of density distribution and are considered quite disordered. Recently, imaging of tablet density has been possible with X-ray micro-tomography, where cross sections of the tablet can be visualised showing the density distribution (Wu *et al.*, 2004). This may provide information about how pressure can affect density and consequently strength and the growth of fracture lines.

Leuenberger proposed a relationship shown in equation 7.6 between indentation hardness (P) and relative density (ρ):

$$P = P_{\max} (1 - e^{-x\delta\rho})$$

equation 7.6

where P_{\max} holds for maximal hardness, x is the pressure susceptibility, δ equals the compression pressure, and ρ is the relative density. The parameter x determines the degree of porosity reduction under pressure and P_{\max} provides a measure of the bonding strength required for the formation of the tablet. A new model for tablet hardness was proposed by Kuenz and Leuenberger (1999) as a function of relative density. They concluded that the lowest porosity can be used as a reference point where bonding in a compact first occurs and begins the strengthening process.

7.2.3 The effect of compression on tablet characteristics

Higuchi *et al.* (1952) and Train and Hersey (1960) were probably the first to investigate the compression of pharmaceutical powders into tablets. They investigated the effect of compression on density, disintegration, hardness, porosity, specific surface and the distribution of pressure in a die press. Knowledge of how compression affects the properties of powders aids the selection of appropriate excipients to optimise solid dose formulations.

7.2.3.1 Density and Porosity

True densities are measured using helium gas since it will penetrate every surface flaw down to about one Angstrom, thereby enabling the measurement of powder volumes with great accuracy. The true volume of solid materials is measured by employing Archimedes' principle of fluid (gas) displacement and the technique of gas expansion. The measurement of density by helium displacement often can reveal the presence of impurities and occluded pores which cannot be determined by any other method.

Porosity is a measure of the volume of air-filled pores in a compressed tablet. It is important when testing compacts to consider porosity, as tablet hardness can greatly increase with increasing density. As particles are forced closer together, the cohesive forces holding them together increase which will consequently increase hardness.

Hiestand *et al.* (1971 and 1977) found that the logarithm of the hardness is a linear function of the relative density. Kuentz and Leuenberger (2000) developed a new model for tablet hardness based on the Leuenberger theory of powder compression. It describes indentation hardness as a function of relative density. For the model to be valid a large porosity range must be considered, for the pharmaceutical polymers used, porosity was obtained between 3-66%. A typical drug has a porosity range between 0-30% so will only represent a portion of the model. It is usual to compare hardness values at zero porosity so excluding the effect of void spaces and the model is required to accurately predict the maximal hardness at zero porosity even at low porosity ranges.

7.2.3.2 Fracture

The ability of a tablet to withstand mechanical handling and transport is a required property, measured by abrasion, bending, indentation, hardness, diametrical crushing. Destructive tests can also be employed to assess the properties of the compacts and to obtain optimum tableting conditions, *e.g.* effect of particle size and punch velocity. Hardness is determined by the mechanical properties of the material not the particle size, although a reduction in particle size can result in stronger compacts, *e.g.* for spray-dried lactose (Takeuchi *et al.*, 1998). The hardness of Avicel 101 was unaffected by particle size (McKenna and McCafferty, 1982). Sebhatu and Aldebarn (1999) also found an increase in tensile strength with a reduction in particle size for lactose.

The effect of punch velocity was investigated by Roberts and Rowe (1985) for a variety of materials including materials that deformed plastically (polymers and maize starch) and those known to consolidate by fragmentation (magnesium and calcium carbonates). For the organic materials, an increase in punch velocity reduced plastic deformation or induced brittleness in the material. No change in yield pressure with increasing punch velocity was observed with the inorganic materials. Yang *et al.* (1997) investigated the effect of punch velocity with a compaction simulator on a solid dosage form and also found increased punch velocities induced brittle behaviour. The tablets laminated at higher punch velocities.

7.2.3.3 Disintegration and dissolution

Usually, as the applied pressure used to prepare a tablet is increased, the disintegration time is increased. For substances that exhibit plastic deformation, with low compression pressures there are large voids in the tablet that result in rapid disintegration while with high compression forces a dense tablet can be made with low porosity. Dense tablets will disintegrate slowly as inter-particle bonding will be greater and there are less void spaces to allow water molecules to penetrate. Dissolution can therefore be controlled in some respects by compaction pressures. If the mechanism of compaction is by fragmentation, then an increase in applied pressure will result in faster dissolution because fragmentation increases the specific surface area.

Yu *et al.* (2004) found that as compression force increased the dissolution of compressed disks was not affected. Dissolution of two drugs, metoprolol, a BCS high solubility drug and furosemide, a BCS low solubility drug was not significantly altered by a change in compression pressure.

7.2.4 Mechanical Properties

The Tableting Indices proposed by Hiestand based on particle bonding and attraction began the investigations into predicting tableting properties from experimental information. Indentation hardness and tensile strength experiments are extensively used to assess the mechanical properties of compacts and are used for the Tableting Indices. Heckel plots can also give essential information about the type of bonding present in a material.

7.2.4.1 Young's Modulus

Hiestand's indentation hardness testing has evolved into a more specific measurement of recovery, elasticity. Elasticity has been assessed as either a fundamental property (Young's modulus), referring to zero porosity (E_0) or as a property of compacted material (% elastic recovery, % radial elastic recovery, and 'apparent' Young's modulus), referring to a particular porosity (Malamataris *et al.*, 1996). Young's modulus is the ratio of stress to strain or the stiffness of the material and is described in equation 7.8.

Young's modulus of elasticity:

$$\text{Young's modulus} = \frac{\text{stress}}{\text{strain}} \quad \text{equation 7.8}$$

For pharmaceutical compacts, Young's modulus is calculated for zero porosity which will be a derived value from experimental data because tablets contain pores. Decompression behaviour which is the relief of elastic strain by fragmentation or plastic deformation will affect the size and shape of the particles and the pores. Extrapolation of the data curve to zero, to give a single value is the most appropriate way of comparing the mechanical properties of many different materials. Previous models have made it difficult to compare data sets if different experimental conditions were used (Heckel analysis). Tableting Indices consider the brittleness of the compact but Young's modulus is able to describe the elastic or plastic nature of the bonding within the compact.

Several methods have been applied to determine the elastic deformation of compacts which involve either compression or bending. Roberts (1991) and Bassam *et al.* (1990) used three-point and four-point bending techniques on specially constructed rectangular wafer compacts to measure the Young's modulus of pharmaceutical powders (excipients). Kachrimanis and Malametris (2004) subjected cylindrical compacts to radial stress and measured the displacement with a linear variable displacement transducer (LVDT). The load was measured together with the displacement and Young's modulus calculated from the data. For four-point beam testing, the sample is supported symmetrically and two loading points on the upper surface of the beam are symmetrical about the mid-point. Roberts (1991) successfully applied the test to a selection of pharmaceutical powders using the Spriggs (1961) equation to extrapolate Young's modulus to zero porosity.

An equation for the calculation of Young's modulus for four-point beam testing was derived by Church (1984) which is described by equation 7.9:

$$E = \frac{F}{\xi_o} \frac{6\alpha}{h^3 b} \left(\frac{l^2}{8} + \frac{\alpha l}{2} + \frac{\alpha^2}{3} \right) \quad \text{equation 7.9}$$

where E is the Young's modulus, F is the total load, b is the width of the beam, l is the length of the beam, α is the distance between beams and ξ_o is the central deflection. The Young's modulus is obtained from the slope of total load *versus* central deflection.

The three-point bend is a simpler and consequently an easier geometry to use than the four-point test (equation 7.10):

$$E = \frac{Fl^3}{4st^3w} \quad \text{equation 7.10}$$

where l is the length of the beam, s is the deflection from the mid-point, t is the thickness and w is the width. It has been used successfully by Roberts (1991) with the Spriggs relationship (equation 7.11) to measure the Young's modulus of a variety of materials.

The Spriggs relationship:

$$E = E_o \exp^{-bP} \quad \text{equation 7.11}$$

where E is the measured modulus at porosity P and b is a constant. E_o is the modulus at zero porosity.

The Spriggs equation (equation 7.11) is an empirical relationship between porosity and E but its applicability is restricted over a narrow, typically low porosity range (Kachrimanis and Malamartaris, 2004). For better prediction of Young's modulus over

a larger porosity range, a semi-empirical power law equation (Phani and Niyogi, 1987) has been proposed (equation 7.12).

Phani and Niyogi power law equation:

$$E = E_0 \left(1 - \frac{P}{P_c} \right)^f \quad \text{equation 7.12}$$

where P_c is the tapped porosity, the critical porosity when E is equal to zero and f is a characteristic exponent of pore structure and particle morphology.

Kachrimanis and Malamatris (2004) calculated the Young's modulus at zero porosity for pregelatinized starch, microcrystalline cellulose and calcium hydrogen phosphate dehydrate using both the Spriggs and Phani and Niyogi relationships. Considerable differences in Young's modulus were obtained, the Spriggs equation giving higher modulus readings at zero porosity.

The equipment used for the measurement of strain has to be very accurate as compacts are usually quite brittle and any elastic relaxation will be very small. Typically a texture analyser with a LVDT and crosshead rate of 1 mm/min allows sufficient measurement of the displacement data calibrated with appropriate loads. Thermal Mechanical Analysis has also been utilised to determine Young's modulus of wafer compacts (Roberts, 1991), uncoated pellets (Bashaiwoldu *et al.*, 2004) and coated pellets (Bashaiwoldu *et al.* 2004b). Atomic Force Microscopy (AFM) has been successfully used to determine the elasticity and surface morphology of polymers (Nie *et al.*, 1996; Lubarski *et al.*, 2004). AFM indentation offers many advantages over conventional techniques as the sample can be very small and the indenter tip can be used to image the indent as well as measure the mechanical properties. It is possible to indent a single crystal, however the crystals required are often much larger than those routinely produced during the drug development process. Nano-indentation techniques can also be used to investigate mechanical properties with even the smallest of samples. The penetration depth of the indenter is recorded as a

function of load and the data is presented as a hysteresis curve, Young's modulus and hardness are derived from the unloading. Hence, mechanical properties can be measured with or without crack formation which is a major advantage over conventional techniques.

7.2.5 The effect of crystallographic forms on tableting behaviour

7.2.5.1. Crystal Habit

The tableting behaviour of drugs can be affected by changes in crystal habit. Habit is the description of the outer appearance of a crystal, only the external shape of a crystal is affected, the internal structure remains the same. The effect of crystal habit on mechanical properties has been well demonstrated. Shell (1963) described crystal habits by measurement of preferred particle orientation that is related to the compression characteristics of the powder. Staniforth *et al.* (1981) used different crystallisation conditions to optimise the compression of mannitol. Garekani *et al.* (1999) compared Heckel plots of the compression for different crystal forms of paracetamol. Polyhedral and plate-like crystals were compressed and found to have different characteristics, the polyhedral crystals were more compressible than the plate-like crystals. Jbilou (1999) produced a directly compressible form of ibuprofen by spherical agglomeration. In both cases the production of small, more spherical particles, improved flowability and compressibility due to enhanced binding connected with spherical particles (Szabo-Revesz *et al.*, 2001).

7.2.5.2 Crystal form

Polymorphism can affect the mechanical properties of a material as a conformational change in the crystal structure will change the modulus of elasticity. Payne *et al.* (1996) investigated the Young's modulus of forms A and B of primidone. The values for primidone A and B were quite close and it would be difficult to differentiate between the two experimentally. However knowledge of the crystal structure and preferred orientation helps distinguish between the two forms. If the crystal structures

of the two polymorphs were different this would be expected to affect the mechanical properties considerably.

Hancock *et al.* (2002) investigated the properties of the crystalline and amorphous forms of an active pharmaceutical ingredient (API). The amorphous sample was found to flow well yet it was found to be less ductile, more brittle and more elastic than its crystalline counterpart. There were no major differences in the tensile strength or the viscoelasticity of the samples. The amorphous material behaviour was glass-like, it shattered on indentation and was noticeably brittle. This was consistent with the measurement of its glass transition at 120 K, so at room temperature existed in a glassy state. Because amorphous material is not arranged in an orderly way, as in a crystal there is no accommodation of plastic flow or bonding therefore brittleness is expected. Within a crystal, hydrogen bonds allow for slip of planes and covalent and ionic bonds allow for the accommodation of pressures involved with compression.

The incorporation of water into the crystal lattice may alter tableting behaviour. Sun and Grant (2004) discovered that the incorporation of water into the crystal lattice of *p*-hydroxybenzoic acid resulted in greater tablet strength. Crystal structures of the anhydrous (HA) and monohydrate (HM) forms of *p*-hydroxybenzoic acid were downloaded from the CSD. HM crystals consist of *p*-hydroxybenzoic acid dimers held together by hydrogen bonds and water molecules which form layers. HM results in a more rigid crystal lattice that lessens fragmentation, therefore the better consolidation is attributed to superior plasticity. The presence of water between layers of dimers maintains separation between the planes and facilitates slip. Bonding strength of HM is enhanced by the presence of water by forming a three-dimensional hydrogen bonding network.

Busignies *et al.* (2004) studied the compaction of different forms of lactose: amorphous lactose, lactose monohydrate (α), anhydrous lactose (α & β). The choice of crystal form was found to dramatically affect the mechanical properties of the material. The monohydrate was found to have poor compression properties; it had a

low modulus and a capping tendency. It is therefore important to consider crystal structures when selecting an appropriate form for tableting.

7.2.6 Molecular structure and the prediction of mechanical properties

It is very difficult to make precise measurements on the small particles present in powders so generally data is gathered from instrumented tablet presses or from testing compacts. This is not an ideal way of assessing a material's mechanical properties as defects and a propensity to lamination contribute to errors. Also as each prepared compact has pores, the extrapolation to zero porosity for each material causes variations according to which model is used (Kachrimanis, 2004). Therefore a theoretical route to predict mechanical properties would be useful to eliminate any experimental measurements.

Payne *et al.* (1996) modelled molecular mechanics providing a route to the second derivatives of the lattice energy, with respect to the lattice parameters and atomic coordinates and hence values of mechanical properties. Therefore the crystal structure must be known beforehand. The Young's modulus is calculated from the stiffness of the crystal using the Reuss or the Voigt methods if the crystal has symmetry. Payne *et al.* (1996) investigated the polymorphic forms of primidone and successfully predicted the mechanical properties from their crystal structures. This was compared to experimental data performed using beam three-point bending and the Spriggs equation fit to the data. Aspirin was expected to be more flexible (lower modulus) than primidone as it exists as dimers arranged in pairs of sheets and the hydrogen bond motif does not confer strength that extends throughout the lattice. Primidone is arranged around a central ribbon of hydrogen bonds with a line of symmetry running down the middle, as seen in flurbiprofen cyclohexylamine (Chapter 6). Primidone has extended hydrogen bonding patterns which confer considerable resistance to forces applied in the planes of the extended motifs. Crystal structures and the number of hydrogen bonds present are therefore important in the rigidity of

the crystal and of the bulk compact for the calculation of Young's modulus. For this technique to be successful, the crystal structure must be determined either by single crystal or powder X-ray crystallography, which is challenging if the molecule is large. If the molecule contains a lot of disorder then the crystal structure will be mean of all the structures present and this may not represent the correct conformations present if the material was compressed.

Roberts *et al.* (1999) used the program Cerius² Mechanical Properties module which uses the atom-atom potential method to calculate the second differential of the lattice energy with respect to lattice parameters and atomic co-ordinates. The program was used to predict the mechanical properties for polymorphs of sulphathizole and carbamazepine. The results were compared to experimental data to investigate the effects of crystal morphology on the elastic moduli. Crystal morphology was found to be an important determinant of elastic moduli as long needle-like crystals prefer to align themselves in the x direction of the beam. If this is considered in the calculation of Young's modulus then the agreement between experimental and prediction is good. This work followed on from Payne *et al.* (1996) and confirmed that it was a robust method for the prediction of mechanical properties from structural information.

7.3 Experimental

7.3.1 Introduction

Much work has been undertaken to characterise pharmaceutical excipients in order to improve our understanding of powder compaction mechanics and to develop testing methods to accurately determine Young's modulus or other hardness measurements. Pharmaceutical excipients such as microcrystalline cellulose, starch and lactose are well characterised now, they are easily compressible and used to improve the compressibility of drug substances. Drug substances have not been extensively studied as they are poorly compressible and difficult to test. Of a list of literature data for Young's modulus of pharmaceutical materials (Roberts, 1991) 4% were drug substances (aspirin and paracetamol) the remaining 96% were excipients.

Roberts (1991) looked at a range of drug substances that ranged from hard and stiff materials to very flexible ones, listed in table 7.1 below.

Table 7.1 Young's modulus of drug substances as determined by three-point beam testing (Roberts, 1991)

Material	E ₀ GPa
Theophylline	12.93
Paracetamol	11.65
Caffeine	8.73
Sulfadiazine	7.70
Aspirin	7.45
Tolbutamide	5.22
Ibuprofen	5.02
Testosterone propionate	3.16
Phenylbutazone	3.33

Roberts (1991) was able to produce enough compacts of sufficient quality to use three-point beam testing on nine drugs. It was shown that the technique was accurate and applicable for use with a wide range of materials with different E values. The compacts prepared were 20 x 7 mm to an approximate thickness of 1 mm, different porosities were produced using different loads. Beams were the preferred geometries because of ease of measuring the dimensions and are ideal for three-point bending. Roberts chose these dimensions to reduce the sample size and to eliminate ejection problems i.e. reduce the area of contact with the die wall and reduce lamination or capping type effects. The beams were expected to be fragile and thin so would require low loads for bending. Highly accurate deflection measurements were collected on a Thermal Mechanical Analyser (TMA) with an accuracy of 0.005 μm . The instrument was capable of applying static and dynamic loads of 0.5 N and ± 0.25 N respectively to an accuracy of 4 nm for the range ± 0.2 mm. Young's modulus for the beams was plotted against porosity for each of the samples and the Spriggs (1961) equation was used as the equation of preference to extrapolate to zero porosity, as it gives the best fit for pharmaceutical materials and therefore is representative as the true modulus of the material.

Roberts and Rowe (1996) used the same apparatus and method to determine the Young's modulus of polymorphs of carbamazepine, sulfathiazole and sulfanilamide. The most stable form has the highest Young's modulus, yield stress, true density and an increased dwell time is required to allow sufficient plastic flow and bond formation to occur. The differences in Young's modulus for each material were attributed to the arrangement of hydrogen bonds in the crystal structure of the polymorphs. The higher Young's modulus for carbamazepine form III (13.19 GPa) was due to a compact crystal structure and the formation of dimers which were held together in chains. Form I consists of a very open structure with sheets of carbamazepine molecules stabilised by hydrogen bonded dimers and van der Waals interactions stacked in layers which results in a very low Young's modulus (3.67 GPa).

There is no literature regarding measuring the Young's modulus of salts and the effect of counterion on the mechanical properties. This would be useful to investigate, as prediction of a material's mechanical properties would aid the formulation scientist select the most appropriate form for ease of tableting. This may only be important if the dose of the material is high (e.g. 500 mg) because the active ingredient occupies a large part of the tablet and its mechanical properties become important. Knowledge and prediction of a materials properties, e.g. mechanical properties and aqueous solubility, from structural information would provide a powerful tool in selecting the best salt form for a formulation.

7.3.2 Experimental Aims

The experiments were designed to use in-house equipment to test the mechanical properties of compacts of drug and salt powders. Tensile strength of the compacts was tested by compression and the Young's modulus of the material determined by either bending or stretching. The effect of the addition of the counterion was assessed for each drug and rules established to improve tableting behaviour.

7.3.3 Experiment 1

7.3.3.1 Equipment

7.3.3.1.1 QTS-25 Texture Analyser from CNS Farnell (UK)

Technical Specification: load range 0-25 kg in 1g increments, load accuracy of 0.5% of full scale, position accuracy 0.02 mm \pm 0.1% of set distance, test speed range of 10-1000 mm/min, speed accuracy better than 0.1% of full scale. The software used was Texture Pro V2.0.

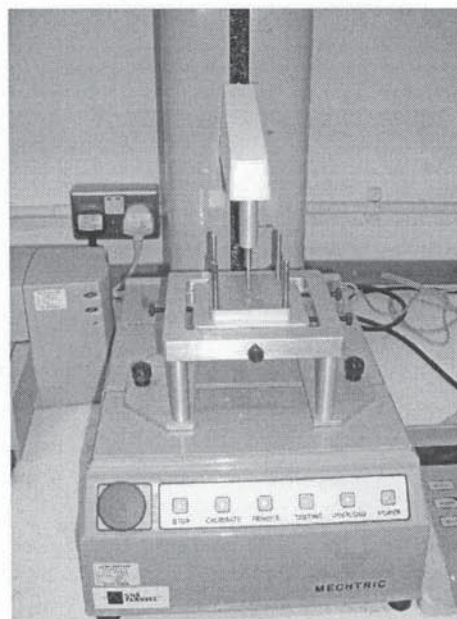


Figure 7.1 The QTS-25 Texture Analyser

The machine has a compression or extension speed of 10 mm per minute or above, and a 4 mm diameter probe with a flat end was used. The machine can be set to compress at a specified speed. It is not possible to perform indentation hardness experiments as a static load cannot be applied for a set time. However, tensile strength can be measured by studying the load required to indent the probe a specified distance (2 mm), which will inevitably result in tablet fracture.

A program was developed that used the lowest speed in order to collect the most data points for accuracy. It was to indent the tablet up to 2 mm and measure the force required for fracture, in grams, against distance. The maximum load detected was collected for each compact.

7.3.3.1.2 Specac Die and Press

A Specac KBr hydraulic press was used to make the compacts with a manual pressure valve which could apply pressures up to 10 tonnes with graduations of 0.2 tonnes. A Specac 13 mm KBr die was used to form the cylindrical tablets. The material to be compressed was placed between the shiny faces of the die and compressed to a maximum of 10 tonnes.

7.3.3.2 Methods

0.02 moles of each salt were made as described in section 3.2. DSC was used to confirm the form and used in subsequent experiments on compression.

The densities of the drug and salt powders together with Avicel PH105[®] were tested using a Gemini Helium Pycnometer. The pycnometer was calibrated before use. Each sample was kept at 40 °C for 12 hours before analysis. Powder was inserted into the sample vial until it was approximately three quarters full and accurately weighed. The sample vial was transferred to the pycnometer and the weight was entered. The pycnometer provided three readings and produced a mean and standard deviation.

250 ± 2 mg of drug was accurately measured on a balance and transferred to the 13 mm die cavity. It was gently tapped down to ensure an even distribution of powder throughout the die cavity. The die was assembled and 8 tonnes of pressure was applied for 2 minutes after which, the tablet was ejected manually. These conditions were the same as required for KBr disk compression for FTIR spectroscopy. The pressure was varied to produce tablets with different porosities, while the weight of powder in the die remained the same.

If the tablet was ejected intact then it was used for tensile strength testing. It was placed in the centre of the QTS platform and the probe was lowered until it met resistance. The force and displacement data was collected by the software as the probe was pressed 2 mm into the tablet.

It was not possible to make intact tablets of etodolac, flurbiprofen and gemfibrozil. These materials are very brittle and laminated on ejection from the die. Different pressures were used (2 – 8 tonnes) and various dwell times (30 secs – 2 mins) were tried to optimise the compression and ejection process. No variable improved the tablets' properties. Gemfibrozil was considered the most brittle material as fracture occurred throughout the tablet on ejection. Etodolac and flurbiprofen experienced lamination of the top faces of the tablet whereas ibuprofen compressed easily into tablets.

To improve the compression of the drug powders Avicel PH105[®] was added to produce whole tablets that were suitable for testing. Gemfibrozil was the most brittle so it was decided to investigate the minimum quantity of Avicel required to produce intact tablets. Once the concentration had been found, it was to be used throughout the experiments as a component of each powder so the Avicel contribution was consistent. The Avicel content in gemfibrozil tablets was either: 1, 5, 7.5, 10, 15, 20, 50 % (w/w). Powders were accurately weighed and mixed using the doubling-up method to improve homogeneity. Tablets were made as described previously.

10% (w/w) Avicel PH105[®] was found to be the lowest concentration that allowed complete gemfibrozil tablets to be ejected from the die. All the tablets were used for tensile strength testing to study the effect of Avicel on tablet hardness. The remaining drug and salt powders were mixed with 10% (w/w) Avicel PH105[®] by the doubling-up method. 300 mg was accurately weighed and inserted in the die, 8 tonnes of pressure was applied for 2 minutes to produce tablets. The tablets were left for 24 h to allow for relaxation then weighed again and the dimensions measured with a micrometer directly before tensile strength testing.

7.3.3.3 Results

The true density measurements for all of the drug and salt powders are listed in table 7.2 and 7.3, below.

Avicel PH105[®] had a mean density of 1.59 ±0.001 g/cm³.

Table 7.2 The true density of etodolac and flurbiprofen amine salts as measured by a helium pycnometer (n=3; mean ±SD)

Etodolac			Flurbiprofen		
	Mean density g/cm ³	SD		Mean density g/cm ³	SD
Drug	1.24	0.001	Drug	1.29	0.001
Butylamine	1.15	0.001	Butylamine	1.16	0.002
Hexylamine	1.10	0.004	Hexylamine	1.12	0.001
Octylamine	1.08	0.013	Octylamine	1.10	0.002
Benzyamine	1.20	0.001	Benzyamine	1.21	0.001
Cyclohexylamine	1.60	0.001	Cyclohexylamine	1.20	0.002
Tert-butylamine	1.15	0.001	Tert-butylamine	1.17	0.002
AMP1	1.24	0.002	AMP1	1.24	0.001
AMP2	1.25	0.001	AMP2	1.32	0.033
Tris	1.24	0.001	Tris	1.32	0.002

The results of tensile strength testing for the drug and salt powders containing 10% Avicel are shown in figures 7.2-7.5.

Table 7.3 The true density of gemfibrozil and ibuprofen amine salts as measured by a helium pycnometer (n=3; mean ±SD)

Gemfibrozil			Ibuprofen		
	Mean density g/cm ³	St Dev		Mean density g/cm ³	St Dev
Drug	1.09	0.001	Drug	1.11	0.001
Butylamine	1.07	0.002	Butylamine	1.07	0.001
Hexylamine	1.05	0.002	Hexylamine	0.98	0.004
Octylamine	1.04	0.001	Octylamine	0.75	0.001
Benzyamine	1.10	0.001	Benzyamine	1.08	0.001
Cyclohexylamine	1.09	0.001	Cyclohexylamine	1.12	0.001
Tert-butylamine	1.04	0.002	Tert-butylamine	1.02	0.001
AMP1	1.12	0.003	AMP1	1.11	0.001
AMP2	1.18	0.001	AMP2	1.15	0.001
Tris	1.20	0.001	Tris	1.2	0.001

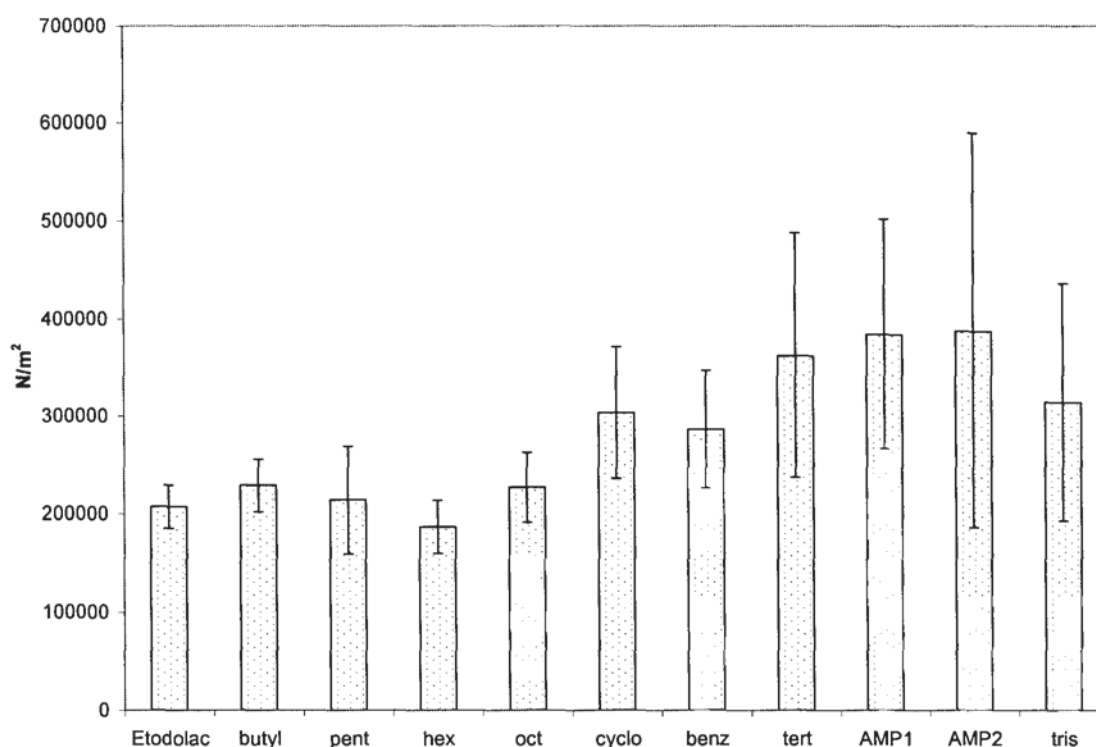


Figure 7.2 Tensile strength of etodolac and its amine salt compacts with 10% Avicel PH 105. n=4; \pm SD.

Etodolac is a brittle material and prone to lamination. The tablets of the amine salts of etodolac are less brittle and so form tablets much more easily, little or no lamination occurs. This could be a function of the material but it could also be due to the presence of Avicel in the tablets. The hardness of the tablets is between $2 \times 10^5 \text{ N/m}^2$ and $4 \times 10^5 \text{ N/m}^2$, although the deviations are large. The fracture of the tablets began with crack formation at the site of the applied pressure, the cracks spread with increasing pressure which resulted in immediate breakage where the tablet split into 2-3 pieces and commonly flew off the sample stage. No obvious relationship was observed between hardness and counterion (figure 7.3). This indicated the mechanism was brittle fracture which implies the bonding within the tablet is strong and there is little elastic bonding.

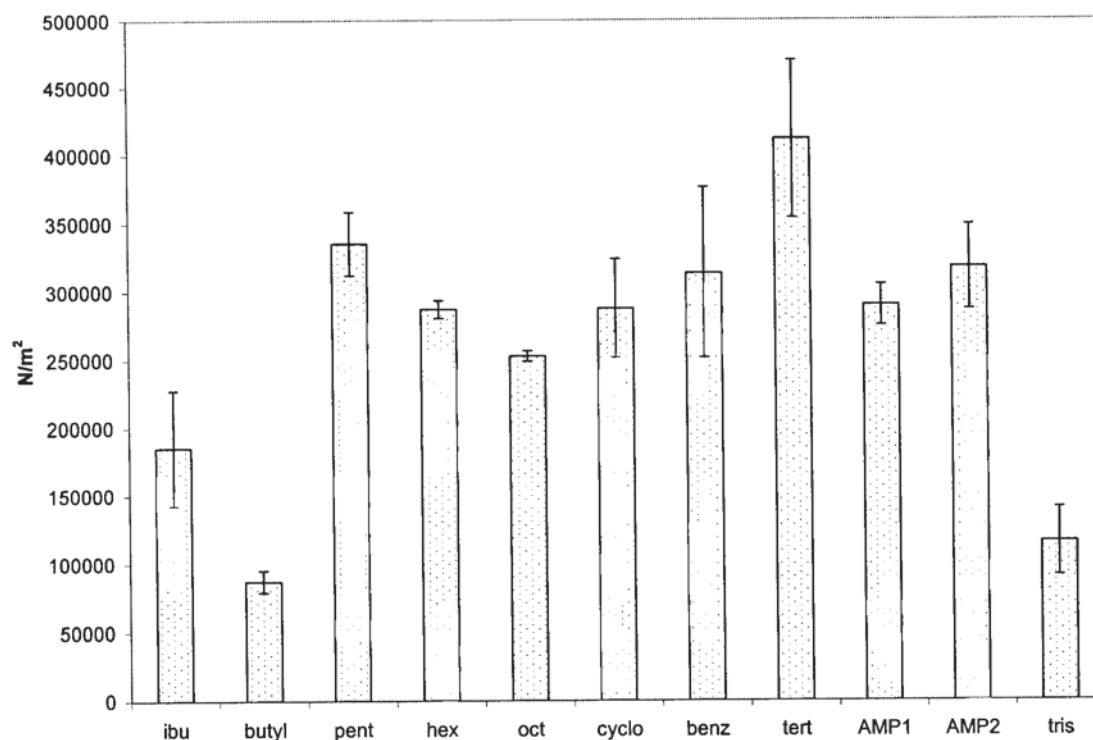


Figure 7.3 Tensile strength of ibuprofen and its amine salts with 10% Avicel PH 105. n=4; \pm SD.

Ibuprofen tablets are easily compressible and have a hardness range approximately the same as etodolac and its salts (figure 7.3). The butylamine and tris salts are the only powders with a reduced hardness value compared to the parent molecule. The other salts have increased hardness compared to the parent, with a hardness range of $2.5 \times 10^5 \text{ N/m}^2$ to $4 \times 10^5 \text{ N/m}^2$. The fracture mechanism of ibuprofen salts is quite different than etodolac, although the hardness values are quite similar the tablets appeared 'soft'. As the pressure increased the probe was indented into the tablet and crushed the tablet only in the area of contact. The result was a tablet with a hole in it, rather like a polo mint. This could indicate that the bonding in the tablet was characterised by plastic deformation or that the inter-particle bonding/attraction was quite weak overall. The bonding of the area in contact with the probe was strong but the bonding did not extend to areas other than that in contact with the probe.

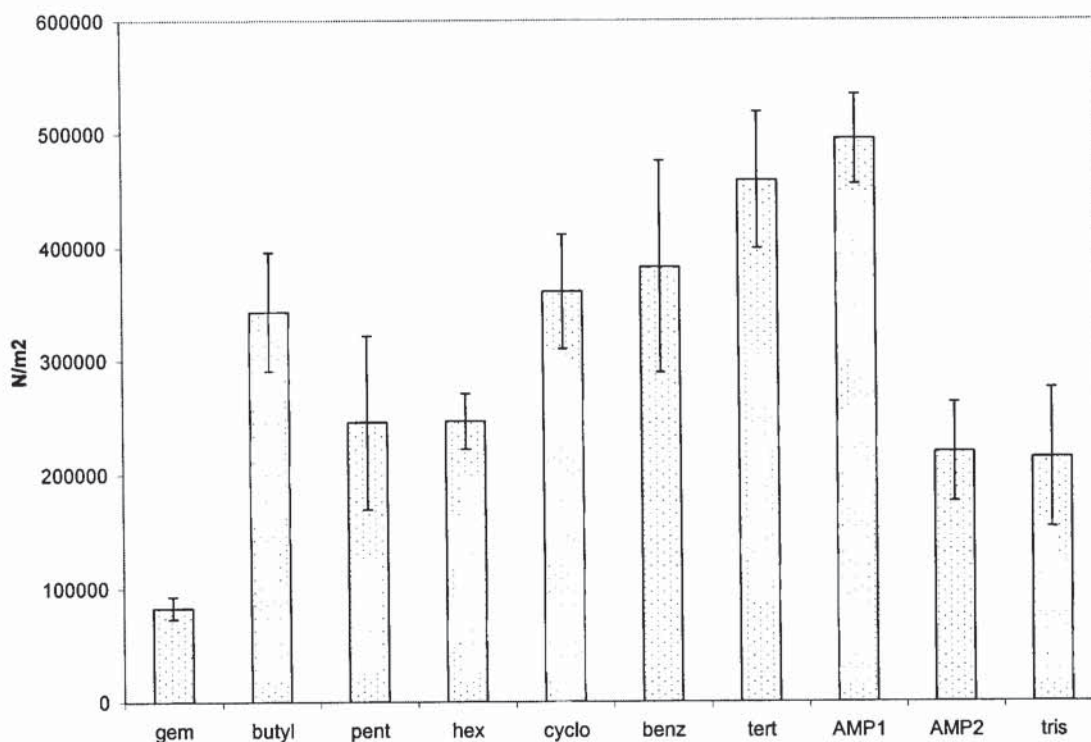


Figure 7.4 Tensile strength of gemfibrozil and its amine salts with 10% Avicel PH 105. n=4; \pm SD

Gemfibrozil is characterised by brittle bonding hence lamination is a common cause of tablet failure. It has a hardness of $1 \times 10^5 \text{ N/m}^2$, a low value which indicates the bonding within the tablet is weak and easily broken. The tablets of the amine salts of gemfibrozil are much harder than the parent molecule, with a hardness range of $2 \times 10^5 \text{ N/m}^2$ to $5 \times 10^5 \text{ N/m}^2$ (figure 7.4).

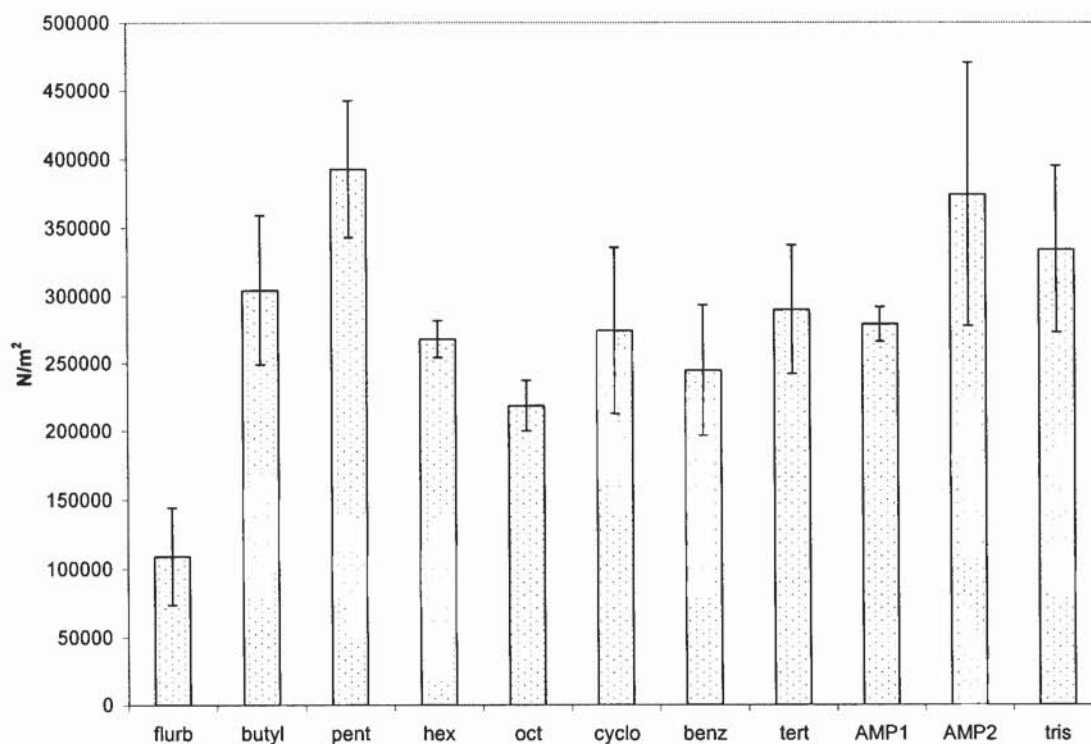


Figure 7.5 Tensile strength of flurbiprofen and its amine salts with 10% Avicel PH 105. n=4; \pm SD

The tensile strength of flurbiprofen salts is between 2×10^5 N/m² and 4×10^5 N/m² (figure 7.7). The salt compacts are much harder than the drug itself. Flurbiprofen is a very brittle material which is liable to extensive lamination on compression. The deviations in the results are large and no obvious relationship was observed between tensile strength and salt.

7.3.3.4 Experimental Limitations

It was not possible to produce tablets with different porosities using this method of tablet compression. Therefore the results of the experiments must be viewed with caution because the results are not comparable. This was the main reason for abandoning the QTS experiments using cylindrical tablets. Also, the use of round tablets increases the propensity of lamination, which was a common defect in the samples. The experiments also contained Avicel, to improve compressibility. This is not ideal as it is not possible to attribute mechanical properties to the drug or salt. As

the materials to be tested are prone to brittle behaviour, it was essential to develop an alternative die that minimised lamination.

On a more practical level, the texture analyser (QTS-25) was very difficult to use as the software crashed continuously, losing any data collected at the time. This was unsatisfactory as each experiment was destructive. The number of samples required for a valid experiment increased and there were small amounts of material available at any one time because the salts were manufactured in-house and using small batches.

7.3.4 Experiment 2

7.3.4.1 Equipment

7.3.4.1. Variable depth die (120 x 7 mm)



Figure 7.6 Roberts 20 x 7 mm four piece stainless steel die held together with screws.

The exact die that Roberts (1991) (figure 7.6) used in his thesis to make wafers for three-point beam testing was inherited from Bradford University. The whole die was made of stainless steel. It consisted of a four part die wall chamber that was put together before use and held together with screws, tightened with an Allen key. The inside faces of the walls were shiny, buffed steel, the die faces were of two parts: one face had a 2 mm elevation and the other a 20 mm elevation. Roberts used this die

successfully to make wafers of many excipients and drug substances. A range of porosities was obtained using different loads while maintaining the same volume.

An attempt was made to make wafers of Avicel PH105 at different porosities using the Roberts die and reproducing the experiments detailed in the thesis to obtain a range of porosities. It was found that the die was unsuitable in its current format for our purposes as it was not possible to produce wafers of different porosities. It was very cumbersome and time-consuming putting the die together to make the wafer and taking it apart to release the wafer. It was decided to approach a local toolmaker to design a more convenient die that would release the wafer easily and maintain the die cavity at a set volume so different porosities could be achieved.

7.3.4.1.2 Bespoke die (20 x 7 x 1 mm)

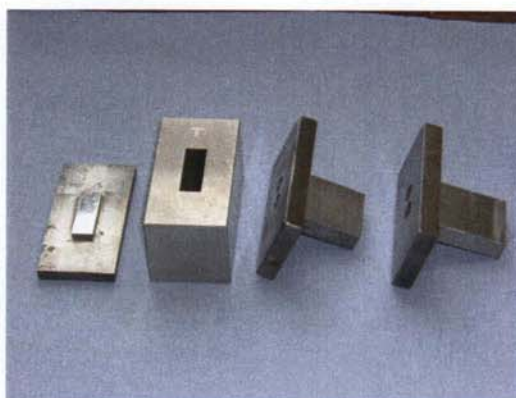


Figure 7.7 New punch and die set. One piece hardened steel die of 20 x 7 mm made to fit existing punches with 1 mm gap and longer punch (far right) for ejection.

G & F Press Tools LTD, Brierley Hill, Birmingham constructed a hardened steel die that was made of a single piece of steel (die walls) with a 20 x 7 mm hole in the centre. The bottom (die face) piece was from Roberts die and made to fit the new equipment. The longer shaft was fashioned so that there was a 1 mm gap when the die was complete and each face of the die was of shiny steel. An extra punch was made with a longer shaft to aid the ejection of the wafer from the die (figure 7.7). The maximum tolerance of the die was 4 tonnes; this was used as the standard pressure for wafer manufacture.

7.3.4.1.3 Hounsfield Universal Tester S Series H10KS-0393

The Hounsfield S Series was supplied by Tinius Olsen Ltd (Surrey, UK) with Q-Mat 2.18 software including Test Generator, Testzone and File examination. A 5 N load cell was selected for maximum accuracy as wafers were expected to be fragile. The 5 N load cell was calibrated by Tinius Olsen prior to use and operated with an accuracy of $\pm 0.5\%$. Other load cells of above 5 N were available but were too inaccurate to measure small loads. The crosshead was able to move at jog speeds of 0.001 to 1000 mm/min, with an extension accuracy of ± 0.01 mm and a speed accuracy of $\pm 0.05\%$ of the set speed (figure 7.8).



Figure 7.8 The Hounsfield S Series Universal Testing Machine

The software program calculates Young's modulus from the linear part of the force against displacement graph; a standard linear regression analysis is applied. The dimensions of the sample are required fields for the accurate determination of Young's modulus (see section 7.2.5)

7.3.4.1.4 Stretching apparatus

The wafer was held between two clamps while the crosshead moved upwards at a rate of 1 mm/min (figure 7.9). It was important to determine whether there was any slippage of the wafer occurring as the clamps were moving apart as this would invalidate the results. Also, the wafers were not expected to be elastic along the length of the wafer so the displacement measurements would be small and accurate measurement of small displacements was essential. Insertion of the wafer between the clamps required considerable dexterity and care not to break the wafer during this process. This was a particular problem for high porosity wafers which were very fragile.



Figure 7.9 Avicel PH105 wafer held between upper and lower clamps for elongation

Analysis of the data for Avicel PH105 and ibuprofen wafers of different porosities revealed no difference in calculated Young's modulus values. The modulus was expected to increase as porosity reduced, as described in the literature (Roberts, 1991). This is because the strength of the tablet is expected to increase as it becomes more dense as the number of bonding sites increases therefore improving the overall strength. This did not occur in the samples tested and the calculated Young's modulus values were attributed to movement of the clamps and the friction

of the sample against the clamps, not elongation of the wafer. The Young's modulus readings were between 9 and 11 for all the materials tested, these included Avicel PH105[®], ibuprofen and its benzylamine salt and, flurbiprofen cyclohexylamine.

This method was deemed unsuitable for the accurate measurement of Young's modulus for wafers of pharmaceutical powders. The elongation method or stretching of an inherently brittle sample cannot be used to assess the mechanical properties of a material using the current apparatus.

7.3.4.1.5 Bespoke miniature three-point bend apparatus

Roberts (1991) validated the use of a three-point bend apparatus for the accurate determination of Young's modulus of wafers of pharmaceutical powders. Tinius Olsen were approached to design a miniature three-point bend jig for testing a typical 20 x 7 mm wafer on the Hounsfield S-series. Tinius Olsen were to manufacture a jig to house the wafer and they had to ensure the machine could collect enough accurate information to be able to calculate Young's modulus. The 5 N load cell was calibrated so that loads of 0 to 5 N could be measured accurately. The cross head was not able to measure the movement of the wafer so a Linear Displacement Unit (LDU) was required. It was calibrated to accurately measure movement up to 1 mm, the thickness of the wafer. Figure 7.10 shows the three-point bend jig with an Avicel wafer, the LDU is connected to the back of the machine and there are adjusting screws either side that allow for the testing of different sized wafers. The black shaft is located in the centre of the supports and is attached to the load cell.

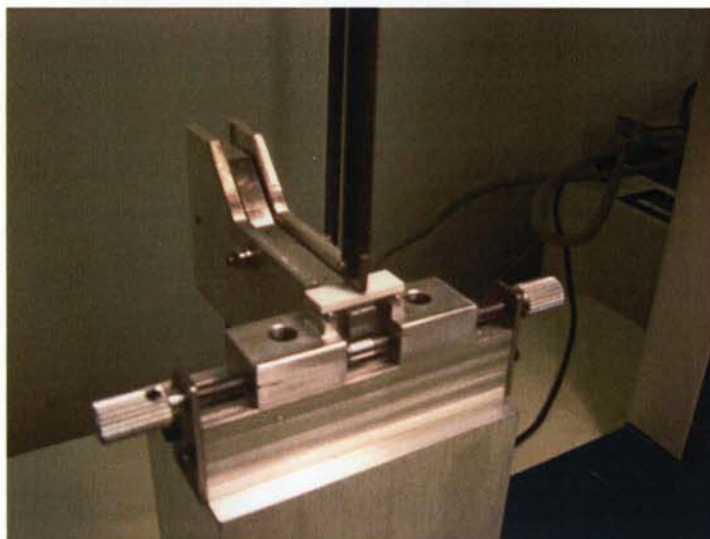


Figure 7.10 Bespoke miniature three point bend jig

7.3.4 Three-point bend determination of Young's modulus

7.3.4.1 Method

The powders were sieved through 750 μm to ensure there were no large particles present. At least six wafers were made of each powder at four different porosities; if more material was available additional wafers were made. An initial mass of 100 mg was accurately weighed and placed in the die; the powder was tapped to evenly distribute the powder in the die. 4 tonnes of pressure was applied for 30 seconds. If the tablet was not intact on ejection the mass was increased by 10 mg each time to obtain the minimum mass required to form a compact; this was the most porous sample. Once the minimum mass was found, the mass was increased by approximately 15 mg each time to obtain wafers with a range of porosity values. Porosity was a ratio of theoretical volume (calculated from true density and die volume dimensions) against measured volume.

A suspension of 1% (w/v) magnesium stearate in ethanol was painted onto the punch faces and walls and left to dry if necessary to provide lubrication before use.

The wafer was ejected from the die and any broken or fractured wafers were discarded. The intact wafers were kept for 24 h to allow for stress relaxation. The dimensions of the wafer were measured with a Linear Tools electronic digital calliper

with an accuracy of $\pm 0.02\text{mm}$ directly before the experiment. The depth of the wafer was measured at four points and the average was used for the Young's modulus calculation (see equation 7.8).

7.3.4.2 Results

Typical force against displacement graphs for Avicel PH105[®] and ibuprofen are displayed in figures 7.11 and 7.12, respectively. The Young's modulus is determined by the gradient of the curve (equation 7.4). The gradient for the Avicel graph is steeper than for ibuprofen and so is expected to have a higher modulus than ibuprofen. The graphs are characterised by a short lag period before the parameters can be measured (figure 7.11), if the probe has to move to contact the wafer or a "burst" (figure 7.12) if the probe is in slight contact with the wafer before the experiment. A linear region is then observed which represents the elastic behaviour of the compact. A third region in which there is breakage of the wafer, usually into two pieces (figure 7.11) characterised by a sharp peak at the maximal force, or plastic deformation of the wafer (irreversible bending) where the curve tails off (figure 7.12). This final section can be used to identify the type of bonding present in the compact; if the wafer is prone to breakage then brittle bonding is the main mechanism yet if it bends rather than breaks, plastic flow is present.

Avicel has ideal mechanical properties, it has a relatively high E_0 (10-12 GPa) which indicates it is resistant to deformation and it is a ductile material which exhibits plastic flow because it compresses well. Resistance to deformation is desirable because it will resist tablet handling processes *e.g.* coating processes, storage and transportation conditions. Plastic flow is the preferred method of compression because brittle material is hard but it can be very fragile and elastic material is prone to breaking apart under decompression.

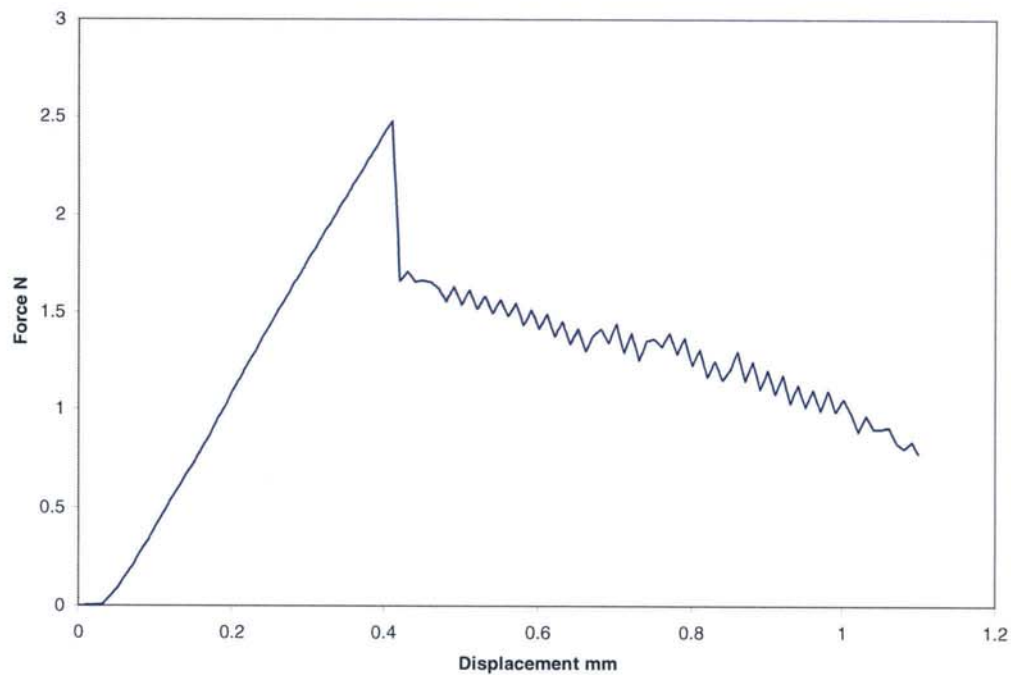


Figure 7.11 Typical force against displacement data for an avicel PH105 wafer of porosity 0.67, using QMAT Testzone for Hounsfield S series.

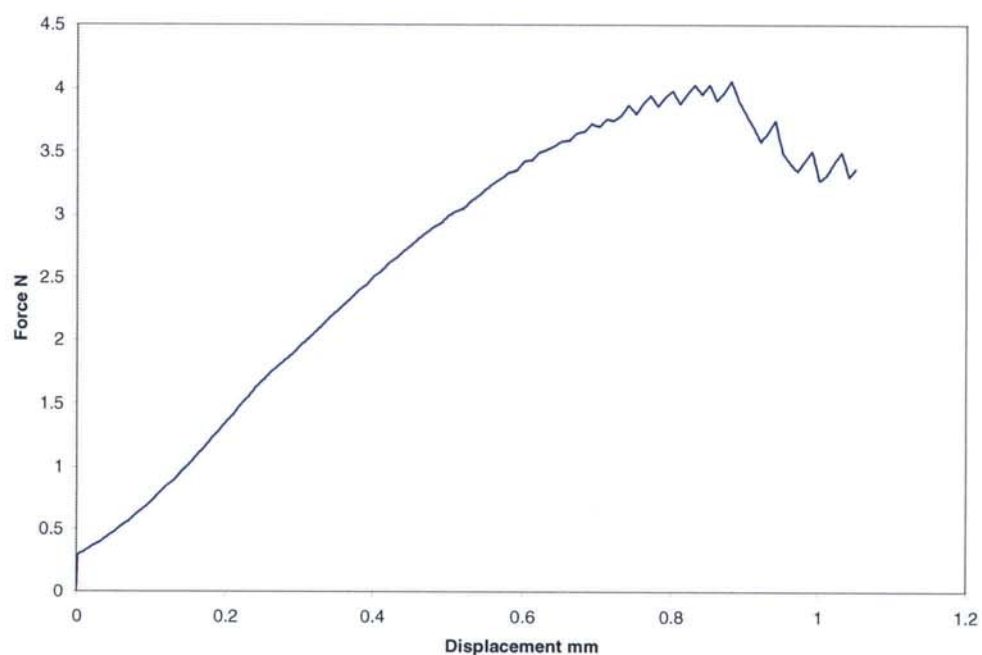


Figure 7.12 Typical force against displacement data curve of an ibuprofen wafer of porosity 0.08, using QMAT Testzone for Hounsfield S series.

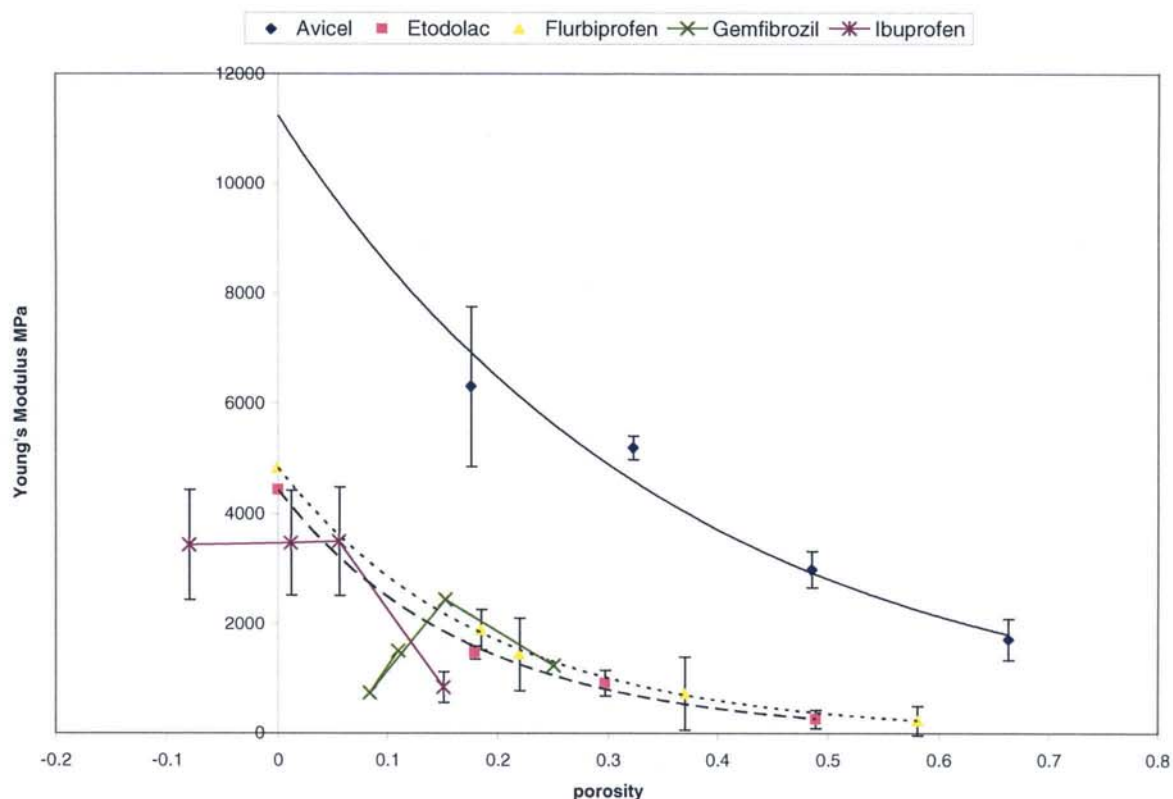


Figure 7.13 Young's Modulus versus porosity for Avicel PH105[®], etodolac, flurbiprofen, ibuprofen and gemfibrozil. n=6; \pm SD.

Figure 7.13, shows the extrapolated Young's modulus data for Avicel PH105[®] and the drugs etodolac, gemfibrozil and flurbiprofen using the Spriggs exponential relationship. It was possible to create wafers of a typical porosity range of 0.2 to 0.6; this is a wide range and provides confidence in the extrapolated Young's modulus value. It is interesting to note that Roberts (1991) was able to look at a much narrower porosity range, e.g. 0.10 to 0.35 for microcrystalline cellulose, 0.07 to 0.17 for paracetamol and 0.02 to 0.20 for theophylline. The larger porosity range achieved in this experiment was attributed to the superior punch and die set.

Etodolac and flurbiprofen have similar modulus values at zero porosity (4.43 and 4.84 GPa respectively) and as powders they behave in very similar ways; they are both prone to lamination at low porosities, they compress well between 0.2 and 0.6 porosity, they are soft, chalky materials at high porosities. In each case the standard deviations are low and the regression fit is high ($r^2 = 0.994$ and $r^2 = 0.999$).

respectively) which may indicate reproducible bonding or sliding of planes during compression. It is interesting to observe that the line does not pass through all data points for Avicel PH105® and the standard deviations are much larger than for the drugs. Avicel has a much higher modulus than etodolac and flurbiprofen (11.23 GPa) and is therefore much more robust and is not prone to lamination. The bonding within the pure Avicel compact is strong and rigid.

Gemfibrozil compacts at lower porosities suffered from crack formation, resulting in weak compacts. The wafers below 0.15 porosity had compromised strength due to a section of the upper surface becoming separated from the main wafer after ejection from the die. This left a porosity range of 0.25 to 0.15 that consistently produced flawless compacts. This was deemed to small a range for an accurate determination of Young's modulus. Gemfibrozil bonding was confirmed to be very brittle and no modulus was determined.

Negative porosity was observed with ibuprofen wafers (figure 7.14) it is therefore not meaningful to extrapolate to zero porosity. There were four data points collected over a wide range of initial masses, these resulted in a relatively small porosity range (-0.1 to 0.15). The powder was easily compressed into wafers with no lamination observed and a slight adherence to the die faces which was addressed by lubrication with magnesium stearate. The strength of the wafers is compromised at porosities below 0.05 where the Young's modulus is consistently 3.5 GPa and the compacts were observed to bend on application of force. Negative porosity has been observed by Roberts (1991) with compacts of stearic acid and phenylbutazone. He speculated that the errors could be due to the inaccurate measurement of true density, or conversion of polymorphic forms. In that study, the first scenario was concluded to be the main source of error as only small fractions of the material were converted to a different form. Comparison of true density measurements of ibuprofen from Roberts and experimental data (table 7.3) concur that the density is 1.11g/cm³. Polymorphic changes were investigated by DSC using compacts with porosity below 0.5. There may be evidence of preferred orientation which would explain negative porosity and would affect the modulus. At low porosities (high densities), for the material to compress, the molecules may be encouraged to orientate themselves in the same

direction to achieve a stable conformation. For the modulus to be truly representative of the material, the particles should be randomly oriented to eliminate the effect of the modulus of a particular orientation (see section 7.3.4.4 and 7.3.4.5).

Roberts (1991) was able to produce wafers for ibuprofen of a range of porosity (0.04 to 0.18) which compares well with the data collected here, although the range is possibly too low for an accurate determination of Young's modulus. It is clear from the gemfibrozil and ibuprofen data that low porosity compacts (below 0.10) have undesirable characteristics, the added pressure and the increased density compound the propensity for failure, either by lamination if the bonding is brittle and strong or lack of strength due to plastic flow and flexible. Avicel PH105[®] has a E_0 of 11.23 and a r^2 of 0.975.

Table 7.4 Young's modulus of all the materials as determined by three-point bend testing for etodolac and gemfibrozil salt compacts. Modulus values could not be obtained for all materials, indicated by a (-).

Etodolac			Gemfibrozil		
Material	E_0 GPa	Correlation coefficient	Material	E_0 GPa	Correlation coefficient
Drug	4.43	0.994	Drug	-	
E butylamine	4.41	0.942	G butylamine	3.61	0.966
E hexylamine	-		G hexylamine	-	
E octylamine	3.32	0.918	G octylamine	-	
E tert-butylamine	2.88	0.911	G tert-butylamine	2.45	0.508
E AMP1	5.35	0.997	G AMP1	-	
E AMP2	8.16	0.954	G AMP2	7.95	0.924
E tris	-		G tris	18.81	0.993
E cyclohexylamine	5.20	0.998	G cyclohexylamine	5.10	0.870
E benzylamine	4.78	0.996	G benzylamine	-	

Table 7.5 Young's modulus of all the materials as determined by three-point bend testing for flurbiprofen and ibuprofen salt compacts. Modulus values could not be obtained for all materials, indicated by a (-).

Flurbiprofen			Ibuprofen		
Material	E ₀ GPa	Correlation coefficient	Material	E ₀ GPa	Correlation coefficient
Drug	4.84	0.999	Drug	-	
F butylamine	3.62	0.992	I butylamine	2.65	0.123
F hexylamine	7.29	0.984	I hexylamine	-	
F octylamine	-		I octylamine	-	
F tert-butylamine	5.95	0.892	I tert-butylamine	4.40	0.980
F AMP1	-		I AMP1	11.11	0.995
F AMP2	9.97	0.990	I AMP2	7.16	0.998
F tris	4.69	1	I tris	-	
F cyclohexylamine	10.54	0.896	I cyclohexylamine	5.80	0.489
F benzylamine	5.23	0.824	I benzylamine	2.82	0.725

7.3.4.3 Discussion of the mechanical properties of the salts; the effect of the counterion

7.3.4.3.1 Etodolac and salts

The etodolac salts were prone to lamination at low porosities (below 0.1) and the powders had a propensity to stick (bond) to the die walls, making ejection difficult, however lubrication with magnesium stearate overcame the problem. Overall, the compression of the salt powders was much easier than the parent drug; the resulting wafers were more robust and less prone to lamination. They were therefore much easier to work with, however this is not reflected in the Young's modulus results derived from the data in table 7.4. The modulus information helps understand what type of bonding is present in the compact and how robust the material is. A high modulus material has very rigid bonding whereas a low modulus tells us the bonding is more elastic (or plastic), easily deformed or more dynamic.

Etodolac butylamine, hexylamine and octylamine salts (figure 7.14) have chain lengths C4, C6 and C8 respectively. The modulus is reduced as chain length increases, characterised by a reduction in gradient as chain length increases. Also there is a sharp reduction in modulus as the porosity is reduced below 0.15, observed in chain lengths 6 and 8, hexylamine and octylamine salts. The E_0 of the parent drug etodolac is approximately the same as that of the butylamine salt (4.43 and 4.41 GPa respectively), the addition of a small counterion of a flexible nature confers little change in modulus but reduces the propensity for brittle behaviour. As the chain length increases, the degree of flexibility within the counterion increases and this reduces the E_0 which is an indication that the bonding within the compact is more flexible. Deformation increases as chain length extends, at low porosities there may be evidence of preferred orientation which would reduce the modulus, see section 7.3.4.5.

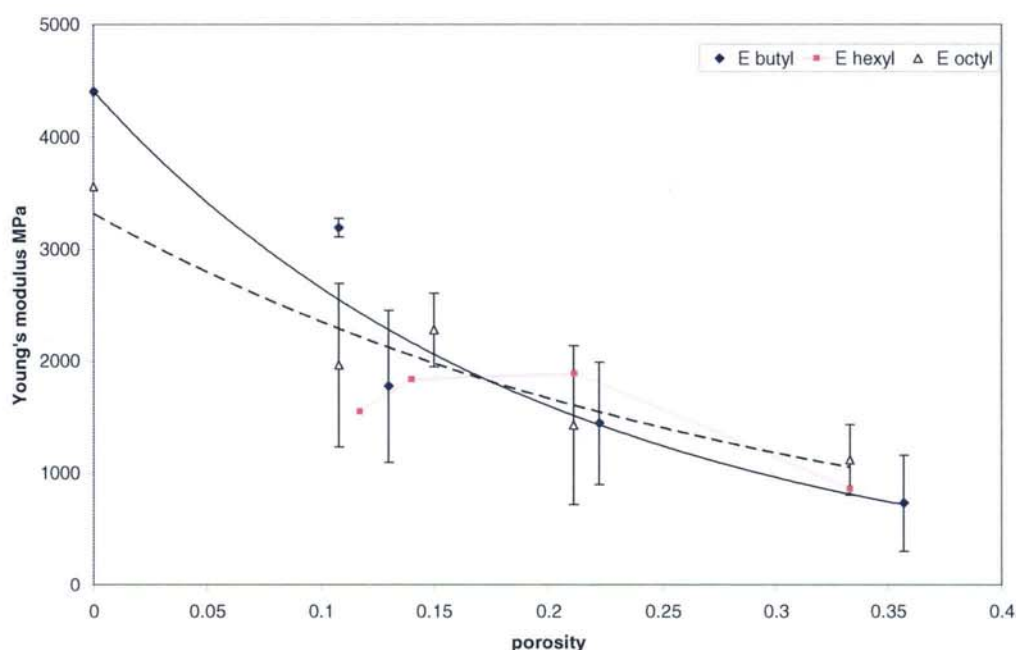


Figure 7.14 Young's modulus *versus* porosity for etodolac butylamine, etodolac hexylamine and etodolac octylamine, $n=6$; mean \pm SD.

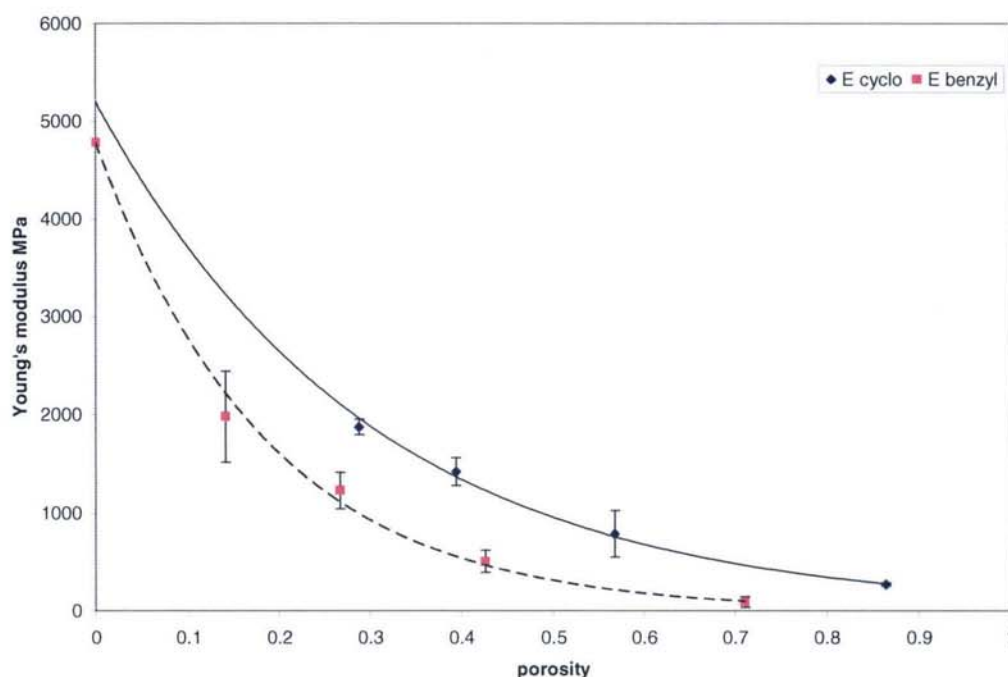


Figure 7.15 Young's modulus versus porosity for etodolac cyclohexylamine and etodolac benzylamine, $n=6$; mean \pm SD.

The inclusion of a cyclical counterion increased the E_0 above the parent drug (figure 7.15), etodolac cyclohexylamine has a greater E_0 (5.20 GPa) than the parent (4.43 GPa). Addition of a saturated cyclic molecule, benzylamine, had little affect on the modulus of the parent drug (4.78 GPa). Both materials are easily compressible and have a high r^2 value, each data point lies on the line of best fit and the deviations are quite small. The achieved porosity range was wide so there is confidence that the extrapolation to zero porosity for this data set is reliable.

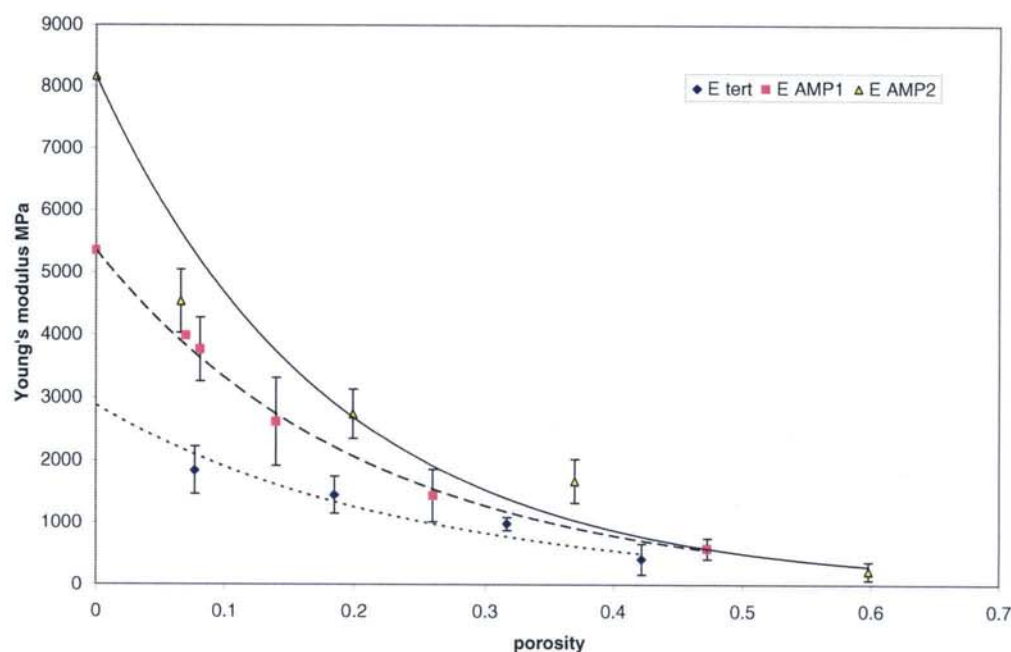


Figure 7.16 Young's modulus *versus* porosity for etodolac tert-butylamine, etodolac AMP1, etodolac AMP2, n=6; mean \pm SD.

The hydrophilic series is based on the tert-butylamine counterion. As hydroxyl groups are added, the counterion becomes more bulky and hydrophilic (AMP1, AMP2 and tris). As the number of hydroxyl groups increases the possible sites for additional hydrogen bonding increases, which would be expected to result in stronger inter-particle bonding and more robust compacts. From the data displayed in figure 7.16, as hydroxyl groups are added to the basic tert-butylamine structure, the E_0 of the compacts increases. Addition of tert-butylamine counterion reduced the E_0 compared to the parent, although powder was easily compressible, the bonding had become more flexible. Etodolac AMP1 and AMP2 have a higher E_0 than the parent; these materials were easily compressible and produced very robust compacts. Etodolac AMP1 has a additional hydrogen bond due to the hydroxyl group as compared to the parent, this may confer added rigidity and strength to the crystal lattice resulting in plastic deformation upon compression. The addition of two hydroxyl groups to the counterion (AMP2) improves the mechanical properties because the increase in hydrogen bonds increases the strength of the crystal lattice and improves plastic deformation. Etodolac tris compacts could not be tested as they laminated on

ejection, at all porosity values. The presence of the tris counterion resulted in strong bonding within planes but weak bonding between planes, leading to lamination.

7.3.4.3.2 Gemfibrozil and salts

Gemfibrozil itself is a brittle material and has poor compression characteristics; the addition of an amine counterion makes the powder quite sticky. The stickiness is characterised by bonding of the powder to the faces of the punch which makes ejection of a complete compact with no surface defects difficult. Lubrication with magnesium stearate was required to minimise this effect. Formation of compacts of gemfibrozil octylamine, AMP1 and benzylamine was not possible because of material sticking to the punch faces and lubrication was not effective at eliminating this. Stickiness reduced as the porosity decreased but the compacts became waxy in appearance and behaviour. The compacts would be expected to have very low modulus values if they could be prepared successfully.

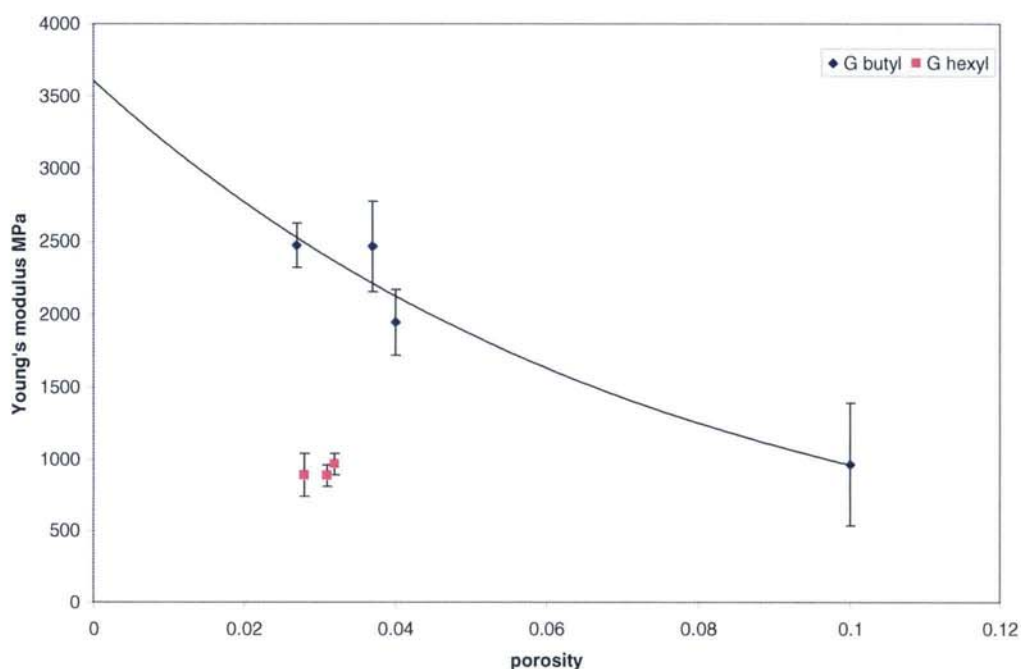


Figure 7.17 Young's modulus versus porosity for gemfibrozil butylamine and gemfibrozil hexylamine, $n=6$; mean \pm SD.

The mechanical properties of gemfibrozil were improved by the addition of the butylamine counterion although it has a relatively low modulus of 3.61 GPa (figure 7.17) compared to Avicel. The porosity range that was possible with this material was very narrow (0.04 to 0.1) therefore the accuracy of the E_0 determination could be questioned. Lamination effects were reduced by the addition of a small amine counterion and the bonding within the wafer has become more flexible. Addition of a longer chained amine (6C) results in compacts within a smaller porosity range than the butylamine salt, the powder also suffered from stickiness to the punch faces which was overcome using large volumes (over 200 mg). It was also noted that the waxy appearance to the compacts increased and the modulus fell as porosity reduced.

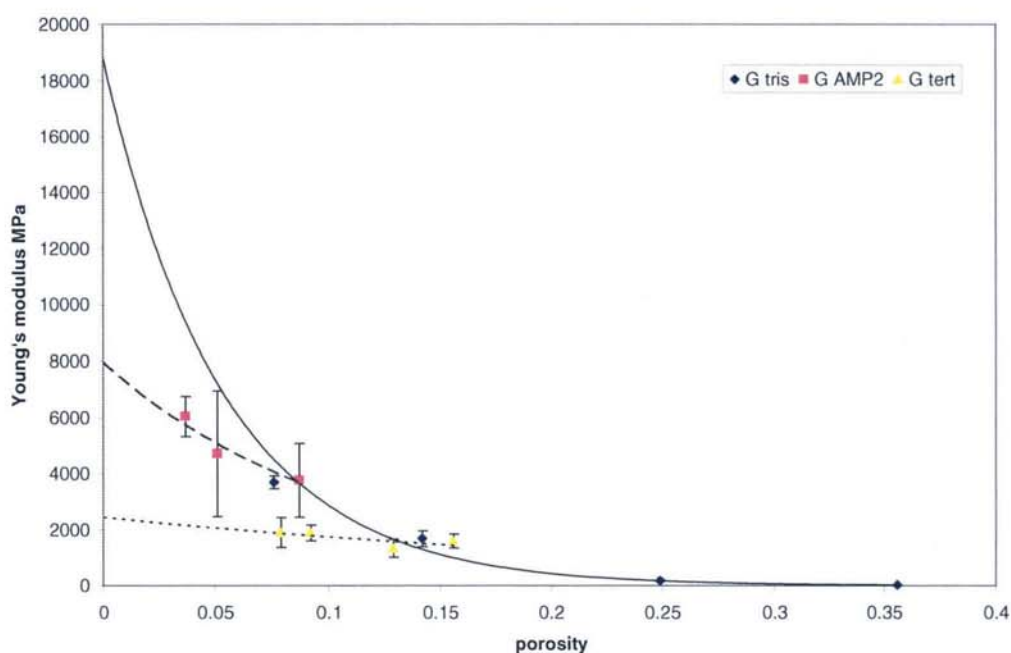


Figure 7.18 Young's modulus *versus* porosity for gemfibrozil tert-butylamine, gemfibrozil AMP2 and gemfibrozil tris, $n=6$; mean \pm SD.

The tert-butylamine, AMP2 and tris salts were easily compressed but, gemfibrozil AMP1 was too sticky for compression into wafers even when lubricated with magnesium stearate. Gemfibrozil tert-butylamine has a relatively low E_0 (2.45 GPa) representing low inherent strength and flexible bonding (figure 7.18). When one hydroxyl group is added the compact is not usable, but when two hydroxyl groups are

added the mechanical properties improve, stickiness is eliminated and the E_0 rises to 7.95 GPa. If three hydroxyl groups are used E_0 increases to 18.81 GPa. This is an uncharacteristic result as tris salts usually have poor compression properties (table 7.4) and the tris salts of ibuprofen and etodolac could not be tested. Knowledge of the crystal structure of the salts would aid understanding of the mechanism of compression of these molecules and help explain why some powders compress more easily than others. Some work has been done to suggest that the presence of water could aid compression by lubricating between layers of drug molecules, improving the slip of planes. Sun and Grant (2003) investigated the crystal structure of p-hydroxybenzoic acid anhydrate and monohydrate by collecting powder X-ray diffraction patterns (PXRD) of compacts. When the monohydrate form is compressed, zig zag layers of molecules mechanically interlock, inhibiting slip and reducing plasticity. However the water molecules in the monohydrate separate the layers of zig zag hydrogen-bonded molecules. This allows for easier slip between layers and provides greater plasticity. The overall effect is for the interparticulate bonding area to increase and the water molecules form a three dimensional hydrogen-bonding network. The presence of one hydroxyl group in the current series does not provide any additional sites for hydrogen bonding, hence its poorly compressible characteristics. The increased strength of the AMP2 compacts may be therefore due to an increased interparticulate bonding area and the formation of additional hydrogen bonds that increase the plasticity of the bonding. The crystal structure of gemfibrozil AMP2 suggests that hydrogen bonding in three dimensions facilitates compression to form strong compacts (section 6.3.3). Gemfibrozil tris has all three hydroxyl groups available for hydrogen bonding as it compresses, increasing the plasticity and strength of the bonding within the tablet. Gemfibrozil tris has the highest modulus value which may be because the hydrogen bonds are present in the x- and y-directions allowing slip of planes in the z-direction which confers extra strength upon compression (section 6.3.3).

7.3.4.3.3 Flurbiprofen and salts

The salts of flurbiprofen are the most compressible of all the drug groups, with only flurbiprofen AMP1 prone to severe lamination which resulted in no suitable wafers

that could be tested. Flurbiprofen octylamine was very sticky and compacts could only be made filling the die with over 200 mg of powder. Above this mass, the compacts were very waxy in appearance and were suspected to be very weak (low E_0). Flurbiprofen butylamine (figure 7.19) was easily compressible but had a lower E_0 than the parent. As the chain length increased, the propensity for the powder to stick to the punch faces increased. The hexylamine salt was also sticky and the compacts had a waxy appearance. There is evidence that at lower porosities (below 0.12) the strength of the compact reduces as observed in etodolac hexylamine. Addition of a saturated cyclic counterion (cyclohexylamine) to flurbiprofen resulted in a material with a high modulus (E_0 10.54 GPa), good compression properties resulting in strong, robust compacts. The E_0 of Avicel PH105 is 11.23 GPa which is close to the derived E_0 of flurbiprofen cyclohexylamine, which suggests it is behaving as a ductile material which is an improvement over the mechanical properties of the drug itself. The addition of an unsaturated cyclic counterion to flurbiprofen results in no real difference in Young's modulus (5.23 and 4.84 GPa for benzylamine salt and flurbiprofen respectively). There is no improvement in mechanical properties when the benzylamine salt form is made (table 7.5). Young's modulus versus porosity plots for flurbiprofen cyclohexylamine and benzylamine are displayed as a scatter graph to observe the distribution of the points about the regression analysis (figure 7.20).

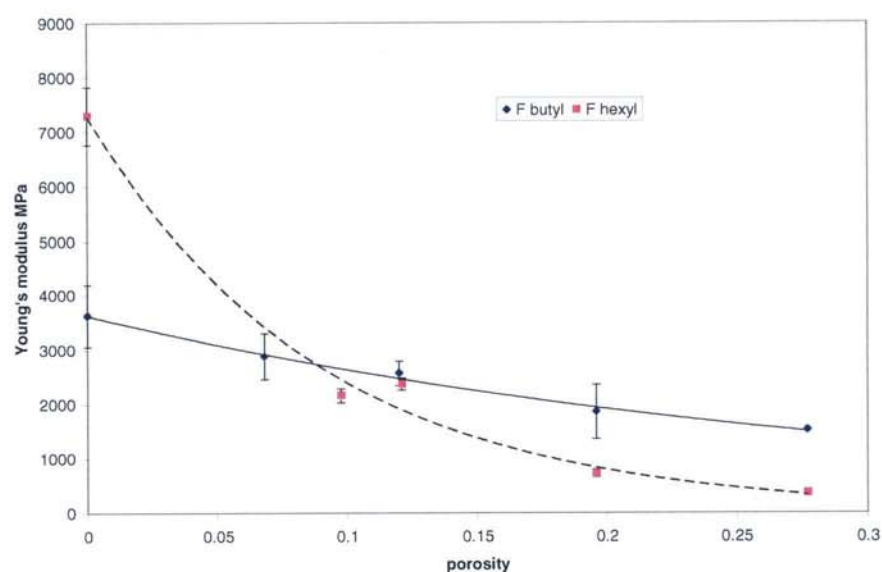


Figure 7.19 Young's modulus *versus* porosity for flurbiprofen butylamine and flurbiprofen hexylamine, $n=6$; mean \pm SD.

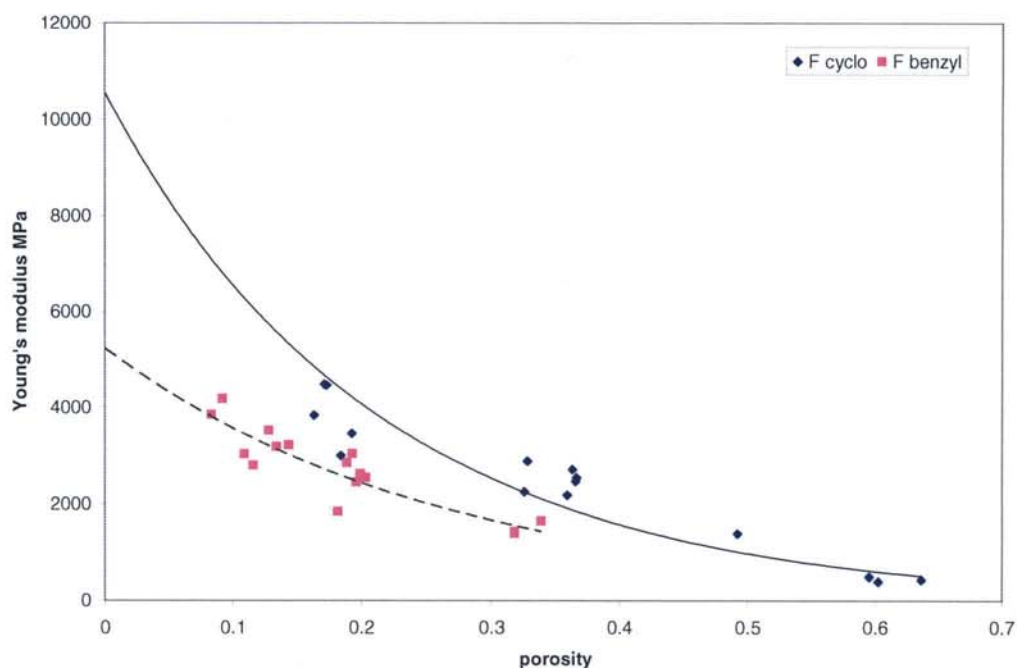


Figure 7.20 Young's modulus *versus* porosity for flurbiprofen cyclohexylamine and flurbiprofen benzylamine.

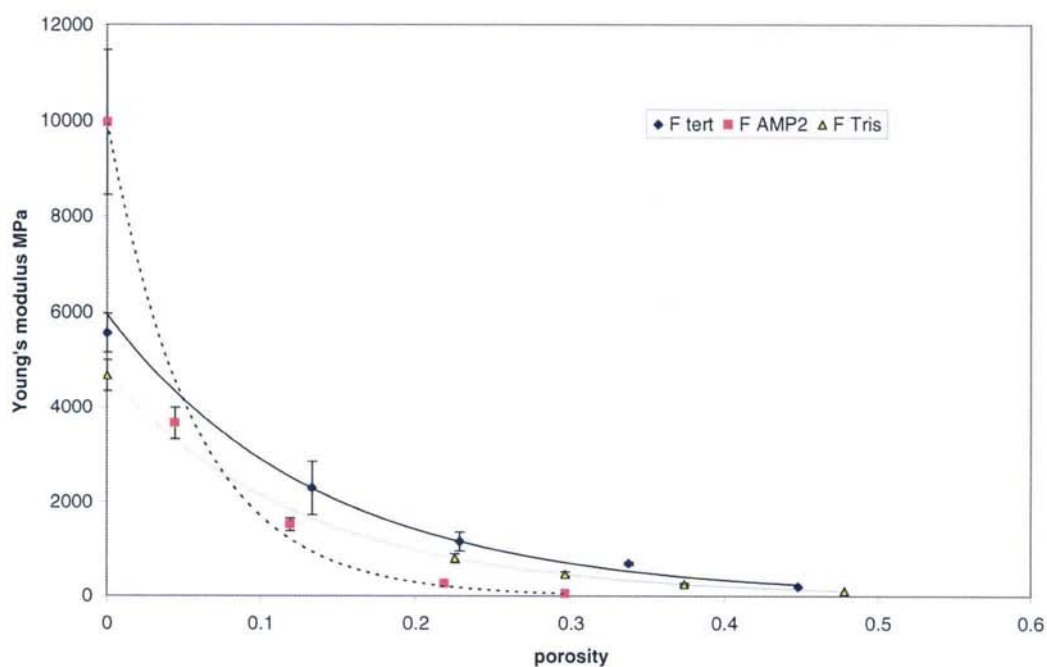


Figure 7.21 Young's modulus *versus* porosity for flurbiprofen tert-butylamine, flurbiprofen AMP2 and flurbiprofen tris, $n=6$; mean \pm SD.

The E_0 of flurbiprofen tert-butylamine was derived to be 5.95 GPa (figure 7.21), which is a slight improvement compared to the drug itself (4.84 GPa) and the tert-butylamine salt form is less likely to laminate at low porosities. As a hydroxyl group is added to the parent (AMP1), the resulting salt form was very difficult to compress and prone to lamination. Lamination was the main source of failure of the prepared compacts at lower porosities and, at high porosities the compacts were extremely fragile and disintegrated on handling. The addition of two hydroxyl groups (AMP2) to flurbiprofen results in a material with a high E_0 value of 9.97 GPa, which is similar to Avicel. The AMP2 salt form has good compression characteristics with strong, tough bonding throughout the compact. This result confirms that the presence of two hydroxyl groups and a greater number of hydrogen bonds increases the plasticity and strength of the bonding within the compact. Compacts were made with flurbiprofen tris and the E_0 was found to be 4.69 GPa, which is no improvement over the drug itself. The tris counterion does not improve compression properties of flurbiprofen probably due to the hydroxyl groups being inhibited from forming extra bonding sites by preventing slip of planes.

7.3.4.3.4 Ibuprofen and its salts

Ibuprofen was easily compressed into wafers, although negative porosities were observed at high die volumes (200 mg) and low porosities, affected the strength and the type of bonding in the compact. At low porosities the wafers exhibited bending and plastic flow due to flexible bonding within the compact. Negative porosity was not observed for any of the salts.

The addition of a butylamine counterion to ibuprofen resulted in very fragile compacts that were difficult to make and test. The E_0 was derived to be 2.65 GPa although the individual readings were quite varied and the regression fit was very poor (0.123), therefore it is difficult to have confidence in this value. Ibuprofen butylamine powder became slightly sticky on compression; this was overcome by lubrication with magnesium stearate. As the chain length of the counterion is increased the propensity for stickiness to the punch faces increased and it was impossible to produce compacts of the hexylamine and octylamine salts.

Ibuprofen cyclohexylamine was easily compressible and produced strong, robust compacts. The E_0 was extrapolated to 5.80 GPa, although the regression fit for this data is low (0.489) it is over a small porosity range (0.1 to 0.2) and unfortunately it was not possible to extend this as at high porosities the wafers disintegrated due to poor inter-particle bonding. Between porosities 0.1 to 0.2 the wafers that were produced were easily compressible and strong. The addition of benzylamine to ibuprofen did not improve the mechanical properties of the drug; the E_0 was derived as 2.82 GPa which is an indication of a weak compact with flexible inter-particle bonding.

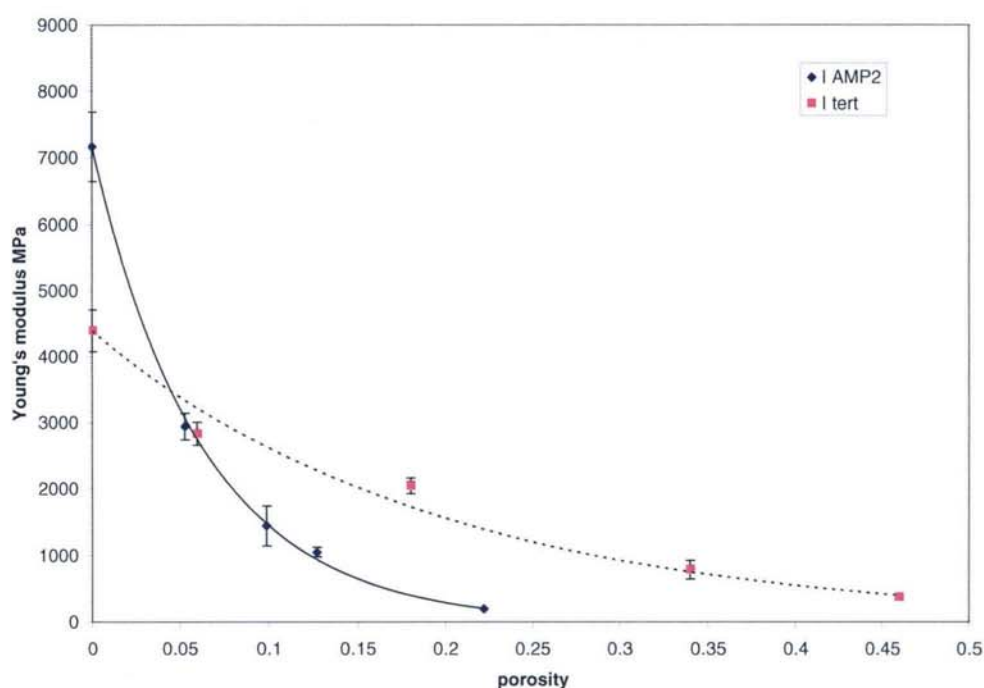


Figure 7.22 Young's modulus *versus* porosity for ibuprofen tert-butylamine and ibuprofen AMP2, n=6; mean \pm SD.

It was not possible to form compacts with ibuprofen tris as on application of pressure the powder did not bond together. Upon ejection from the die the material had formed clumps of denser powder that disintegrated as the punch was removed. Ibuprofen tert-butylamine was easily compressible and gave reasonably strong compacts with E_0 of 4.40 GPa (figure 7.23). The compression properties were improved with the addition of a hydroxyl group (AMP1) which was a ductile material with a high E_0 of

11.11. Ibuprofen AMP1 is characterised by a reduction in modulus at low porosities (below 0.09) which is shown in figure 7.23, the points where the modulus has reduced due to deformation of the bonding and the flexibility of the bonding increasing. Ibuprofen AMP2 also has good compression characteristics producing strong, robust compacts with an E_0 of 7.16 GPa (figure 7.22) indicating the presence of two hydroxyl groups is the optimum hydrogen bonding arrangement within the compact. The addition of three hydroxyl groups (tris) to the counterion reduces the compressibility of ibuprofen because on ejection each compact disintegrated, regardless of porosity.

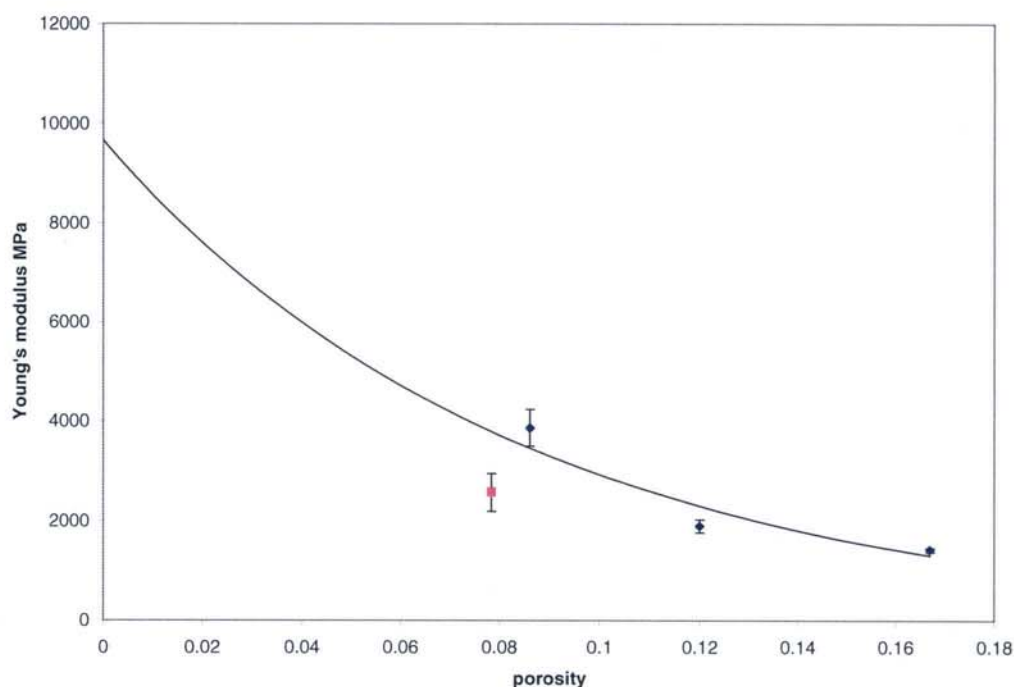


Figure 7.23 Young's modulus versus porosity for ibuprofen AMP1 demonstrating eliminated points (pink), $n=6$; mean \pm SD.

7.3.4.4 DSC

DSC was performed on the compacts of negative porosity to investigate whether possible polymorphic changes or other form changes due to the compression process had occurred. Compacts were prepared with 175 mg and 215 mg ibuprofen,

which produces a compact with negative porosity. Etodolac compacts were also prepared, of mass 115 mg and 155 mg, which produce negative porosity. Three samples were prepared of each compact. The compacts were lightly ground to a powder and approximately 3 mg was accurately weighed and placed in DSC sample pans and analysed according to the method described in section 3.4.2.3. The results (figure 7.24 and 7.25) indicate that no form change was observed in either ibuprofen or etodolac. There is no substantial change in onset temperature between samples and ΔH in J/g to indicate a form change.

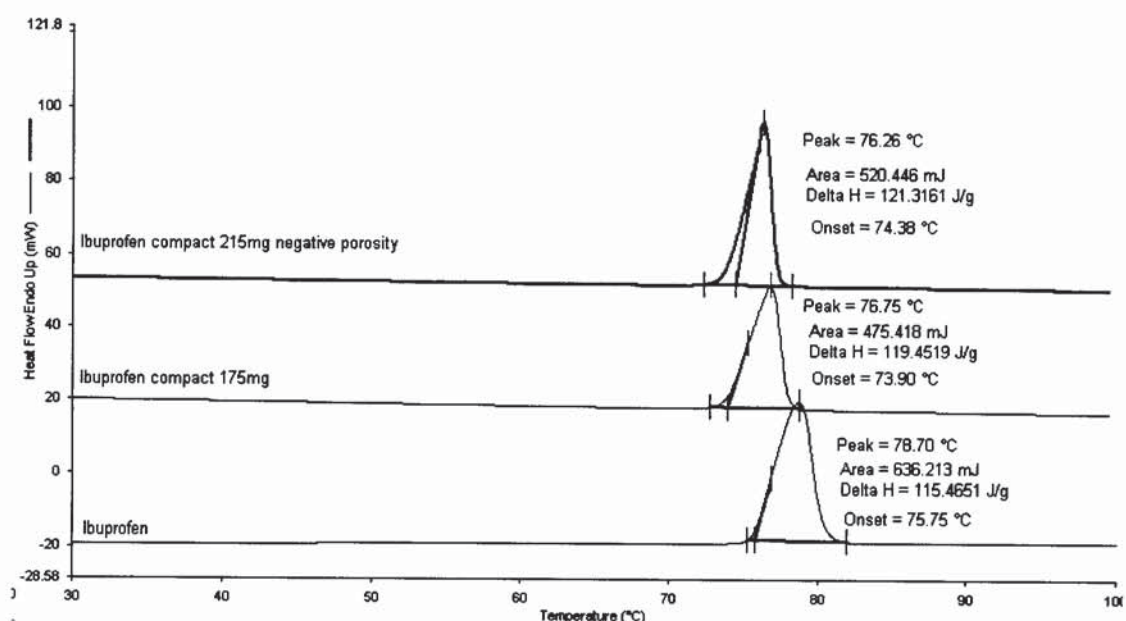


Figure 7.25 The DSC traces of Ibuprofen and its compacts with a scan rate of 10 °C/min

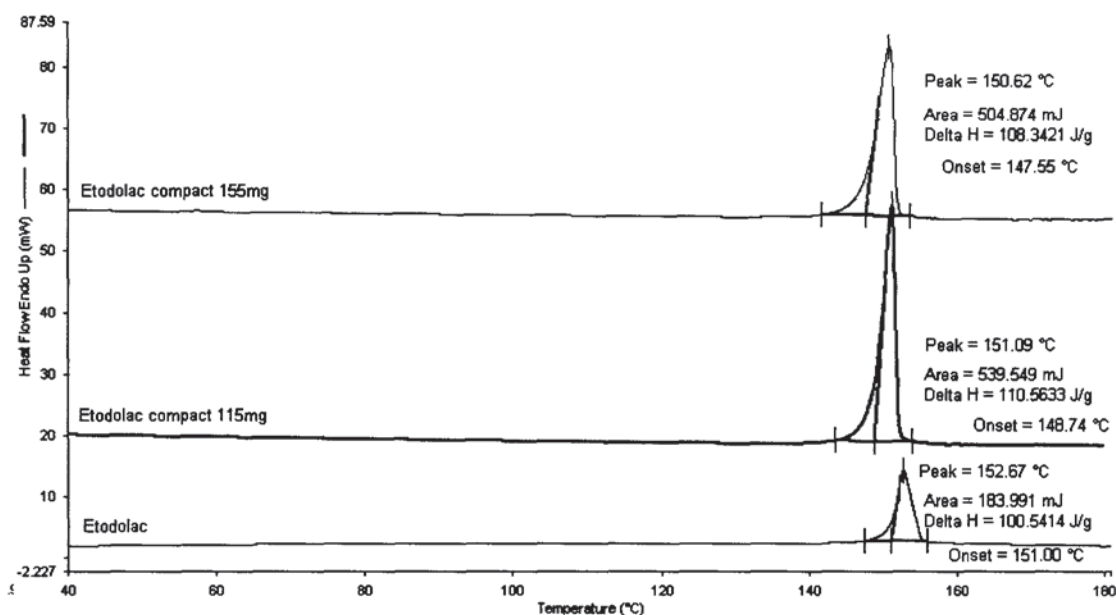


Figure 7.25 The DSC traces of etodolac and its compacts with a scan rate of 10 °C/min

7.3.4.5 X-ray

The crushed compacts of ibuprofen were used from section 7.3.4.4. Particles were used of at least 0.4 μm and were viewed under a light microscope with 8x magnification before mounting on a capillary and fixed on a goniometer head. The sample was attached to the Enraf-Nonius CAD4 diffractometer (as described in section 6.2.2). Polaroid 52 film of dimensions 9 x 12 cm was fixed at right angles to the X-ray beam using a Polaroid film holder. The X-ray beam was directed on the compressed sample for approximately 10 minutes using the pola command and repeated three times for each sample. Etodolac compacts could not be tested due to equipment failure and time constraints.

The results from this experiment show that ibuprofen molecules in compacts of positive porosity (figure 7.26) are randomly oriented. The photographic picture is characterised by rings surrounding the centre of the beam (central white area). Ibuprofen molecules in compacts of negative porosity (figure 7.27) show preferred orientation. The photograph does not show the characteristic rings of random orientation and the photograph has white dots surrounding the beam. These results confirm that negative porosity is due to the particles within the compact re-orienting and the consequences of this are weaker compacts.

**PAGE
NUMBERING
AS ORIGINAL**

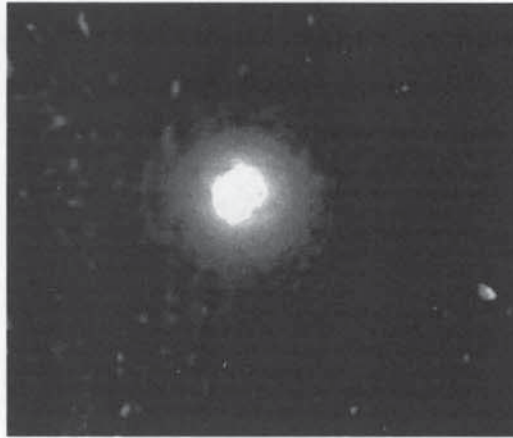


Figure 7.26 X-ray image of ibuprofen compact of positive porosity, the rings indicate random orientation



Figure 7.27 X-ray image of ibuprofen compact of negative porosity, the white dots indicate preferred orientation

7.3.4.6 Conclusions

In general the compressibility of the drugs was improved by salt formation. The E_0 was unaffected by the addition of a butylamine, benzylamine or tert-butylamine counterion. The compressibility was improved with the addition of a cyclohexylamine or AMP2 counterion characterised by an increased E_0 value compared to the drug itself. The mechanism for improvement is not known but it may be due to the arrangement of the crystal structure.

With an increase in chain length, the mechanical properties of the material deteriorate, resulting in a lowering of E_0 . As the chain length is increased there is an increase in flexibility of the counterion, this reduces the strength of the bonding within the compact and makes the bonding more flexible.

Addition of a hydroxyl group to the counterion (AMP1) results in unpredictable mechanical properties, for ibuprofen and etodolac, the compressibility was slightly improved but for gemfibrozil and flurbiprofen crack formation and lamination was severe. Two hydroxyl groups on the counterion conferred improved mechanical properties, improving the E_0 of the parent drug and it forms strong, robust compacts. Tris salts, with three hydroxyl groups resulted in poor compression properties, apart from gemfibrozil tris which formed a very strong compact. The mechanism of the improvement in compression properties for these molecules is not known, it is likely that it can be related to the crystal structure.

Salt selection to optimise mechanical properties:

- Small counterion (C4) should be selected in preference to longer chains
- A saturated cyclic counterion should be selected in preference to an unsaturated one.
- Inclusion of two hydroxyl groups optimises performance for the carboxylic acid drugs studied.

Chapter 8 Concluding remarks and further work

The use of amine counterions in salt formation of poorly soluble acidic drugs has produced materials with different properties compared to the parent molecule. Solubility and dissolution in water has been improved by salt formation which will alter the bioavailability and may reduce the time taken for a clinical effect. The compressibility of the parent drugs has been improved. It was possible to form compacts of the salt powders with higher Young's modulus values than the parent drug, indicating the salt powders were stronger and more resistant to deformation than the parent drug.

Salt formation with butylamine produced the greatest enhancement in solubility for the homologous chain amine series (chapter 3). This was concluded to be due to the ability of the small butylamine counterion to alter the pH of the microenvironment of the dissolving particle to a favourable pH that drives dissolution. As the chain length increases, the lipophilicity of the counterion inhibits dissolution. The mechanical properties of the butylamine salts are not a significant improvement compared to the parent drug. The Young's modulus does not improve but the salts are less brittle than the parent drug (chapter 7). As chain length increases the compression properties of the salt deteriorate. The unit cell has been determined for gemfibrozil butylamine, pentylamine and hexylamine salts. There is no change in the hydrogen bonding arrangement in each crystal structure. As the length of the chain increases, the additional degrees of freedom in the counterion which increase the amount of disorder and this leads to a more dense unit cell. The added hydrophobic nature of the counterion and the dense unit cell may contribute to reduced solubility.

Cyclical counterions do not increase the solubility of the parent drugs significantly, compared to the other counterions (chapter 3). Benzene and cyclohexyl rings are very stable, rigid structures and are large, compared to butylamine. The additional molecular weight does not significantly improve the solubility of the parent drug. The unit cell of flurbiprofen cyclohexylamine has been found by single crystal X-ray crystallography and it reveals that the molecules are arranged in a ladder-like

structure with the benzene rings of flurbiprofen and the rings of cyclohexylamine associating either side of the carboxylic acid function (chapter 6). There are hydrophobic domains on either side of the ionic bond between acid and base; it may be more difficult for water to penetrate this type of structure, explaining the salts poor solubility.

With addition of hydroxyl groups to the tert-butylamine counterion an increase in solubility of the salts is seen. The addition of one hydroxyl group (AMP1) results in an improvement in solubility, compared to the parent drug. The addition of two hydroxyl groups (AMP2) further improves the solubility and confers surfactant-like activity to etodolac and ibuprofen AMP2 salts. Tris, however, does not further increase the solubility of the parent drug. The unit cell has been found for gemfibrozil tris and it shows that all the hydroxyl groups on the counterion are involved in hydrogen bonding in the salt crystal. This confers excellent strength characteristics when the powder is compressed resulting in a strong compact that is resistant to deformation. The AMP2 salts consistently compress well producing strong tablets, the crystal structures of these salt would help explain the results.

The homologous alkyl series and the tert, AMP1, AMP2 and tris salts of the gemfibrozil series were the only samples that were analysed by XRPD to obtain the unit cell information. It was not possible to test any other powders for inclusion in this thesis. Examination of the crystal structures of the other salts would reveal valuable information regarding hydrogen bond arrangement and formation and the arrangement of molecules in the unit cell. This information coupled with solubility and mechanical data collected in this thesis would help explain the properties observed in the experiments.

The solubility data could not be fully explained by the physicochemical analysis that was performed on each drug and its salts. Examination of the heat of solution for each drug and salt may provide important information, together with the unit cell data to help explain the solubility data gathered in this thesis.

The common-ion effect is an important event that cannot currently be predicted and that can affect a drug's solubility in buffers. The solubility information may not be comparable if the molar concentrations of each ion are not quoted. Future work would concentrate on identifying the molecules susceptible to the common-ion effect and assessing the consequences in-vivo, if any. Modelling the common-ion effect may help in prediction of solubilities in electrolyte solutions of known concentrations.

Negative porosity has been attributed to orientation effects within the compact. The effect of orientation must always be considered when compressing powders, its effect may not only be negative porosity but it may explain other problems encountered when compressing powders. Examination of the consequences of preferred orientation would be a valuable area of future research.

To summarise, solubility can be enhanced by salt formation with small compact amine counterion (butylamine). Using this type of counterion may improve the compression properties of the parent drug but will not have a significant effect on E_0 . Cyclical amine counterions, both saturated and unsaturated should not be used as potential salt formers as they do not improve solubility or E_0 significantly. Salt formation with a hydroxyl-containing amine counterion improves solubility. Counterions containing two hydroxyl groups show greatest improvement in solubility and compressibility of the parent drug, consistently increasing E_0 . Amine counterions that are small, compact and contain hydrophilic hydrogen bonding moieties (*e.g.* hydroxyl groups) have the potential to be used as future salt formers. Future research may investigate whether these rules can be applied to other drugs and other amine series.

Appendix A

A.1 Structures of materials

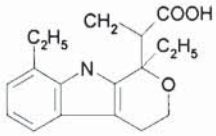
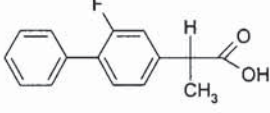
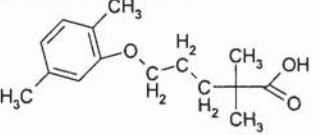
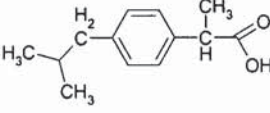
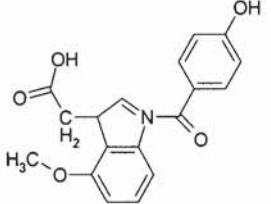
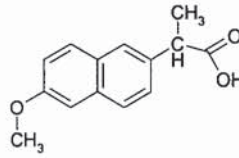
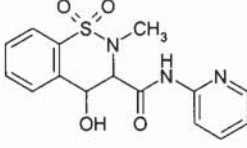
 <p>Etodolac</p>	 <p>Flurbiprofen</p>	 <p>Gemfibrozil</p>
 <p>Ibuprofen</p>	 <p>Indomethacin</p>	 <p>Naproxen</p>
	 <p>Piroxicam</p>	

Figure A-0-1 Chemical structures of the NSAIDs studied

Appendix B

B.1 Gemfibrozil HPLC assay

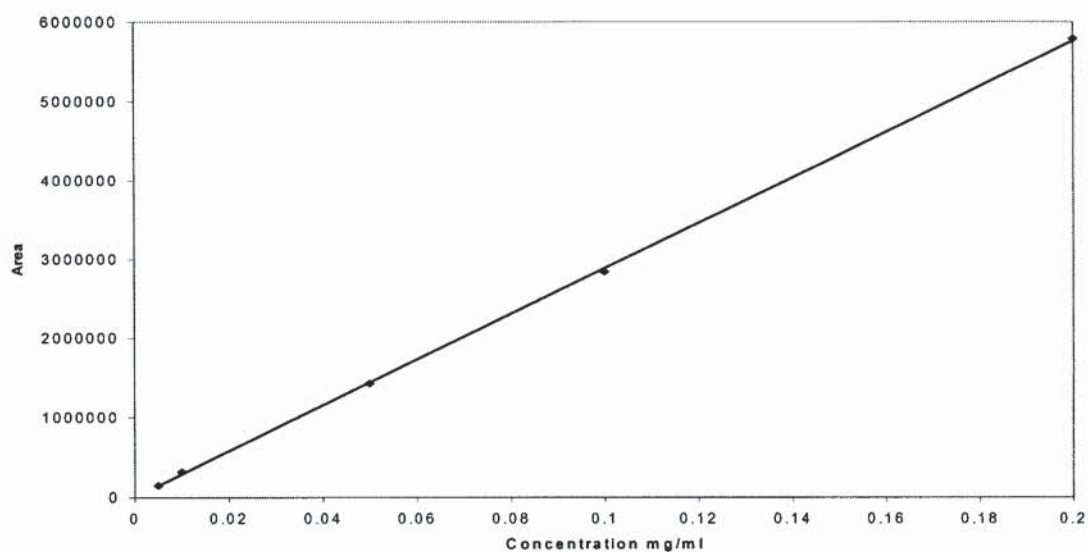


Figure B.1 Typical calibration graph for gemfibrozil assay by HPLC. $R^2 = 0.9998$ and $Y = 3 \times 10^7 X + 2788$

B.2 Gemfibrozil UV scan

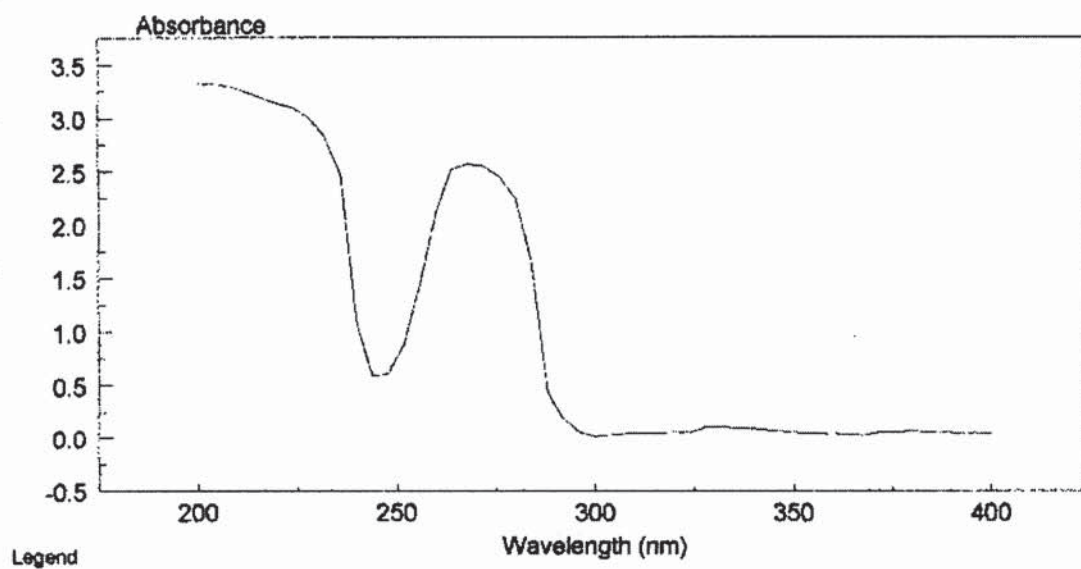


Figure B.2 UV scan gemfibrozil

B.3 Flurbiprofen HPLC assay

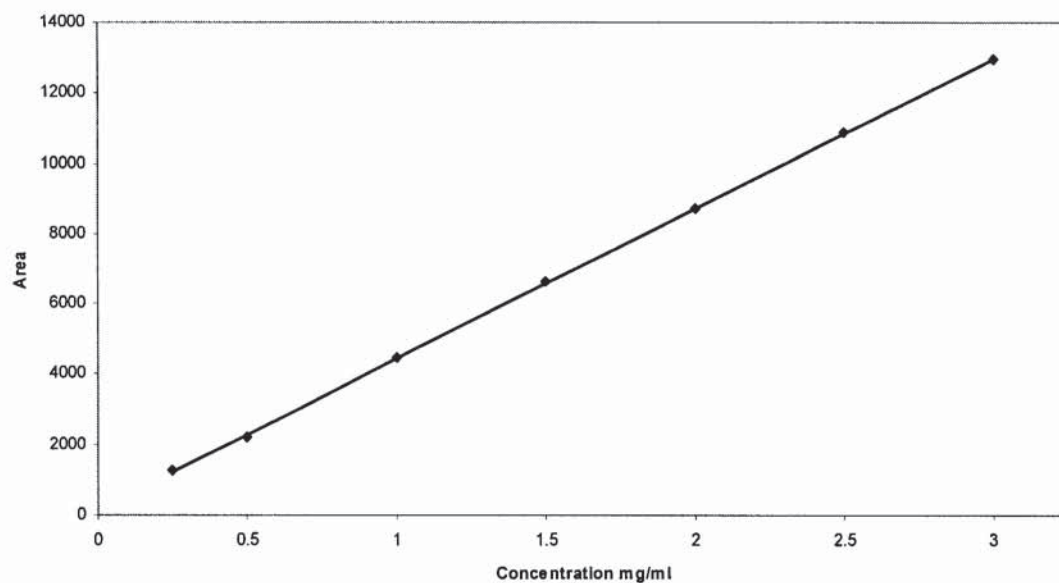


Figure B.3 Typical calibration graph for flurbiprofen assay by HPLC. $R^2=0.9998$, $Y=4273.3X+162.73$

B.4 Flurbiprofen UV scan

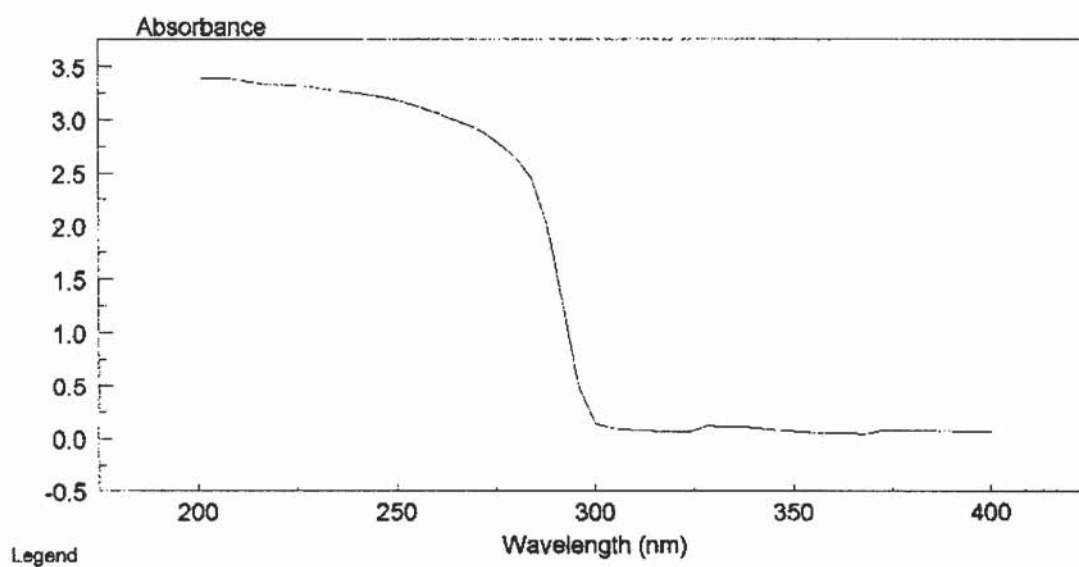


Figure B.4 Scanning UV absorbance spectra for flurbiprofen

B.5 Ibuprofen HPLC assay

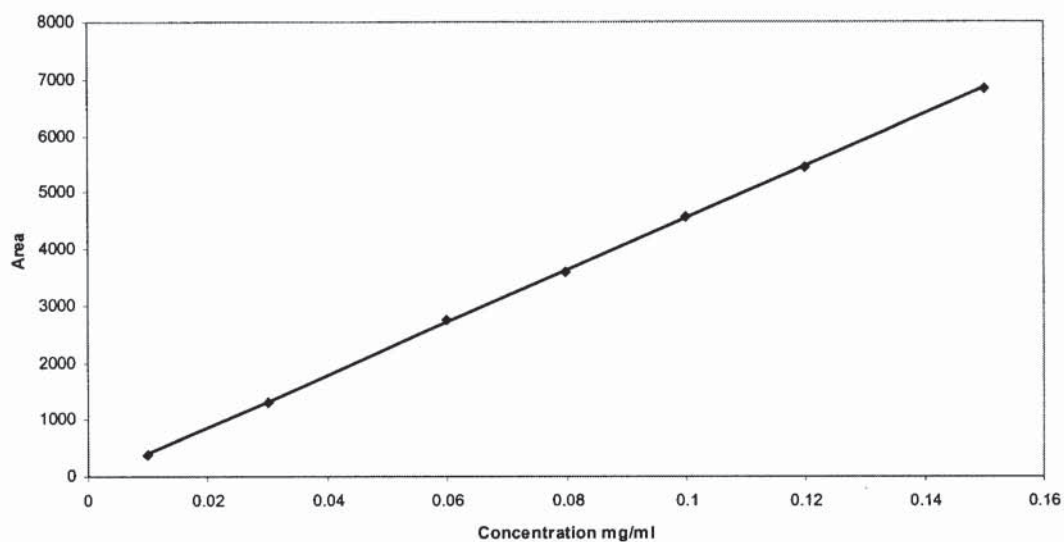


Figure B.5 Typical calibration graph for ibuprofen assay by HPLC . R^2 0.9999 and $Y=46050X-61.138$

B.6 Ibuprofen UV scan

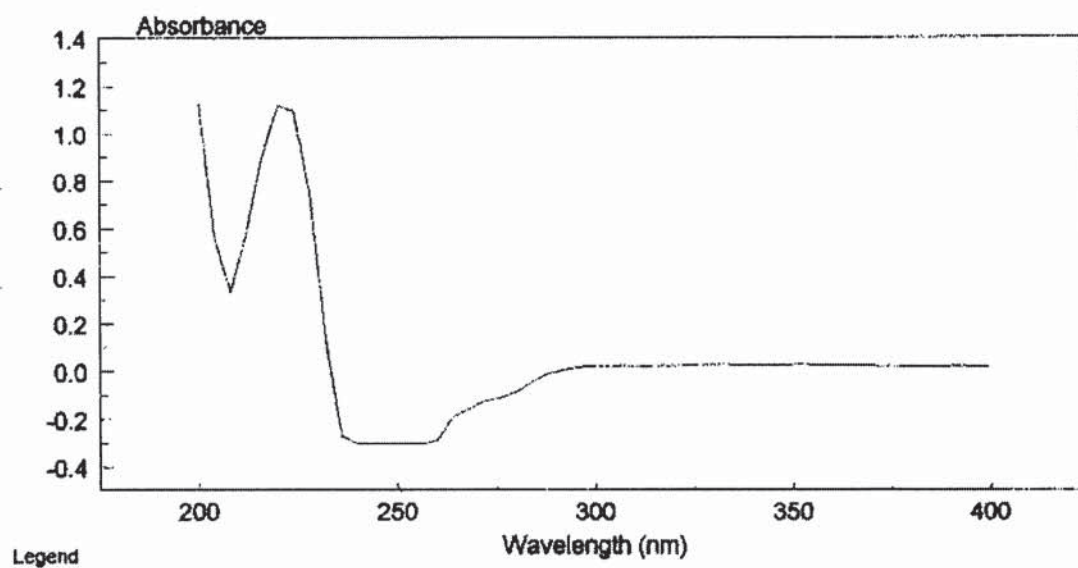


Figure B.6 UV scan of ibuprofen

B.7 Etodolac HPLC assay

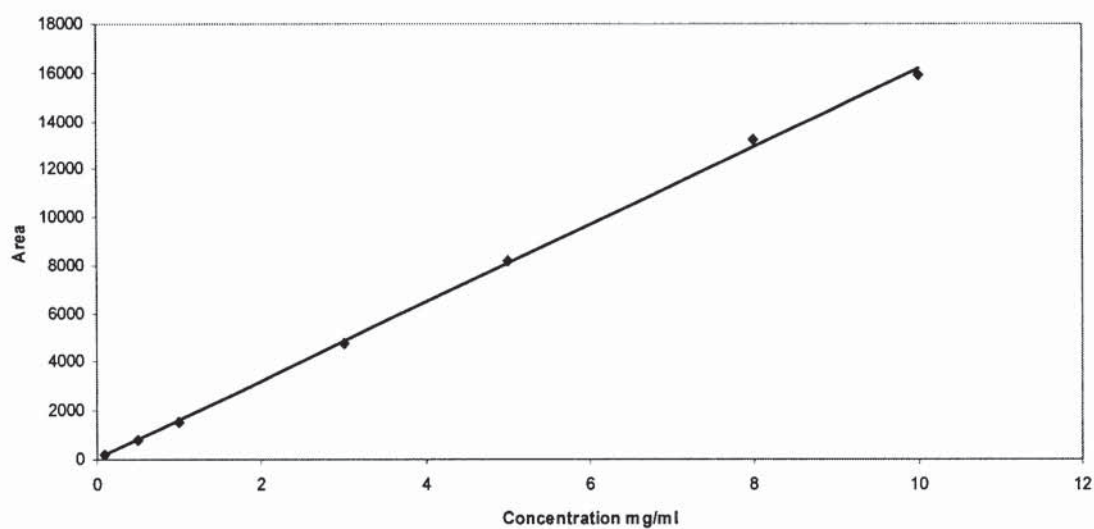


Figure B.7 Typical calibration graph for etodolac assay by HPLC. R^2 0.9993 and $Y=1615X+19.552$.

B.8. Etodolac UV scan

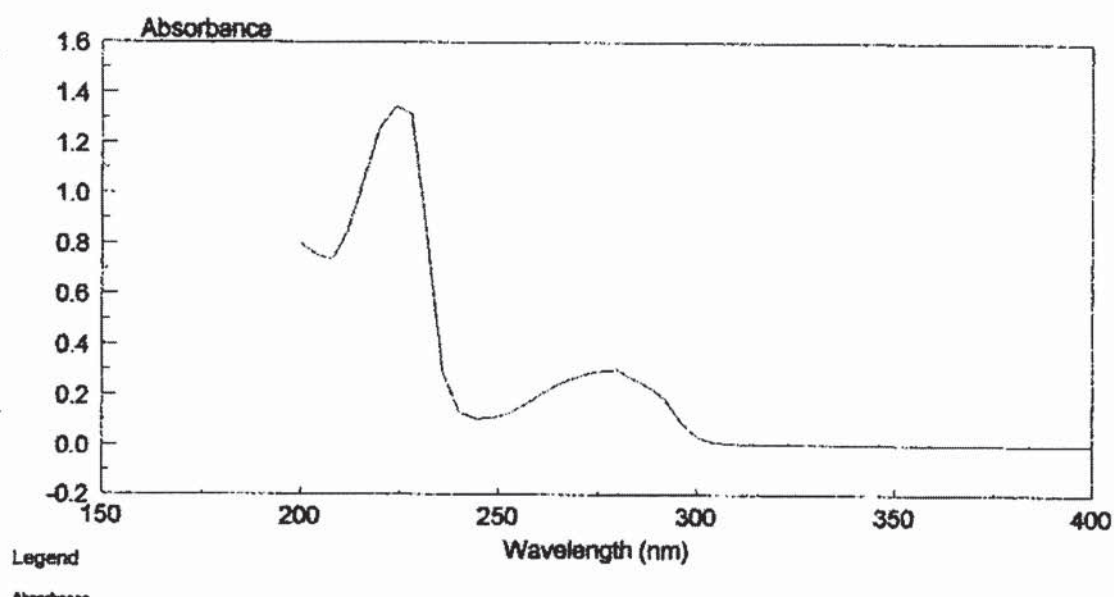


Figure B.8 UV scan for etodolac

B.9 Naproxen assay by HPLC

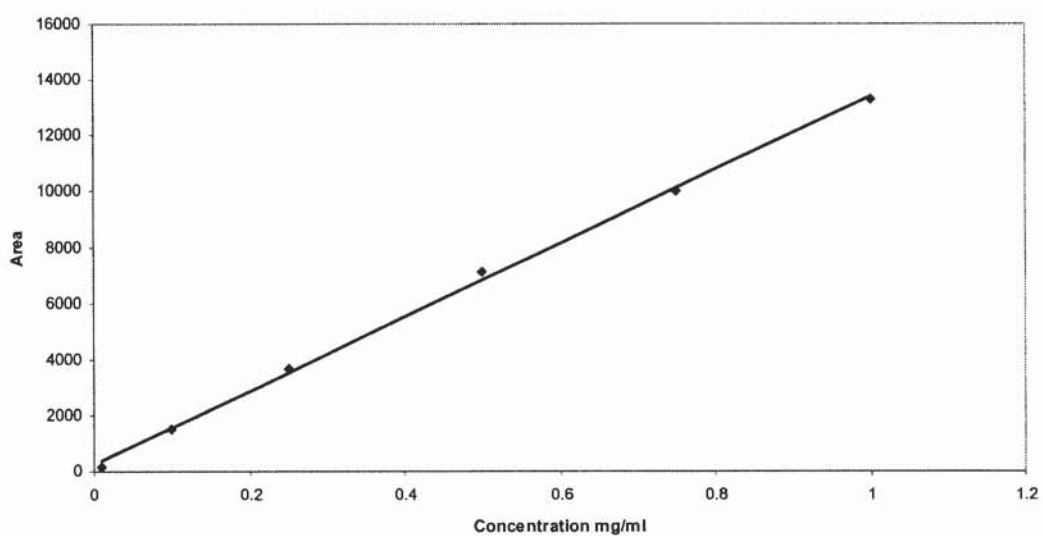


Figure B.9 Typical calibration graph for naproxen assay by HPLC. R^2 0.9987 and $Y=13188X+232.6$.

B.10 Piroxicam assay by HPLC

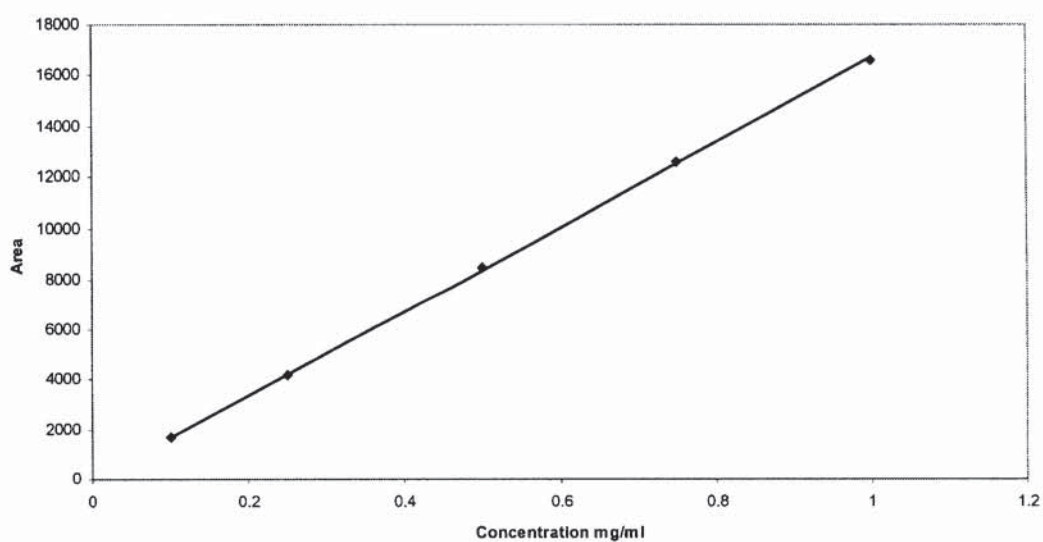


Figure B.12 Typical calibration graph for piroxicam assay by HPLC. $R^2=0.9998$ and $Y=16651X+44.776$

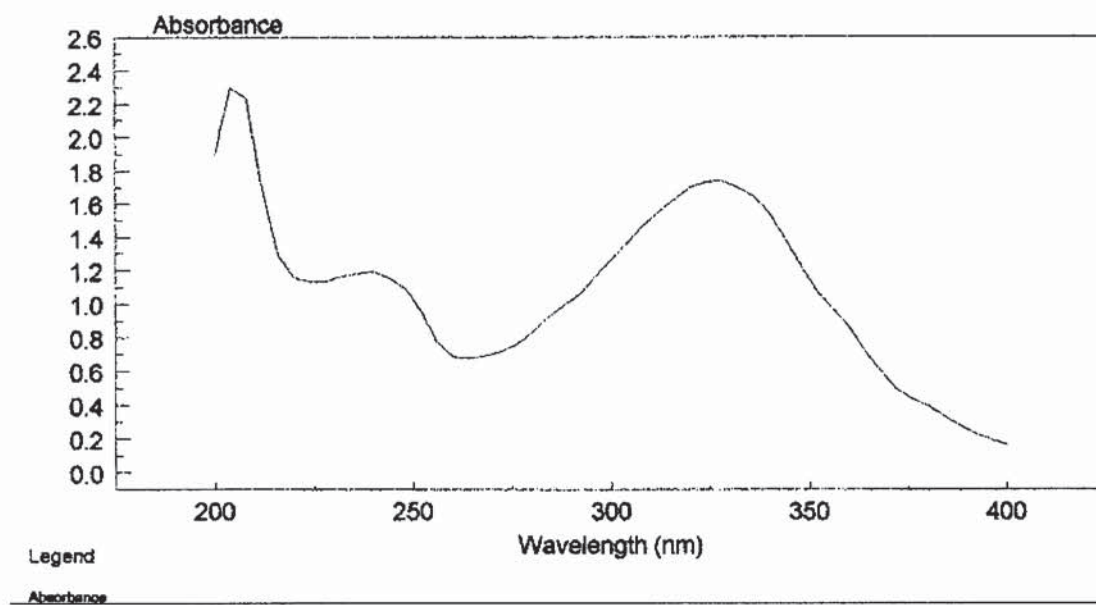


Figure B.13 Typical UV scan of piroxicam

Appendix C

Composition of buffers

Buffer	Ingredient A	Ingredient B	Final Volume
pH 3	34 g potassium dihydrogen orthophosphate	Adjust pH with orthophosphoric acid	250 ml
pH 4	6.8 g potassium dihydrogen orthophosphate in 700 ml water	Adjust pH with a 10 % v/v solution of orthophosphoric acid	1000 ml
pH 5.5	Dissolve 13.61 g of potassium dihydrogen orthophosphate in 1000 ml water	Dissolve 35.81 g disodium hydrogen orthophosphate in 1000 ml water	Add 96.4 ml A and 3.6 ml B to give 100ml
pH 6.0	50 ml of 0.2M potassium dihydrogen orthophosphate	5.70 ml 0.2M sodium hydroxide	200ml
pH 6.8	50 ml of 0.2M potassium dihydrogen orthophosphate	23.65 ml 0.2M sodium hydroxide	200ml
pH 7.2	50 ml of 0.2M potassium dihydrogen orthophosphate	35.00 ml 0.2M sodium hydroxide	200ml
pH 8	50 ml of 0.2M potassium dihydrogen orthophosphate	46.80 ml 0.2M sodium hydroxide	200ml
pH 9	1.74 g potassium dihydrogen orthophosphate in 80 ml water	Adjust pH with 1M potassium hydroxide	100

Appendix D

D.1 Typical physicochemical data

D.1.1 Typical NMR data

Below are two NMR scans for flurbiprofen (figure 3) and flurbiprofen benzylamine (figure 4). The resonance spectra are plotted against the deviation in parts per million (ppm) from a tetramethylsilane (TMS) standard on the right hand side. Groups that are in the aliphatic region have typical ppm values between 0-4 i.e. they have no electronegative groups that may shift the resonance. The CH₃ and H group attached to the aliphatic C and these groups would be expected to resonate at about 1-2 ppm. It should appear as a quartet since it is next to 3 hydrogen atoms, but it should integrate to 1. The CH₃ group is next to 1 H so should appear as a doublet that integrates to 3; see Figure D3. Flurbiprofen has a COOH group attached to the aliphatic C, oxygen is electron withdrawing so a shift to higher ppm value is expected, to about 3.75. This electron withdrawing effect is much more severe at the ionisable COOH proto, which appears as a singlet at 12.5 ppm. There is one peak between 7-8 ppm and at this chemical shift aromatic groups are expected, the nine remaining protons present in the aromatic rings resonate at this position.

The integration parameters were calculated by the software and represent the total number of protons resonating in the sample; these are presented on the left of the axis. The total number of protons in the sample is calculated by adding these numbers up, the total is 14 which is the number of hydrogen's in flurbiprofen. This confirms that the sample is flurbiprofen.

On the far left is the peak splitting data for the individual peaks, this data allows one to identify the next door neighbour of the group you are trying to locate. If you are looking at a highly complex structure this data helps identify the position of groups that may have the same number of protons, because each environment surrounding the group may be different. For the purposes of this thesis knowledge of the interpretation of peak splitting is not required and only the integration parameters will be used to confirm salt formation.

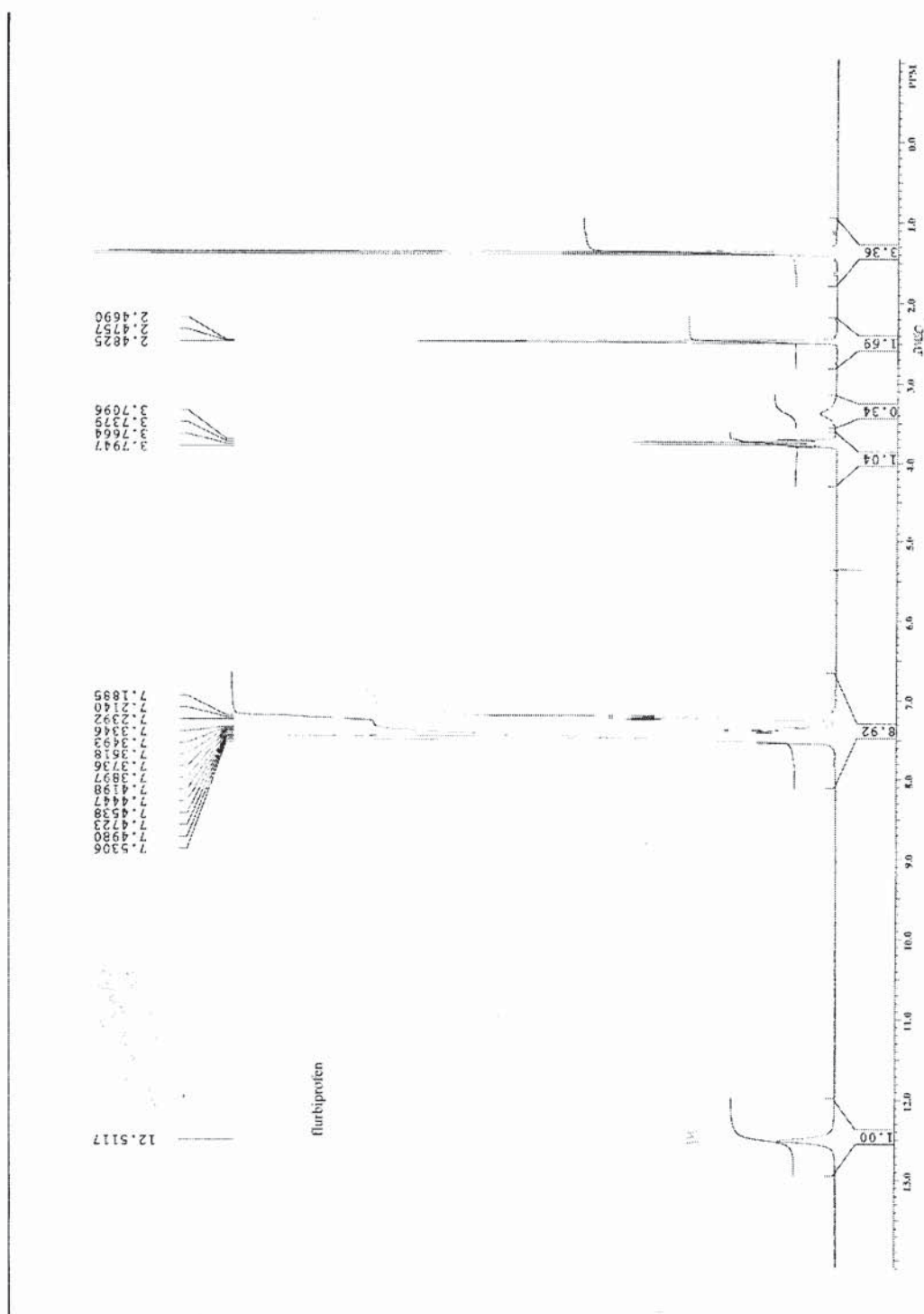


Figure D.1 Proton NMR data for flurbiprofen in DMSO

The NMR data for flurbiprofen benzylamine is displayed in figure 4, below. The additional C_6H_5 and NH_2 group are represented by the peaks at 6 and 4 ppm respectively. The total number of protons present confirms the formation of the benzylamine salt of flurbiprofen.

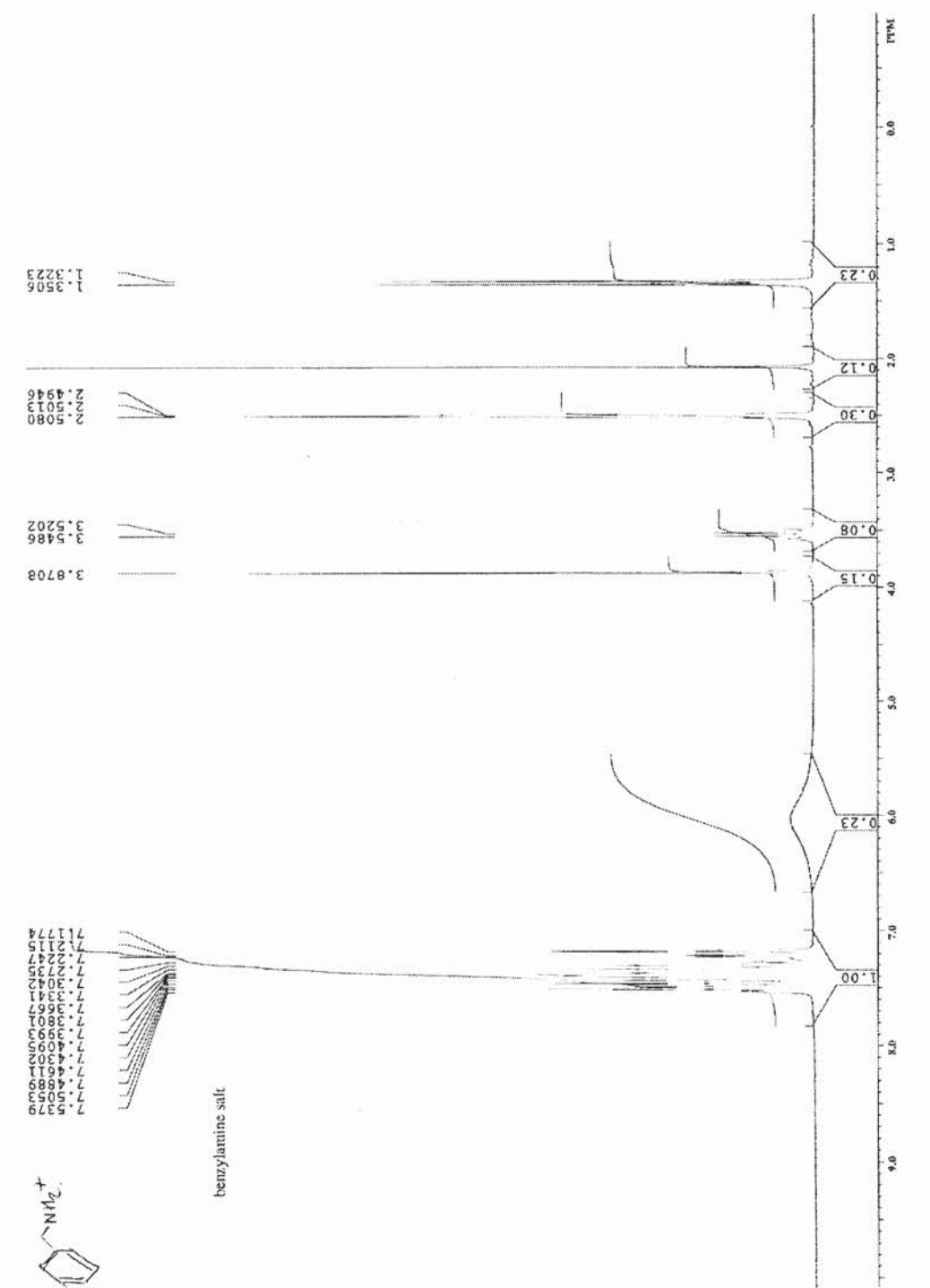


Figure D.2 Proton NMR data for flurbiprofen benzylamine in chloroform

D.1.2 Typical FTIR data

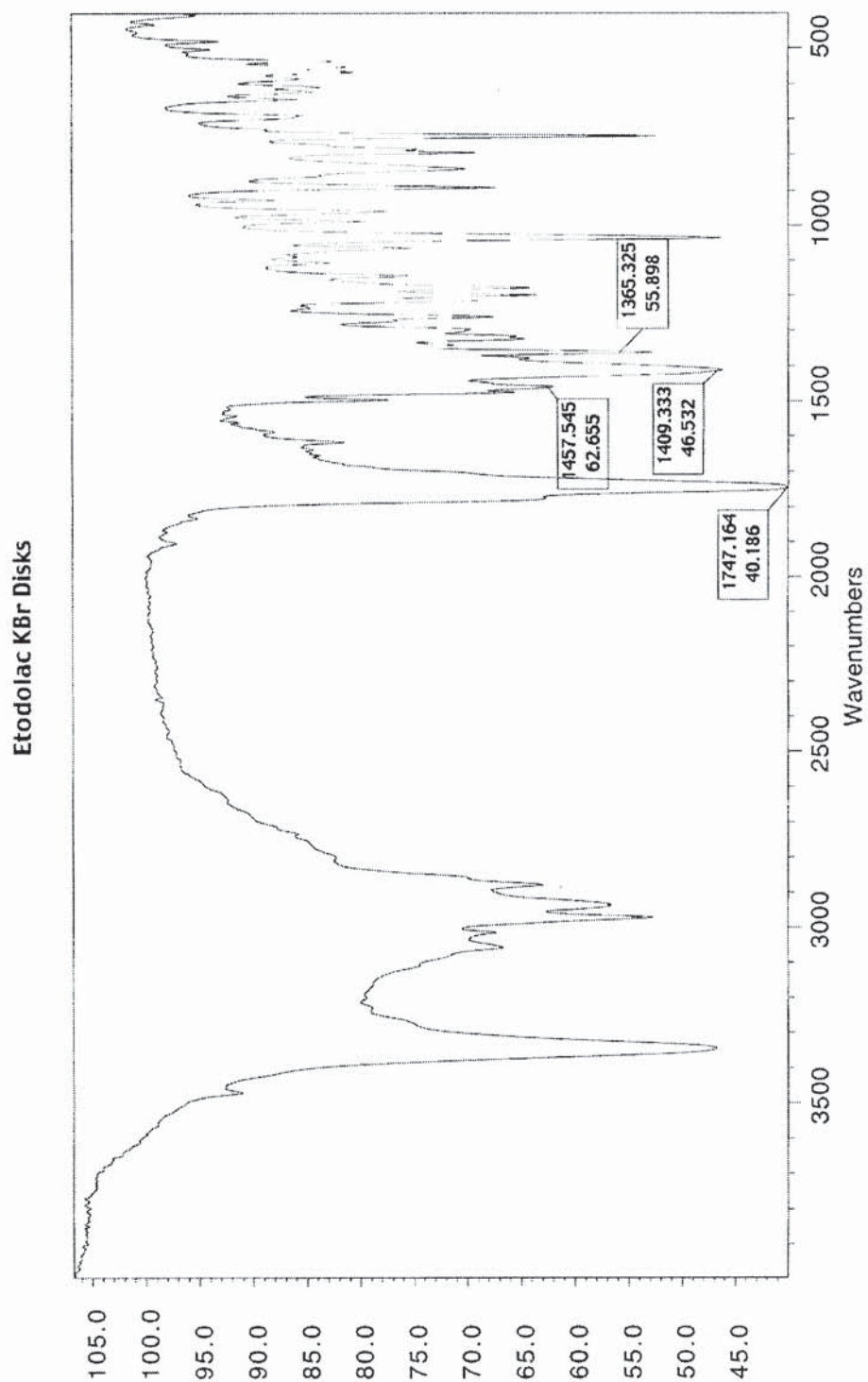


Figure D.3 Typical FTIR scan for etodolac in KBr disks

Etodolac butylamine

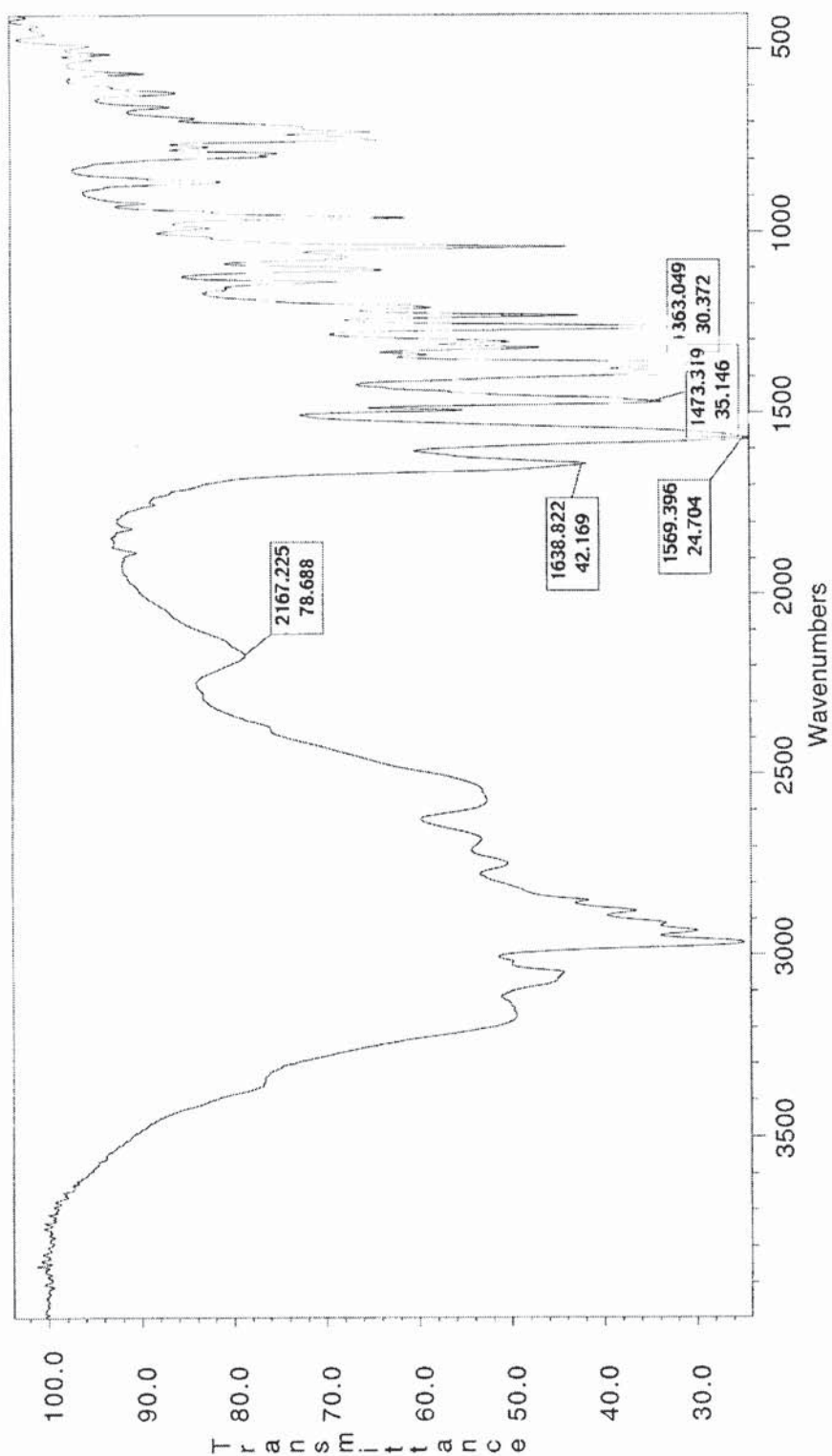


Figure D.4 Typical FTIR scan for etodolac butylamine in KBr disks

D.1.3 Typical DSC data

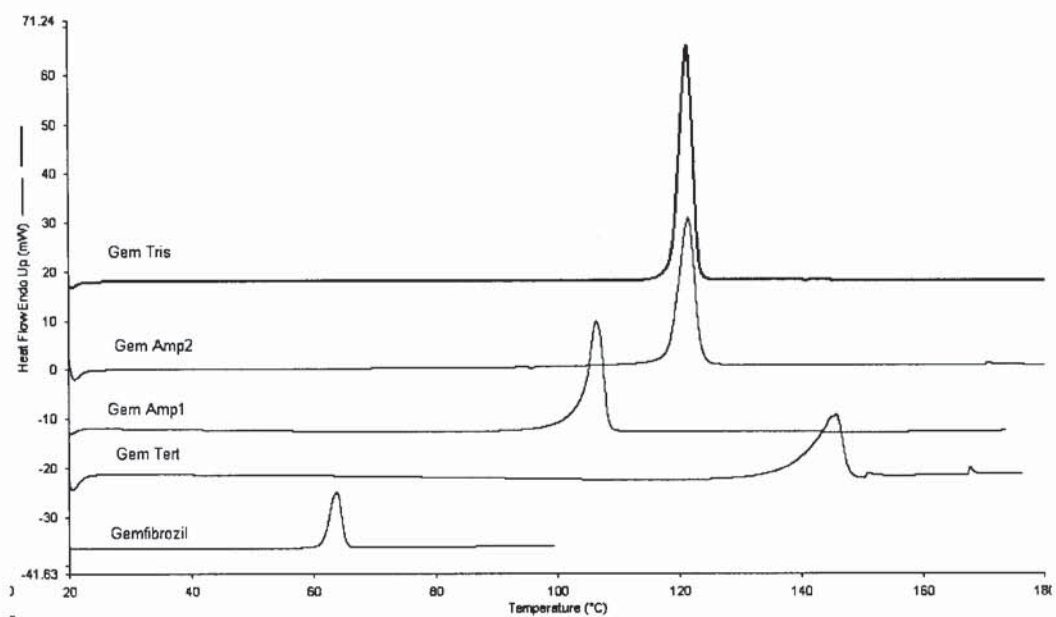


Figure D.5 Typical DSC traces for gemfibrozil and its tert, AMP1, AMP2 and tris salt forms

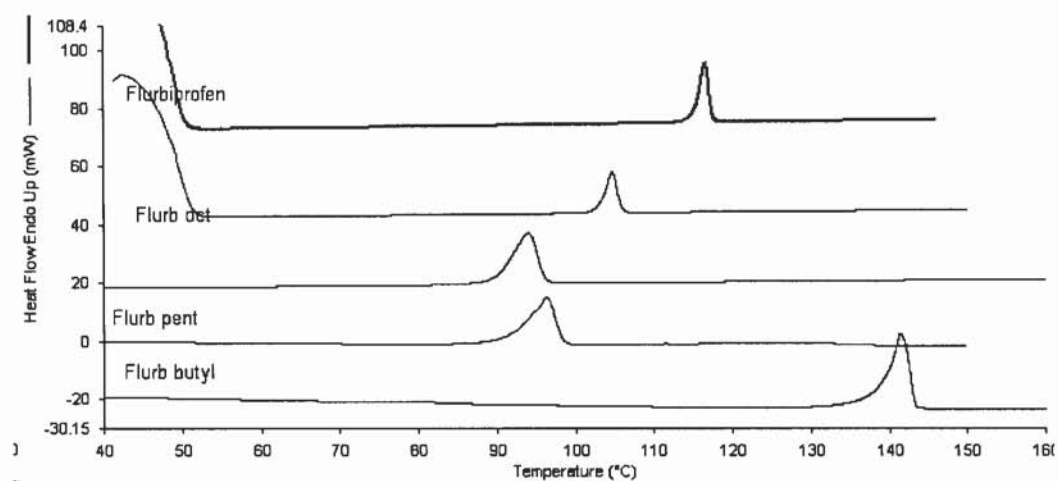


Figure D.6 Typical DSC traces for flurbiprofen and its butylamine, Pentylamine, and octylamine salt forms

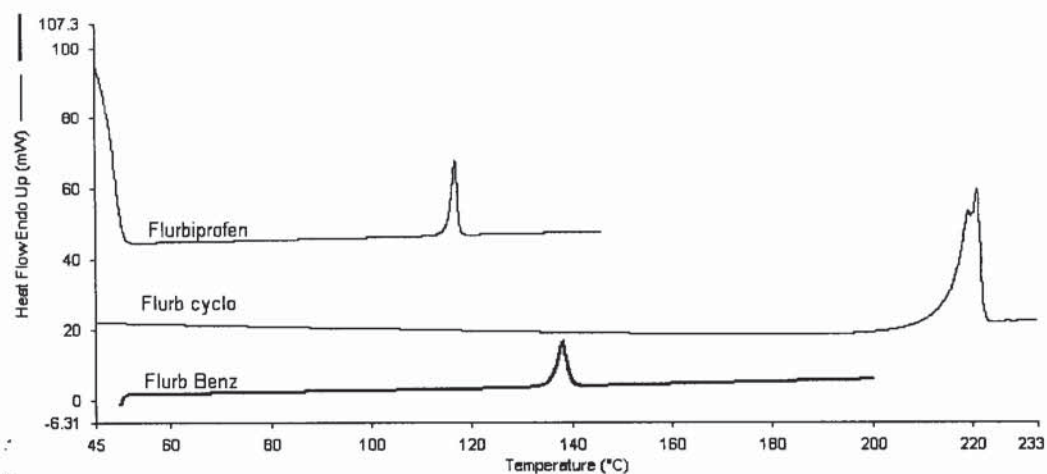


Figure D.7 Typical DSC traces for flurbiprofen and its cyclohexylamine and benzylamine salt forms

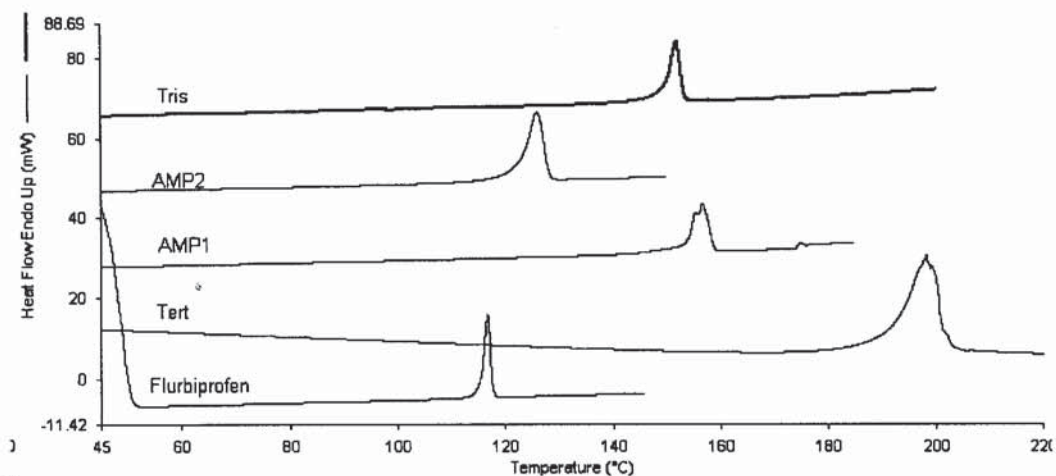


Figure D.8 Typical DSC traces for flurbiprofen and its tert, AMP1, AMP2 and tris salt forms

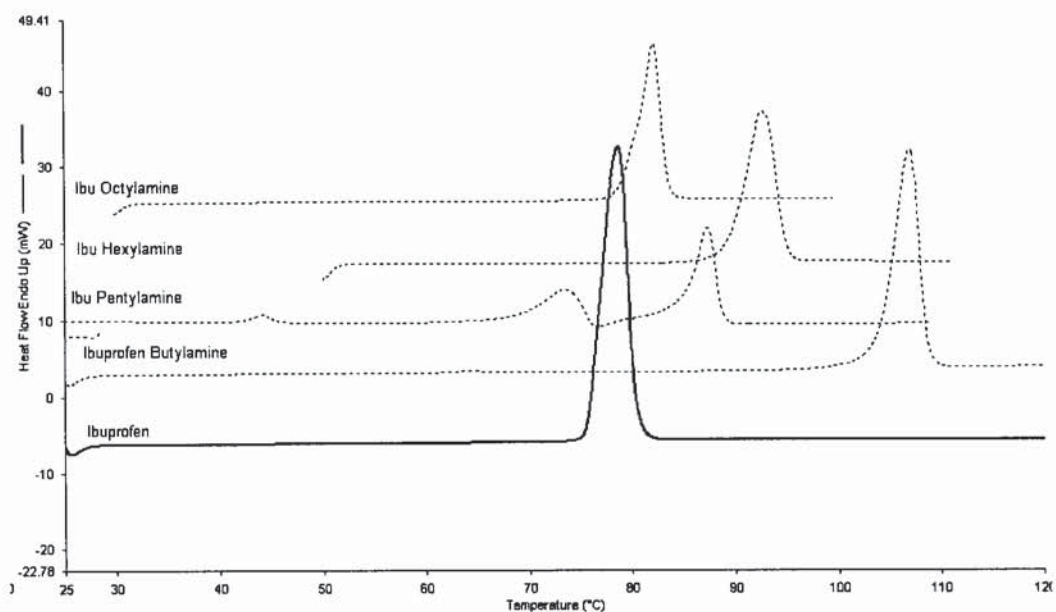


Figure D.9 Typical DSC traces for ibuprofen and its butylamine, Pentylamine, hexylamine and octylamine salt forms

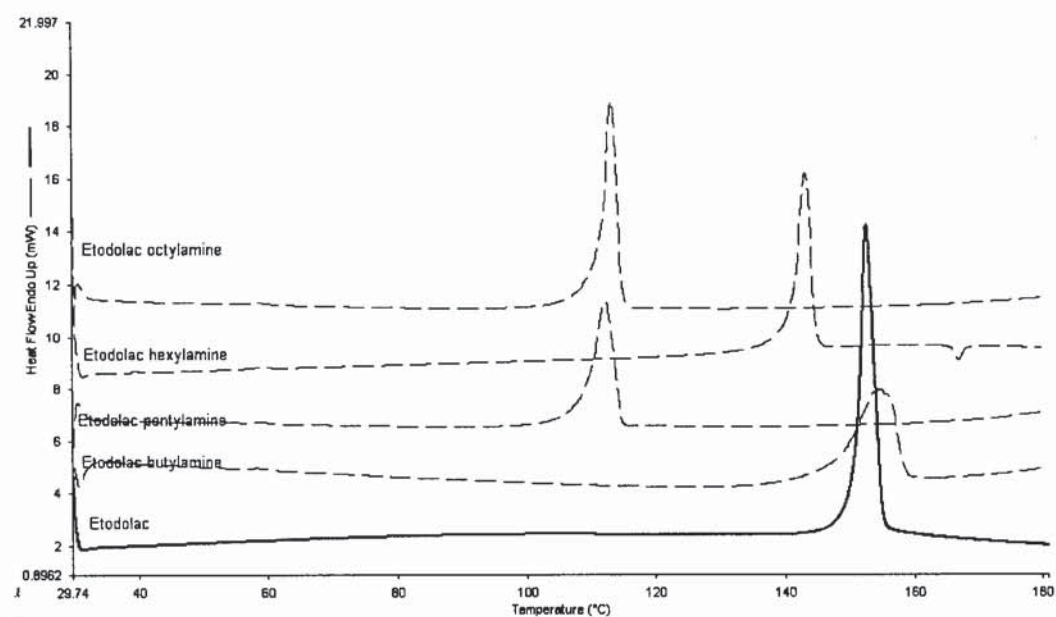


Figure D.10 Typical DSC traces for etodolac and its butylamine, hexylamine, Pentylamine and octylamine salt forms

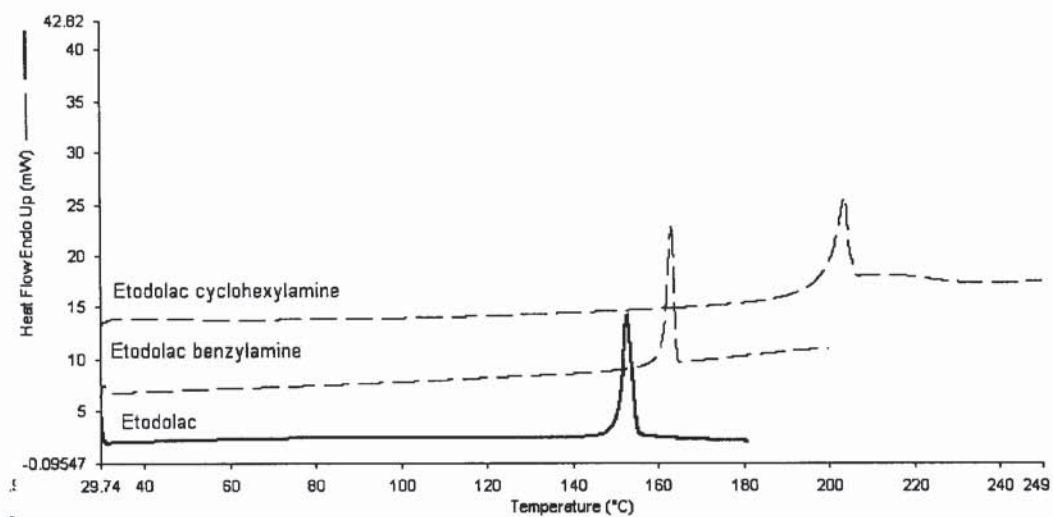


Figure D.11 Typical DSC traces for etodolac and its benzylamine and cyclohexylamine salt forms

Agharkar S, Lindenbaum S, Higuchi T. Enhancement of solubility of drug salts by hydrophilic counterions: properties of organic salts of an antimalarial drug. *J Pharm Sci.* 1976; 65 (5):747-749.

Agrawal S, Pancholi SS, Jain NK, Agrawal GP. Hydrotropic solubilization of nimesulide for parenteral administration. *Int J Pharm.* 2004; 274(1-2):149-155.

Ahfat NM, Buckton G, Burrows R, Ticehurst MD. An exploration of inter-relationships between contact angle, inverse phase gas chromatography and triboelectric charging data. *Eur J Pharm Sci.* 2000; 9:271-176

Alexandridis P, Hatton TA. Poly(ethylene oxide)---poly(propylene oxide)---poly(ethylene oxide) block copolymer surfactants in aqueous solutions and at interfaces: thermodynamics, structure, dynamics, and modeling. *Colloids Surf.* 1995; 96(1-2):1-46

Al-Saidan SM. Transdermal self-permeation enhancement of ibuprofen. *J Control Release.* 2004; 100(2):199-209.

Amidon GL, Lennernas H, Shah VP, Crison JR. A theoretical basis for a biopharmaceutic drug classification: the correlation of *in vitro* drug product dissolution and *in vivo* bioavailability. *Pharm Res.* 1995; 12(3):413-420

Anderson BD, Conradi RA. Predictive relationships in the water solubility of salts of a nonsteroidal anti-inflammatory drug. *J Pharm Sci.* 1985;74(8):815-820.

Anderson BD, Smith SW. *The Practice of Medicinal Chemistry*, CG Wermuth, Ed., Academic Press, London, 1996

Andreu JM, Bordas J, Diaz JF, Garcia de Ancos J, Gil R, Medrano FJ, Nogales E, Pantos E, Towns-Andrews E. Low resolution structure of microtubules in solution. Synchrotron X-ray scattering and electron microscopy of taxol-induced microtubules assembled from purified tubulin in comparison with glycerol and MAP-induced microtubules. *J Mol Biol.* 1992 Jul 5;226(1):169-84.

Arakawa T, Timasheff SN. Mechanism of protein salting in and salting out by divalent cation salts: balance between hydration and salt binding. *Biochemistry.* 1984 ;23(25):5912-5923.

Atherton AD, Barry BW. Photon correlation spectroscopy of surface active cationic drugs. *J Pharm Pharmacol.* 1985;37(12):854-862.

Attwood D, Udeala OK. Aggregation of antihistamines in aqueous solution: effect of counterions on self-association of pyridine derivatives. *J Pharm Sci.* 1976;65(7):1053-1057.

Attwood D, Natarajan R. Effect of pH on the micellar properties of amphiphilic drugs in aqueous solution. *J Pharm Pharmacol.* 1981;33(3):136-140.

Attwood D, Fletcher P. Self-association of local anaesthetic drugs in aqueous solution. *J Pharm Pharmacol.* 1986;38(7):494-498.

Attwood D, Fletcher P, Boitard E, Dubes JP, Tachoire H. A calorimetric study on the self-association of an amphiphilic phenothiazine drug in aqueous electrolyte solutions. *J Phys Chem.* 1990a; 94(15); 6034-6041.

Attwood D, Boitard E, Dubès J -P and Tachoire H. Association models for an amphiphilic drug in aqueous solutions of high ionic strength from calorimetric studies. *Colloids Surf.* 1990b; 48:35-46

Attwood D, Blundell R, Mosquera V V, Garcia M. Association and surface properties of amphiphilic benzodiazepine and benzothiazepine drugs in aqueous solution. *J Colloid Interface Sci.* 1993; 161:19-23.

Attwood D, Waigh R, Blundell R, Bloor D, Thevand A, Boitard E, Dub`es JP, Tachoire H. Self association of verapamil in aqueous electrolyte solution. *Mag Res Chem.* 1994; 32: 468

Attwood D, Mosquera V V, Garcia M, Suarez, M, Sarmiento F. A comparison of the micellar properties of structurally related antidepressant drugs. *J Colloid Interface Sci* 1995; 175:201-206.

Attwood D, Mosquera V V, Lopez-Fontan JL, Garcia M, Sarmiento F. self-association of phenothiazine drugs: Influence of the counterion on the mode of association. *J Colloid Interface Sci.* 1996;184(2):658-662.

Attwood D, Boitard E, Dubes J, Tachoire H. A calorimetric study of the influence of electrolyte on the micellisation of phenothiazine drugs in aqueous solution. *J Phys Chem.* 1997; 101:9568-9592.

Attwood D, Boitard E, Dubes J, Tachoire H. A calorimetric study of the influence of temperature on the self-association of amphiphilic antidepressant drugs in aqueous solution. *J Colloid Interface Sci.* 2000; 227(2):356-362.

Aunins JG, Southard MZ, Myers RA, Himmelstein KJ, Stella VJ. Dissolution of carboxylic acids. III: The effect of polyionizable buffers. *J Pharm Sci.* 1985; 74(12):1305-1316.

Aulton ME, *Pharmaceutics- The science of dosage form and design.* Churchill Livingstone, London. 2002

Avdeef A. Physicochemical profiling (solubility, permeability and charge state). *Curr Top Med Chem.* 2001;1(4):277-351.

Banerjee S, Yalkowsky SH, Valvani SC. Water solubility and octanol/water partition coefficients of organics. Limitations of the solubility-partition coefficient correlation. *Environ Sci Technol.* 1980; 14: 1227-1229.

Bashaiwoldu AB, Podczek F, Newton JM. Application of dynamic mechanical analysis (DMA) to the determination of the mechanical properties of pellets. *Int J Pharm.* 2004a;269(2):329-342.

Bashaiwoldu AB, Podczek F, Newton JM. Application of dynamic mechanical analysis (DMA) to the determination of the mechanical properties of coated pellets. *Int J Pharm.* 2004b;274(1-2):53-63.

Bassam F, York P, Rowe R, Roberts R. Young's Modulus of powders used as pharmaceutical excipients. *Int J Pharm.* 1990; 64:55-60

Bergstrom CA, Luthman K, Artursson P. Accuracy of calculated pH-dependent aqueous drug solubility. *Eur J Pharm Sci.* 2004; 22(5):387-398.

Bogardus JB, Blackwood RK Jr. Solubility of doxycycline in aqueous solution. *J Pharm Sci.* 1979;68(2):188-194

Bogardus JB. Common ion equilibria of hydrochloride salts and the Setschenow equation. *J Pharm Sci.* 1982;71(5):588-90.

Boultif A, Louër D. Indexing of powder diffraction patterns for low-symmetry lattices by the successive dichotomy method. *J Appl Cryst.* 1991; 24:987-993.

Bragga D, Fabrizia G. Crystal engineering; from molecules and crystals to materials. Kulwer Scientific, Boston, USA, 1999.

Bragg L. X-Ray Crystallography. *Scientific American* 1968 219(2);58-70.

Busignies V, Tchoreloff P, Leclerc B, Hersen C, Keller G, Couarraze G. Compaction of crystallographic forms of pharmaceutical granular lactoses. II. Compacts mechanical properties. *Eur J Pharm Biopharm.* 2004; 58(3):577-586.

Causon D, Gettins J, Gormally J, Greenwood R, Natarajan R, Wyn-Jones E. Relaxations associated with aggregation in drugs. *J Chem Soc Faraday Trans.* 1981; 2:143 – 151.

Church MS. Mechanical characterization of pharmaceutical powder compacts. 1984 Nottingham University, UK. Thesis

Coffin-Beach D, Hollenbeck RG. Determination of the energy of tablet formation during compression of selected pharmaceutical powders. *Int J Pharm.* 1983; 17:313-324.

Dash BH, Bank RG, Schachtel BP, Smith AJ. Ibuprofen tablets dissolution *versus* bioavailability. *Drug Dev Ind Pharm.* 1988; 14(11):1629-1645.

Datta S, Grant D. Crystal structures of drugs: Advances in determination, prediction and engineering. *Nature*; 2004. 3: 42-57.

David WIF, Shankland K, Shankland N. Routine determination of molecular crystal structures from powder diffraction data. *Chem Comm (Camb)* 1998; 8:931-932.

Desiraju GR. Crystal engineering. From molecules to materials. *J Mol Struc.* 2003; 656:5-15.

- Di Martino P, Scoppa M, Joiris E, Palmieri GF, Andres C, Pourcelot Y, Martelli S. The spray drying of acetazolamide as method to modify crystal properties and to improve compression behaviour. *Int J Pharm.* 2001;213(1-2):209-21.
- Dittert LW, Higuchi T, Reese DR. Phase solubility technique in studying the formation of complex salts of triamterene. *J Pharm Sci.* 1964;53:1325-1328.
- Erb DM. Solution Calorimetry- An alternative method for the quantification of the solid state properties of drugs. 1985. Thesis University of Iowa, Iowa City, USA
- Ernandes JR, Chaimovich H, Schreier S. Spin label study of detergents in the region of critical micelle concentration. *Chem Phys Lipids.* 1977;18(3-4):304-315.
- Fendler JH. Membrane mimetic chemistry. 1982. Wiley-Inter-Science, New York, USA
- Florence AT., Attwood D. Physicochemical Principles of Pharmacy. 1988. Palgrave Macmillan, London, UK
- Frezzatti WA Jr, Toselli WR, Schreier S. Spin label study of local anesthetic-lipid membrane interactions. Phase separation of the uncharged form and bilayer micellization by the charged form of tetracaine. *Biochim Biophys Acta.* 1986;860(3):531-538.
- Gao D, Rytting H. Use of solution calorimetry to determine the extent of crystallinity of drugs and excipients. *Int J Pharm.* 1997; 151:183-192.
- Gavezzotti A. PROMET5.3 A program for the generation of possible crystal structures from the molecular structure of organic compounds. 1997. University of Milan, Milan, Italy. Thesis
- Gohel MC, Panchal MK. Refinement of the lower acceptance value of the similarity factor f_2 in comparison of dissolution profiles. *Diss Tech.* 2002; 9(1)1-5.
- Gould PL. Salt selection for basic drugs. *Int J Pharm.* 1986; 33:201-217.
- Gray VD. Simulated intestinal fluid TS- Change to pH 6.8. *Pharmacopeial Forum* 1996; 22:1943-1945.
- Gu L, Strickley RG. Preformulation salt selection. Physical property comparisons of the tris(hydroxymethyl)aminomethane (THAM) salts of four analgesic/anti-inflammatory agents with the sodium salts and the free acids. *Pharm Res.* 1987; 4(3):255-257.
- Guillory JK., Erb DM. Using solution calorimetry to quantitate binary mixtures of three crystalline forms of sulphamethoxazole.. *Pharm Manuf.* 1985; Sept 28-30.
- Guillory J.K. Polymorphism in Pharmaceutical Solids. 1999. Marcell Dekker, New York, USA.
- Habershon S, Harris KDM., Johnson RL., Turner GW, Johnson J.M. Gaining insights into the evolutionary behaviour in genetic algorithm calculations, with applications in structure solution from powder diffraction data. *Chem Phys Lett.* 2002;353:185-194.

- Garekani HA, Ford JL, Rubinstein MH, Rajabi-Siahboom AR. Formation and compression characteristics of prismatic polyhedral and thin plate-like crystals of paracetamol. *Int J Pharm.* 1999; 187(1), :77-89.
- Hancock BC, Carlson GT, Ladipo DD, Langdon BA, Mullarney MP. Comparison of the mechanical properties of the crystalline and amorphous forms of a drug substance. *Int J Pharm.* 2002;241:73-85.
- Hao Y, Mucklick F, Petzow G. Correlation between the dislocation of HCP single crystals by application of the Fourier transformation approach. *Comp MaterialsSci.* 1996; 7:167-172.
- Harris KDM., Tremayne M. Crystal structure determination from powder diffraction data. *Chem Mater.* 1996; 8:2554-2570.
- Harris KDM., Johnston RL., Kariuki BM. The genetic algorithm: foundations and applications in structure solution from powder diffraction data. *Acta. Cryst. A.* 1998; 54:632-645.
- Healy AM. and Corrigan O I. The influence of excipient particle size, solubility and acid strength on the dissolution of an acidic drug from two-component compacts. *Int J Pharm.* 1996;143, (2): 211-221.
- Heckle RW. An analysis of powder compression phenomena. *Trans Metall Soc.* 1961; AIME 221:1001
- Hersey JA., Rees J. Deformation of particles during briquetting. *Nature (Phys. Sci.)* 1971; 230:96
- Hendriksen BA. Characterization of calcium fenoprofen 1. Powder dissolution rate and degree of crystallinity. *Int J Pharm.* 1990; 60(3):243-252
- Heyrovska R. Physical electrochemistry of strong electrolytes based on partial dissociation and hydration. Quantative interpretation of the thermodynamic properties of NaCl(aq) from zero to saturation. *J Electrochemical Soc.* 1996; 143(6):1789-1793.
- Hiestand EN, Bane JM, Strezlin EP. Impact test for hardness of compressed powder compacts. *J Pharm Sci.* 1971; 60(5): 758-763
- Hiestand EN, Wells JE, Peot CB, Ochs JF. .Physical processes of tableting. *J Pharm Sci.* 1977; 66 (4): 510-519.
- Hiestand EN. Dispersion forces and plastic-deformation in tablet bond. *J Pharm Sci.* 1985; 74 (7): 768-770.
- Hiestand E. N. Tablet bond. I. A theoretical model. *Int J Pharm.* 1991; 67 (3): 217-229.
- Hiestand EN, Smith DP. Tablet bond .2. Experimental check of model. *Int J Pharm.* 1991;67(3): 231-246..
- Hiestand EN. Principles, tenets and notions of tablet bonding and measurements of strength. *Eur J Pharm Bio.*1997; 44 (3):229-242.

- Higuchi T, Arnold RD, Tucker SJ, Busse LW. The physics of tablet compression. Studies on aspirin, lactose and sulphadiazine tablets. *J Am Pharm Assoc Sci Ed.* 1954; 41:93-96.
- Higuchi WI, Parrott E, Wurster D, Higuchi T. Investigation of drug release from solids II. Theoretical and experimental study of influences of bases and buffers on rates of dissolution of acidic solids. *J Am Pharm Assoc Sci Ed.* 1958 ; 47:376-389
- Hilal SH, Carreira LA, Karickhoff SW. A rigorous test for SPARC's chemical reactivity models: estimation of more than 4300 Ionization pKas. *Quant Struct Act Relat.* 1995; 14 348-360
- Hilal SH, Carreira LA, Karickhoff SW. A comprehensive study of molecular speciation: calculation of microscopic and zwitterionic ionization constants. *Talanta.* 1999;827: 50-68
- Hill JO, Öjelund G, Wadsö I. Thermochemical results for "tris" as a test substance in solution calorimetry. *J Chem Thermodynamics* 1969;1:111-116.
- Hodson AC, Ferrie PG, Dennis AB. Identification of a hydrate using the complementary techniques of dynamic vapour sorption (DVS), DSC, TGA and hot stage microscopy. *Eur J Pharm Sci.* 4(1) *Page S181*
- Hogan SE, Buckton G. The quantification of small degrees of disorder in lactose using solution calorimetry. *Int J Pharm.* 2000;207 (1-2):57-64.
- Holbrook SR. Crystallographic analysis of RNA structure. 1998. CSHL, New York, USA
- Holden JR., Du Z, Ammon, HL. MOPACK. *J Comput Chem.* 1993; 12:422-436.
- Holman LE., Leuenberger H. The relationship between solid fraction and mechanical properties of compacts — the percolation theory model approach. *Int J Pharm.* 1988; 46 (1-2), 35-44.
- Hu J, Johnston KP, Williams III, RO. Spray freezing into liquid (SFL) particle engineering technology to enhance dissolution of poorly water soluble drugs: organic solvent versus organic/aqueous co-solvent systems. *Eur J Pharm Sci.* 2003;20 (3): 295-303.
- Hwang PM, Vogel HJ. Structure-function relationships of antimicrobial peptides. *Biochem Cell Biol.* 1998; 76(2-3):235-246.
- Jbilou M, Ettabia A, Guyot-Hermann AM, Guyot JC. Ibuprofen agglomerates preparation by phase separation. *Drug Dev Ind Pharm.* 1999;25(3):297-305.
- Johansson B, Wikberg M, Ek R Alderborn G. Compression behaviour and compactability of microcrystalline cellulose pellets in relationship to their pore structure and mechanical properties. *Int J Pharm.* 1995; 117(1): 57-73.
- Johansson B, Alderborn G. The effect of shape and porosity on the compression behaviour and tablet forming ability of granular materials formed from microcrystalline cellulose. *Eur J Pharm Biopharm.* 2001; Crystallography analysis 52 (3):347-357.

Jones PG. Crystal growing. Chem Br. 1981;17:222-225.

Kachrimanis K, Malamataris S. "Apparent" Young's elastic modulus and radial recovery for some tableted pharmaceutical excipients. Eur J Pharm Sci. 2004;21(2-3):197-207.

Karhhoﬀ SW., McDaniel VK., Melton C, Vellino AN., Nute DE., Carreira LA. Predicting chemical reactivity by computer. Environ Toxicol Chem. 1991; 10:1405-1416.

Kendrew JC, Bodo G, Dintzis HM, Parrish RG, Wykoff H, Phillips DC.. A three-dimensional model of the myoglobin molecule obtained by X-ray analysis. Nature 1958; 181:662-666.

Khalil E, Najjar S, Sallam A. Aqueous solubility of diclofenac diethylamine in the presence of pharmaceutical additives: a comparative study with diclofenac sodium. Drug Dev Ind Pharm. 2000;26(4):375-381.

Kiang YH, Xu W, Kaufman MJ. Ab initio structure determination of rofecoxib from powder diffraction data using molecular packing analysis method and direct space method. Int J Pharm. 2003 Feb 18;252(1-2):213-23.

King SY, Basista AM, Torosian G. Self-association and solubility behaviors of a novel anticancer agent, brequinar sodium. J Pharm Sci. 1989;78(2):95-100.

Ko GH., Fink WH. A combined quantum chemistry and classical molecular interaction energy method for the determination of crystal properties and energies. J Chem Phys. 2002;116:747-754.

Kopecky F. Micellization and other associations of amphiphilic antimicrobial quaternary ammonium salts in aqueous solutions. Pharmazie. 1996;51(3):135-144.

Krumme M, Schwabe L, Fromming K. Development of computerised procedures for the characterisation of the tableting properties with eccentric machines: extended Heckel analysis. Eur J Pharm Biopharm. 2000; 49(3):275-286.

Kuentz M, Leuenberger H. A new model for the hardness of a compacted particle system, applied to tablets of pharmaceutical polymers. Powder Tech. 2000; 111(1-2):145-153.

Lamy-Freund MT, Ferreira VF, Schreier S. Polydispersity of aggregates formed by the polyene antibiotic amphotericin B and deoxycholate. A spin label study. Biochim Biophys Acta. 1989;981(2):207-212.

Lamy-Freund MT, Schreier S, Peitzsch RM, Reed WF. Characterization and time dependence of amphotericin B: deoxycholate aggregation by quasielastic light scattering. J Pharm Sci. 1991;80(3):262-266.

Larson AC. and Von Dreele RB., "General Structure Analysis System (GSAS)", Los Alamos National Laboratory Report LAUR, 2000; 86-748.

Ledwidge MT. The effects of pH, crystalline phase and salt formation on the solubility of ionisable drugs.1997. University of Dublin, Dublin, Ireland. PhD thesis.

- Ledwidge MT. , Corrigan O.I. Effects of surface active characteristics and solid state forms on the pH solubility profiles of drug-salt systems. *Int J Pharm.* 1998; 17: 187-200
- Lee YJ, Padula J, Lee HK. Kinetics and mechanisms of etodolac degradation in aqueous solutions. *J Pharm Sci.* 1988;77(1):81-86.
- Lieberman H. A. ed. *et al.* Pharmaceutical Dosage Forms Tablets. 1990. Volume 2 Second Edition. 201-243. Marcell Dekker, New York, USA
- Letinski DJ, Connelly MJ Jr, Peterson DR, Parkerton TF. Slow-stir water solubility measurements of selected alcohols and diesters. *Chemosphere.* 2002;48(3):257-265.
- Leuenberger H. The compressibility and compactibility of powder systems. *Int J Pharm.* 1982; 12 (1): 41-55.
- Leuner C, Dressman J. Improving drug solubility for oral delivery using solid dispersions. *Eur J Pharm Biopharm.* 2000;50(1):47-60.
- Liang Z, Westlund P, Wikander G. A quantitative electron-spin resonance line shape study of the local motion in the micellar and liquid crystalline lamellar phases of the oleoyllysolecithin water system. *J ChemPhys.*1993; 99(9):7098-7107.
- Liu JP., Choe MC. Statistical analysis on the FDA conjugates oestrogen tablets of bioequivalence guidance. *Drug Info J.* 1996; 30:881-889.
- Liu JP, Ma MC, Chow SC. Statistical evaluation of similarity factor f2 as a criterion for assessment of similarity between dissolution profiles *Drug Info J.* . 1997; 31:1255-1271.
- Louër D,Vargas R. Indexation automatique des diagrammes de poudre par dichotomies successives. *J. Appl. Cryst.* 1982;15: 542-545.
- Lubarsky GV, Davidson MR, Bradley RH. Elastic modulus, oxidation depth and adhesion force of surface modified polystyrene studied by AFM and XPS. *Surface Science* 2004; 558 (1-3): 135-144.
- Lund, W, ed. *The Pharmaceutical Codex: Principles and Practice of Pharmaceutics.* 1994. 12th edition, London: The Pharmaceutical Press. UK
- Macheras P, Reppas C Crystallography analysis B. *Biopharmaceutics of orally administered drugs.* 1995. Ellis Horwood, London, UK.
- Malamataris S, Hatjichristos Th. and Rees J. E. Apparent compressive elastic modulus and strength isotropy of compacts formed from binary powder mixes. *IntJ Pharm.* 1996; 141 (1-2):101-108.
- Malheiros SVP, de Paula E, Meirelles NC. Contribution of trifluoperazine/lipid ratio and drug ionization to hemolysis. *BiochimBiophys Acta - Biomembranes,* 1998; 1373 (2): 332-340.

- McGovern SL, Caselli E, Grigorieff N, Shoichet BK. A common mechanism underlying promiscuous inhibitors from virtual and high-throughput screening. *J Med Chem.* 2002;45(8):1712-1722.
- McKenna A, McCafferty DF. Effect on particle size on the compaction mechanism and tensile strength of tablets. *J Pharm Pharmacol.* 1982;34(6):347-351.
- Meylan W.P, Howard P.H and Boethling R.S. Improved method for estimating water solubility from octanol/water partition coefficient. *Environmental Toxicology and Chemistry* 1996;15(2): 100–106.
- Miyazaki S, Oshiba M and Nadai T. Unusual solubility and dissolution behavior of pharmaceutical hydrochloride salts in chloride-containing media. *Int.J Pharm.* 1980;6(1): 77-85.
- Miyakazi S, Oshiba M, Nadai T. Precaution on use of hydrochloride salts in pharmaceutical formulation. *J Pharm Sci.* 1981; 70 (6): 594-596.
- Moffat AC. Clarke's isolation and identification of drugs. The Pharmaceutical Press, London, UK 1986.
- Mooij WTM, van Eijck BP, Kroon J. Ab initio crystal structure predictions for flexible hydrogen-bonded molecules. *J Amer Chem Soc.* 2000; 122 (14): 3500-3505.
- Mooney KG, Mintun MA, Himmelstein KJ, Stella VJ Dissolution kinetics of carboxylic-acids .1. Effect of pH under unbuffered conditions. *J Pharm Sci.* 1981; 70 (1): 13-22.
- Moore JW., Flanner HH. Mathematical comparison of dissolution profiles. *Powder Tech.* 20:64-74.
- Mullin JW. Crystallisation. 2001. Butterworth-Heinmann, Boston, USA.
- Murali Mohan Babu GV, Prasad Ch. DS, Ramana Murthy KV. Evaluation of modified gum karaya as carrier for the dissolution enhancement of poorly water-soluble drug nimodipine. *Int.J Pharm.* 2002; 234(1-2):1-17.
- Muster TH, Prestidge CA. Application of time-dependent sessile drop contact angles on compacts to characterise the surface energetics of sulfathiazole crystals. *Int. J Pharm.* 2002; 234(1-2):43-54.
- Mysels KJ, Princen LH. Light Scattering by Some Laurylsulfate Solutions. *J. Phys. Chem.* 1959; 63(10); 1696-1700.
- Neubert R, Dittrich T. Ion pair approach of ampicillin using *in vitro* methods. *Pharm Acta Helv.* 1990 ;65(7):186-188.
- Neumann AW, Good RJ. Surface and Colloid Science. 1979. Plenum Press, New York, USA.

Ni N and Yalkowsky S.H. Prediction of Setschenow constants. *Int. J Pharm.* 2003; 254 (2):167-172.

Nicklasson F, Johansson B, Alderborn G. Tableting behaviour of pellets of a series of porosities--a comparison between pellets of two different compositions. *Eur J Pharm Sci.* 1999a ;8(1):11-17.

Nicklasson F, Johansson B, Alderborn G. Occurrence of fragmentation during compression of pellets prepared from a 4 to 1 mixture of dicalcium phosphate dihydrate and microcrystalline cellulose. *Eur J Pharm Sci.* 1999b;7(3):221-231

Nie HY, Motomatsu M, Mizutani W, Tokumoto H. Local elasticity measurement on polymers using atomic force microscopy. *Thin Solid Films* 1996; 273 (1-2): 143-148.

Nimmo J, Heading RC, Tothill P, Prescott LF. Pharmacological modification of gastric emptying: effects of propantheline and metoclopramide on paracetamol absorption. *Br Med J.* 1973;1(5853):587-589.

O'Connor KM, Corrigan OI. Comparison of the physicochemical properties of the N-(2-hydroxyethyl) pyrrolidine, diethylamine and sodium salt forms of diclofenac. *Int J Pharm.* 2001a;222(2):281-293.

O'Connor KM, Corrigan OI. Preparation and characterisation of a range of diclofenac salts. *Int J Pharm.* 2001b;226(1-2):163-179.

O'Dowd PJ, Corrigan OI. Dissolution kinetics of three component non-disintegrating compacts: theophylline, benzoic acid and salicylamide. *Int J Pharm.* 1999; 176(2): 231-240.

Ohtaki H, Fukushima N. A structural study of saturated aqueous-solutions of some alkali-halides by x-ray-diffraction. *J Sol Chem.* 1992; 21 (1): 23-38.

Ohtaki H. A rapid direct analysis of the structure of reaction intermediates by the EXAFS method combined with a stopped-flow technique. *Pure Appl Chem.* 1993; 65 (12): 2589-2592.

Palomo ME, Ballesteros MP, Frutos P. Analysis of diclofenac sodium and derivatives. *J Pharm Biomed Anal.* 1999;21(1):83-94.

Panunto TW, Lipkowska ZU, Johnson R, Etter MC; Hydrogen-bond formation in nitroanilines: the first step in designing acentric materials. *J. Am. Chem. Soc.* 1987; 109(25): 7786-7797.

Parshad H, Frydenvang K, Liljefors T, Larsen CS. Correlation of aqueous solubility of salts of benzylamine with experimentally and theoretically derived parameters. A multivariate data analysis approach. *Int. J Pharm.* 2002; 237 (1-2): 193-207.

Parshad H, Frydenvang K, Liljefors T, Sorensen HO and Larsen CS. Aqueous solubility study of salts of benzylamine derivatives and p-substituted benzoic acid derivatives using X-ray crystallographic analysis. *Int.J Pharm.* 2004; 269(1), 157-168.

- Payne RS, Roberts RJ, Rowe RC, McPartlin MB, Ash A. The mechanical properties of two forms of primidone predicted from their crystal structures. *Int. J Pharm.* 1996; 145 (1-2), 165-173.
- Payne RS, Roberts RJ, Rowe RC, Docherty R. Examples of successful crystal structure prediction: polymorphs of primidone and progesterone. *Int. J Pharm.* 1999a; 177 (2): 231-245.
- Payne RS, Roberts RJ, Rowe RC, Charlton MH, Docherty R. Potential polymorphs of aspirin. *J Comput Chem.* 1990b. 20:262-273.
- Perlovich GL, Bauer-Brandl A. Thermodynamics of solutions I: Benzoic acid and acetylsalicylic acid as models for drug substances and the prediction of solubility. *Pharm Res.* 2003; 20 (3): 471-478. Crystallography analysis
- Perlovich GL, Kurkov SV, Bauer-Brandl A. Thermodynamics of solutions. II. Flurbiprofen and diflunisal as models for studying solvation of drug substances. *Eur J Pharm Sci.* 2003;19(5):423-432.
- Perlovich GL, Kurkov SV, Kinchin AN, Bauer-Brandl A. Thermodynamics of solutions III: comparison of the solvation of (+)-naproxen with other NSAIDs. *Eur J Pharm Biopharm.* 2004; 57 (2): 411-420.
- Phani KK, Noyogi SK. Young modulus of porous brittle solids. *J Mat Sci.* 1987; 22 (1): 257-263.
- Pikal MJ, Lukes AL, Lang JE, Gaines K. Quantitative crystallinity determinations for beta-lactam antibiotics by solution calorimetry: correlations with stability. *J Pharm Sci.* 1978;67(6):767-773.
- Rades T, Müller-Goymann CC. Investigations on the micellisation behaviour of fenoprofen sodium. *Int. J Pharm.* 1997; 159(2) :215-222.
- Rades T, Mueller-Goymann CC. Interactions between fenoprofen sodium and poly (ethylene oxide). *Eur J Pharm Biopharm.* 1998; 46(1):51-59.
- Rescigno A. Bioequivalence. *Pharm Res.* 1992;9(7):925-928.
- Rietveld WJ, MacKay DM. Electroencephalogram potentials evoked by accelerated visual motion. *Nature.* 1968 Feb 17;217(129):677-8.
- Roberts RJ, Rowe RC. The effect of punch velocity on the compaction of a variety of materials. *J Pharm Pharmacol.* 1985;37(6):377-384.
- Roberts RJ, Rowe RC. Brittle fracture propensity measurements on 'tablet-sized' cylindrical compacts. *J Pharm Pharmacol.* 1986;38(7):526-528.
- Roberts RJ. The elasticity, ductility and fracture toughness of a variety of pharmaceutical powders. 1991 Thesis. University of Bradford, Bradford, UK.

Roberts RJ, Rowe RC. Influence of polymorphism on the Young's modulus and yield stress of carbamazepine, sulfathiazole and sulphanilamide. *Int. J Pharm.* 1996; 129(1-2):79-94.

Roberts RJ, Payne RS, Rowe RC. Mechanical property predictions for polymorphs of sulphathiazole and carbamazepine. *Eur J Pharm Sci.* 2000;9(3):277-83.

Rubino JT. Solubilities and solid state properties of the sodium salts of drugs. *J Pharm Sci.* 1989;78(6):485-489.

Rue PJ, Rees JE. Limitations of the Heckel relation for predicting powder compaction mechanisms. *J Pharm Pharmacol.* 1978;30(10):642-643.

Ruso JM, Attwood D, Rey C, Taboada P, Mosquera V, Sarmiento F. Light scattering and NMR studies of the self-association of the amphiphilic molecule propranolol hydrochloride in aqueous electrolyte solutions. *J Phys Chem, B* 1999; 103 (34): 7092-7096.

Sarmiento,F, Lopez-Fontan,JL, Prieto,G Attwood D. Mixed micelles of structurally related antidepressant drugs. *Colloid Polym Sci.* 1997; 275:114-117.

Saunders M, Podluzi K, Shergill S, Buckton G, Royall P. The potential of high speed DSC (hyper-DSC) for the detection and quantification of small amounts of amorphous content in predominantly crystalline samples. *Int J Pharm.* 2004;274(1-2):35-40.

Schrier SL, Zachowski A, Devaux PF. Mechanisms of amphipath-induced stomatocytosis in human erythrocytes. *Blood.* 1992;79(3):782-786.

Scurlock JE, Curtis BM. Tetraethylammonium derivatives: ultralong-acting local anesthetics? *Anesthesiology* 1981; 54(4):265-269.

Sebhatu T, Alderborn G. Relationships between the effective interparticulate contact area and the tensile strength of tablets of amorphous and crystalline lactose of varying particle size. *Eur J Pharm Sci.* 1999; 8(4):235-242.

Serajuddin AT, Jarowski CI. Effect of diffusion layer pH and solubility on the dissolution rate of pharmaceutical acids and their sodium salts. II: Salicylic acid, theophylline, and benzoic acid. *J Pharm Sci.* 1985;74(2):148-154.

Serajuddin AT, Sheen PC, Augustine MA. Common ion effect on solubility and dissolution rate of the sodium salt of an organic acid. *J Pharm Pharmacol.* 1987;39(8):587-591.

Sevelius H, Runkel R, Segre E, Bloomfield SS. Bioavailability of naproxen sodium and its relationship to clinical analgesic effects. *Br J Clin Pharmacol.* 1980;10(3):259-263.

Shaw LR. The development of a novel *in vitro* model suitable for the prediction of bioavailability. 2001. Thesis. University of Aston, Birmingham, UK.

Shell JW. X-ray and crystallographic applications in pharmaceutical research. III. Crystal habit quantitation. *J Pharm Sci.* 1963; 52:100-101

Sherwood L. Human Physiology, from cells to systems. 2004. Thompson Learning, London, UK.

Shinoda K, Yamanaka T, Kinoshita K. Surface chemical properties in aqueous solutions of non-ionic surfactants octyl glycol ether, α -octyl glyceryl ether and octyl glucoside. *J Phys Chem.* 1959; 63(5): 648-650.

Silverstein RM., Webster FX. Spectrometric identification of organic compounds. 1998. John Wiley & Sons, New York, USA.

Socrates G. Infrared characteristic group frequencies. 1994. John Wiley & Sons, New York, UK

Sonnergaard JM. A critical evaluation of the Heckel equation. *Int J Pharm.* 1999;193(1):63-71.

Spriggs RM. Expression for effect of porosity on elastic modulus of polycrystalline refractory materials, particularly aluminium hydroxide. *J Am Ceram Soc.* 1961;44:628-629.

Stahl PH and Wermuth G. (editors). Handbook of Pharmaceutical Salts: Properties, Selection, and Use. 2002. Wiley-VCH, Zurich.

Staniforth JN, Rees JE, Kayes JB, Priest RC, Cotterill NJ. The design of a direct compression tablet excipient. *Drug Dev Ind Pharm.* 1981; 7:179-190.

Streng WH, Hsi SK, Helms PE, Tan HG. General treatment of pH-solubility profiles of weak acids and bases and the effects of different acids on the solubility of a weak base. *J Pharm Sci.* 1984;73(12):1679-1684.

Sun CQ, Grant DJW. Improved tableting properties of p-hydroxybenzoic acid by water of crystallization: A molecular insight . *Pharm Res.* 2004; 21 (2): 382-386.

Szabo-Revesz P, Goczó H, Pintye-Hodi K, et al. Development of spherical crystal agglomerates of an aspartic acid salt for direct tablet making. *Powder Tech.* 2001; 114 (1-3): 118-124.

Takehiko HT, Hino YT, Yamamoto H, Kawashima Y. Spray-dried composite particles of lactose and sodium alginate for direct tableting and controlled releasing. *Int. J Pharm.* 1998; 174 (1-2): 91-100.

Thomas E, Rubino J. Solubility, melting point and salting-out relationships in a group of secondary amine hydrochloride salts. *Int J Pharm.* 1996; 130 (2): 179-185. Threlfall TL. Analysis of organic polymorphs, a review. *Analyst* 1995;120:2435-1460.

Train D, Hersey J.A. The use of laminar lubricants in compaction processes. *Powder Metall.* 1960; 6:20-32

Turner GW, Tedesco E, Harris KDM, Johnson RL, Kariuki BM. A method for understanding characteristics of multi-dimensional hypersurfaces, illustrated by energy and powder profile R-factor hypersurfaces for molecular crystals. *Z Kristallogr.* 2001; 216 (4): 187-189.

Urbanetz NA, Lippold BC. Solid dispersions of nimodipine and polyethylene glycol 2000: dissolution properties and physico-chemical characterisation. *Eur J Pharm Biopharm.* 2005; 59 (1): 107-118.

Visser JW. A fully automated program for finding the unit cell from powder data. *J Appl Cryst.* 1969; 2:89-95.

Watson DG. *Pharmaceutical Analysis.* 1999. Churchill Livingstone, London, UK

Werner P Crystallography analysisE, Eriksson L, Westdahl M. TREOR, a semi-exhaustive trial-and-error powder indexing program for all symmetries. *J App Cryst.* 1985; 18:367-370.

Westesen K, Wehler T. Investigation of the particle size distribution of a model intravenous emulsion. *J Pharm Sci.* 1993 Dec;82(12):1237-44.

Williams DE. Program MPA/MPG. Molecular Packing Graphics. Thesis. Department of Chemistry, University of Louisville, KY 40292, USA.

Wu CY, Ruddy OM, Bentham AC, Hancock BC, Best SM, Elliot JA. Modelling the mechanical behaviour of pharmaceutical powders during compaction. *Powder Tech.* 2005; 152 (1-3): 107-117.

Yang LB, Venkatesh G, Fassihi R. Compaction simulator study of a novel triple-layer tablet matrix for industrial tableting. *Int J Pharm.* 1997; 152 (1): 45-52.

Yff BTS, Royall PG, Brown MB, Martin GP. An investigation of calibration methods for solution calorimetry. *Int J Pharm.* 2004; 269 (2): 361-372.

Yokoyama S, Fujino Y, Kawamoto Y, Kaneko A. Micellization of an aqueous-solution of piperidolate hydrochloride in the presence of acetylcholine chloride. *Chem Pharm Bull.* 1994; 42 (6): 1351-1353.

York P. A consideration of experimental variables in the anaysis of powder compaction behaviour. *J Pharm Pharmacol.* 1979; 31:244-246

Yu LX, Carlin AS, Amidon GL, Hussain ASI. Feasibility studies of utilizing disk intrinsic dissolution rate to classify drugs. *Int J Pharm.*2004; 270 (1-2): 221-227.

Approved Drug Products. 1992. Rockville, MD, USA

British Pharmacopoeia. 2002. The Stationary Office, London, UK

BNF, No 49. 2005. www.bnf.org/bnf. London, UK

Martindale, The complete drug reference. 1999. Pharmaceutical Press, London, UK

Therapeutic Drugs. 1991. Churchill Livingstone, London, UK

The United States Pharmacopoeia and the National Formulary. 2003. Webcom Ltd., Toronto, Canada.

